MODULATION OF IMMUNE RESPONSES BY HUMAN PARAINFLUENZA VIRUS

By Cariosa Noone

Supervised for the award of Doctor of Philosophy by

Dr. Patricia Johnson

School of Biotechnology

March 2007

DECLARATION

I hereby certify that this material, which I now submit for assessment on the programme of study leading to the award of Ph.D. is entirely my own work and has not been taken from the work of others save and to the extent that such work has been cited and acknowledged within the text of my work.

Signed: Carissa Moore

ID No.: 55154239

Date: 30/3/2007

ACKNOWLEDGEMENTS

First and foremost, I would like to thank my supervisor, Dr. Patricia Johnson for all her help and support throughout the years. She has been a constant source of advice and guidance during my studies and always had an open door. Over the years we have both been through many trials and tribulations, so I want to thank her not only for her supervisory skills, but also for her friendship.

I would also like to thank our EU collaborators, Wolfgang Neubert, Sascha Bossow, Marian Wiegand, Grazia Cusi and Marius Loetscher for providing me with an unlimited supply of essential reagents, needed for my thesis. Not only were they the bearer of gifts, they also offered continuous support and technical advice throughout my research. I also need to thank the European Union for their financial support of my project.

Last but not least, I would like to thank my family and friends for all their help and support during my studies. I would especially like to thank my mum, Katherine and my sister, Tracy for their endless support and patience, through the highs and lows of my life in research. I would also like to thank my boyfriend, Aidan who has been my rock throughout the four years and who has always encouraged me when times were tough. I want to thank all my friends in NUI Maynooth, especially Ellen and Jane, who were my buddies in crime. Also, a special thanks to the lymphocyte biology lab (our next door neighbours) for all their help and advice, especially in flow cytometry techniques. A final thanks to everyone at DCU for being so welcoming and supportive when we relocated labs and a special thanks to all in the vascular lab, for always being there to lend a helping hand.

PUBLICATIONS

Publications leading up to this thesis:

Noone, C.M., Lewis, E.A., Frawely, A.B., Newman, R.W., Mahon, B.P., Mills, K.H., Johnson, P.A. (2005) Novel mechanism of immunosuppression by influenza virus haemagglutinin: selective suppression of interleukin 12 p35 transcription in murine bone marrow-derived dendritic cells. *J Gen Virol.* **86**, 1885-90.

Publications arising from this thesis:

Noone, C.M., Lewis, E.A., Newman, R.W., Johnson, P.A. (2007) Artificially generated dendritic cells misdirect antiviral immune responses. *J Leukoc Biol* (accepted for publication).

Noone, C.M., Lewis, E.A., Loetscher, M., Newman, R.W., Johnson, P.A. Human CD56+ natural killer cells regulate T cell proliferation during viral infection by inducing cell cycle arrest via an IL-2 dependent/p27 mechanism (submitted to blood # MS #BLOOD/2006/055913).

Noone, C.M., Lewis, E.A., Johnson, P.A. Natural killer cells regulate human proliferative responses (manuscript in preparation).

Bossow, S., Wiegand, M., Cusi, G., Noone, C.M., Johnson, P.A., Neubert, W.J. A novel replication deficient Sendai virus vector expressing chimeric HPIV3 HN and F proteins induces robust antibody and cell mediated immunity (manuscript in preparation).

CONTENTS

CHAPTER 5: IMMUNE RESPONSES TO A NOVEL REPLICATION DEFICIENT HPIV3 VACCINE

CHAPTER 6

APPENDICES

ABBREVIATIONS

Ab	Antibody
Abs	Absorbance
ADCC	Antibody-dependent cell-mediated cytotoxicity
Ag	Antigen
AO	Acridine orange
APC	Allophycocyanin
APC	Antigen presenting cell
BCR	B cell receptor
BSA	Bovine serum albumin
CD	Cluster of differentiation
Cdks	Cyclin dependent kinases
cDNA	Complimentary deoxyribonucleic acid
CTL	Cytotoxic T lymphocyte
DC	Dendritic cell
dsRNA	Double-stranded ribonucleic acid
EAE	Experimental autoimmune encephalomyelitis
EB	Ethidium bromide
EDTA	Ethylenediaminetetraacetic acid
ELISA	Enzyme linked immunosorbent assay
F	Fusion protein
FITC	Fluorescein isothiocyanate
FSC	Forward scatter
GM-CSF	Granulocyte-macrophage colony-stimulating factor
HA	Hemagglutinin
HBSS	Hanks balanced salt solution
HCMV	Human cytomegalovirus
HCV	Hepatitis C virus
HIV	Human immunodeficiency virus
HLA	Human leukocyte antigen
HN	Hemagglutinin-neuraminidase
HPIV	Human parainfluenza virus

HRP	Horse-radish peroxidase
HSV	Herpes simplex virus
IFN	Interferon
Ig	Immunoglobulin
IL	Interleukin
i.n	Intranasal
i.p	Intraperitoneal
L	Large protein
LCMV	Lymphocytic choriomeningitis virus
LPS	Lipopolysaccharide
M	Matrix protein
mAb	Monoclonal antibody
MCMV	Murine cytomegalovirus
mDC	Myeloid dendritic cell
MEM	Minimum essential medium
MHC	Major histocompatibility complex
mRNA	Messenger RNA
MS	Multiple sclerosis
NA	Neuraminidase
NK	Natural killer
NP	Nucleocapsid protein
OD	Optical density
P	Phosphoprotein
PAMP	Pathogen-associated molecular pattern
PBMC	Peripheral blood mononuclear cell
PBS	Phosphate buffered saline
PCR	Polymerase chain reaction
pDC	Plasmacytoid dendritic cell
Pe	Phycoerythrin
PMA	Phorbol 12-myristate 13-acetate
PMN	Polymorphonuclear
PRR	Pattern-recognition receptor
RA	Rheumatoid arthritis
rh	Recombinant human

RPMI	Roswell park memorial institute
RSV	Respiratory syncytial virus
RVI	Respiratory viral infection
SARS	Severe acute respiratory syndrome
SeV	Sendai virus
SIV	Simian immunodeficiency virus
SSC	Side scatter
TCR	T cell receptor
Th	T helper
TLR	Toll-like receptor
TMB	Tetramethylbenzidine
TNF	Tumour necrosis factor
Treg	Regulatory T cell
UV	Ultra violet

MODULATION OF IMMUNE RESPONSES BY HUMAN PARAINFLUENZA VIRUS

Cariosa Noone

ABSTRACT

Human Parainfluenza virus type 3 (HPIV3) is a key respiratory pathogen responsible for bronchiolitis, pneumonia and croup. The persistent nature of this virus and its ability to reinfect within a short space of time has led to successive failures in the design of a vaccine against this virus. To understand the lack of protective immunity observed after HPIV3 infections, a comprehensive study investigating immune responses to this respiratory pathogen was undertaken. A human *ex vivo* model of viral infection was developed. Priming by HPIV3 was compared to immune responses induced by influenza A virus, which unlike HPIV3 primes immunity to reinfection with the same strain. HPIV3 infection generated potent and mature dendritic cells (DCs). However, unlike influenza A generated DCs, allogeneic human mixed leukocytes (MLR) failed to proliferate to HPIV3 generated DCs. Conversely purified CD3+T cells were capable of expanding to these DCs. Further investigation revealed that autologous CD14-CD3- cells in the MLR were responsible for this control of T cell proliferation. Inhibition was contact dependent and reliant on the absence of IL-2. Follow on studies demonstrated that T cell proliferation control was due to CD56+ natural killer (NK) cells. Of interest, the regulation was not exerted by NK cytotoxicity but by partial arrest of cell cycle progression via regulation of p27 cyclin dependent kinase (cdk) inhibitor. Moreover, there was an overall control of T cell expansion by NK cells. The human *ex vivo* model was then used to assess the immunogenicity of a novel HPIV3 vaccine. Parallel studies involving murine immune models were also investigated. Studies revealed that the vaccine did not elicit the suppressive effects associated with HPIV3 whole virus infections. In conclusion, these studies identified a novel mechanism of immune regulation by NK cells in HPIV3 infections and demonstrated the potential of a novel vaccine against HPIV3.

For my mum,
my guidance,
my life

GENERAL INTRODUCTION

1.1 RESPIRATORY VIRAL INFECTIONS

Viruses are obligate parasites that can infect all living organisms. Composed of either DNA or RNA, these subcellular organisms have no metabolic activity outside the host cell and so are totally dependent on these cells for life (Harper 1998). Respiratory viral infections (RVIs) are a leading cause of morbidity, hospitalization and mortality, throughout the world (Abed and Boivin 2006, Armstrong *et al* 1999). Clinical manifestations range from acute upper respiratory tract infections to more serious lower respiratory infections, such as pneumonia (Abed and Boivin 2006). As RVIs are airborne diseases, they can spread rapidly from one individual to the next and so must be monitored closely. This is especially true for influenza virus, as it has the potential to change rapidly, producing a virulent strain, which could result in a pandemic (Fauci 2006). Furthermore, recurrent infections are quite common amongst certain respiratory viruses, such as respiratory syncytial virus (RSV) and parainfluenza viruses (PIV) (Hall 2001) and evidence for viral persistence has also been reported (Goswami *et al* 1984). Viral persistence is a consequence of viral immune modulation or evasion of the hosts immune system, enabling the virus to reside in a latent state, in the cells that they infect. Immune modulation by viruses can also interfere with essential immune responses, such as the antiviral interferon response and critical immune cells, such as dendritic cells, which play a critical role in adaptive immunity (Andrejeva *et al* 2004, Hengel *et al* 2005, Fernandez-Sesma *et al* 2006). In addition to their clinical attributes, RVIs can have huge socio-economic consequences; accounting for 20 million absences from work, yearly, in the United States (US) (Brooks *et al* 2004) and costing the US economy, approximately 40 billion dollars annually, for non-influenza related RVIs alone (Fenderick *et al* 2003). Thus, prevention and control of these RVIs is a major goal for researchers. Some efforts have been made to try and combat these viruses, through the development of vaccines, such as the trivalent inactivated vaccine for influenza and antiviral agents, such as neuraminidase inhibitors, adamantanes (antiviral drugs) and fusion inhibitors (Abed and Boivin 2006). However, although these antivirals may inhibit certain aspects of viral replication, they are only a 'quick fix' to the problem, as they do not

prevent reinfection by the virus. Thus, vaccines are still the most effective treatment for viral infections, as they can induce lifelong immunity to a particular virus strain. Also, although there is a trivalent vaccine available for influenza, it needs to be changed annually, to accommodate the ever growing new viral strains, that emerge from this mutating virus (Doherty *et al* 2006). Consequently, in the event of a pandemic millions would die, due to the time constraints associated with sequencing the new virus and developing a new vaccine. Therefore, other avenues should be explored for developing influenza vaccines. Also, many other respiratory viruses, such as RSV, coronaviruses and PIV have as yet, no licensed vaccines (Abed and Boivin 2006), emphasising the complex nature of the virus/ host relationship and the obstacles it must impose on vaccine development. Thus, understanding the immune responses to these respiratory viruses is critical to the development of new and more efficient vaccines.

1.1.1 Parainfluenza Viruses

Human parainfluenza viruses (HPIV) are a major cause of respiratory illness in adults, neonates and infants. They belong to the *paramyxoviridae* family and contain four different serotypes: HPIV1, 2, 3 and 4. HPIV1-3 are major causes of lower respiratory infections in infants, which are commonly characterised by illness such as croup, pneumonia and bronchiolitis (Denny and Clyde 1986). HPIV-4, induces similar clinical symptoms to HPIV1-3, however, symptoms are usually less severe (Henrickson 2003, Chanock 2001).

1.1.1.1 Structural organisation

HPIV are nonsegmented, negative, single-stranded RNA viruses. They encode at least six common structural proteins (3′-N-P-C-M-F-HN-L-5′), critical for viral replication. Integral to immunity and pathogenesis are the large envelope glycoproteins, which consist of a fusion (F) protein and the hemagglutinin-neuraminidase (HN) protein (figure 1.1). Their main function is in attachment and fusion of host cells. The matrix (M) protein is thought to be involved in mediating attachment of completed

nucleocapsids to the envelope. The large (L) polymerase protein, phosphoprotein (P) and nucleocapsid protein (NP), are closely associated with the viral RNA (vRNA) and are involved in viral replication. Also, the P gene of some paramyxoviruses can produce small non-structural proteins, such as the C and V proteins. These proteins appear to play in role in inhibiting the interferon response (Andrejeva *et al* 2004, Gotoh *et al* 2002), which is an important immune defence mechanism (Henrickson 2003, Chanock 2001, Hall 2001).

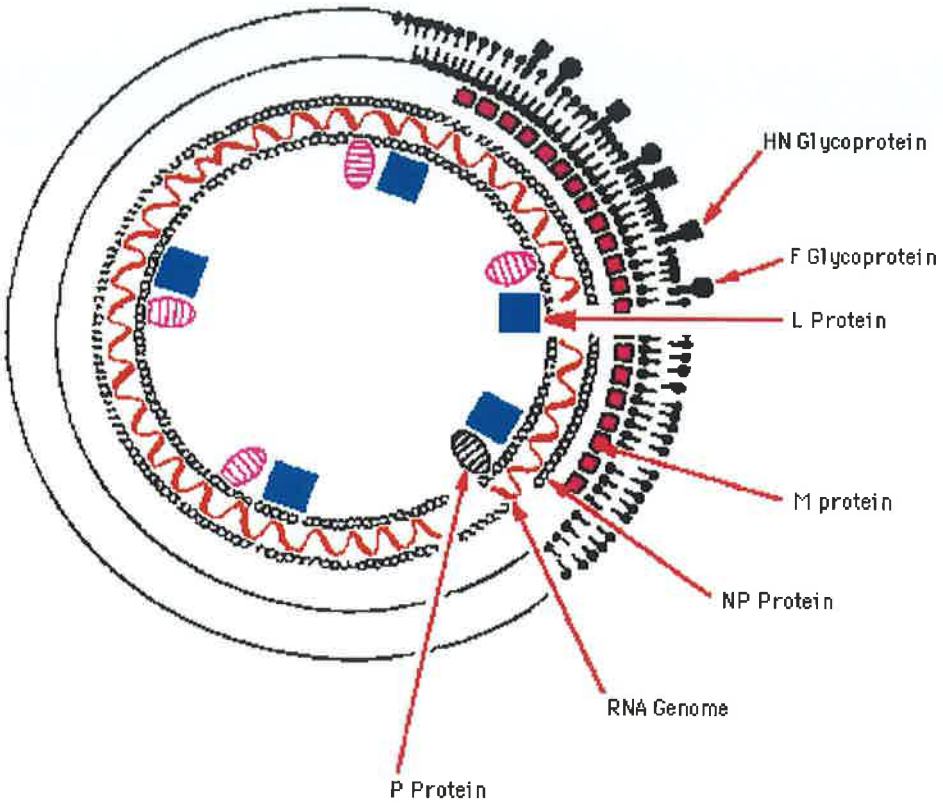

Figure 1.1 Structure of human parainfluenza virus.
(Taken from: www.microbios.com.ar/galeria-u2.htm)

1.1.1.2 Viral replication

The virus attaches to sialic acid receptors on the host cell and fuses with the cell membrane, enabling the nucleocapsid entry into the cytoplasm (figure 1.2). Once inside the cell, transcription takes place using the polymerase L protein (RNA-dependent RNA polymerase) and P protein. The virus uses host ribosomes to help

translate the viral messenger RNA (mRNA) into viral proteins, which direct replication of the virus genome, firstly to a positive sense strand and then into a negative sense strand. These negative sense strands are encapsidated with NP and can be released from the cell by budding (Chanock 2001, Henrickson 2003, Moscona 2005).

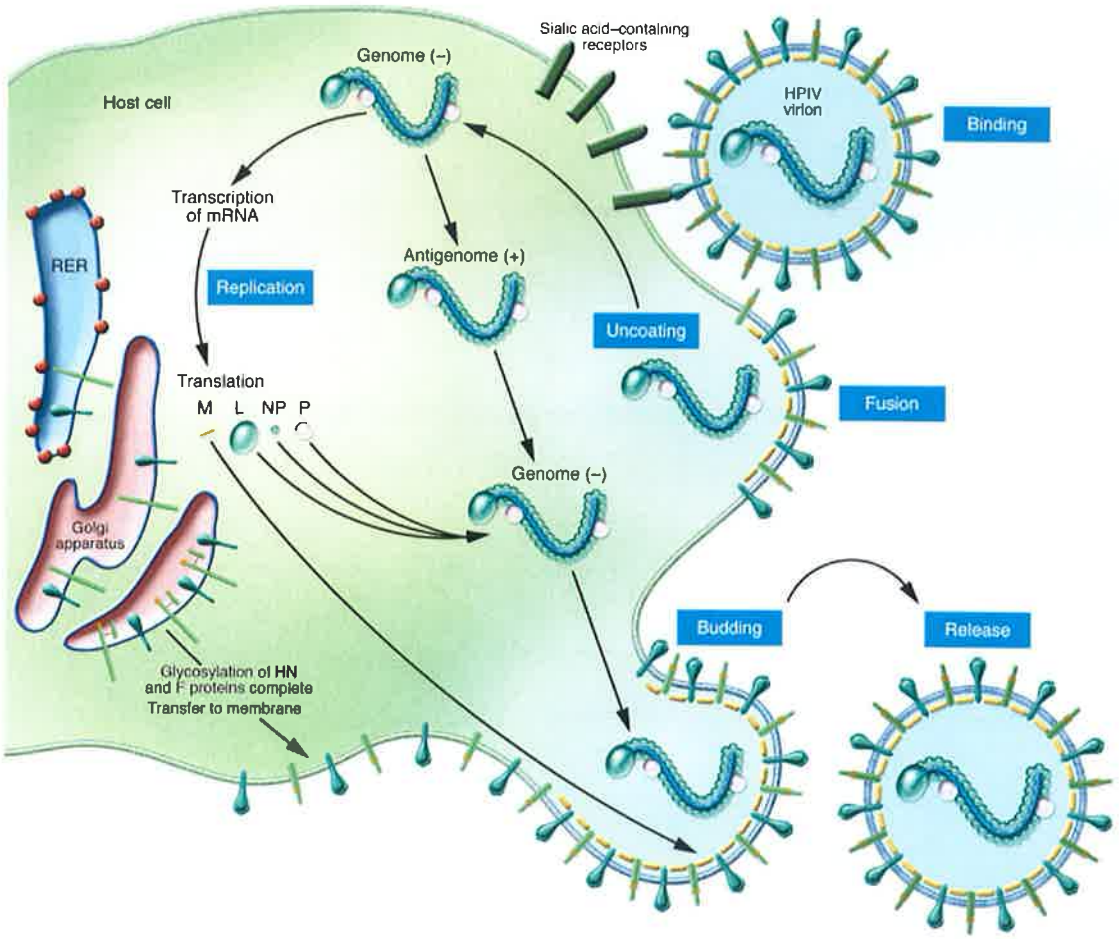

Figure 1.2 Schematic representation of the life cycle of parainfluenza virus.
(Taken from Moscana 2005)

1.1.1.3 Pathogenesis

HPIV replicates in the respiratory epithelium, resulting in inflammation of the airways or bronchiolitis. This inflammation is accompanied by a large influx of inflammatory cells. However, the damage to epithelial cells appears to result from inflammation, rather than the virus itself, but this concept remains unclear. In most cases, the virus is non-cytopathic and can lead to persistent infections. Tissue damage leads to necrosis

of cells and increased mucus secretions, obstructing airflow, resulting in wheezing or coughing. Recovery from infection usually occurs within a few days of symptoms (Moscona 2005, Henrickson 2003, Hall 2001).

1.1.2 Influenza Virus

Human viral influenza is a highly contagious, acute respiratory disease of global importance that has afflicted humans since ancient times. It is responsible for yearly epidemics and sporadic pandemics, representing a major cause of morbidity and mortality worldwide (Wright and Webster 2001, Cox and Subbarao 1999). Influenza viruses belong to the *orthomyxoviridae* family, which contains four groups: influenza A, B and C viruses and thogotovirus; of which influenza A is clinically the most important, as it can introduce new influenza viruses into the human population, through antigenic drift and shift. Influenza A viruses are further divided into subtypes, based on the antigenic nature of their hemagglutinin and neuraminidase proteins. Infection is characterized by fever and chills, accompanied by headache, myalgias and a dry cough (Cox and Subbarao 1999, Hilleman 2002, Wright and Webster 2001, Lamb and Krug 2001).

1.1.2.1 Structural organisation

Influenza A virus, is an enveloped, negative single-stranded RNA virus. Its genome is segmented, containing 8 RNA segments that encode at least 10 polypeptides. The viral envelope contains spike-like projections, which are the membrane glycoproteins, hemagluttinin (HA) and neuraminidase (NA) (figure 1.3). The HA attaches to the host cell and initiates membrane fusion with the endocytic vesicle inside the cell, while NA functions in the release of new viral progeny from the cell, by preventing viral aggregation. The matrix protein (M1) lies under the viral envelope where it interacts with the viral genome and nuclear export protein (Nep) and functions in viral assembly. The other matrix protein (M2) forms an ion channel between the virus interior and the surrounding microenvironment, enabling M2 to provide a low pH for

HA synthesis and virus uncoating. The RNA gene segments form loops and are encapsidated by the nucleocapsid protein (NP), in the inner core of the virus. Associated at one end of each gene segment is the polymerase complex, which is involved in viral transcription and consists of proteins PB1, PB2 and PA and this polymerase complex, along with the RNA segments and NP, are known as the ribonucleoprotein (RNP) core of the virus. It also contains two non-structural proteins, NS1 and Nep, which function in interferon suppression and nuclear export of viral RNA, respectively (Lamb and Krug 2001, Hilleman 2002).

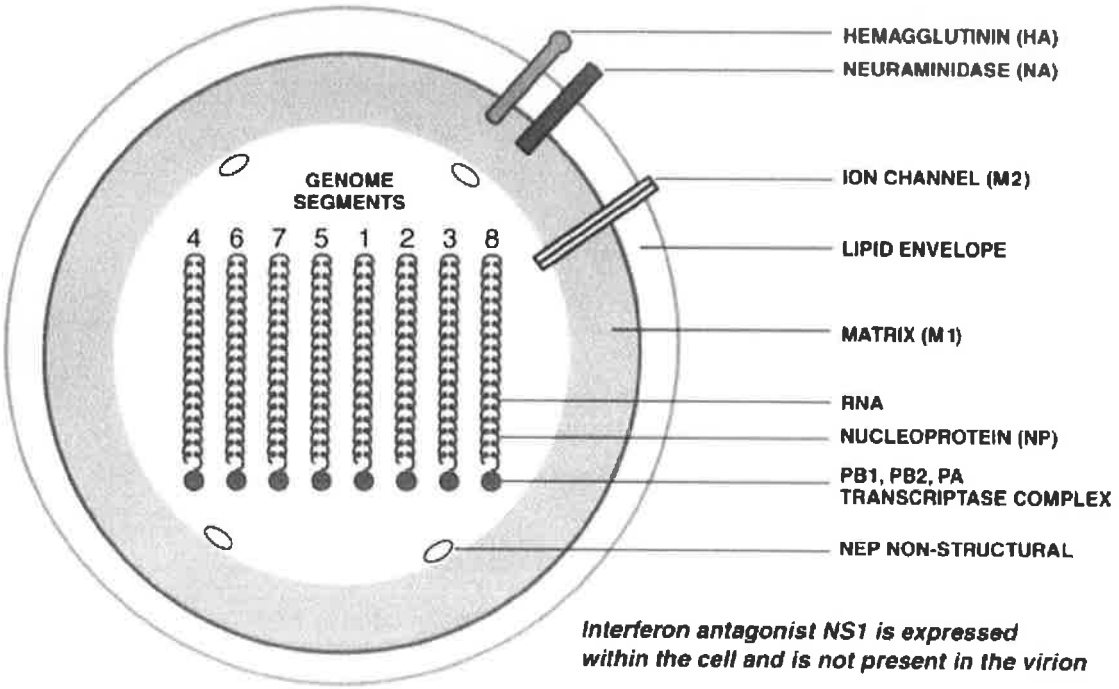

Figure 1.3 Structure of influenza virus.
(Taken from Hilleman 2002)

1.1.2.2 Viral replication

Influenza virus HA binds to sialic acid receptors on the host cells, initiating receptor-mediated endocytosis and the formation of a membrane bound vesicle around the virus (figure 1.4). This vesicle then fuses with endosomes, which can lower its pH, triggering conformational changes in HA, enabling the virus to fuse with cell membranes and expel its viral genome into the hosts' cytosol. From there, the viral

genome enters the nucleus to begin transcription. Influenza can then use its endonucleases to cleave 10-13 nucleotides and the 5′-methyl guanosine cap, from the host cells nuclear RNA, producing capped RNA fragments. These fragments can then serve as primers for transcription of each of the eight viral gene segments, where six of the newly transcribed mRNAs are translated into viral structural proteins, while two original RNA transcripts are each spliced into two mRNAs coding for non-structural proteins. The new virions are then assembled at the host cell membrane, where they are released from the cell by budding, through cleavage of sialic acid receptors by NA (Lamb and Krug 2001, Harper 1998).

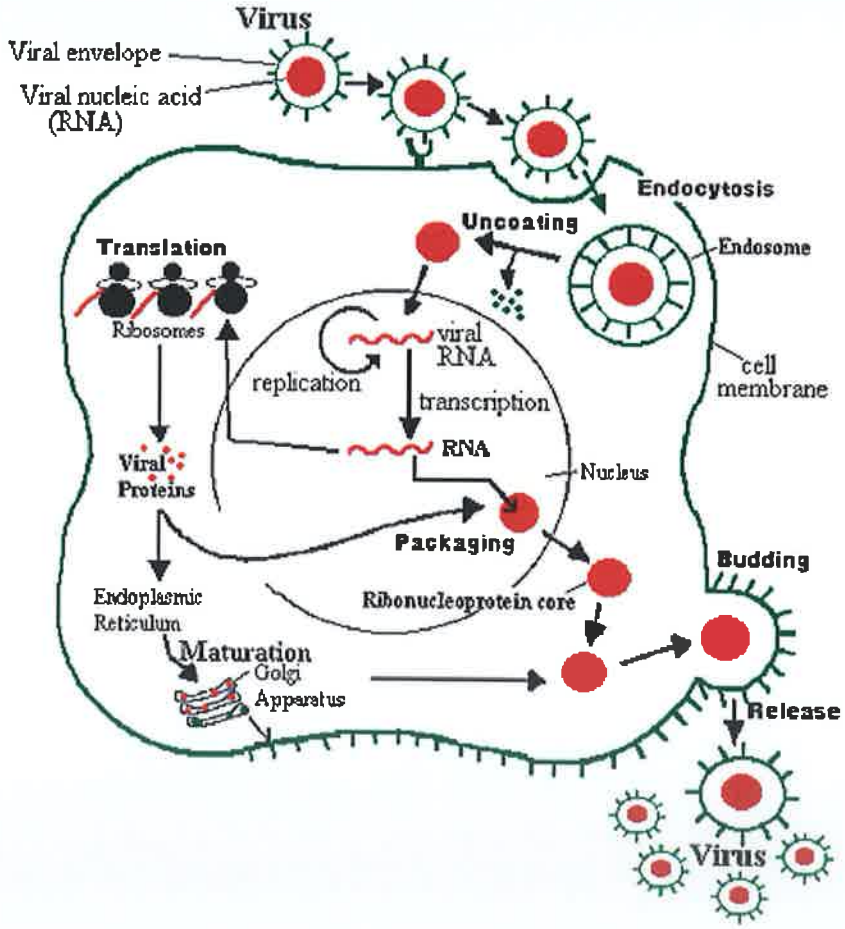

Figure 1.4 Schematic illustration of the life cycle of influenza virus.
(Taken from Access Excellence@ the National Health Museum 1999)

1.1.2.3 Pathogenesis

Influenza virus replicates in the epithelial cells of the respiratory tract. It induces pathological changes throughout the respiratory tract, especially in the lower respiratory tract. These infected epithelial cells induce inflammation of the larynx, trachea and bronchi, which is accompanied by a strong infiltration of leukocytes. Infection usually results in desquamation of the ciliated epithelial cells. All these features contribute to the clinical symptoms of the disease, such as fever, myalgia and dry cough. However, most individuals recover from influenza infection within a few days. Also, infection of the respiratory tract may give rise to primary pneumonitis, especially in immunocompromised individuals and this may lead to secondary bacterial infections, such as those caused by streptococcal and staphylococcal bacteria. These secondary infections can cause severe pulmonary complications, which can result in a fatal form of pneumonia (Wright and Webster 2001, Hilleman 2002).

1.2 IMMUNITY TO VIRUSES

Viral infections will always represent a stringent challenge to immunologists because of the continual emergence of new diseases, such as the severe acute respiratory syndrome (SARS) and avian influenza; as well as the high mutating rate of some viruses, such as the human immunodeficiency virus (HIV) (Kawai and Akira 2006, Doherty *et al* 2006). The war between the virus and the immune system is one of high complexity and could be compared to a type of guerilla warfare, in which both sides try to outwit their opponent. The virus tries to evade recognition by the immune system, but once exposed, the immune system with its highly complex network, sets up its defence by eliminating this "danger", thereby protecting the host or "self" from disease (Matzinger 1994). Thus, the immune system is critical to the outcome of viral infections. However, although the immune response is highly complex, it can be divided into two arms; the innate (or 'non-specific') immune response and the adaptive (or 'specific') immune response; that work in synergy to provide the quickest and most efficient protective immunity (Janeway *et al* 2001, Harper 1998).

1.2.1 Innate Immunity

The innate immune response provides the first line of defence against invading pathogens. It provides a rapid and fairly primitive non-specific response to infections. Firstly, it tries to limit pathogen entry to the body through physical and chemical barriers, such as epithelia, digestive enzymes and antimicrobial peptides. If these surface defences are overcome by invading pathogens, they subsequently encounter the innate immune cells and plasma proteins of the complement system. These plasma proteins can be activated from pathogen infections, resulting in enhanced opsonization and phagocytosis of the pathogen and microbial lysis (Tosi 2005, Janeway *et a*l 2001). The innate immune cells encompass various leukocytes, such as natural killer (NK) cells, monocytes and dendritic cells (DCs). Other leukocytes include phagocytic cells that engulf and destroy microorganisms, such as macrophage and neutophils (Abbas *et al* 1997, Tosi 2005). These cells express germ-line encoded receptors, often termed pattern-recognition receptors (PRRs), as they are capable of

recognising common microbial molecules or pathogen-associated molecular patterns (PAMPs), such as complex carbohydrates or lipopolysaccharides (LPS) found in the cell wall of most bacteria or double stranded RNA (dsRNA) produced in virus infected cells (Janeway and Medzhitov 2002, Akira *et al* 2001, Kawai and Akira 2006). These PAMPs are not found in the host cell and so are used to identify 'danger' molecules, enabling the host to destroy only pathogen-infected cells. The most characterised PRRs in mammalian species are the toll-like receptors, which are homologous to the insect Toll receptors that also mediate essential innate immune protection for the insect against fungal pathogens (Akira and Takeda 2004).

1.2.1.1 Pattern recognition receptors: Toll-like receptors

The Toll-like receptor (TLR) family of transmembrane proteins, is the best characterised class of PRRs in mammalian species. To date, 10 to 15 TLRs have been identified in mammalian species, but this number may differ between species. TLRs are expressed on many leukocytes, in addition to epithelial cells lining respiratory, intestinal and urogenital tracts (Iwasaki and Medzhitov 2004, Ashkar et al 2003, Kagnoff and Eckmann, 1997). TLRs can detect multiple PAMPs from a variety of microbes including bacteria, protozoa and viruses (Kawai and Akira 2006, Akira *et al* 2001). TLRs 1, 2, 4, 5 and 6 mainly specialise in the recognition of bacteria through bacterial cell wall components or products, such as bacterial lipoproteins and lipoteichoic acids (detected by TLR 1, 2, 6), LPS (detected by TLR 4) and flagellin (detected by TLR 5). However TLRs 3, 7 and 8 mainly focus on the detection of viruses, recognising nucleic acids that are not normally produced in host cells, such as dsRNA (detected by TLR 3) and single-stranded RNA (ssRNA) (detected by TLR 7 and human TLR8). TLR9 also recognises unfamiliar nucleic acids produced in host cells, such as unmethylated CpG DNA of viruses and bacteria (Akira et al 2001, Iwasaki and Medzhitov 2004, Kawai and Akira 2006, Heil *et al* 2004). TLR 1, 2 and 4 are usually expressed on the cell surface while TLR 3, 7, 8 and 9 are mainly localised to intracellular compartments where they can detect nucleic acids in late endosomes or lysosomes (Akira and Takeda 2004, Diebold *et al* 2004, Kawai and Akira 2006). Stimulation through TLRs activates various signal transduction pathways, ultimately resulting in the nuclear translocation and activation of nuclear factor κB (NF-κB).

NF-κB is an important transcription factor that activates the promoters of numerous genes, transcribing proteins involved in the inflammatory response such as cytokines and chemokines (Akira and Takeda 2004, O'Neill 2004). Chemokines and cytokines play a complex role in the immune response to viruses and various other pathogens, where chemokines main function is to control or direct leukocyte trafficking or migration and cytokines are involved in the activation and regulation of numerous cells (Coelho *et al* 2005, Tosi 2005). Also, there are TLR-independent mechanisms for the recognition of pathogens, which involve cytoplasmic proteins, such as retinoic acid-inducible gene 1 (RIG-1) and melanoma differentiation-associated gene 5 (Mda 5). These are RNA helicases that can bind to viral dsRNA in the cytoplasm, leading to activation of various signalling pathways, including the NF-κB pathway and secretion of type I interferon antiviral cytokines and other inflammatory proteins (Kawai and Akira 2006, Akira and Takeda 2004).

1.2.1.2 Interferons

Some of these innate immune cells, notably macrophage, DCs and NK cells, can secrete large amounts of cytokines, which can activate other immune cells and stimulate inflammation (Tosi 2005). In a viral infection, the interferons (IFNs) are the most important cytokines produced, as they have antiviral properties and are secreted from many different cells, early after infection. They can be separated into two main families consisting of the type I IFNs, of which IFNα and IFNβ are the best characterised and a type II interferon family, encompassing the related but distinct IFNγ (Collier and Oxford 2006, Guidotti and Chisari 2000, Garcia-Sastre and Biron 2006). IFNα and IFNβ share a common heterodimeric receptor (IFNAR), which is ubiquitously expressed on many different cells (Theofilopoulos *et al* 2005). Binding of IFNα/β to its receptor activates kinases that are associated with the receptors cytoplasmic tail; the Janus-activated kinase 1 (JAK1) and tyrosine kinase 2 (TYK2). This results in the tyrosine phosphorylation and activation of the signal transducer and activator of transcription (STAT) 2 and STAT1, leading to the formation of the STAT1-STAT2- IFN regulatory factor 9 (IRF9) complexes, known at the IFN-stimulated gene factor 3 (ISGF3) complexes. Type I IFNs can also induce the

formation of STAT1-STAT1 homodimers, known at the IFNγ-activated factor (GAF) complexes. These complexes translocate to the nucleus and ISGF3 binds IFN-stimulated response elements (ISREs) and GAF binds IFNγ-activated sites (GAS) in DNA to initiate transcription of numerous IFN-stimulated genes that code for antiviral proteins. These proteins are involved in preventing or inhibiting viral replication in that cell. Other signalling pathways are used by type I IFNs, involving the activation of different STATs, such as STAT3, 4 and 5, but the STAT1-STAT1 and STAT1-STAT2 pathways are the most common signalling pathways induced by type I IFNs in cells (Garcia-Sastre and Biron 2006, Platanias 2005). Figure 1.5 illustrates the major components of the classical JAK-STAT pathway induced by type I IFNs.

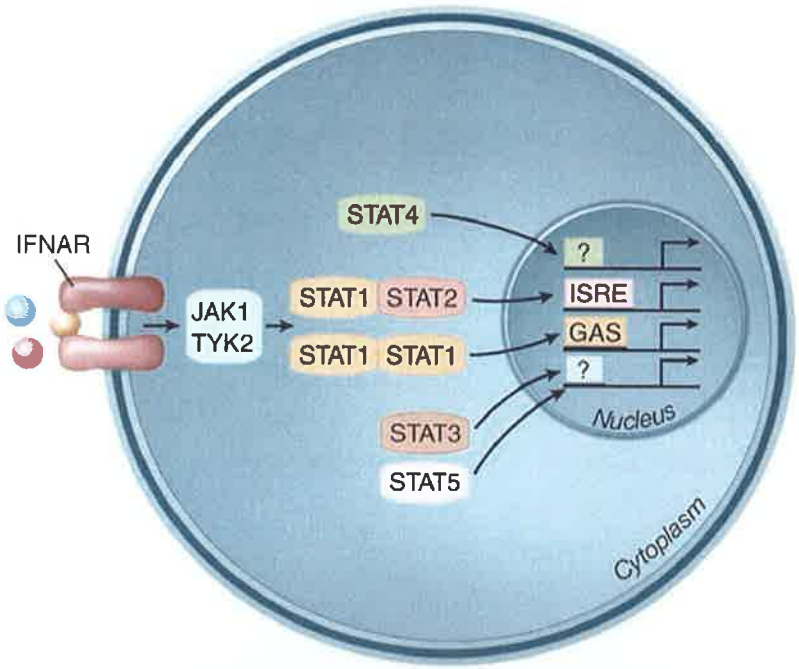

Figure 1.5 Summarises the JAK-STAT signalling pathway induced by type I IFNs.
(Taken from Garcia-Sastre and Biron 2006)

Several antiviral enzymes can be produced, resulting from the signalling pathway above; for example, a serine-threonine kinase, protein kinase R (PKR) and 2′-5′ oligoadenylate synthetases (OAS) are among the best characterised enzymes involved in antiviral immunity. PKR is activated by dsRNA through autophosphorylation. This in turn leads to the phosphorylation of downstream substrates, including the elongation factor eIF2α, thereby inactivating it and inhibiting protein synthesis. Also,

dsRNA activates the OAS enzymes, generating 2′-5′ oligoadenylates, which in turn activates ribonuclease L (RNAse L), leading to viral and cellular degradation of RNA. Although this may lead to programmed cell death or apoptosis of the cell, it limits viral spread to other cells. The effects of IFNα/β are paracrine, in that they will bind to IFN receptors on uninfected neighbouring cells and induce an antiviral state in that cell (Collier and Oxford 2006, Garcia-Sastre and Biron 2006, Mayer 2003). The interferon induced antiviral pathway is summarised in figure 1.6.

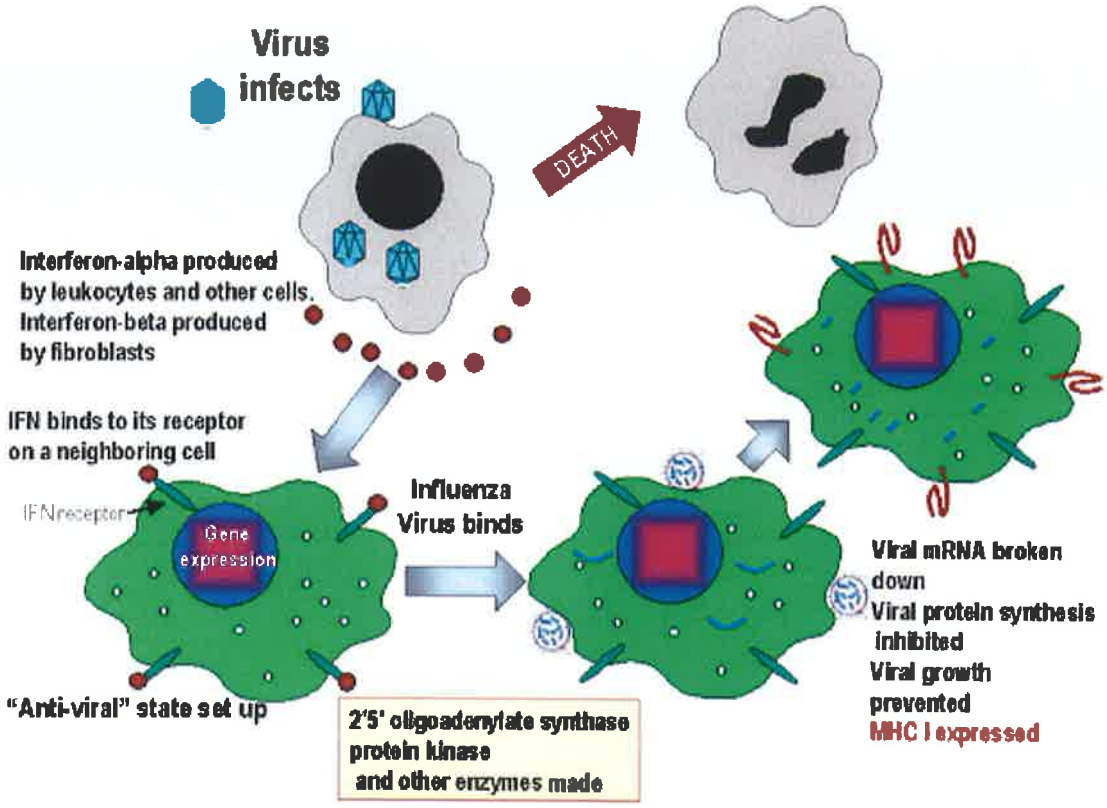

Figure 1.6 Schematic representation of interferon induced antiviral immunity.
(Taken from Mayer 2003)

As type I interferons are proinflammatory cytokines, they can also activate and enhance the activity of other immune cells, such as macrophages, DCs and NK cells (Guidotti and Chisari 2000). Type I IFNs can lead to DC maturation, resulting in the upregulation of MHC and costimulatory molecules, on the surface of DCs, which is essential for T cell activation (Theofilopoulos *et al* 2005). Also type I IFN induced DC maturation following viral infection, can promote cross priming (process whereby a captured extracellular antigen can be presented on MHC class I molecules) of antigens to CD8+ T cells, resulting in T cell activation (Le Bon *et al* 2003). Thus,

type I IFNs play an important role in bridging innate and adaptive immune responses and directing appropriate T cell responses.

IFNγ is a proinflammatory type II IFN cytokine that can modulate many aspects of the immune response, including antiviral immunity. It is mainly secreted from T cells and NK cells and is a critical cytokine involved in activating macrophages. Activated macrophages can produce nitric oxide (NO) and oxygen radicals, which have potent antimicrobial activity. As IFNγ is associated with many protective functions, it is one of the most important cytokines involved in shaping or directing adaptive immune responses (Janeway *et al* 2005, Guidotti and Chisari 2000, Harper 1998).

1.2.1.3 NK cells

NK cells are lymphoid derived cells, that play and important role in innate immune responses, particularly in antiviral and tumour immunity. They express a large repertoire of activatory and inhibitory receptors and are capable of directly lysing virus infected cells and tumour cells (Miller 2001, Hammerman *et al* 2005). They recognise decreased levels of self major histocompatability complex (MHC) class I molecules, which are highly polymorphic glycoproteins expressed on the surface of nucleated cells. In a healthy cell, inhibitory signals are delivered by self MHC class I molecules to NK cells, thereby protecting the cell from lysis. Often virus infected cells and transformed cells express reduced levels of MHC class I, which limits the inhibitory signals delivered from the target cell to the NK cell inhibitory receptors, resulting in NK cell activation and target cell lysis (Tosi 2005, Raulet and Vance 2006, Walzer et al 2005, Delgi-Esposti and Smyth 2005). In addition to its activatory receptors, NK cells can be activated by various cytokines, including IFNα, IFNβ, IL-12, TNFα and IL-15, which are produced by activated DCs and macrophages and IL-2 secreted by T cells. Activated NK cells use two main pathways for inducing apoptosis of target cells: 1) granule exocytosis (discussed in section 1.2.2.5.2) (Trapani and Smyth 2002) and 2) death-receptor-engagement, such as that mediated by the tumour necrosis factor-related apoptosis-inducing ligand (TRAIL). TRAIL

expressed on NK cells can bind to its receptor, the TNF receptor, inducing apoptosis through caspase activation and target cell DNA damage (Smyth *et al* 2003). Antibodies can also bind to viral antigens on infected cells and Fc receptors, such as FcγRIII (CD16) found on NK cells can bind to these antibodies and induce apoptosis of the infected cell through the release of cytotoxic granules, known as antibody-dependent cell-mediated cytotoxicity (ADCC) (Collier and Oxford 2006). Also activated NK cells can secrete large amount of IFNγ, which can limit tumour growth and promote the development of specific protective immune responses (Miller 2001, Wallace and Smyth 2005).

1.2.2 Adaptive Immunity

Pathogens are continuously trying to avoid detection by the immune system and so have generated mechanisms to evade detection; for example, some viruses, such as HIV can mutate readily, altering the viral genome, thereby making it harder for the immune system to detect it (Kawaii and Akira 2005). As the innate immune system only recognises conserved structures or patterns on pathogens, it is limited in its capabilities and is unable to recognise or cope with highly diverse and mutating pathogens. Thus, the immune system has evolved a more specific way of dealing with pathogens that have evaded the innate immune response, which is adaptive immunity. The adaptive immune response can be divided into two arms; 1) humoral immunity, mediated by B lymphocytes and 2) cell-mediated immunity, mediated by T lymphocytes. Both B and T lymphocytes express specific receptors that are capable of recognising an infinite number of pathogens. However only a single type of receptor that is specific to a particular antigen will respond and generate effector functions to that antigen. This unique antigen specificity is achieved through the generation of a large and diverse repertoire of receptors, generated from recombination of gene segments encoding the T cell receptor (TCR) and B cell receptor (BCR). Lymphocytes whose receptors bind with high affinity to self-antigens during the developmental stages are deleted from this repertoire, ensuring that only lymphocytes, which are tolerant to the host cells will survive, a process termed 'negative selection'. Once B and T lymphocytes encounter a particular virus or pathogen, which is specific

for their receptor, they become activated through various signals and proliferate to form a clone of antigen specific effector and memory cells. After the infection is cleared, these memory cells reside in the circulation in a resting state, until they become restimulated again by encountering the same antigen. This second encounter causes a rapid and more efficient immune response to the pathogen and in many cases enables the adaptive immune response to confer lifelong protection to the host against that pathogen (Janeway *et al* 2005, Abbas *et al* 1997).

1.2.2.1 B lymphocytes

B cells are a type of antigen presenting cell (APC), that originate from hematopoietic stem cells in the bone marrow, where they mature, before entering the circulatory network. Their main function is to eliminate extracellular pathogens through the production of specific proteins called antibodies. As most intracellular pathogens disseminate from cell to cell, these antibodies found in extracellular spaces can also help prevent the spread of intracellular infections (Janeway *et al* 2001). B cells recognise and bind particular pathogens or antigens through their immunoglobulin BCR, which then transmits signals to the cells interior and delivers the antigen to intracellular compartments, where it is degraded and returned to the cell surface as peptides bound to MHC class II molecules. This antigen:MHC complex can then be recognised by effector T cells, known as CD4+ T helper cells, which can activate B cells through secretion of cytokines, such as IL-4 and binding of particular stimulatory molecules on the surface of both T and B cell, such as the CD40 ligand (CD40L)(high expression on activated T cells) and CD40 (expressed on B cells). This activated B cell can proliferate to form a clone of identical cells, which then differentiate into antibody secreting plasma cells and memory cells (Abbas *et al* 1997, Janeway *et al* 2001, McHeyzer-Williams 2003). However some microbes can activate B cells directly, without the aid of T cell help, such as bacterial polysaccharides, but they can usually only induce antibody secretion of a particular class and are unable to induce memory B cells (Janeway *et al* 2001).

Antibodies are immunoglobulins (Igs) composed of two polypeptide heavy chains and two light chains, joined together by disulfide bonds. Each chain contains constant and variable regions (figure 1.7). These variable heavy and light chains form a groove or site where the antigens bind and this region along with the constant light chain and heavy chain 1 (CH1), are known as the fragment antigen binding (Fab) region. The constant region is the functional part of the molecule, encompassing the Fc fragment composed of CH2 and CH3 domains. Antibodies can be divided into five different classes or isotyes based on their heavy chain function; IgM, IgA, IgD, IgG and IgE. Cytokines present at the site of infection, such as IL-4, IL-5 and IFNγ, can influence isotype switching. Each of these Igs exerts specific effects, thereby shaping the immune response (Abbas *et al* 1997, Janeway *et al* 2001).

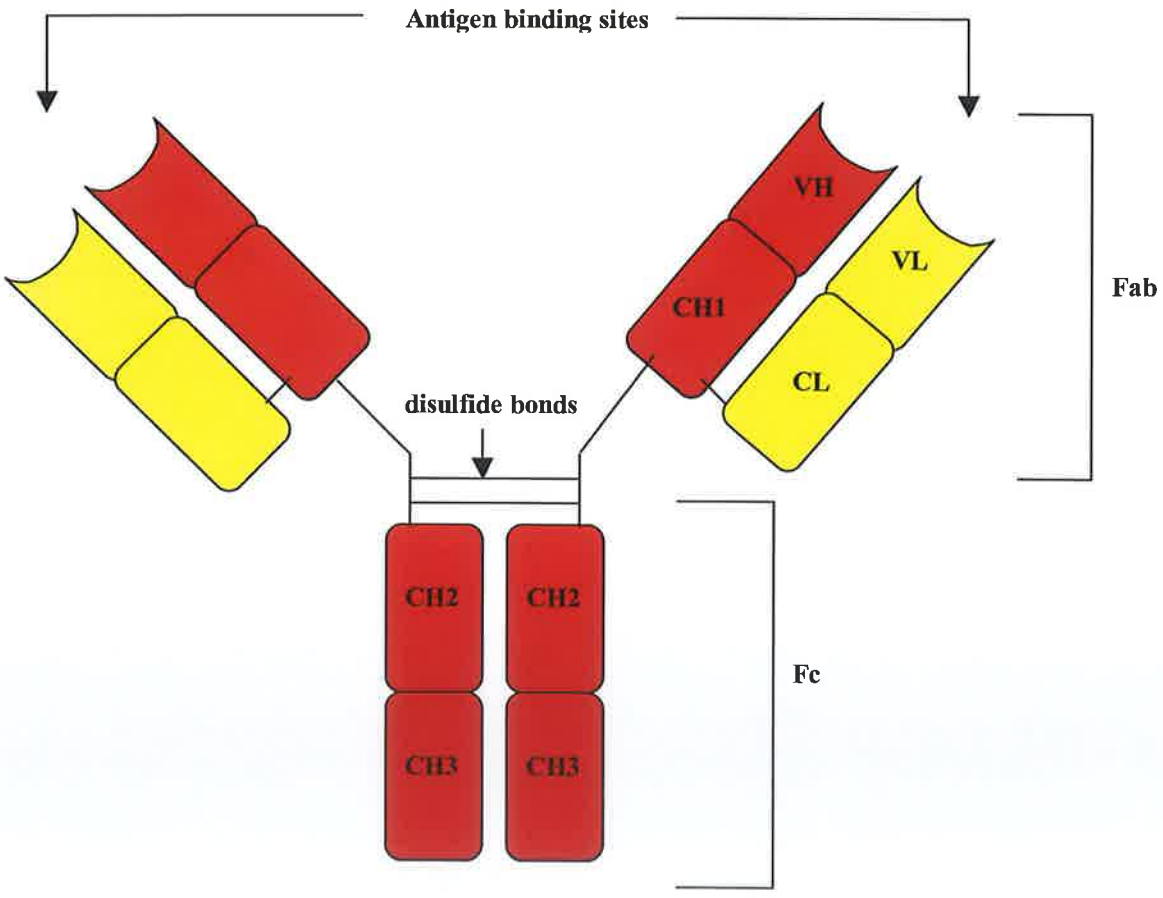

Figure 1.7 Structure of an antibody molecule. Antibody molecules are composed of heavy (H) chains and light (L) chains, linked together by disulfide bonds, containing constant (C) and variable (V) regions.

Antibodies destroy or eliminate pathogens or viruses by several mechanisms, including neutralisation, opsonization and complement activation. Binding of antibodies to antigenic determinants or epitopes on pathogens or toxins, blocks pathogen entry and neutralises harmful toxins, respectively. They can bind or coat antigens, a process known as opsonization, enabling pathogens to be recognised and ingested by various phagocytic cells, expressing Fc receptors that can bind to the Fc region of antibodies. Lastly, antibody binding to pathogens can activate proteins of the complement system, leading to the increased opsonization and death of many pathogens (Janeway *et al* 2001).

This natural defence is imperative to the hosts' survival and eradication of viruses. Thus, the main goal of vaccination is to induce a robust antibody response to the invading virus. In a respiratory virus infection, IgG and IgA are the most crucial antibodies required for the hosts' protection (Crowe and Williams 2003). IgG is the principal antibody found in the blood and it mainly functions in opsonization, complement activation and induction of ADCC, thereby acting systemically. Alternatively, IgA acts locally and is found in secretions of the digestive, urogenital and respiratory tract and its chief responsibility is to neutralise infectious viruses (Collier and Oxford 2006).

1.2.2.2 T lymphocytes

T cells also originate from hematopoietic stem cells in the bone marrow, but unlike B cells, they mature in the thymus before entering the bloodstream. From there, they recirculate between the blood and peripheral lymphoid tissues, until they encounter their specific antigen. They are pivotal cells to the adaptive immune response, playing essential roles in protection against intracellular pathogens or viruses and immunoregulation. Individuals with defects in cellular immunity often suffer more prolonged virus shedding and more severe illnesses with respiratory viruses, such as RSV, influenza and HPIV (Crowe and Williams 2003). The TCR resembles that of the immunoglobulin BCR, in that both receptor gene groups have the potential to generate a diverse repertoire of receptors, through somatic recombination. However, TCRs recognise and respond to peptide antigens, presented to them by MHC

molecules. Each T cell is specific for a particular antigen and contains approximately 30,000 identical receptors that are capable of recognising that antigen. The TCR is a heterodimeric protein, composed of a transmembrane glycoprotein α chain and β chain, which are linked together by a disulfide bond (figure 1.8). Each chain contains a constant and variable region, where the variable region binds the peptide:MHC complex. A CD3 molecule is also associated with the TCR, as it is required for signalling. This antigen receptor binding, along with stimulatory signals, activates the T cells, enabling them to proliferate and differentiate into effector and memory cells. However, there is a smaller group of T cells which express a different TCR, composed of a γ and δ chain, but these cells recognise antigens in a non-MHC restricted manner (Janeway *et al* 2005). T cells acquire many different effector functions, including cytokine production and cytotoxicity and can be divided into three major groups; 1) helper T cells (Th), 2) cytotoxic T lymphocytes (CTLs) and 3) regulatory T cells (Treg). Helper T cells express the co-receptor molecule CD4, and can be subdivided into two main groups: Th1 cells and Th2 cells, whose main function is in cytokine secretion. Cytotoxic T cells express the co-receptor CD8 and their main function is target cell lysis and regulatory T cells can suppress or regulate T cell responses (Janeway *et al* 2005, Schwartz 2005).

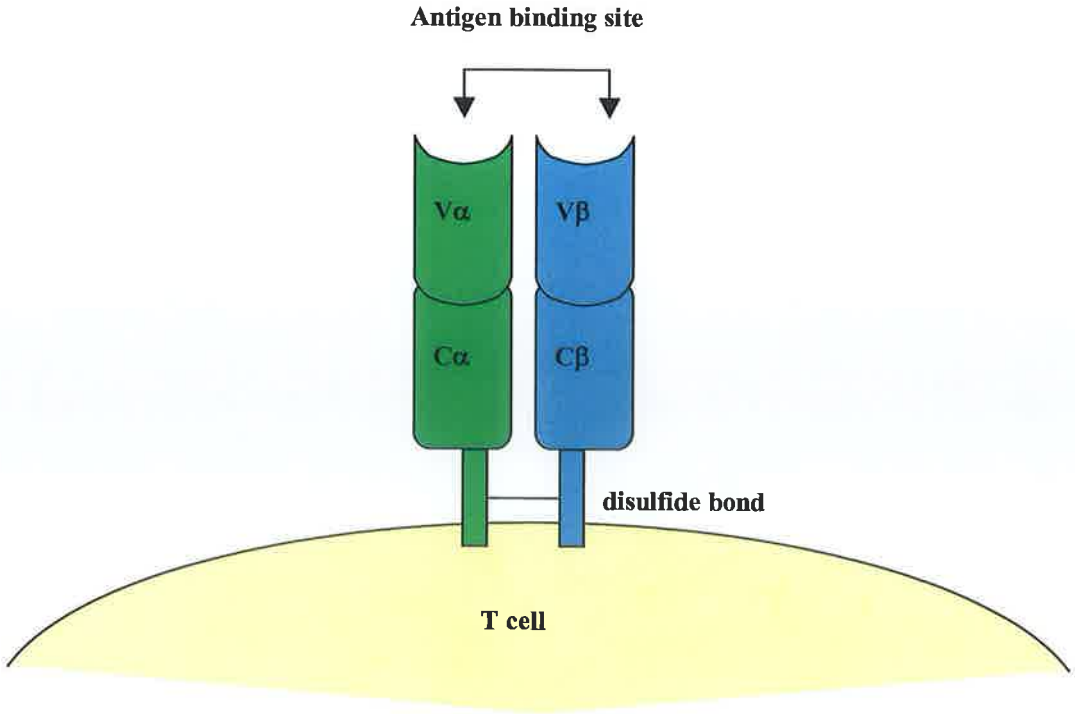

Figure 1.8 Structure of an αβ TCR. The TCR is composed of two polypeptide chains, α and β chains, that contain constant (C) and variable (V) regions and are linked together by a disulfide bond.

1.2.2.3 Major histocompatability complex (MHC)

The major histocompability complex (MHC) is a cluster of genes, which codes for cell surface glycoproteins that bind antigenic peptides to present to T cells. Two classes of MHC molecules exist; 1) MHC class I, which presents endogenous peptides to CD8+ T cells and 2) MHC class II, which presents exogenous peptides to CD4+ T cells. MHC class I is expressed on the surface of most nucleated cells, while MHC class II is mainly expressed by APCs and lining cells, such as epithelial cells. MHC class I molecules contain two Ig-like, polypeptide chains; one α chain, encoded in the MHC locus, that is anchored to the membrane and a second non-MHC encoded chain, β_2-microglobulin. In contrast, MHC class II molecules contain one α and one β chain, encoded in the MHC locus, that traverse the membrane (figure 1.9A and B). Both MHC molecules fold to form a peptide binding groove, which is highly polymorphic, enabling the MHC molecule to present a diverse repertoire of peptide antigens. In humans, the MHC is called the human leukocyte antigen (HLA) gene complex, where HLA-A, B and C, are the main genes of the MHC class I molecule and HLA-DR, DP and DQ, are the main genes of the MHC class II molecule. Endocytosed antigens are processed in acidic intracellular vesicles or endosomes, generating class II associated antigens, whereas antigens present in the cytosol, such as *de novo* synthesised viral proteins, are processed to generate class I associated antigens. This peptide:MHC complex is then delivered to the cell surface to present to T cells (Abbas *et al* 1997, Janeway *et al* 2005, Parham 2005).

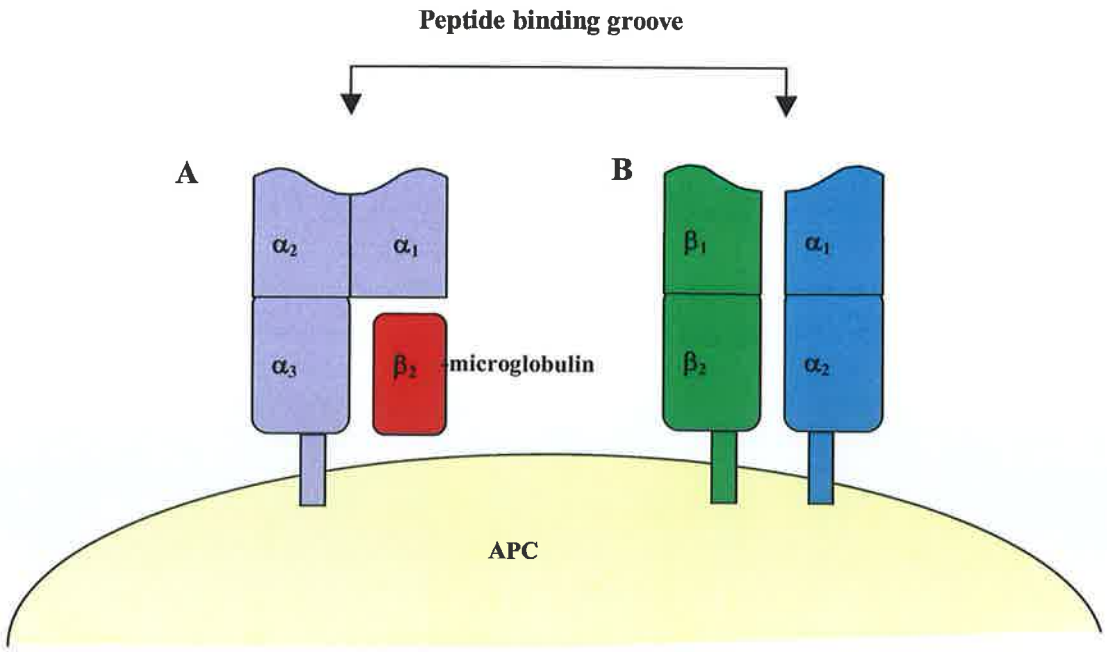

Figure 1.9 Structure of MHC class I and class II molecules. A) Represents MHC class I molecule, which contains an α chain which is non covalently linked to β_2-microglobulin and B) represents the MHC class II molecule, consisting of a non covalently linked α and β chain.

1.2.2.4 Antigen presentation and T cell activation

APCs, such as immature dendritic cells, circulate between the bloodstream and lymphoid tissues until they recognise a particular pathogen or virus, capture and process it into antigenic peptides complexed with MHC molecules (Banchereau and Steinman 1998). Various 'danger signals', recognised by TLRs and other receptors, activates the APC, resulting in phenotypic changes to its cell surface, such as, increased expression of MHC class I and II molecules and upregulation of costimulatory molecules, such as CD80, CD86 and CD40 (Reis e Sousa 2004). This activated APC then migrates to secondary lymphoid organs, such as the spleen and lymph nodes, where it can present these antigenic fragments to naïve T cells. If the naïve T cell recognises this particular antigen and receives the appropriate costimulatory signals from the APC, such as those generated from the binding of CD80 and CD86 molecules on the APC, to CD28 molecules on the T cell, it becomes activated, thereby initiating an immune response. Also, T cells express coreceptors CD4 and CD8 on their surface, which bind to invariant sites on MHC molecules,

increasing cell-cell adhesion and strengthening signal transduction. Activated T cells secrete IL-2, which promotes T cell growth and proliferation in an autocrine manner, thereby sustaining the T cell response (Janeway *et al* 2005). However, if the engagement of the TCR with its peptide:MHC complex (signal 1) occurs in the absence of costimulation (signal 2), this T cell cannot respond and proliferate to its cognate antigen, resulting in T cell anergy. This enables self antigens expressed by tissue cells to induce peripheral T cell tolerance, as only activated APCs express the stimulatory ligands required for signal 2, thus limiting the activation of autoreactive T cells and autoimmunity (Appleman and Boussiotis 2003). After the activated T cells have elicited their response, they need to be switched off to avoid immunopathology. Thus, they upregulate inhibitory receptors, such as CTLA-4 on their cell surface, which has a higher affinity for CD80 and CD86, than the activatory molecule CD28 does, which shuts down the proliferative response (Janeway *et al* 2005).

1.2.2.5 T cell effector functions

1.2.2.5.1 CD4+ T cells

CD4+ T cells recognise peptide antigens, presented to them by MHC class II molecules. Their primary effector function, is to activate other immune cells, hence they are know as 'helper T cells'. After activation, naïve CD4+ T cells differentiate into two main effector T cell subsets, depending on the cytokine milieu present at the site of activation (O'Garra 1998). Activated APCs, such as dendritic cells, can secrete various different cytokines in response to a particular pathogen, which can influence T cell polarisation and differentiation (figure 1.10). Proinflammatory cytokines, such as IL-12, can direct the T cell to differentiate into a Th1 cell, which is capable of secreting large amounts IFNγ (Watford *et al* 2003, O'Garra 1998). IFNγ can activate other immune cells, such as NK cells and macrophages, which can kill intracellular pathogens. Similarily, IL-4 production can influence the differentiation of CD4+ T cells, into Th2 cells, which secrete various cytokines, including IL-4, IL-5 and IL-13 and are mainly involved in protection against extracellular pathogens (O'Garra 1998, Janeway *et al* 2005). Th2 cells play a critical role in humoral immunity, through B cell activation and antibody secretion. In general, the cytokines produced by Th1 and

Th2 cells antagonise the development of the opposing effector phenotype. An immature effector cell, Th0, also exits and is capable of secreting both Th1 and Th2 cytokines (O'Garra 1998). Furthermore, another CD4+ helper T cell has emerged recently, the Th17 cell. Its developmental pathway is thought to be distinct from Th1 and Th2 cells and involves transforming growth factor (TGF)-β1 and IL-6 in promoting Th17 development. IL-23 also plays an important role in clonal expansion of this population (Mangan *et al* 2006). IL-17 is produced from this subset and is involved in mediating inflammation and provides defence against extracellular bacteria (Dong 2006, Tato and O'Shea 2006, Mangan *et al* 2006)

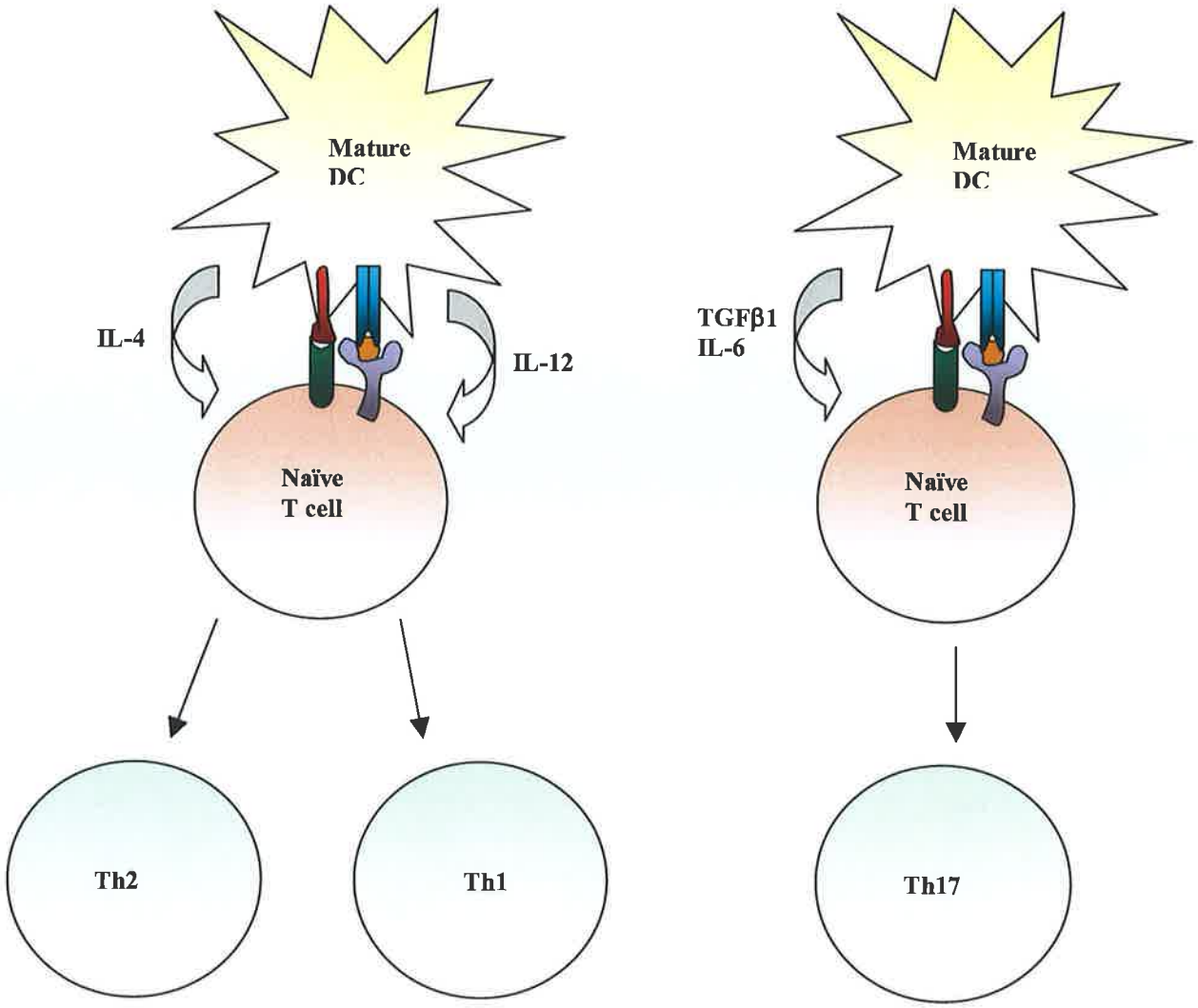

Figure 1.10 Schematic representation of the different developmental pathways of Th cells.

Virus specific CD4+ T cell responses play a major role in antiviral immunity through the secretion of cytokines and the activation of essential protective cells including B cells, NK cells, macrophage and CD8+ T cells (Collier and Oxford 2006). *In vivo* studies using mice depleted of CD4+ T cells have highlighted the importance of these cells in virus elimination and control (Harandi *et al* 2001, Hou *et al* 1992). One such study investigating herpes simplex virus (HSV) 2 infection in mice, demonstrated that CD4+ T cell deficient mice reinfected with HSV 2, succumbed to a lethal infection, implicating a crucial involvement for these IFNγ secreting CD4+ T cells in virus protection (Harandi *et al* 2001). Virus specific CD4+ T cells can also enhance

antibody titres *in vivo* (Brown *et al* 2006), strengthening the humoral immune response.

1.2.2.5.2 CD8+ T cells

CD8+ T cells recognise peptide antigens, presented by MHC class I molecules, on APCs. They can be activated directly by the APC, if the APC can provide the required costimulatory signals; however, if the APC expresses low levels of costimulatory molecules, it cannot activate naïve CD8+ T cells, until it receives help from armed CD4+ T cells, which can activate and upregulate expression of its costimulatory molecules, thereby enabling the APC to activate the CD8+ T cell. The activated CD8+ T cell or cytotoxic T lymphocyte (CTL) can secrete cytokines, such as IFNγ and directly kill target cells, such as virus infected cells or tumour cells (Collier and Oxford 2006, Janeway *et al* 2005). These CTLs store effector proteins, such as perforin and granzymes (proteases) in vesicles. CTLs induce apoptosis of the target cell, by releasing these effector proteins, perforin and granzymes (proteases), into the target cell. Perforin forms holes in the target cell membrane, enabling granzymes to enter, where they can activate caspases in the cell, leading to nuclease activation and DNA degradation (Russel and Ley 2002). Other pathways, such as the Fas pathway, can also induce apoptosis of target cells. CTLs express Fas ligand, which binds to its receptor, Fas on target cells, resulting again in caspase activation and target cell killing, from nuclease induced DNA degradation (Janeway *et al* 2005).

CTLs are the principal cells involved in controlling and clearing most viral infections (Collier and Oxford 2006). In the case of respiratory viral infections, effector CTLs can be detected in the lungs 7 days post infection and optimal levels appear by day 10 (Woodland 2003). Lack of CD8+ T cells can be associated with delayed viral clearance and exacerbated illness, which has mainly been demonstrated in studies investigating CD8+ T cell responses to virus infections in class I deficient mice (Hou *et al* 1992).

1.2.2.5.3 Regulatory T cells

Protection from pathogens is achieved by effector cells, which can secrete large amounts of proinflammatory cytokines, thereby activating other immune cells and strengthening the immune response. However, this inflammatory response can damage self tissues and so must be tightly regulated (Artavanis-Tsakonas *et al* 2003). Also, autoreactive cells that can respond and become activated by self antigens, pose a threat to that individual, if the response is not controlled. Thus, the immune system contains subsets of T cells, known as regulatory T cells, which can suppress or regulate T cell responses. These cells can be classified as, natural or inducible regulatory T cells (Schwartz 2005, Mills 2004, Janeway *et al* 2005).

Natural regulatory T (Treg) cells develop in the thymus and so may represent a distinct T cell population (Schwartz 2005). They can suppress the activation of self reactive T cells, through mechanisms involving cell-cell contact and cytokine production (Cozzo *et al* 2003). Inducible regulatory T cells are generated from naïve T cells in the periphery that have encountered antigen presented to them by semi-activated DCs. They can suppress T cell proliferation of effector cells, through the production of immunosuppressive cytokines, such as IL-10 and transforming growth factor (TGF) β. Inducible T regulatory cells include, Tr1 cells, which secrete large amounts of IL-10 and Th3 cells, which secrete TGFβ (Mills 2004).

During certain viral infections, such as HCV and HIV infections, regulatory T cells can act as double-edged swords (Weiss *et al* 2004, Boettler *et al* 2005). This phenomenon can be demonstrated by the fact that during chronic HCV infections, regulatory T cells have been shown to suppress virus specific T cell responses, thus protecting host cells; however, consequently dampening down effector responses, leading to increased viral load and persistence (Boettler *et al* 2005).

1.3 DENDRITIC CELLS

Dendritic cells (DCs) are sentinels of the immune system, linking innate and adaptive immunity. They are potent antigen presenting cells (APCs) that can regulate T cell responses. DCs are derived from hematopoietic stem cells in the bone marrow, where they function mainly in the uptake, transport and processing of pathogenic antigens, for presentation to T cells. In their 'immature' state, they circulate peripheral tissues, sampling the local microenvironment for pathogens. After they encounter a pathogen, through various recognition receptors, such as TLRs, they migrate to the lymph nodes and process these pathogenic antigens and present them on MHC molecules. This recognition process activates the DC, which also upregulates costimulatory molecules on its surface which are important for T cell activation. This mature DC is now capable of triggering an immune response, by presenting its peptide:MHC complex to a particular T cell, whose TCR is specific for the peptide:MHC complex (Banchereau and Steinman 1998, Matzinger 1994, Janeway *et al* 2001, Banchereau *et al* 2000).

1.3.1 Activation of dendritic cells

Immature DCs express various TLRs that recognise conserved molecular patterns on pathogens or PAMPs (figure 1.11) (Reisa e Sousa 2004). They can also recognise pathogens by intracellular receptors, such as the dsRNA binding receptor, protein kinase R (PKR), which recognises viral dsRNA in the host cells cytoplasm (Diebold *et al* 2003). This recognition leads to the activation of signal transduction pathways, resulting in the upregulation of MHC and costimulatory molecules and the secretion of cytokines, such as IL-12, IL-1, IL-15, type I IFNs, IL-10, IL-6 and TNFα and various chemokines, such as MIP3β, from the DC (Banchereau and Steinman 1998, Iwasaki and Medzhitov 2004, Cella *et al* 1999, Morelli *et al* 2001, McGurik *et al* 2002, Ngo *et al* 1998). These mature DCs are morphologically and phenotypically distinct from immature DCs, exhibiting a veiled-like appearance, when viewed microscopically and usually express high levels of CD40, CD86 and CD80 costimulatory molecules, in addition to specific DC maturation markers, such as DC-SIGN, CD83 and DC-LAMP (Van Kooyk and Geijtenbeek 2003, Janeway *et al* 2001,

Banchereau and Steinman 1998). This activation also upregulates chemokine receptors, such as CCR7 on the surface of DCs, enabling them to migrate to lymph nodes (Forster *et al* 1999). Other innate cells, such as activated NK cells, NKT cells (recognise glycolipids) and γδT cells (recognise microbial and tumour antigens) can activate DCs, through cytokine production and cell contact dependent mechanisms (figure 1.11) (Munz *et al* 2005, Degli-Esposti and Smyth 2005). These mature DCs can then activate naïve T cells, through antigen-TCR ligation, costimulation and cytokine secretion, enabling them to differentiate into effector T cells, such as Th1, Th2 and CTLs (Janeway *et al* 2005). They can also activate other immune cells such as NK cells and γδT cells, through cytokine secretion and direct cell contact (Degli-Esposti and Smyth 2005, Munz *et al* 2005).

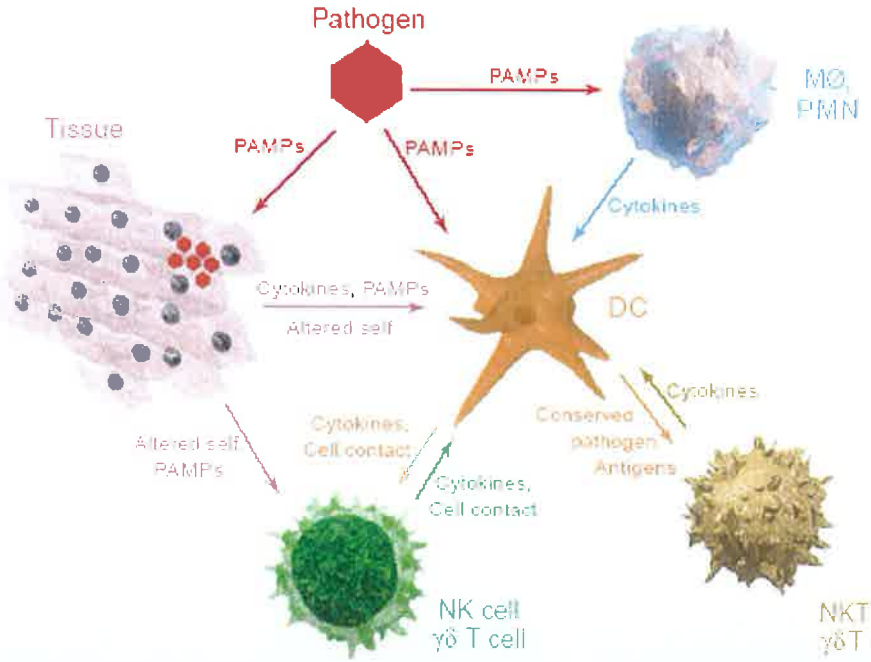

Figure 1.11 Signals involved in innate dendritic cell activation. DCs can sense potential pathogens or PAMPs through TLRs or endogenous signals from infected 'self' tissue. These signals are detected directly or indirectly (cytokines) by the DC, resulting in its activation. Other innate cells, such as NK cells, NKT cells, γδT cells, macrophage (MØ) and polymorphonucleocytes (PMN) can also activate DCs.
(Taken from Reis e Sousa 2004)

1.3.2 Dendritic cell subsets

In mice, there are at least two distinct pathways for DC generation, myeloid and lymphoid. Both mature myeloid and lymphoid DCs express high levels of CD11c, MHC class II and costimulatory markers CD40, CD80 and CD86. Myeloid precursor cells appear to give rise to at least five DC subtypes in lymphoid tissue of uninfected mice. They can be distinguished from each other based on their surface marker expression, mainly by CD4 and CD8 (an $\alpha\alpha$ homodimer on DCs) expression on their cell surface. $CD4^-CD8^+CD11b^+$, $CD4^+CD8^-CD11b^+$ and $CD4^-CD8^-CD11b^+$ DCs can be found in the spleen and lymph nodes. Lymph nodes also contain $CD4^-CD8^-CD11b^+$ DCs, which express CD205 (specific DC marker) and these DCs are thought to be the mature form of tissue interstitial DCs. Also, skin draining lymph node DCs express the same markers as the interstitial DCs, but also express langerin and so are believed to be the mature form of epidermal Langerhans cells. $CD4^-CD8^+CD11b^-CD205^+$ DC population are located in the thymus, however, a small percentage of these DCs can be found in the spleen and lymph nodes. Lastly, plasmacytoid DCs (pDCs), which are thought to be lymphoid derived, express $CD11c^{lo}B220^+$ (CD45) and alternative levels of CD4 and CD8 in their immature state. In general, there exists a large degree of functional plasticity between myeloid and lymphoid derived DCs, as both precursor populations can differentiate into myeloid DCs (mDCs) and pDCs (Shortman and Liu 2002, Banchereau *et al* 2000, Traver *et al* 2000).

In humans, blood is a major source of DCs and contains two main subsets, myeloid derived DCs (mDCs) and lymphoid derived plasmacytoid DCs (pDCs), which are $CD11c^+$ and $CD11c^-$, respectively. Very few lymphoid DCs have been isolated from humans and those DCs that have been isolated show varying expression of CD4, CD11b and CD11c markers. Most human thymic DCs resemble mouse $CD8^+$ thymic DCs and express $CD11c^+CD11b^-CD45RO^{lo}$ phenotype, but appear to lack many myeloid markers. In addition to these primary DC populations, monocytes (CD14+) and CD34+ hematopoietic cells are precursor cells that can differentiate into immature DCs *in vitro*, with various cytokines, including granulocyte-macrophage colony-stimulating factor (GM-CSF), IL-4 and type I IFNs. As these precursor cells

are relatively easy to obtain in high numbers, compared to primary DC subsets, such as immature blood DCs, these cytokine generated DCs are frequently used in *in vitro* assays to assess DC function (Ito *et al* 2005, Shortman and Liu 2002, Banchereau *et al* 2000).

1.3.2.1 Myeloid dendritic cells

Human mDCs express myeloid lineage surface markers such as CD11c, CD11b and CD33. They not only differ phenotypically from pDCs but also functionally. They express different TLRs, enabling them to recognise and respond to different pathogens compared to pDCs. Most mDCs express a variety of receptors, including TLR 1, 2, 3, 4, 5 and 8, which are mainly involved in the recognition of bacterial components and viral products (Kadowaki *et al* 2001, Iwasaki and Medzhitov 2004). They are potent APCs with strong endocytic abilities and are very efficient at processing and presenting antigens to T cells. Once activated, they mainly drive the differentiation of naïve T cells towards Th1 cells, through the production of proinflammatory cytokines, such as IL-12. However, certain pathogens, such as extracellular parasites, induce mDCs to secrete Th2 cytokines that drive Th2 cell development (DeJong *et al* 2002, Ito *et al* 2005, O'Garra 1998).

1.3.2.2 Plasmacytoid dendritic cells

Human plasmacytoid DCs are specialised cells capable of producing large amounts of type I IFNs in response to viruses and so are often referred to as 'interferon producing cells' (IPCs). They express high levels of IL-3 receptor α chain (CD123) and lack myeloid markers, such as CD11c and CD11b and so are characterized as $CD4^+CD45RA^+CD123^+ILT3^+ILT1^-$ cells. They also express additional distinguishing markers such as blood dendritic cell antigen (BDCA)-2 and BDCA-4, which are unique to human pDCs (Barchet *et al* 2005, Colonna *et al* 2004, Lui 2005, McKenna *et al* 2005)). The developmental pathway for pDCs is still unclear, but Flt-3 ligand (Flt-3L) is thought to play a role in the generation of pDCs from hematopoietic stem cells in both humans and mice and *in vitro* these cells can survive and differentiate

into mature pDCs, by addition of IL-3 and CD40L, respectively (Blom *et al* 2000, Gillet *et al* 2002, Grouard *et al* 1997). They express TLR7, TLR8 and TLR9, equipping pDCs with the sensors necessary to detect viral pathogens (Lui 2005, Kadowaki *et al* 2001). Once activated, they secrete large amounts of type I IFNs, necessary for antiviral immunity and activation of other APCs and NK cells (Collier and Oxford 2006, Guidotti and Chisari 2000, Wallace and Smyth 2005). Freshly isolated pDCs are not as potent APCs as mDCs, as they have poor endocytic abilities and so are weak inducers of T cell proliferation (Grouard *et al* 1997). Thus, it is not clear whether they can activate naïve T cells directly. However, they can induce expansion of memory T cells (Krug *et al* 2003). Also, activated pDCs can induce the proliferation of antigen specific T cells, such as influenza specific CD4+T cells *in vitro* and direct Th1 polarisation of these cells (Cella *et al* 2000).

Lastly, a new mouse DC subset has emerged recently, known as the interferon-producing killer dendritic cell (IKDC). This DC subset is distinct from mDCs or pDCs as it also expresses NK cell activatory markers, such as NKG2D, in addition to DC markers. Once activated through various TLRs, such as TLR9, they can kill target cells directly using activatory receptors, much in the same was as NK cells can induce cytotoxicity of target cells. These cells can also secrete type I IFNs, IFNγ and IL-12 upon stimulation. After inducing cytotoxicity, these cells were found to lose expression of NK cell activatory markers and to gain expression of MHC class II and costimulatory molecules, associated with antigen presentation. Thus, these unique IKDCs are capable of directly killing target cells and then differentiating into highly potent APCs that can activate T cells (Chan *et al* 2006).

1.3.3 Dendritic cells and T cell tolerance

In addition to their potent ability to activate T cells, DCs also perform immunoregulatory functions, through the induction of T cell tolerance. In the thymus, DCs present self antigens to immature T cells, where they can either be deleted (negative selection) or selected (positive selection) to survive and develop into mature

T cells, depending on their binding affinity for the self antigen. This helps to prevent self reactive T cells from entering the circulatory system, thereby limiting autoimmunity. Also, immature DCs can perform a similar function in peripheral tissues. Immature DCs express low levels of MHC class II and costimulatory molecules and can capture and present self antigens derived from tissues or apoptotic cells, in the periphery. This can induce peripheral tolerance, possibly resulting from T cell anergy (Banchereau and Steinman 1998, Janeway *et al* 2001, Lutz and Schuler 2002).

Dendritic cells can also regulate immune responses, through the induction of regulatory T cells. DC subsets that are only partially activated, expressing high levels of MHC class II molecules and some costimulatory molecules, but secreting little or no proinflammatory cytokines, exhibit a 'semi' mature phenotype. This semi mature DC phenotype can be induced by certain pathogens, such as components of the bacteria *Bordetella pertussis*, which stimulate these DCs to secrete IL-10 and promote the induction of Tr1 cells that can suppress T cell responses (Lutz and Schuler 2002, Mills 2004, McGuirk *et al* 2002). Thus, semi mature DCs can induce T cell tolerance through the generation of regulatory T cells.

1.4 IMMUNITY TO RESPIRATORY VIRUSES: HUMAN PARAINFLUENZA VIRUSES AND INFLUENZA VIRUS

1.4.1 Immunity to HPIV

The mechanisms of viral clearance and immune responses to HPIV are unclear. However, antibodies against HPIV are produced, mainly in response to the two major viral envelope proteins, HN and F. The majority of serum antibodies produced against these glycoproteins, are IgG antibodies and IgA antibodies are found in the mucosa. These antibodies protect against upper and lower respiratory tract infections (Henrickson 2003, Chanock 2001, Julkunen *et al* 1984). Also, cytotoxic T cells, that can kill virus infected cells, appear to be important in the clearance of virus from the lower respiratory tract, especially during HPIV3 infections (Henderson 1981). This cell mediated immunity is also important for recovery from viral infection, as HPIV3 infected infants, with a severe T cell deficiency, can lead to a fatal case of pneumonia (Chanock 2001). Therefore, this lack of cellular immunity appears to exacerbate the disease, emphasising the important role of T cells in the immune response to viral infections. However, although adequate protection appears to be mounted against HPIV, no long lasting immunity to these viruses ever develops (Henrickson 2003). Thus, reinfection with HPIV can occur throughout life, suggesting a lack or deficiency in immunological memory.

1.4.2 Modulation of host immune responses by HPIV

HPIV can modulate certain aspects of the immune system, thereby enhancing its own survival. HPIV3 can infect dendritic cells, leading to limited T cell proliferation (Plotnicky-Gilquin *et al* 2001), which is important for viral clearance and inducing memory T cells. Moreover, this virus has also been shown to induce IL-10 secretion from virus infected peripheral blood mononuclear cells, which is a potent immunoregulatory cytokine that can inhibit T cell proliferation (Sieg *et al* 1996).

Also, HPIV can interfere with signalling components of the interferon pathway (Young *et al* 2000), which may affect interferon production and antiviral immunity. Thus, HPIV modulation of host immune responses, may account for the frequent infection rate and lack of lifelong immunity, associated with HPIV.

1.4.3 Prevention and control of HPIV infections

As of yet, there is no licensed HPIV vaccine. However, the live attenuated HPIV3 vaccine is showing considerable promise, as it can induce good humoral immune responses in seronegative children (Belshe *et al* 2004). Also, no antiviral drugs have been approved yet to treat HPIV infections. However, ribavirin, which is a drug that can inhibit viral polymerase acitivity, and the neuraminidase inhibitor, zanamivir, exhibited *in vitro* antiviral activity against HPIV (Abed and Boivin 2006, Henrickson 2003). Thus, progress in this area is evident and will hopefully provide new therapies to treat HPIV infections in future years.

1.4.4 Immunity to influenza virus

Influenza virus can induce robust immune responses. It stimulates the production of antibodies to specific HA and NA antigens of the virus, which is the main method of ensuing protection to the host. These antibodies can neutralise virus growth and include principally, mucosal IgA and serum IgG antibodies. CD4+ T cells also help to promote high quality antibody responses, through their activation of B cells and regulation of antibody class switching, through cytokine secretions. Cytotoxic T lymphocytes can recognise influenza viral peptides, such as those generated from HA, NP, M and PB2 viral antigens, presented to them by MHC class I molecules and kill infected cells directly. These cells help to eliminate virus infected cells from the lungs. Also, epithelial cells and mononuclear cells can secrete various cytokines, such as interferon α, which can activate natural killer cells, enabling them to kill virus infected cells (Doherty *et al* 2006, Wright and Webster 2001, Hilleman 2002). These effector mechanisms help to eradicate the virus and protect the host cell. Also, re-exposure of the host to the same virus strain induces robust memory responses. Thus,

influenza can instill lifelong immunity to the host, provided that the virus does not mutate to form a new viral strain, which is not recognised by the hosts immune system (Wright and Webster 2001).

1.4.5 Modulation of host immune responses by influenza virus

Influenza A virus can mutate, producing new viral strains, so as to avoid detection by the immune system. This attribute is achieved by the viral HA and NA proteins, through two types of antigenic variation, antigenic drift and antigen shift. Antigenic drift, results in minor changes to the virus, occuring from a series of point mutations to the antigenic HA and NA proteins, which can generate new amino acids within these antigenic molecules, rendering circulatory antibodies that had been previously produced by the host cell in response to influenza, ineffective against this new viral strain (Wright and Webster 2001). Antigenic shift occurs when novel subtypes of influenza virus that normally only infect birds or pigs, are transmitted to humans. This reassortment leads to the production of a new influenza virus in the human population, containing a novel HA or HA and NA, derived from a mixture of RNA segments from both parental strains. These new viruses can infect and be transmitted rapidly, through this immunologically susceptible, human population and are responsible for pandemics worldwide (Webby and Webster 2001, Cox and Subbarao 1999, Wright and Webster 2001). Thus, both types of antigenic variation enable the virus to survive, by evading immune detection.

Influenza viruses can also modulate certain aspects of the immune response. The viral NS1 protein of influenza performs a variety of functions to suppress the immune response, such as inhibition of type 1 interferons (interferon α and β) secretion from dendritic cells, which are responsible for initiating antiviral immunity (Fernandez-Sesma *et al* 2006). Also, the NS1 protein can interfere with the antiviral immune response induced by the interferons, as it can bind or sequester double-stranded RNA, produced during viral replication, from the hosts double-stranded RNA cytoplasmic receptor, protein kinase (PKR), which inhibits viral replication (Hengel *et al* 2005, Bergmann *et al* 2000, Garcia-Sastre 2002). Moreover, activation of PKR can also

induce other signal transduction pathways, such as the nuclear factor κB (NF-κB), which is important for the transcription of many cytokines, including interferons (William 1999, Akira and Takeda 2004). This NS1 protein can also suppress dendritic cell maturation, which ultimately results in an attenuated adaptive immune response, through suboptimal stimulation of T cells by the dendritic cells (Fernandez- Sesma *et al* 2006).

1.4.6 Prevention and control of influenza virus

As with HPIV infections, vaccines are the most effective treatment for influenza virus. There are currently two main classes of licensed vaccines for influenza virus. The first is the inactivated trivalent vaccine, which contains one H1N1 strain, one H3N2 strain and one influenza B virus strain. Due to the unpredictable drift and shift in influenza viruses HA and NA antigens, these trivalent vaccines are designed yearly by members of the world health organisation (WHO) surveillance network, to try and predict the drift strain that may occur during the winter season. This vaccine is safe and immunogenic, inducing 60-90% protective immunity to children and adults; however, it appears to be less effective in elderly individuals (Cox and Subbarao 1999). Also, as the virus for these vaccines are grown in eggs and then purified, this process is quite long and laborious, delaying vaccine production. The second major class of vaccine, consists of live attenuated vaccines, which are produced from virus passages at low temperatures, producing a live attenuated or cold adapted vaccine. These vaccines induce protective immune responses in infants and children and are able to stimulate CD8+ T cell memory (Doherty *et al* 2006, Palese 2006, Arvin and Greenberg 2006, Hilleman 2002). Also, antivirals such as amantadines, which inhibit viral replication of influenza by interfering with the M2 protein (involved in viral uncoating) and neuraminidase inhibitors (zanamivir and oseltamir), which prevent virus release from the cell, can provide effective treatment for influenza virus infection (Abed and Boivin 2006).

However, despite the efficacy of both vaccines and antiviral drugs in preventing and controlling influenza virus infections, there is still a need to develop new therapies, as

one major drawback to these vaccines, is their specificity towards a particular strain of virus. Thus, these vaccines would have little or no effect on new viruses, generated from antigenic drift or shift. Therefore, researchers are now trying to develop a vaccine that would target a 'universal' or 'conserved' influenza antigen that is essential for virus function. One such antigen is the viral M2 protein, which forms an ion channel on influenza viruses (Palese 2006, Doherty *et al* 2006, Hilleman 2002). This protein is highly conserved antigenically and can produce protective antibodies as demonstrated by Friers group, which have developed a vaccine, consisting of the ectodomain of M2 fused to the hepatitis B core protein, which is capable of reducing influenza associated death in mice (Neirynck *et al* 1999). Thus, although new developments in influenza vaccines have been made and researchers are now trying to develop a 'universal' influenza vaccine, it is hard to predict whether these therapeutic advances will prevent a major pandemic outbreak, but perhaps they would delay the course of the infection, providing researchers and manufacturers with the time they need, to develop a new vaccine against the pandemic virus strain.

1.4.7 Future Perspectives

However, although advances have been made in prophylaxis of respiratory virus infections, there are still many drawbacks to vaccination. Some vaccines provide only limited protection requiring multiple doses while others have safety concerns (usually involving live attenuated vaccines). In addition, they are generally costly and labour intensive, from a manufacturing point of view. Therefore by researching the intricacies of virus interactions with the host immune system, a broader knowledge of virus/host responses can be compiled and this information can then be used to develop more efficient vaccines or therapies to treat virus infections.

AIMS OF THIS THESIS

Respiratory viruses represent a major threat to human life and have done so for centuries. These viruses can infect individuals of all ages but have profound effects on immunocompromised individuals, neonates, infants and the elderly; attacking those whose immune systems have been weakened through illness or old age, in addition to, naïve or developing immune systems, such as those of neonates and infants. Annually, in the US, parainfluenza viruses alone, account for approximately 33% of lower respiratory tract infections in children younger than five years (Denny and Clyde 1986). Of the human parainfluenza viruses (HPIVs), HPIV3 is the most common virus to infect young infants, those younger than six months and 40% of HPIV3 infections occur within the first year of life (Henrickson 2003). As reinfection with HPIVs are quite common and can occur throughout life, this would suggest that immunity to HPIV is incomplete, resulting in this apparent lack of lifelong immunity. Also, at present there is no licensed vaccine for HPIV, as there still exists many ambiguities surrounding immunity to HPIV. Thus, the main purpose of this thesis is to investigate the immune responses to HPIV3 in particular, focusing on the cell mediated immune responses, which are ultimately responsible for generating memory T cells. As the well documented respiratory virus, influenza A virus, induces robust immune responses and can generate a highly efficient memory response, we performed a comparative study of the immune responses of HPIV3 to influenza virus, to help us elucidate the problems associated with HPIV3 infections.

To approach this study, firstly we investigated innate immune responses to HPIV3 and influenza virus infections, focusing on the dendritic cell (DC) response. DCs are critical to the outcome of many viral infections and play a pivitol role in linking innate and adaptive immunity (Reisa e Sousa 2004a). Also, although animal models have been used extensively to study virus infections, many discrepancies can appear from these results when compared to the human *in vivo* infection. These discrepancies are usually a consequence of the differences that exist between syngenic animal strains, which are genetically identical and humans, which are a genetically diverse species. Thus, murine models of infection, while useful for preliminary data, do not always reflect the exact outcome of infection in humans. The ferret and hamster

models more closely resemble human HPIV3 infection, but studies in these animals are hindered by the lack of immunological reagents and inbred strains. In order to reduce the number of animals used in this study and to provide data concerning the relevance of the observed immunomodulatory properties of HPIV3 in humans, we have proposed to use a human ex vivo immune model instead. Therefore, our first goal was to develop a human *ex vivo* model that would generate DCs, which were similar to naturally occurring virally infected DCs *in vivo*, thus representing a more relevant model for studying virus infections. This model enabled us to comprehensively characterise the phenotype and investigate the functionality of these virally infected DCs, in terms of cytokine production, costimulatory capabilities and induction of T cell proliferation and polarisation. This study enabled us to generate a thorough and clearer picture of both innate and adaptive immune responses to HPIV3 and influenza virus infections.

Lastly, we used this human *ex vivo* model to investigate the immune responses to a novel sendai virus vector RNA vaccine, against HPIV3 and RSV. This model highlighted attributes of both the HPIV3 genome and vaccine construct that exhibited negative and positive immune responses, thus enabling improvements to be made to the vaccine design. Also, murine challenges were performed with the developing vaccine constructs, in addition to the final vaccine, to evaluate their immunogenicity at the humoral and cellular level *in vivo*.

Thus, by understanding the immune responses to HPIV3, this will enable the development of more efficient vaccines and therapeutic agents.

SPECIFIC AIMS:

- To develop a human *ex vivo* model of respiratory infection.
- To use this model to establish the underlying immune mechanism leading to persistence of HPIV3 and the failure to induce immunological memory.
- To compare these immune responses to those generated with influenza A virus, which induces robust immunological memory to the same strain.
- Lastly, to use this model to examine the immune responses to a novel HPIV3 vaccine, in order to see if this vaccine can appropriately prime immune

responses to HPIV3 and thus, enable one to speculate on future predictions for this vaccine in the possible induction of immunological memory.

DEVELOPMENT OF A HUMAN *EX VIVO* MODEL OF RESPIRATORY VIRUS INFECTION

2.1 INTRODUCTION

Circulating monocytes play crucial roles in the maintenance of immune homeostatsis. These precursor cells continuously exit the bloodstream and enter body tissues, where they can give rise to tissue resident macrophages, as well as specialized dendritic cells (DCs) (Gordon and Taylor 2005, Randolph *et al* 1999). It has been well established that dendritic cells are sentinels of the immune response, linking innate and adaptive immunity (Reis e Sousa 2004, Banchereau and Steinman 1998, Reis e Sousa 2004b). In a respiratory viral infection, virus replication occurs in the epithelial layer of the respiratory tract (Brown *et al* 2004, Doherty *et al* 2006, Moscona 2005), which can influence both resident cells, such as immature dendritic cells (van Rijt *et al* 2005) and migratory cells; ultimately resulting in maturation and migration of dendritic cells to secondary lymphoid organs, where they can activate naïve T cells (Banchereau and Steinman 1998, Reis e Sousa 2004, Reis e Sousa 2004b), thereby initiating an immune response. Several studies have highlighted the importance of the microenvironment and in particular, the cytokine milieu generated at the site of an infection, at influencing DC generation and differentiation (Sato and Iwasaki 2004, Svensson *et al* 2004, Vieira *et al* 2000, Qu *et al* 2003). Influenza infected monocytes that were cultured with endothelial cells, have been shown to be capable of differentiating into mature DCs, endowed with the functional capacity to stimulate proliferation of Influenza A virus specific CD4+ and CD8+ T cells (Qu *et al* 2003). Thus, environmental factors may play a critical role in DC development, ultimately affecting the outcome of an infection.

Conventional DCs, representing the monocyte derived DC (IL-4 DC) which are generated in the presence of granulocyte/macrophage colony stimulating factor (GM-CSF) and interleukin 4 (IL-4), have played centre stage for many years in standard *in vitro* assays (Cella *et al* 1999, Senechal *et al* 2004, Jinushi *et al* 2003, Plotnicky-Gilquin *et al* 2001), highlighting their importance in immunology. As they are relatively easy to grow and culture in high numbers compared to freshly isolated

blood DCs, this makes them an attractive alternative to use when studying DC immune responses (Shorman and Lui 2002, Sallusto and Lanzavecchia 1994). They have been useful in unravelling certain characteristics of viruses, such as those demonstrated by Vidalain *et al* 2000. In this report they demonstrated that the TNF-related apoptosis induced ligand (TRAIL) was upregulated on IL-4 DCs following measles virus infection. TRAIL can induce T cell apoptosis resulting in immune suppression (Vidalain *et al* 2000). Other studies using IL-4 DCs have demonstrated that certain viruses, such as the human cytomegalovirus (HCMV) can induce immunosuppression through functional impairment of DCs (Moutaftsi *et al* 2002). However, although these conventional DCs mimic immature DCs found in peripheral tissue (Sallusto and Lanzavecchia 1994), their relevance *in vivo* remains unclear, especially as this DC generation pathway, involving IL-4, can hardly represent the cytokine milieu present at a site of a virus infection (Parlato *et al* 2001).

This has led investigators to explore other avenues for DC generation, resulting in the generation of the type 1 interferon DC (IFN-DC) (Mohty *et al* 2003, Parlato *et al* 2001, Santini *et al* 2003). High levels of type 1 IFN are physiologically produced *in vivo* in response to viral infections or inflammatory stimuli (Diebold *et al* 2003, Cella *et al* 2000), so they appear to be an obvious candidate in generating a more naturally occurring DC population. IFN-DCs, generated in the presence of GM-CSF and IFNα are potent APCs, which appear to be similar to the naturally occurring plasmacytoid DCs (pDCs: are potent producers of type I IFNs following virus infections)(Lui 2005), in so far as they are capable of secreting large amounts of type I IFNs in response to virus infections and they also appear to be potent stimulators of memory T cells but poor inducers of naïve T cell stimulation (Mohty *et al* 2003, Carbonneil *et al* 2004, Krug *et al* 2003, Siegal *et al* 1999). However, although IFN-DCs may be similar to pDCs, they have additional characteristics making them distinct from pDCs, such as the expression of myeloid markers and different TLRs on their surface compared to pDCs (Mohty *et al* 2003, Kadowaki *et al* 2001, Barchet *et al* 2005). Therefore, whether these particular DCs exist *in vivo* remains to be determined.

However, we feel that these artificial methods of DC generation may inappropriately skew immune responses to viral infections and questions still remain as to the

relevance of these DCs in models of *in vivo* immune responses. Also, in light of the critical role DCs play in defining immunological outcomes, not only from infection but inflammation and neoplasia, it is imperative that the most appropriate cell type be generated and examined in a given disease state. Human parainfluenza virus type 3 (HPIV3) is a common respiratory virus that infects adults, neonates and infants. It has the capacity to infect the same individual several times during their life, suggesting that it fails to induce a state of long lasting immunity (Henrickson 2003). Also, little is known about the immune response to HPIV3 infection and in particular innate immunity to this virus. Therefore we comprehensively compared the maturation and cytokine secretion profiles of directly infected monocytes, IL-4 DCs, IFN-DCs and DCs generated from infected epithelial supernatants in response to viral infections, HPIV3 and influenza, TNFα treatment or untreated controls. These virus generated DCs were then cocultured with T cells to investigate their immunostimulatory and polarising abilities. By thoroughly investigating the differences between the virally infected cell populations, we hoped to establish a more relevant model for generating DCs, which could be used in viral studies. Thus, the main aim from this study was to develop a human *ex vivo* model of virus generated DCs that would most likely resemble naturally occurring virus generated DCs *in vivo*, which could then be used to investigate immune responses to HPIV3 infection.

2.2 MATERIALS AND METHODS

Table 2.2.1 Lists the reagents used in this study

Product	Catalog #	Company
sterile 96-well plate (flat bottom)	142475	Nunc, Roskilde, Denmark
sterile 24-well plate (flat bottom)	167008	Nunc, Roskilde, Denmark
tissue culture flask 75cm^2	83.1811	Sarstedt, Wexford, Ireland
tissue culture flask 75cm^2	83.1812	Sarstedt, Wexford, Ireland
tissue culture flask 75cm^2	83.1810	Sarstedt, Wexford, Ireland
acridine orange	A6014	Sigma-Aldrich, Dublin 24, Ireland
30% BSA solution	A1662	Sigma-Aldrich, Dublin 24, Ireland
ethidium bromide	E8751	Sigma-Aldrich, Dublin 24, Ireland
FACS clean	340345	Becton Dickinson, Oxford, England
FACS rinse	340346	Becton Dickinson, Oxford, England
FACS flow	342003	Becton Dickinson, Oxford, England
FACS tubes	falcon 2052	Becton Dickinson, Oxford, England
Foetal calf serum (FCS)	S03590S1820	Biowest, France
Hanks balanced salt solution (HBSS)	24020-091	GIBCO BRL, Paisley, Scotland
HEPES buffer	15630-056	GIBCO BRL, Paisley, Scotland
L-glutamine	25030-024	GIBCO BRL, Paisley, Scotland
RPMI 1640 medium	31870-025	GIBCO BRL, Paisley, Scotland
Penicillin-streptomycin	15070-063	GIBCO BRL, Paisley, Scotland
Minimum essential medium (MEM)	21090-022	GIBCO BRL, Paisley, Scotland
gentamicin solution	15710-049	GIBCO BRL, Paisley, Scotland
lymphoprep	1114547	Nycomed Ltd., Birmingham, England
MACS separation LS columns	130-042-401	Miltenyi Biotec, Gladbach, Germany
MACS separation LD columns	130-042-901	Miltenyi Biotec, Gladbach, Germany
Human micorbeads, CD14	130-050-201	Miltenyi Biotec, Gladbach, Germany
Human micorbeads, CD3	130-050-101	Miltenyi Biotec, Gladbach, Germany
normal goat serum	S-2007	Sigma-Aldrich, Dublin 24, Ireland
sodium azide (NaN_3)	1.06688.0100	Merck, Darmstadt, Germany
potassium dihydrogen phospate (KH_2PO_4)	1.04871.1000	Merck, Darmstadt, Germany
sodium chloride (NaCl)	1.06400.5000	Merck, Darmstadt, Germany
di-sodium hydrogen orthophospate (Na_2HPO_4)	102494C	BDH, Poole, England
potassium chloride (KCl)	P00200	Scharlau Chemie S.A., Barcelona, Spain
sucrose ($C_{12}H_{22}O_{11}$)	302997J	BDH, Poole, England
Bovine serum albumin (BSA)	A4503-50g	Sigma-Aldrich, Dublin 24, Ireland
sodium dihydrogen phospate (NaH_2PO_4)	102454R	BDH, Poole, England
tetramethylbenzidine (TMB) liquid substrate	T8665-1l	Sigma-Aldrich, Dublin 24, Ireland
ethelenediaminetetraacetic acid (EDTA)	Ac0965	Scharlau Chemie S.A., Barcelona, Spain
sulfuric acid (H_2SO_4)	84721	Fluka, Germany
TRIZMA base	T6066	Sigma-Aldrich, Dublin 24, Ireland
paraformaldehyde (PFA)	P6148	Sigma-Aldrich, Dublin 24, Ireland
TWEEN20	T7949	Sigma-Aldrich, Dublin 24, Ireland

phorbal myristate acetate	P8139	Sigma-Aldrich, Dublin 24, Ireland
cystal violet	1.15940	Merck, Darmstadt, Germany
recombinant human TNFα	11133015	Immunotools, Friesoythe, Germany
purified anti-human CD3 Ab	555336	BD pharmingen, Oxford, England
recombinant human interferon alpha 2	11105-1	R&D Systems Europe Ltd., Oxon, UK
recombinant human IL-4	204-IL	R&D Systems Europe Ltd., Oxon, UK
recombinant human GM-CSF	11133125	Immunotools, Friesoythe, Germany
Human Parainfluenza virus type 3	VR-93	ATCC, Manassas, USA
^{3}H-thymidine	TRA310	(Amersham) GE Healthcare UK Ltd., Buckinghamshire, UK
Betaplate scint	1205-440	PerkinElmer, MA, USA
printed filter mat A	1450-421	Wallac, Turku, Finland
plastic cases	1450-432	PerkinElmer, MA, USA
40μm cell strainer	352340	BD Biosciences Europe, Belgium
Annexin V-FITC apoptosis detection kit I	556547	BD pharmingen, Oxford, England

Table 2.2.2 Lists equipment used in this study.

Equipment	Model	Company
Centrifuge	Eppendorf 5804	Eppendorf, Hamburg, Germany
Ultracentrifuge	L8-70M	Beckman, UK
Flow cytometer	FACSCalibur	Becton Dickinson, Oxford, UK
Haemocytometer	Improved, 2-grids	Neubaurer
Irradiator	Gamma-cell 1000 Elite	Nordion, Ottowa, Canada
Midi MACS separation unit		Miltenyi Biotec, Gladbach, Germany
Fluorescent microscope	Eclipse E200	Nikon, USA
Inverted microscope	Eclipse TS100	Nikon, USA
Plate reader	MCC/340	Titertek Multiscan
Micro 96 harvester		Skatron Instruments, Lier, Norway
Scintillation counter	Trilux microbeta counter 1450	Perkin-Elmer, Life Sciences, MA, USA

Cell culture and viral infections were carried out in accordance with the Safety and Health Policy of Dublin City University and where appropriate, with the notification of the Health and Safety Authority and Environmental Protection Agency.

2.2.1 Separation of peripheral blood mononuclear cells

Buffy coats of healthy donors were obtained from The Irish Blood Transfusion Service (St. James's Hospital, Dublin). The peripheral venous blood (approximately 50ml) was mixed with 5ml of a 5% solution of the anticoagulant ethylenediaminetetraacetic acid (EDTA) and diluted 1:1 with Hank balanced salt

solution (HBSS) containing 1% foetal calf serum (FCS; enodtoxin free) (heat inactivated for 30mins at 56°C) and 10mM HEPES buffer. The diluted blood was layered onto 7ml of Lymphoprep™ solution in a 30ml sterilin tube and centrifuged at 400g for 25mins with the accelerator and brake switched off, to prevent the layers from mixing. The Lymphoprep™ solution with a density of 1.077g/ml provides a gradient that enables the blood components to be separated according to their density. Thus, during centrifugation, the higher density erythrocytes and polymorphonuclear cells (PMNs) or granulocytes sediment to the bottom of the tube, while the lower density mononuclear cells form a distinct cloudy layer at the interface of the sample (figure 2.2.1). This mononuclear layer of cells or buffy coat layer is then removed using a Pasteur pipette and the cells are washed twice with 10ml of the supplemented HBSS solution, with centrifugation at 800g for 5mins. After the final wash, the pelleted cells were resuspended in 2ml of complete Roswell Park Memorial Institute (cRPMI)-1640 medium (RPMI 1640 supplemented with 10% FCS and 1% L-glutamine and penicillin/streptomycin solution). To remove clumps from these peripheral blood mononuclear cells (PBMCs), the cells were then filtered through 40um filters and washed through with cRPMI and the cell yield was calculated as described in section 2.2.2.

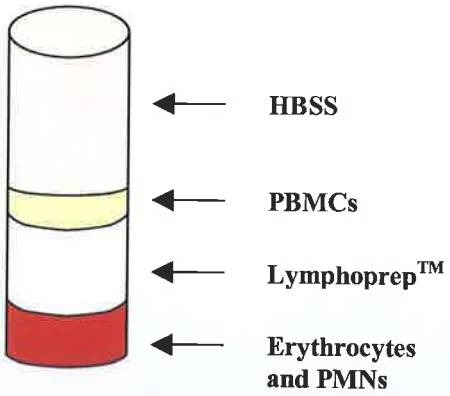

Figure 2.2.1 Separation of PBMCs by density centrifugation. Peripheral blood was layered onto Lymphoprep™ in a 30ml sterilin tube. Following centrifugation the blood components were separated into layers according to density; with the erythrocytes and PMNs sedimenting to the bottom of the tube and PBMCs gathering at the interface between the medium and Lymphoprep™.

2.2.2 Determination of cell viability and yield

Background

Ethidium bromide (EB) intercalates and stains double-stranded DNA and fluoresces orange under halogen or ultra violet (UV) light. It can only stain cells with permeable membranes, such as those in the final stages of apoptosis and so can detect dead cells. Acridine orange (AO) is a cell permeable dye that can bind to double-stranded DNA of live cell, emitting a green fluorescence under halogen or UV light. These dyes are useful for the detection of viable cells from a cell suspension. An EB/AO solution was made by adding EB stock solution (0.8ml of 4mg/ml solution) to AO stock solution (2ml of 1mg/ml solution) and then made up to 200ml with 0.85% weight/volume (w/v) sodium chloride (NaCl).

Method

The Improved Neubauer Haemacytometer slide was used to determine the number of cells in a defined volume. The microscopic slide contains a grid etched onto its surface and the volume of a solution in an area of the grid can be calculated from the area of the grid and the height between the grid and cover slip (0.1mm) (figure 2.2.2). Cells to be counted were diluted in EB/AO and pipetted onto the slide beneath a cover slip, ensuring that the solution covered the entire surface of the counting chamber or grid. The number of live (green) and dead (orange) cells was determined by counting the four corners of the grid and cell yield was calculated as follows:

(Average cell number from grid corners) X (dilution factor) X 10^4 = cell number/ml

* The number 10^4 is the volume correction factor for the slide: each square is 1 X 1mm and the depth is 0.1mm.

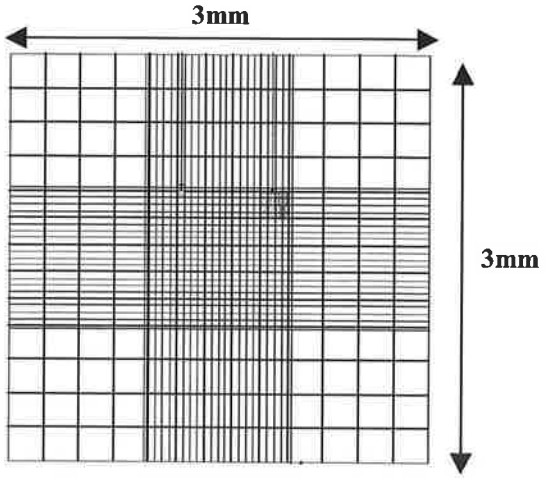

Figure 2.2.2 Diagram of the grid of the Improved Neubauer Haemocytometer.
(Taken from: http://www.ruf.rice.edu/~bioslabs/methods/microscopy/cellcounting.html)

2.2.3 Viral Stocks

HPIV3 (VR93-ATCC) with a stock concentration $TCID_{50}$/ml = 9 was provided by Marius Loetscher (Berna Biotech AG, Switzerland), who was a collaborator on our project. HPIV3 (VR93-ATCC) stocks were also prepared internally as described below. Influenza A Virus H3N2 (A/Panama/2007/99) in allantonic fluid with a $TCID_{50}$/ml = 8.8 was kindly provided by Robert Newman (NIBSC, Hertfordshire, UK).

2.2.3.1 Infection of Vero cells for HPIV3 propagation

Vero cells (African green monkey kidney cell line) were kindly provided by Marius Loetscher (Berna Biotech AG, Switzerland). The cells were grown in T175 flasks with culture medium, consisting of minimum essential medium (MEM), supplemented with 5% FCS, 0.6mg/ml L-glutamine and 50µg/ml gentamicin. Vero cells grow very quickly and needed to be split every 24-48h, when the cells are ~80-90% confluent. For subculture, the culture medium was removed and replaced with 10-15ml of 0.05% trypsin and left to incubate at 37°C for approximately 5mins. Trypsin is a proteolytic enzyme that cleaves protein bridges which attach adherent cells to the surface of tissue culture flasks. Thus, trypsin enables adherent cells to be

collected by dislodging them from the surface of flasks. After incubation with trypsin, the cells were visualised using an inverted microscope to confirm cell detachment from the flask surface. Then 10-15ml culture medium (containing FCS) were added to flasks to neutralise the toxic effects of the trypsin and the cells were spun at 1200rpm for 7min. The pellet was resuspended in 2-3ml culture medium and added to three flasks containing ~29ml.

Before Vero cell infection with HPIV3, cells were left to grow until they were 80% confluent, which took approximately 1-2 days. HPIV3, with a stock concentration tissue culture infectious dose/ml ($TCID_{50}$/ml) of $10^{9.2}$ (VR-93, ATCC), was diluted to a $TCID_{50}$/ml of 10^7 in serum-free medium (the $TCID_{50}$ of a virus is the dilution of virus that can be expected to infect 50% of culture cells and is used to measure virus concentration). The culture medium was removed from the cells and they were washed 3X with PBS. The HPIV3 containing serum-free medium (128µl virus/20ml MEM) was then added to the Vero cells (T175) and left to incubate for 4 days at 37°C.

2.2.3.2 Harvesting and purifying HPIV3

On the day of HPIV3 harvest, Vero cells were subjected to 3 freeze-thaw cycles to break up the cells (-80°C). The cell suspension, containing the virus and cell debris in medium, was transferred to 50ml tubes and centrifuged at 4°C for 45min at 3500rpm, to sediment the cell debris. The supernatant was collected and carefully overlayed on ~5ml of a 30% sucrose solution (made in 1X phosphate buffered saline (PBS) pH 7.2 [PBS- 400g NaCl, 58g Na_2HPO_4, 10g KCl, 10g KH_2PO_4 and 5l distilled water = 10X PBS solution]) in ultracentrifuge tubes (sucrose =1/5 of the total volume added to the ultracentrifuge tubes). The sucrose solution was used as a density gradient. The tubes were then ultracentrifuged (fixed angle rotor) at 5°C for 15h at 50000rpm. The delicate ultracentrifuged pellets (figure 2.2.3) with some of the overlaying cushion-sucrose solution were transferred to 50ml tubes, using transfer pipettes. Some PBS was added to the tubes to dilute the sucrose and the pelleted fragments were spun down at 4°C for 45min at 3500rpm. The supernatant was carefully removed and the

pellet was washed with PBS and centrifuged at 4°C for 10min at 3500rpm. The final pellet or purified virus was then resuspended in approximately 160µl of PBS (1/1000 of the volume subjected to the ultracentrifuge) and aliquoted and stored at –80°C.

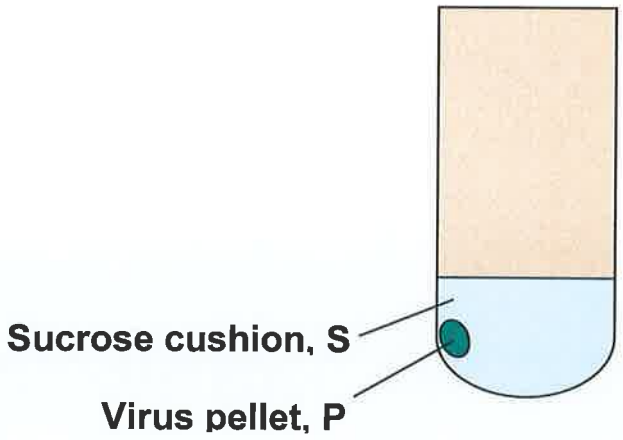

Figure 2.2.3 Schematic illustration of the virus pellet following ultracentrifuation.

2.2.3.3 Calculating the concentration of HPIV3

To calculate the concentration of HPIV3, a titration assay was carried out which determines the $TCID_{50}$/ml of the virus. Vero cells in culture medium were plated at a concentration of $1X10^4$ cells/well (100µl/well), in a flat-bottomed 96 well plate and left to incubate at 37°C for 24h. Following their 24h incubation, the Vero cells were confluent and ready for infection. For infection, virus was diluted in serum-free medium, starting at a 1:1000 dilution of the virus for the top working concentration and then diluting 1:10 down the plate (100µl virus/well of Vero cells). Table 2.2.3 shows the titration scheme for the virus on the 96 well plate.The plate was left to incubate for 5-6 days and then the titre was read. For this purpose, all medium was removed from the Vero cells and replaced with 50µl/well of 1% crystal violet staining solution. After 15mins the staining solution was removed and the cells were air-dried. Cells were then examined by light microscopy for the presence of syncytia, which are densely grouped cell nuclei and wells were marked as positive or negative for the presense of syncytia. The $TCID_{50}$/ml of the virus was calculated by the following equation:

Log $TCID_{50}$/ml = (number of positive wells, between 0 and 40) X 0.2 – log(lowest dilution, usually 10^{-3}) + 0.5

(Equation from Marius Loetscher, Berna Biotech AG, Switzerland)

Table 2.2.3 Shows the plate plan for titrating the virus.

No virus	10^{-3}	10^{-3}	10^{-3}	10^{-3}	10^{-3}
No virus	10^{-4}	10^{-4}	10^{-4}	10^{-4}	10^{-4}
No virus	10^{-5}	10^{-5}	10^{-5}	10^{-5}	10^{-5}
No virus	10^{-6}	10^{-6}	10^{-6}	10^{-6}	10^{-6}
No virus	10^{-7}	10^{-7}	10^{-7}	10^{-7}	10^{-7}
No virus	10^{-8}	10^{-8}	10^{-8}	10^{-8}	10^{-8}
No virus	10^{-9}	10^{-9}	10^{-9}	10^{-9}	10^{-9}
No virus	10^{-10}	10^{-10}	10^{-10}	10^{-10}	10^{-10}

2.2.4 Flow cytometry

Background

Flow cytometry is a process used to characterise the properties of individual cells as they pass by laser beams of light. It can provide us with information about the cells size, granularity and expression of protein markers on or in a particular cell. To analyse protein expression, cells are incubated with particular monoclonal antibodies which can bind to the protein of interest. These antibodies are usually conjugated to fluorochromes that emit light at various wavelengths after excitation in the laser beam, enabling the proteins to be detected (Janeway *et al* 2005).

After cells have been labelled with fluorochrome conjugated antibodies, the cell suspension is forced, along with sheath fluid through a nozzle, that enables the cells to be individually spaced in this stream of liquid (figure 2.2.4). As each cell passes the laser beam, which is usually an argon light with an excitation wavelength of 488nm, the cells scatter the laser light and the fluorochrome conjugated antibodies, fluoresce at different wavelengths. The scattered light is detected by photomultiplier tubes, that

can measure both the size of a cell, detected as forward scatter (FSC) and cell granularity, detected as side scatter (SSC). This enables one to distinguish between different cell subsets based on their size and granularity, such as macrophage, which are large and granular cells compared to lymphocytes, which are a much smaller and less granular cell population than macrophages.

The fluorescence emitted from the fluorochrome conjugated antibodies are also detected by photomultiplier tubes. There are four main fluorochromes used in flow cytometry: fluorescein isothiocyanate (FITC)- emits light at a maximum intensity at 530nm and is detected by the fluorescent detector FL1, phycoerythrin (Pe)- emits light at 578nm and is detected by FL2, peridin chlorophyll protein (PerCP)- emits light at 675nm and is detected by FL3 and allophycocyanin (APC)- emits light at 660nm and is detected by FL4. The information from the flow cytometer (FACS [fluorescence activated cell sorter] calibur; Becton Dickinson) is then fed to a computer where the data can be analysed (http://www.petermac.org/pdf/Intro%20to%20Flow%20Cytometry%20.pdf).

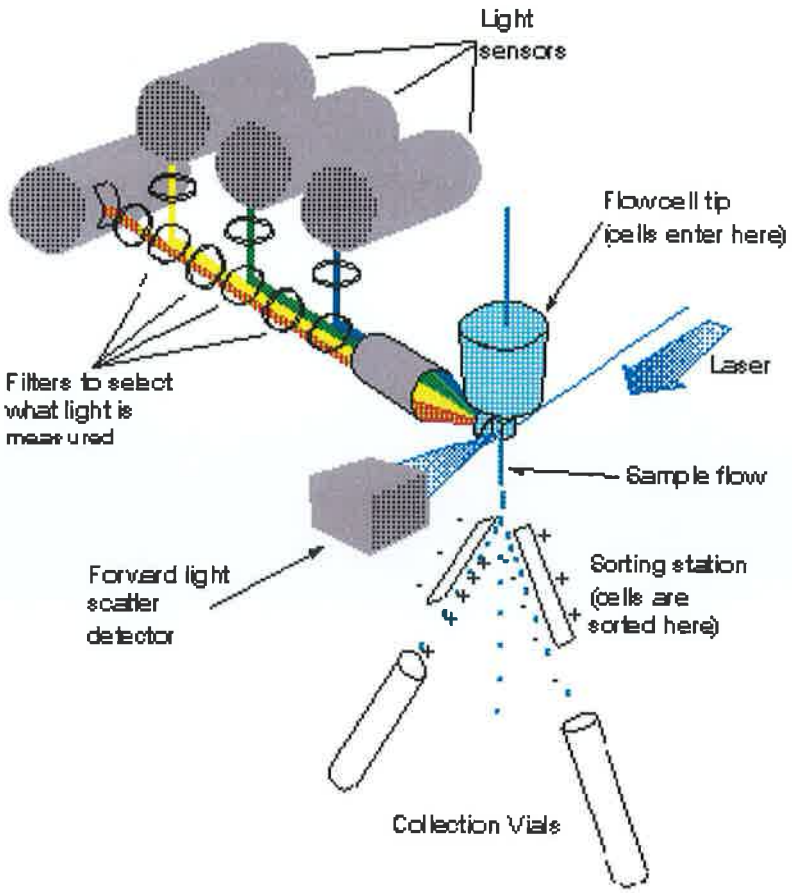

Figure 2.2.4 Simplified schematic displaying the principles of flow cytometry.
(Taken from: http://meds.queensu.ca/qcri/flow/cri-fc-getstarted.htm)

2.2.5 Cell surface staining for flow cytometry

Cells were centrifuged at 3000rpm for 10mins and resuspended in 1X PBS, containing 1% bovine serum albumin (BSA) and 0.02% sodium azide, known as PBA buffer (50µl PBA/2X10^5 cells). This is an isotonic buffer and the sodium azide helps to prevent endocytosis of the monoclonal antibodies (mAb) and the BSA prevents non-specific binding of antibodies. 5µl of fluorochrome labelled mAbs that are specific for a particular surface marker, were added to FACS tubes, along with the resuspended cells and incubated in the dark for 30min at 4°C. Numerous fluorochrome labelled antibodies can be applied to the same FACS tube, provided that they contain different fluorochromes and the flow cytometer used has the capacity to detect them. After incubation, the cells were washed with ~2ml PBA and centrifuged at 3000rpm for 10mins. The supernatants were discarded and the pellets were resuspended in 0.5ml

PBA and read on the flow cytometer FACScalibur and data was analysed using Cellquest software (Becton Dickinson, Oxford). Fluorochrome labelled isotype or control mAbs that were specifically matched to each of the fluorochrome labelled mAbs, were used as controls for non-specific staining of cells (figure 2.2.5). Table 2.2.4 summarises the mAbs used in this study for flow cytometery.

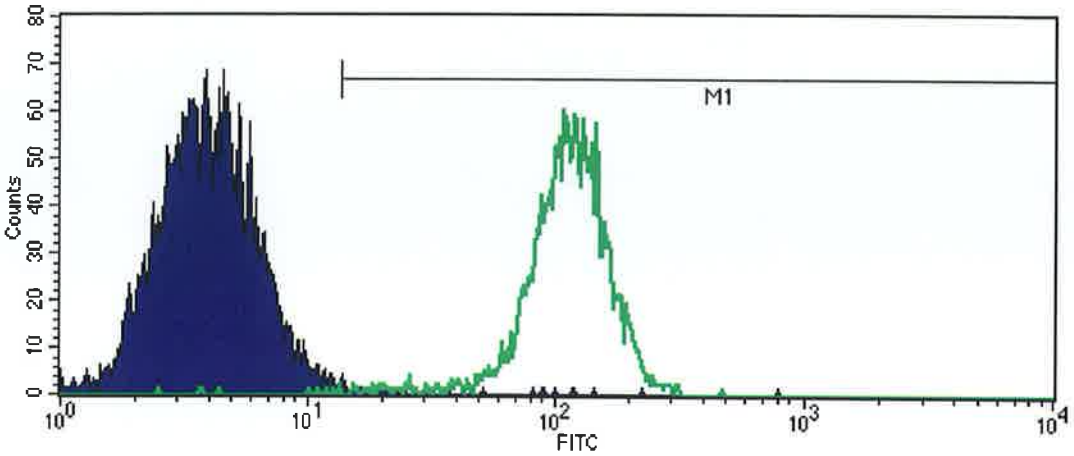

Figure 2.2.5 Histogram depicting background staining. The purple histogram represents the isotype control and the green histogram shows the number of cells and intensity of cells for this FITC conjugated Ab. M1 represents the region that is positive for the particular marker.

Table 2.2.4 Summarises the human cell surface mAbs used in this study.

Antibody	Fluorochrome	Catalog #	Company
CD14	Pe	12-0149	eBioscience
CD83	Pe	12-0839	eBioscience
CD11c	FITC	11-0116	eBioscience
CD86	Pe	12-0869	eBioscience
CD80	FITC	11-0809	eBioscience
HLA-DR	APC	17-9956	eBioscience
CD123	Pe	12-1239	eBioscience
CD3	APC	17-0038	eBioscience
IgG1	Pe	12-0839	eBioscience
IgG1	FITC	11-4719	eBioscience
IgG2b	Pe	12-4732	eBioscience
IgG1	APC	17-4719	eBioscience
IgG2b	APC	17-4732	eBioscience

2.2.6 Separation and purification of cell subsets from PBMCs

2.2.6.1 Principles of magnetic microbead cell separation

Magnetic microbead separation of cells is an efficient way of separating cell subsets of interest. The magnetic microbeads are composed of antibodies that are conjugated to biodegradable beads, which are composed of iron oxide polysaccharide. These microbeads are incubated with cells and can bind to particular cell surface proteins. The cell suspension is then passed through a column, which is held by a magnet (MidiMAC) and this enables the cells labelled with the microbeads to be retained in the column, as a result of magnetic forces. Unlabelled cells are therefore eluted from the column and can be collected as the depleted or unlabelled fraction. To remove the labelled cells from the column, the column is removed from the magnet and the cells are plunged out and collected as the enriched or labelled fraction (figure 2.2.6).

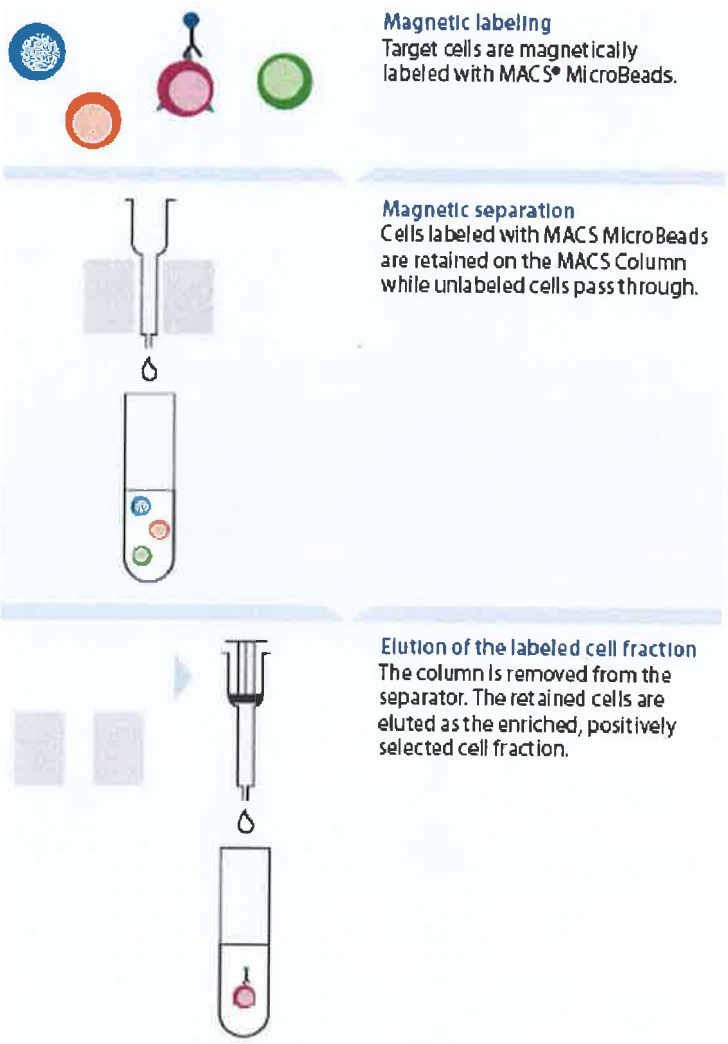

Figure 2.2.6 Summarises the principles of magnetic microbead separation of cells.
(Taken from: www.miltenyibiotec.com)

2.2.6.2 Separation of CD14+ monocytes and CD3+ T cells

Isolation of CD14+ monocyes and CD3+ T cell from human PBMCs, using anti-human microbeads, was performed in accordance to the manufacturers specifications (Miltenyi Biotec). Briefly, PBMCs were centrifuged at 300g for 10mins and resuspended in degassed MACS buffer (80µl of buffer/1X10^7 cells), consisting of sterile PBS, supplemented with 0.5% BSA and 2mM EDTA and incubated with either CD14 for CD3 microbeads (20µl of beads/1X10^7 cells), for 15mins at 4°C. Following incubation, cells were washed by adding MACS buffer and centrifuged at 300g for 10mins. The pellet was resuspended in MACS buffer (approximately 6ml/1X10^8 cells). To positively select CD14+ and CD3+ cells, LS columns were used and placed

in the magnet. The column was firstly washed with 3ml of MACS buffer and then the resuspended cells are added to the column and the column is rinsed with 9ml of buffer. The fraction collected first is the unlabelled cells or depleted fraction. After all the MACS buffer has run through the column, the positively labelled cells are flushed out of the column with a plunger (5ml).

2.2.6.3 Determining cell purity

To determine the purity of the CD14+ monocytes and CD3+ T cells, the cells were stained with their respective mAbs, Pe conjugated anti-CD14 for monocytes and APC conjugated anti-CD3 for T cells, as described in section 2.2.4, in addition to other relevant mAbs useful in determining cell purity. The cells were analysed by flow cytometry and rountinely purity was >90% for CD14+ monocytes and >95% for CD3+ T cells (refer to appendix 1A).

2.2.7 Virus infection and culture of cells

2.2.7.1 Virus infection of monocytes and dendritic cells

CD14+ monocytes which had been purified from PBMCs (described in section 2.2.6.2) were cultured in cRPMI, supplemented with 100ng/ml recombinant human (rh) GM-CSF and 50ng/ml rhIL-4 (IL-4 DC) or 500U/ml rhIFNα2b (IFN-DC), for 6 and 4 days, respectively. This culturing technique generates both immature IL-4 DCs and IFN-DCs. Two main stocks of purified HPIV3 were used in this study (section 2.2.3): 1) HPIV3 propagated and purified internally (stock concentration $TCID_{50}$/ml = 8) and 2) HPIV3 (stock concentration $TCID_{50}$/ml = 9) provided by Marius Loetscher (Berna Biotech AG, Switzerland). Influenza A Virus H3N2 (A/Panama/2007/99) in allantonic fluid with a $TCID_{50}$/ml = 8.8 was kindly provided by Robert Newman (NIBSC, Hertfordshire, UK). CD14+ monocytes, IL-4 DCs and IFN-DCs were infected with HPIV3 at a $TCID_{50}$/ml of 6 or influenza virus at a $TCID_{50}$/ml of 7 for 2h at 37°C (Plotnicky-Gilquin *et al* 2001), then subsequently washed (centrifuged at

3000rpm for 5mins) following incubation to remove excess virus. The cells were then cultured in fresh cRPMI on a 24 well plate ($1X10^6$ cells/ml) for the indicated time points. As a positive control, CD14+ monocytes, IL-4 DCs and IFN-DCs were also cultured with 25ng/ml of rhTNFα, which is a common cytokine used to induce DC maturation (Cella *et al* 1999).

2.2.7.2 Culturing of the human epithelial A549 cell line

A549 cells were kindly supplied by Shirley O' Dea (Institute of Immunology, N.U.I.M). Cells were cultured in 12ml of Dulbecco's basal medium, supplemented with 10% FCS and 1% L-glutamine at 37°C. At appropiate intervals, when the cells were confluent, they were subcultured using 5ml of 0.05% trypsin and then resuspended in 5ml of culture medium when the adherent cells became dislodged from the surface of T75 flasks. The cells were centrifuged at 1200rpm for 7mins and the pellets were resuspended in a ~3ml culture medium and added to three flasks containing ~11ml culture medium.

2.2.7.3 Virus infection of A549 cells

For infection, culture medium was removed from the cells and replaced with 6ml of medium containing either HPIV3 or influenza virus, at a $TCID_{50}$/ml of 6. The cells were left to incubate for 2h at 37°C and then the virus infected medium was removed and the cells were washed and replaced with 12ml cRPMI and incubated for 24h. Following incubation, medium was removed from the cells and centrifuged at 1200rpm for 7 mins. The supernatant (containing the virus) was aliquoted and frozen directly at –20°C or UV inactivated in a petri dish under UV light for 20min (inactivates the virus) and then subsequently, aliquoted and frozen. Some flasks were not infected with virus but were still washed and cultured with 12ml of cRPMI for 24h and supernatants were harvested and frozen for control purposes. CD14+ monocytes ($1X10^6$ cells/ml) were cultured on a 24 well plate with non-infected A549

supernatant, virus infected A549 supernatant or UV inactivated A549 supernatant at 50% volume/volume (v/v) ratio for indicated time points.

2.2.8 Determination of apoptotic cells

Background

Apoptosis (programmed cell death) of cells was determined using the Annexin V-FITC Apoptosis Detection Kit I (BD Pharmingen). Apoptosis can be characterised by certain morphological features, such as the loss of plasma membrane and the condensation of the cytoplasm and nucleus of cells. This detection kit identifies apoptotic cells by the loss of their plasma membranes. When cells are undergoing apoptosis, the membrane phospholipid phosphatidylserine (PS) is translocated from the inner to the outer surface of the cell membrane. PS externalisation occurs in the early stages of apoptosis. Once exposed on the cell surface, annexin V, which is a phospholipid-binding protein that has high affinity and specificity for PS, can bind to PS. As annexin V is conjugated to FITC, its detection can be read by flow cytometry. In this detection kit, cells are also stained with propidium iodide (PI), which is a membrane impermeant dye that can stain DNA and so is useful for identifying cells in the later stages of apoptosis. By staining cells with both annexin V FITC and PI, this allows for the detection of both early and late apoptotic cells (www.bdbiosciences.com).

Method

Cells were stained for apoptosis detection according to the manufacturers guidelines (BD Pharmingen). Briefly, cells were harvested, counted (see section 2.2.2) and then washed (3000rpm for 5mins) with ice cold PBS. Cell pellets were resuspended in 1 X binding buffer (supplied with kit) at a concentration of $1X10^5$ cells/100µl of buffer. 5µl of annexin V FITC and 5µl of PI (Pe) were added to FACS tubes along with 100µl of resuspended cells. Cells were vortexed and incubated in the dark at room

temperature (RT) for 15mins. Then a further 400µl of 1 X binding buffer was added to the FACS tubes and cells were read within the hour by flow cytometry. Unstained cells were used as controls or isotypes to set the parameters needed for FACS. For analyses, quadrants markers were set based on isotype controls and values reflect the percentage of cells in each quadrant; where the lower left (LL) or annexin V^-PI^- quadrant represents living cells, the lower right (LR) or annexin V^+PI^- quadrant represents early apoptotic cells, the upper right (UR) or annexin V^+PI^+ quadrant represents late apoptotic cells and upper left (UL) or annexin V^-PI^+ quadrant represents necrotic or dead cells (figure 2.2.7).

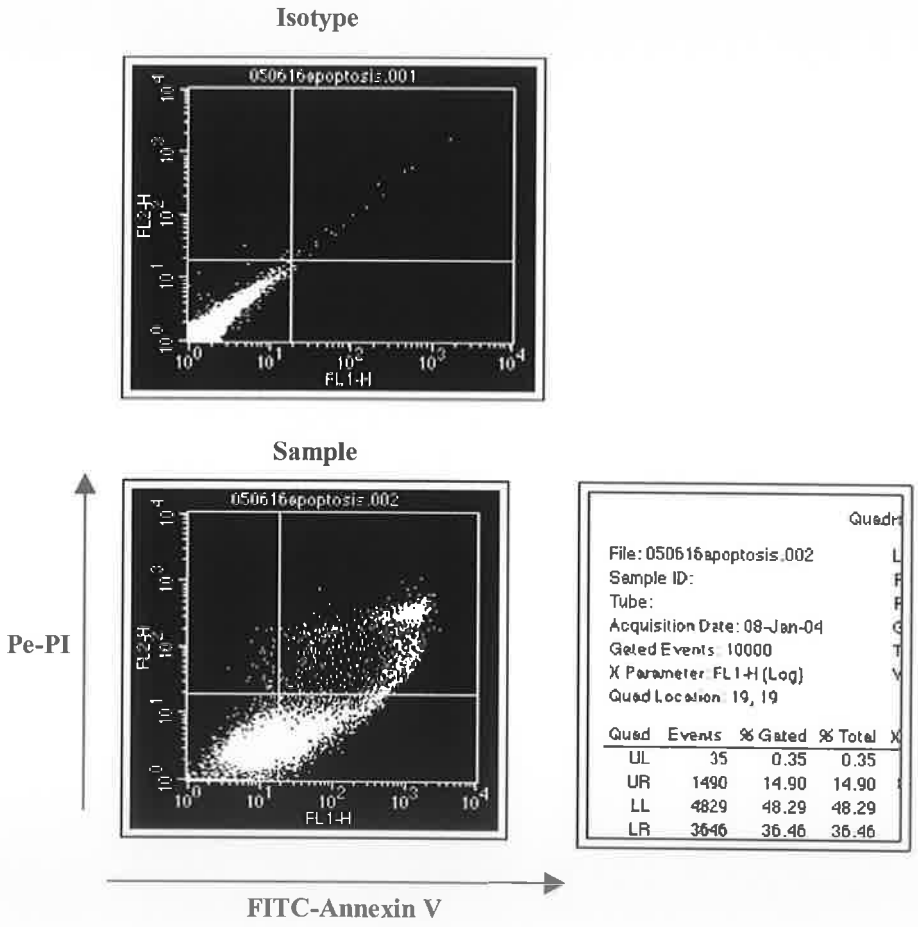

Figure 2.2.7 Dot blot representing isotype control and stained sample. The unstained cells were used as a control for background staining for FL1 and FL2 and quadrant markers were set against this isotype control. The percentage of annexin V and PI positive and negative cells in each quadrant, could then be determined from the stained sample.

2.2.9 Enzyme linked immunosorbent assay (ELISA)

2.2.9.1 Principle of the sandwich ELISA

Background

ELISAs can be used to quantify the amount of cytokine produced in solution. In a sandwich ELISA, a fixed quantity of capture antibody (mAb), specific for the cytokine being detected, is bound to a 96 well plate (the capture antibody is diluted in buffer, such as PBS and usually incubated overnight at 4°C). The plate in then washed to remove excess or unbound antibody and a blocking buffer, usually containing BSA, is added to prevent non-specific binding of subsequently added reagents. Samples of unknown antigen concentration and a series of recombinant cytokine standards of known concentration are added to the plate and incubated overnight at 4°C. The plate is washed again to remove any unbound antigen or cytokine and a biotinylated detection antibody for the cytokine is added and incubated (usually for 2h at RT). After incubation, the plate is washed and then streptavidin-horseradish –peroxidase (HRP) is added to the plate. Streptavidin binds biotin with high affinity and is conjugated to HRP, which is an enzyme that catalyses the oxidation of its substrate tetramethylbenzidine (TMB) by hydrogen peroxide, forming a blue compound. Following streptavidin-HRP incubation the plate is washed again and TMB is added, which forms a blue colour that increases in intensity in the well, if a lot of cytokine has been bound to the well. The reaction is stopped by adding sulphuric acid to the plate, which turns the solution a yellow colour and the absorbance of light at 450nm is read by a plate reader (www.abcam.com/technical). Thus, the rate of colour formation is proportional to the amount of cytokine present. Figure 2.2.8 summarises the principles of a sandwich ELISA.

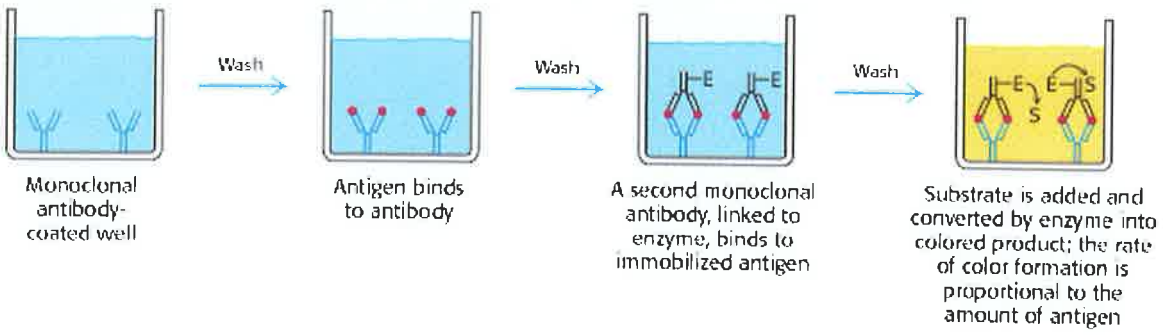

Figure 2.2.8 Schematic illustrating the principles of a sandwich ELISA
(Taken from: http://www.ncbi.nlm.nih.gov/books/bv.fcgi?rid=stryer.figgrp.515)

2.2.9.2 Calculating the results from a sandwich ELISA

Once the absorbance at 450nm has been read, the known standard concentrations are plotted against optical density (OD) or optical absorbance, producing a standard curve (figure 2.2.9). The unknown samples with absorbance readings at 450nm can then be read from the curve to give known sample concentrations.

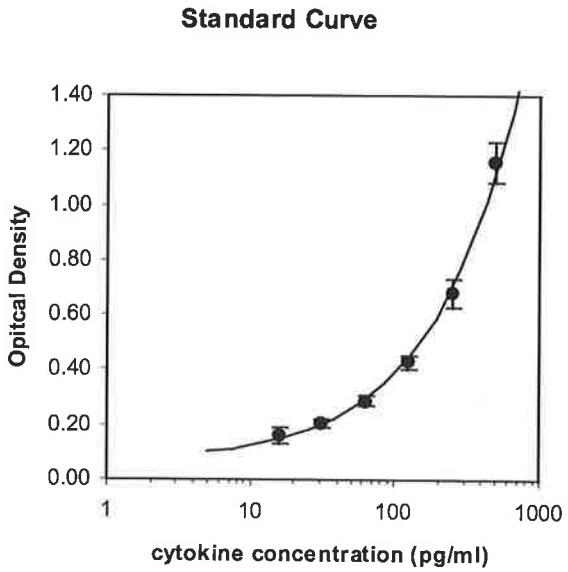

Figure 2.2.9 Typical standard curve depicting OD values ± 2 standard deviations against known cytokine concentrations.

2.2.9.3 Quantifying different cytokines by ELISA

Supernatant from samples were collected at indicated time points and cytokine production was measured by ELISA kits, according to the manufacturers instructions (R&D). Table 2.2.5 represents the different ELISA kits used in this study to detect particular cytokines. Samples and standards were plated either in duplicate or triplicate wells on the 96 well plate to ensure accurate quantitative results were obtained and statistical analyses could be performed on the samples.

Table 2.2.5 Lists the Human ELISA kits used in this study

Human ELISA kit	Catalog #	Company
IL-10 DuoSet ELISA kit	DY217	R&D Systems Europe Ltd. UK
IL-12p40 DuoSet ELISA kit	DY1240	R&D Systems Europe Ltd. UK
TNFα DuoSet ELISA kit	DY210	R&D Systems Europe Ltd. UK
IFNα ELISA kit	41100-1	R&D Systems Europe Ltd. UK
IFNγ DuoSet ELISA kit	DY285	R&D Systems Europe Ltd. UK

2.2.10 Coculture assays

Background

Mixed leukocyte/lymphocyte reaction (MLR) is a common assay used to investigate T cell responses. In this reaction T cells from one individual are usually mixed with APCs from a second individual and if these T cells recognise the other individuals MHC molecules as being foreign (allogeneic) then they will proliferate in response to them. Studies have revealed that approximately 1-10% of all T cells will respond to stimulation in this way (Janeway *et al* 2005).

Method

Control and infected CD14+ monocytes, IL-4 DCs and IFN-DCs were gamma irradiated (stops cells proliferating) with 442 rads/min for 20mins. The cells were then washed and centrifuged at 3000rpm for 5mins, resuspended in cRPMI and counted (section 2.2.2) and seeded at $2x10^4$ (50µl/well) into 96-well flat-bottomed plates. Cocultures of CD14+ monocytes and purified allogeneic CD3+ T cells (section 2.2.4.2) or mixed leukocyte reactions (MLR: CD14 depleted or CD14- population, contains high numbers of allogeneic T cells, ~ 40-50% CD3+ T cells) were performed at 1:10 ratios for all experiments. Thus, $2x10^4$ APCs were cultured with $2x10^5$ (150µl/well) T cells (purified CD3+ T cells or MLR). Allogeneic cells, such as the CD3+ T cells and CD14- population in this case, are from a different donor to the CD14+ monocytes, IL-4 DCs and IFN-DCs and therefore express different MHC molecules to these irradiated cells. When these cells from different donors are mixed together, the non irradiated T cells will divide or proliferate in response to the 'foreign' or non-self MHC molecules, expressed by the irradiated cells. This assay is useful for determining the functional capacity of an APC through its ability to

stimulate T cells. For control purposes, unstimulated T cells were also added to the 96 well plate as a negative control. For a postive control, T cells were stimulated with 50ng/ml of the polyclonal activator phorbol 12-myristate 13-acetate (PMA, stock concentration = 10μg/ml) and 1μg/ml anti-human CD3 mAb (stock concentration = 1mg/ml). PMA directly activates protein kinase C, which in turn can activate various signalling pathways, leading to T cell activation. Anti-human CD3 mAb activates T cells by binding or crosslinking to CD3 on the surface of T cells. The anti-human CD3 mAb was bound to the 96 well plate, in disodium hydrogen phosphate (0.1M Na_2HPO_4 - Na_2HPO_4 was made to 0.1M with sterile distilled water and pH to 9 with 0.1M sodium dihydrogen phosphate) binding buffer for 24h at 37°C, prior to stimulation. After incubation, the antibody solution was removed and wells were washed X2 with sterile PBS, before the addition of cells. Cocultures were incubated for 5 days in total at 37°C. At day 3, supernatants (~160μl) were harvested from cocultures and fresh cRPMI was added to cells. At day 5, cells were assessed for proliferation by tritiated thymidine incorporation. All samples were perfomed in triplicate on the 96 well plates.

2.2.11 ^{3}H-Thymidine incorporation and proliferation

Background

Tritium (^{3}H) is a radioisotope and can be attached to thymidine, which is one of the bases of DNA. ^{3}H-thymidine can be used to determine proliferation of cells by ultimately becoming incorporated into replicating DNA. Thus, the more cell divisions the more ^{3}H-thymidine will be incorporated into the DNA.

Method

After incubating the cocultures (section 2.2.10) for 5 days, ^{3}H-thymidine (Amersham Biosciences- stock concentration = 1mCi/ml) was diluted in cRPMI (25μCi/ml) and then 20μl was added to each well (2.5μCi/well), which had a volume of 200μl. The plate was incubated for a further 5h at 37°C and then the cells were harvested. During

harvesting, the cells are washed from the wells and sucked up through needles. The cells burst releasing their DNA and the cell debris and DNA are passed through a filter membrane, which only allows small particles (<1.5μm) to pass. Thus, intact DNA which has a large fragment length (ranging from mm – cm) cannot pass through the filter and so is collected on the filter membrane (http://www.celldeath.de/apometh/prolif.html). The filter membrane or mat is dried and sealed in plastic bag containing 1-2ml of scintillation fluid and the radioactive sample is read on a scintillation counter. Beta particles emitted from the radioactive sample, transfer energy to molecules in the scintillation fluid, which in turn excites these molecules (fluors), releasing flashes of light. Photomultiplier tubes in the counter detect these tiny flashes of light, which are counted (http://www.shef.ac.uk/physics/teaching/phy311/scintillator.html). The number of flashes of light counted per minute (cpm) reflects the intensity of beta rays emitted from the radioactive sample. Thus, the more DNA present in a sample, the higher its radioactivity will be, resulting in higher numbers of light flashes being counted. The data was plotted as the average cpm $\pm$ the standard error.

2.2.12 Statistical analysis

Different samples were compared using two-sample Student t tests, if the samples being compared were normal ($p>0.05$). If the normality plot was <0.05 for samples being compared, the Mann-Whitney U test was used to determine statistical significance. Results were considered significant at the 5% probability level ($p<0.05$). Statistical analysis were carried out using the Minitab programme.

2.3 RESULTS

2.3.1 Isolation of pure CD14+ monocyte popultions from PBMCs

To begin our study investigating different cell population responses to virus infection, it was imperative to isolate a highly pure population of precursor CD14+ monocytes, as these cells were subsequently used to generate all DC subsets, in this study. Following CD14 positive selection, it was visibly noticeable from the forward and side scatter dot blots, the disappearance of a group of cells from the depleted cell fraction (figure 2.3.1, left panel). More than 90% of this group of cells (CD14 enriched), stained positive for CD14 and CD11c, which are myeloid markers, indicative of cell lineage. Only 1.2% of the CD14+CD11c+ cells were not captured by the positive selection process and were eluted into the depleted fraction (figure 2.3.1, right panel). Contaminating CD3+ cells found in the CD14+ fraction, were < 2% (see appendix 1B). Thus, our selection process was highly successful, providing a pure population of precursor monocytes for subsequent studies.

2.3.2 Characterisation of different cell subsets following viral infection

Firstly, we assessed the phenotype of monocytes, immature IL-4 DCs (cultured for 6 days) and immature IFN-DCs (cultured for 4 days) in terms of cell size and granularity (figure 2.3.2). Monocytes exhibited typical precursor morphology, demonstrated by their forward and side scatter profile, which revealed a population of cells that were small in size with little granules (figure 2.3.2, left panel). In contrast, the pre-primed IL-4 DCs and IFN-DCs, both formed large, granular cell populations, evident from their forward and side scatter profile (figure 2.3.2, middle and right panel).

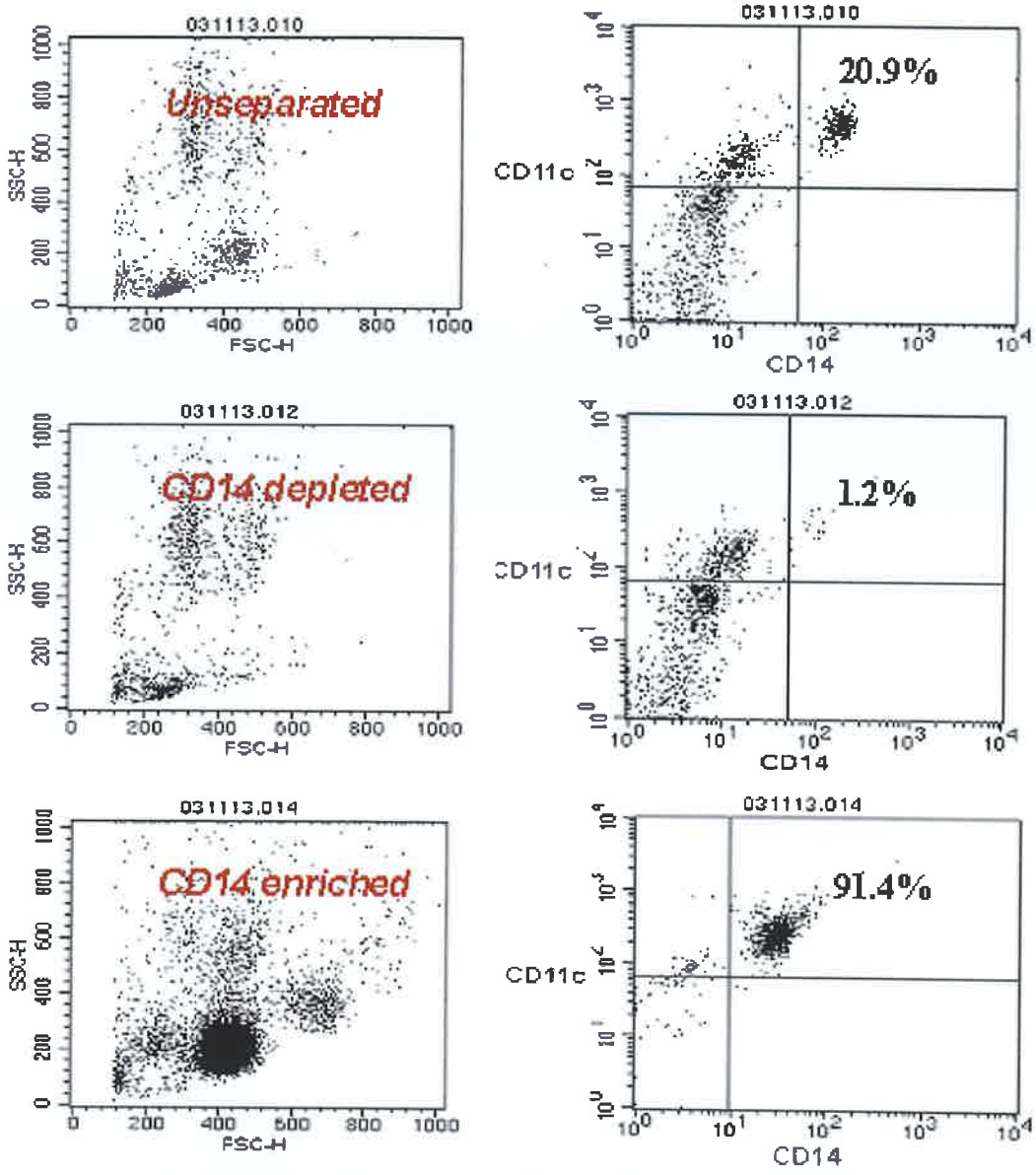

Figure 2.3.1 Purity of CD14+ monocytes isolated from human PBMCs. Cells were stained with human FITC-conjugated anti-CD11c and Pe-conjugated anti-CD14. Unseparated PBMCs contained 20.9% CD14+CD11c+ cells. Only 1.2% CD14+CD11c+ cells escaped positive selection in the column and were collected as the CD14 depleted or negative cell fraction. Following positive selection, the CD14 enriched population had a purity > 90%. Data is representative of >3 independent experiments (for raw data from repeat experiments refer to appendix 8, table 8.A).

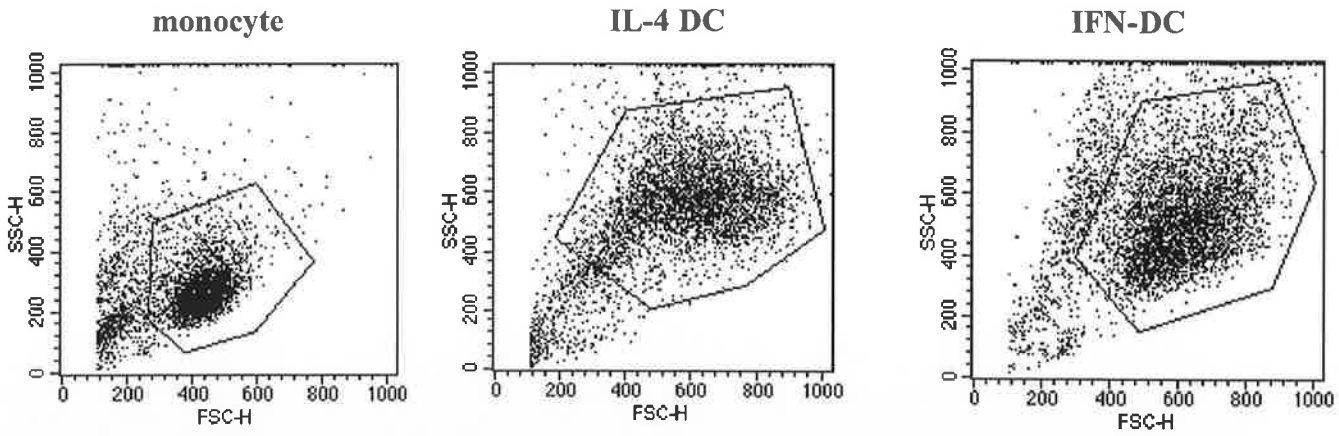

Figure 2.3.2 Cell size and granularity of monocytes, IL-4 DCs and IFN-DCs. Differences in the forward and side scatter of monocytes, immature IL-4 and IFN-DCs were assessed during characterisation of these cells. Monocytes were found to be relatively small in size with little granules compared to the IL-4 DCs and IFN-DCs, which were large, granular cells. Cell populations were gated for phenotypic analysis, ensuring that highly pure cell populations were analysed.

Next, we analysed the surface marker expression profile of monocytes, IL-4 DCs and IFN-DCs, following direct viral infection and A549 DCs generated from culture with infected epithelial cell supernatants for 48h (figure 2.3.3). Interestingly, the A549 DCs seemed to mimic the expression of surface markers on directly infected monocytes, showing upregulation of costimulatory markers CD80 and CD86, downregulation of myeloid markers CD14 and CD11c, and upregulation of the DC maturation marker CD83, MHC class II and the IL-3Rα chain (CD123), following infection with HPIV3 (figure 2.3.3 C and D). This phenotypic pattern was also evident from the A549 DCs generated from culture with the UV inactivated HPIV3 epithelial cell supernatants, indicating that viral replication is not a prerequisite for this viral induced DC maturation. HPIV3 infected IFN-DCs showed a similar expression profile of costimulatory molecules, MHC Class II and CD123 to monocytes (figure 2.3.3B). However, infection of the IL-4 DCs with HPIV3 generated a DC totally distinct from the infected monocyte (figure 2.3.3A). Although there was strong upregulation of the costimulatory marker CD86 compared to its positive control TNFα, the lack of

expression of CD123 and poor upregulation of MHC Class II, would indicate the emergence of two very distinct DCs.

Interestingly, influenza virus infection generated a DC distinct from HPIV3 infected DCs (figure 2.3.3A-D). We observed notable differences, including downregulation of CD11c and CD14, in addition to, upregulation of CD83, CD80, CD123 and MHC Class II, between the HPIV3 and influenza virus infected monocytes (figure 2.3.3D). Similarly, influenza virus generated A549 DCs mimicked direct infection of the monocytes, but with less potency than the HPIV3 generated DCs (figure 2.3.3C and D). We also saw upregulation of costimulatory markers and MHC Class II from influenza infected monocytes, IFN-DCs and IL-4 DCs (figure 2.3.3A-C). However, there was still relatively high levels of CD14 and CD123 on the influenza virus infected monocytes compared to infected IL-4 DCs and IFN-DCs, emphasising their naïve state. These results suggest that different viruses may exert different influences on DC generation, which may be caused by artificial pretreatment of these cells.

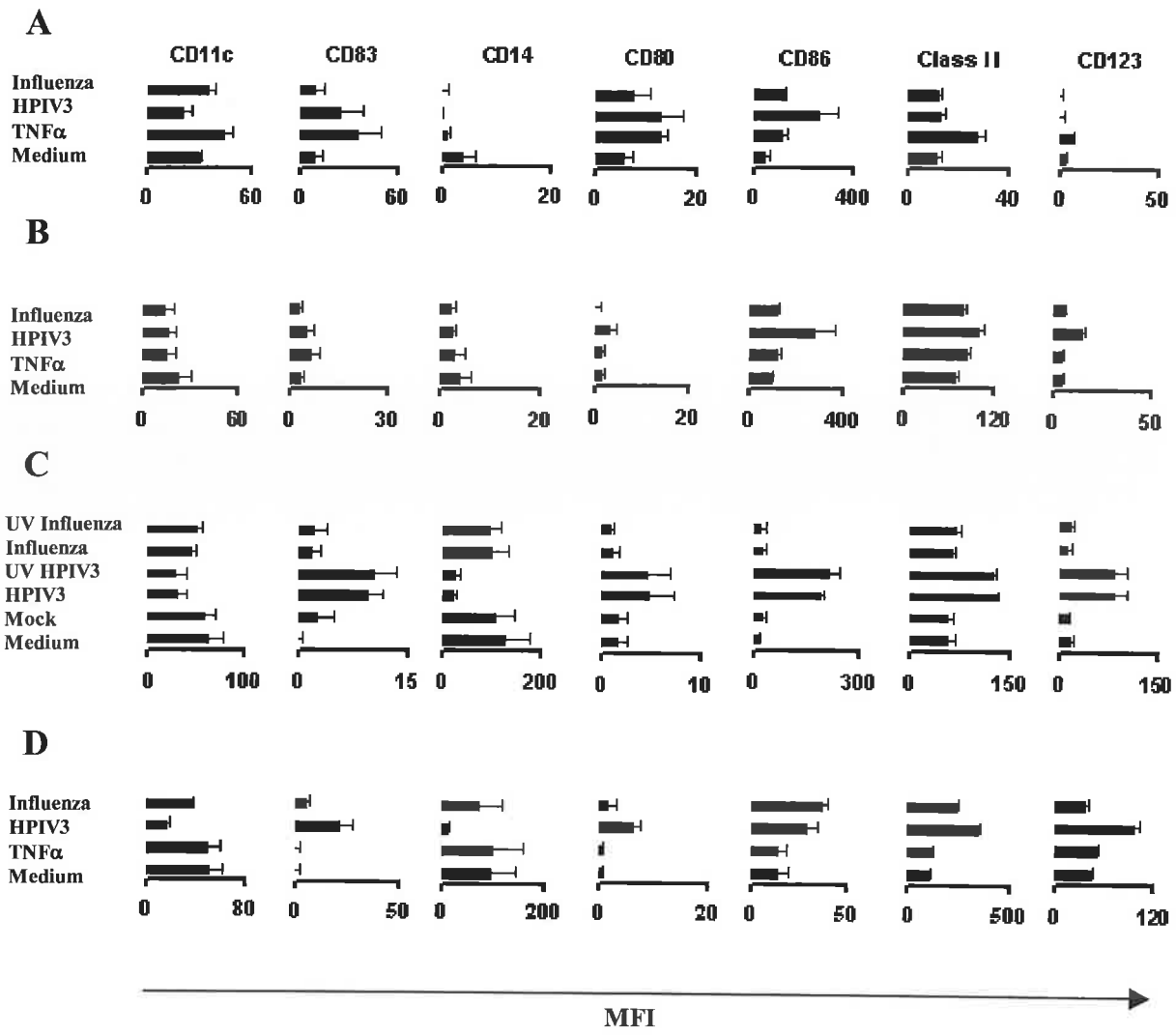

Figure 2.3.3 Phenotypic pattern from direct viral infection of monocytes and A549 DCs versus IL-4 DCs and IFN-DCs. Medium (non-infected), TNFα treated, mock (non infected A549 supernatant) treated and virus infected cells (section 2.2.7) were harvested after 48h and stained with human FITC-conjugated anti- CD80, CD11c; PE-conjugated anti- CD14, CD86, CD83, CD123; and APC-conjugated HLA-DR. Isotype controls included FITC, PE and APC-conjugated mouse IgG1 and FITC and APC- conjugated mouse IgG2b. Data represents the mean fluorescence intensity (MFI) of (A) IL-4 DCs, (B) IFN-DCs, (C) A549 DCs and (D) monocytes, following 48h culture. Results are a culmination of two to four independent experiments.

2.3.3 Cytokine production from the virally infected cell populations

We investigated the cytokine secretion profile from these infected cells, to help us predict what kind of influence they would have on polarising T cells. Strikingly, there was significant levels of the antiviral, proinflammatory cytokine IFNα produced from all cell subsets infected with HPIV3, compared to the various other treatments (figure 2.3.4A-D). To our knowledge, this finding has not been previously reported. Interestingly, IL-4 DCs were the only DC subset capable of secreting large amounts of TNFα in response to HPIV3 infection, strengthening this proinflammatory response (figure 2.3.4A). However, little or no IL-12p40 (a well established Th1 (Brombacher *et al* 2003) inducing cytokine) was produced from HPIV3 infected IL-4 DCs compared to its positive control, TNFα. High levels of the regulatory cytokine IL-10, were only observed in supernatants from the HPIV3 infected IL-4 DCs and monocytes compared to the HPIV3 infected IFN-DC and A549 DC supernatants (figure 2.3.4A-D). Only TNFα treated IL-4 DCs and IFN-DCs were capable of secreting high levels of IL-12p40 compared to their control and virus infected samples (figure 2.3.4A and B), while TNFα treatment, had no stimulatory effect on cytokine production from monocytes (figure 2.3.4C).

In contrast, little or no cytokines were secreted from the influenza infected cells compared to the various other treatments (figure 2.3.4A-D). All subsets infected with influenza exhibit similar cytokine secretion profiles, showing a general lack of IFNα and TNFα production and modest levels of IL-10 and IL-12p40 secretion from cells. Thus, again we demonstrate the importance of different DC generation pathways in influencing the production of distinct cytokine profiles from virally infected cells.

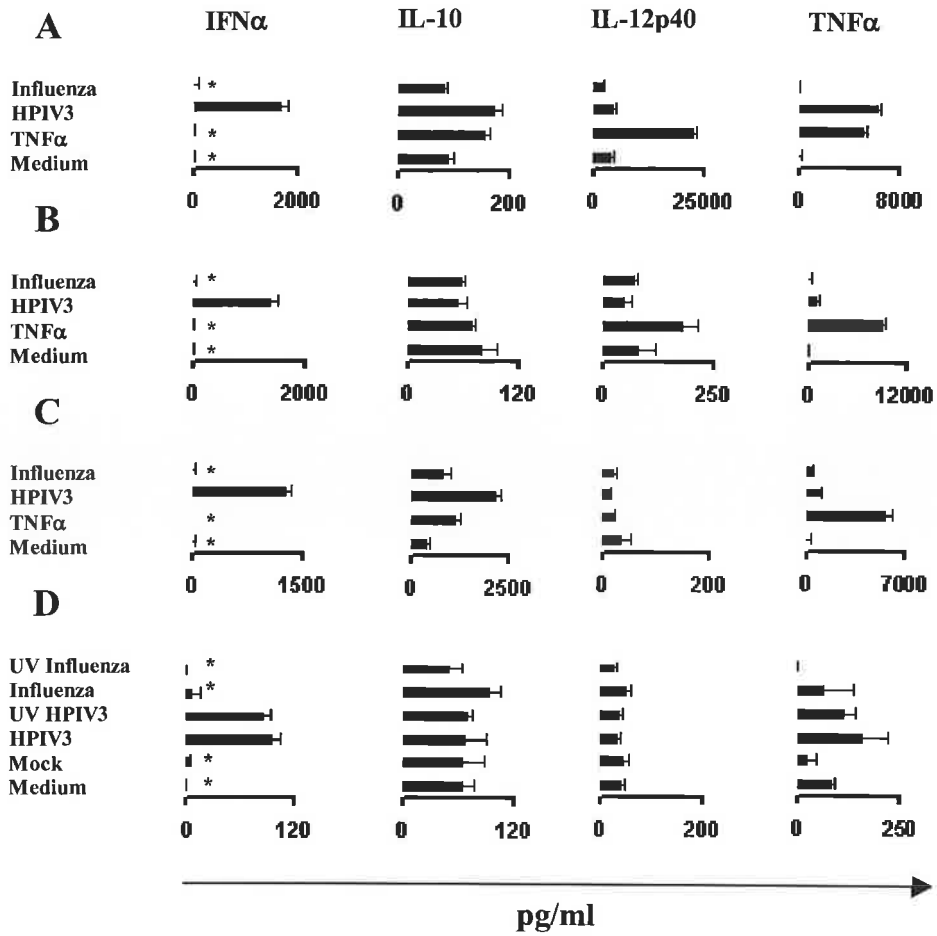

Figure 2.3.4 Cytokine secretion profile of virally infected IL-4 DCs, IFN-DCs, monocytes and A549 DCs. Cells were infected with HPIV3 or influenza and cultured for 48h (section 2.2.7). Supernatants were harvested and IFNα, IL-10, IL-12p40 and TNFα secretion was determined by ELISA. Data reflects the mean concentration ± SD for infected (A) IL-4 DCs, (B) IFN-DCs, (C) monocytes and (D) A549 DCs. Statistical differences between HPIV3 samples and influenza, TNFα treated, mock treated and untreated samples for IFNα production were assessed using two-sample Student *t* tests (for statistics from repeat experiments refer to appendix 7, table 7.A), $*P \leq 0.05$. Results are representative of two to three individual experiments (for raw data from repeat experiments refer to appendix 8, table 8.B).

2.3.4 Virus induced apoptosis of infected cell subsets

The propensity of viruses to induce apoptosis of cells is well documented (Brown *et al* 2004, Plotnicky-Gilquin *et al* 2001) and is critical to the outcome of immune

responses. Therefore, it was imperative to assess the levels of viral induced apoptosis of the different cell subsets. Interestingly, IL-4 DCs exhibited a large amount of apoptosis, >50% in the control cells, compared to the IFN-DCs and monocytes, which did not exceed more than 30% each, respectively (figure 2.3.5A). However, TNFα, which is a potent inducer of DC maturation (Cella *et al* 1999, Sallusto and Lanzavecchia 1994) greatly improved the survival of the IL-4 DCs, with 80% of the cells still surviving, following the two day culture (figure 2.3.5B). Also, TNFα slightly increased the survival of the IFN-DCs but had little or no effect on the monocytes (figure 2.3.5B). Strikingly, HPIV3 induced extremely high levels of apoptosis (>80%) in IL-4 DCs (figure 2.3.5C). There was also strong to moderate levels of apoptosis observed from the monocyte cultures infected with HPIV3, with the IFN-DCs displaying the most resistance to HPIV3 induced apoptosis (figure 2.3.5C). Again, we saw increased levels of apoptosis from the influenza infected IL-4 DCs, with nearly 50% of cells undergoing apoptosis, while similar levels of apoptosis, ranging from 25-35%, were observed from the influenza infected IFN-DCs and monocytes (figure 2.3.5D). Thus, IL-4 DCs appear to be more sensitive to viral induced apoptosis than the IFN-DCs or monocytes.

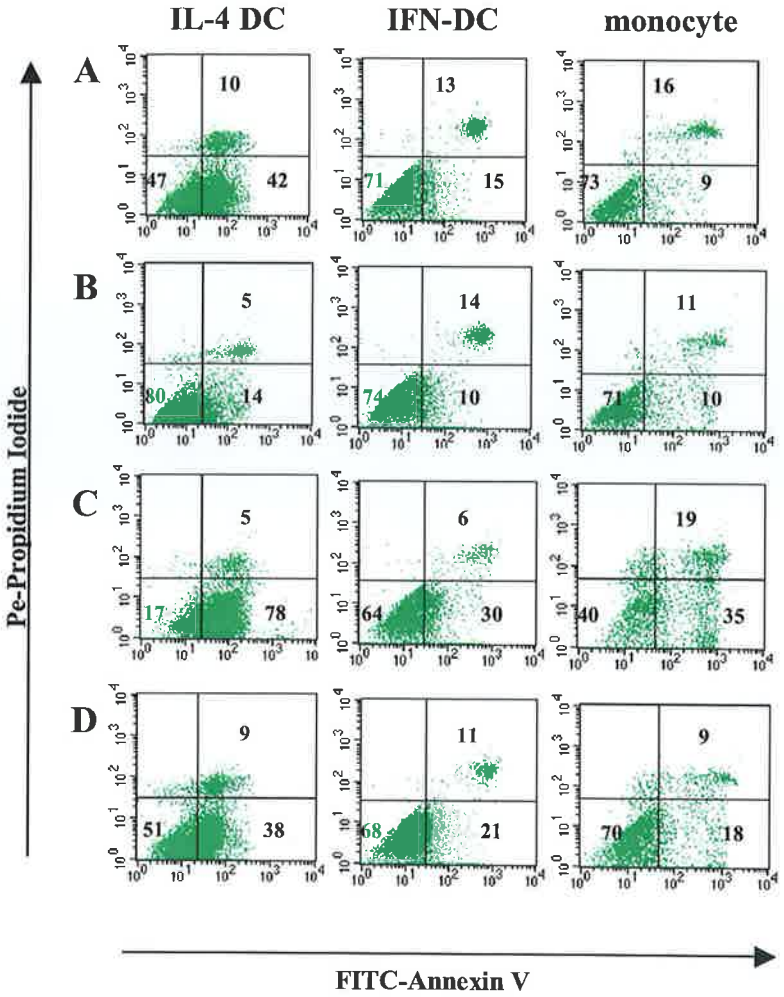

Figure 2.3.5 Differential effects of viral induced apoptosis of IL-4 DCs, IFN-DCs and monocytes. Cells were infected with HPIV3 or influenza and cultured for 48h (section 2.2.7). Apoptosis of cells was determined using the FITC-labelled annexin V detection kit I (section 2.2.8) and samples; A) control, B) TNFα treated, C) HPIV3 and D) influenza infected cells, were analysed by flow cytometry. Quadrants markers were set based on isotype controls and values reflect the percentage of cells in each quadrant; where the lower left quadrant represents living cells, the lower right quadrant represents early apoptotic cells and the upper right quadrant represents late apoptotic cells. Data are representative of two separate experiments (for raw data from repeat experiment refer to appendix 8, table 8.C).

2.3.5 Immunostimulatory properties of the virally infected cell populations

We wanted to test the immunostimulatory capacity of these virally generated DCs. Therefore we cultured virally infected monocytes, IL-4 DCs , IFN-DCs and A549 DCs with purified allogeneic CD3+ T cells and mixed leukocyte populations (mixed leukocyte reaction ; MLR). Interestingly, despite elevated levels of apoptosis in infected IL-4 DCs, these cells induced similar T cell proliferation profiles to the IFN-DCs (figure 2.3.6A and B). There was strong downregulation of T cell proliferation from both the purified CD3+T cell coculture and the MLR of the HPIV3 infected IL-4 DCs and IFN-DCs, compared to the control, TNFα and influenza treated cocultures. Although, there was less proliferation in general from the infected monocytes and A549 DC cocultures, they also exhibited similar T cell proliferation profiles to the infected IL-4 DC and IFN-DC cocultures in the MLR (figure 2.3.6A-D). However, most interestingly we did not observe the same inhibition of proliferation from the purified CD3+T cells that had been cultured with the HPIV3 infected monocytes (figure 2.3.6D). This phenomenon was also evident from the purified CD3+T cells in the UV HPIV3 and live HPIV3 generated A549 DC cocultures, but to a lesser extent (figure 2.3.6C). Thus, infected IL-4 DCs and IFN-DCs exhibit different stimulatory capacities to the infected monocytes and A549 DCs, in terms of their strength (high cpm) and ability to proliferate T cells.

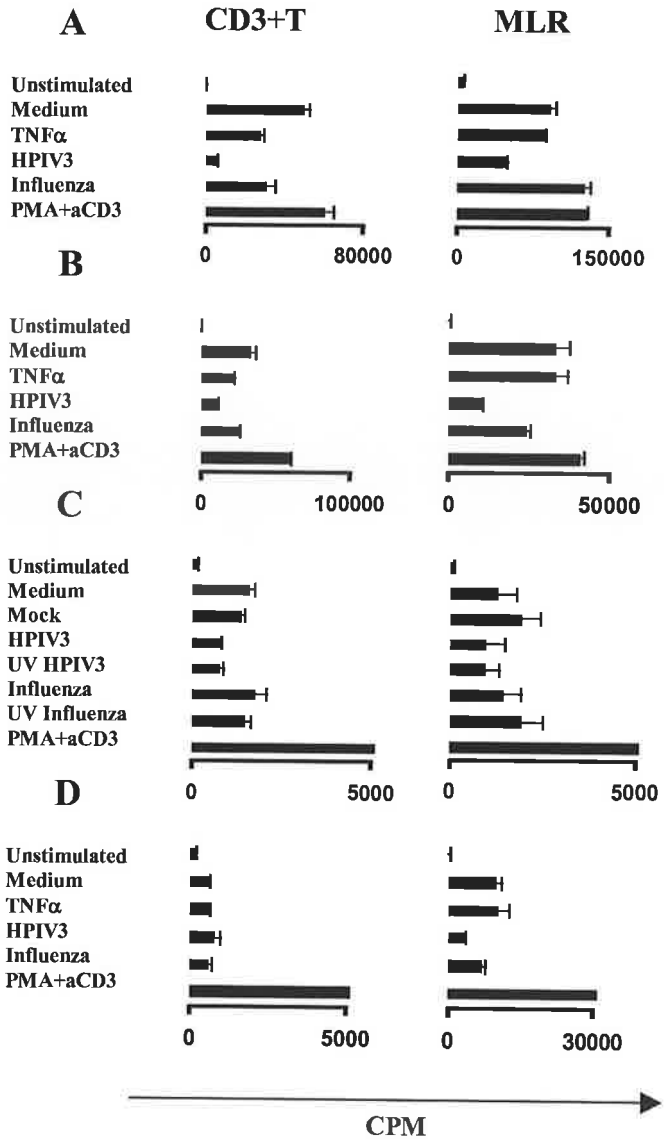

Figure 2.3.6 HPIV3 infected IL-4 DCs and IFN-DCs display different stimulatory properties compared to infected monocytes and A549 DCs. Cells were infected with HPIV3 or influenza virus and were cultured for 24h (section 2.2.7). Cocultures of DCs with allogeneic CD3+ T cells or in mixed leukocyte reactions (MLR: CD14 depleted fraction) were set up at a 1:10 ratio and incubated for 5 days (section 2.2.10). Proliferation was evaluated by the addition of ^{3}H-thymidine to the cocultures for the last 5h of incubation (section 2.2.11). Cells were then harvested and analysed on a scintillation counter. Results reflect the mean cpm $\pm$ SE for (A) IL-4 DC, (B) IFN-DC, (C) A549 DC and (D) monocyte cocultures and are representative of two to four independent experiments (for raw data from repeat experiment refer to appendix 8, table 8.D).

2.3.6 Virus infected cell subsets and T cell polarisation

Lastly, we examined the supernatants from the T cell proliferation assays, to assess if these virus infected cells had the ability to induce T cell polarisation, in addition to proliferation. Firstly, we investigated IFNγ secretion from both the purified CD3+ T cell and MLR cocultures. IL-4 DC cocultures produced similar levels of IFNγ from all treatments, despite the fact that T cell proliferation was reduced in the HPIV3 infected cocultures (figure 2.3.7A). IFN-DCs exhibited similar IFNγ secretion profiles to the IL-4 DCs in the MLR cocultures, but to a lesser extent, while higher levels of IFNγ were produced from both virus infected purified CD3+ T cell cocultures (figure 2.3.7A and B). High levels of IFNγ were secreted from the virus infected monocyte MLR cocultures compared to the other treatments. This pattern was also evident from the virus infected monocytes cocultured with purified CD3+ T cells, but to a lesser extent (figure 2.3.7C). Also, no key variations were observed in IFNγ production from the various samples of the A549 DC MLR cocultures (refer to appendix 2). So, both viruses appear to be inducing a Th1 cell bias, however, the quantitiy of IFNγ produced differs dramatically between the different cell subsets.

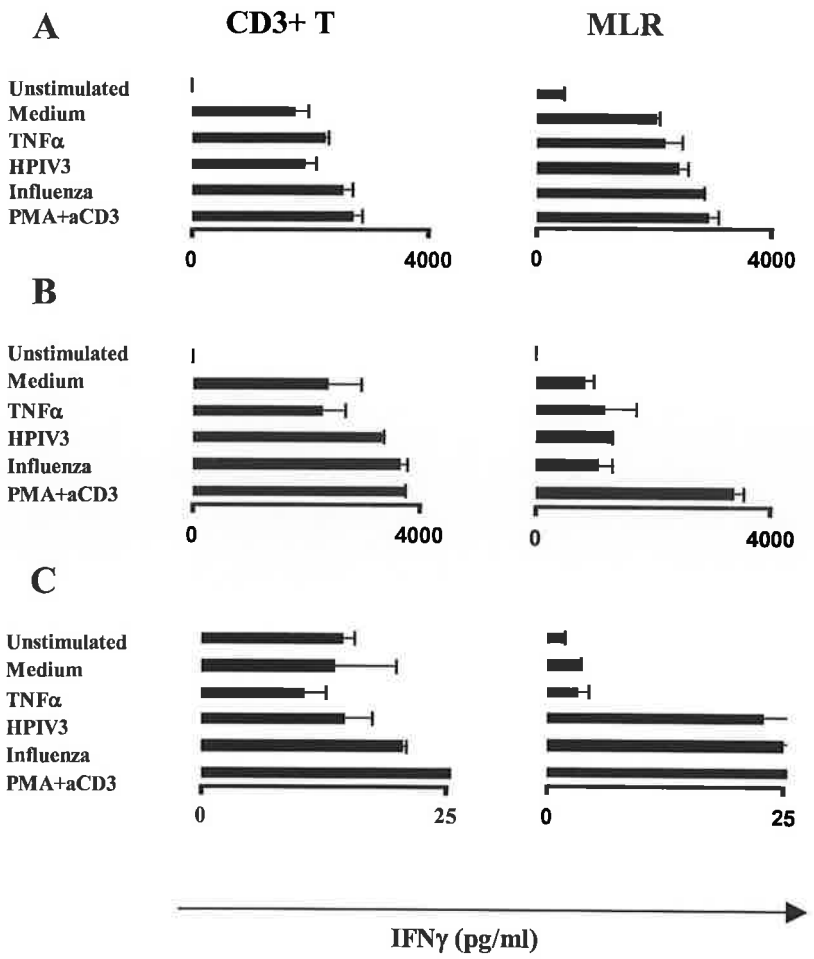

Figure 2.3.7 IFNγ secretion from the cocultures. Cells were cultured with purified CD3+ T cells and MLR, as described above (figure 2.3.6). After 3 days, supernatants were harvested from the cocultures and tested for IFNγ secretion by ELISA. Data reflects the mean ± SD for A) IL-4 DC, B) IFN-DC and C) monocyte cocultures. Results are representative of two to four separate experiments (for raw data from repeat experiment refer to appendix 8, table 8.E).

Noticeable variations were observed in the T cell stimulatory ability of the different cell subsets, hence we speculated that a regulatory cytokine may be responsible for these variations. Therefore we also investigated IL-10 secretion from these cocultures. Interestingly, large amounts of IL-10 were produced from the HPIV3 infected and TNFα treated IL-4 DCs cultured with the purified T cells compared to the influenza infected or control cocultures (figure 2.3.8A). However, when we examined the IL-4 DC MLR cocultures, IL-10 was predominantly secreted from the virus infected cocultures. We also observed strong IL-10 production from the purified T cell coculture of the HPIV3 infected IFN-DCs compared to the other treatments, but saw

little difference in the levels of IL-10 produced from samples of the IFN-DC MLR cocultures (figure 2.3.8B). In general, larger quantities of IL-10 were secreted from the purified CD3+ T cells cultured with the pre-primed DCs, than from the pre-primed DC MLR cocultures. Noticeably, there was a similar trend in IL-10 production from all HPIV3 infected cells, cultured with purified T cells (figure 2.3.8A-C). However, unlike the HPIV3 infected pre-primed MLR cocultures, HPIV3 infected monocytes retained this IL-10 secretion pattern in the MLR coculture, which exhibited higher IL-10 production from the HPIV3 infected monocyte MLR coculture compared to the other treatments (figure 2.3.8C). Also, no differences were observed in IL-10 production from samples of the A549 DC cocultures (see appendix 2). Thus, again striking differences in IL-10 secretion were observed from the infected cocultures, depending on the type of subset used in each coculture. These results also show that IL-10 secretion does not appear to be related to reduced T cell proliferation.

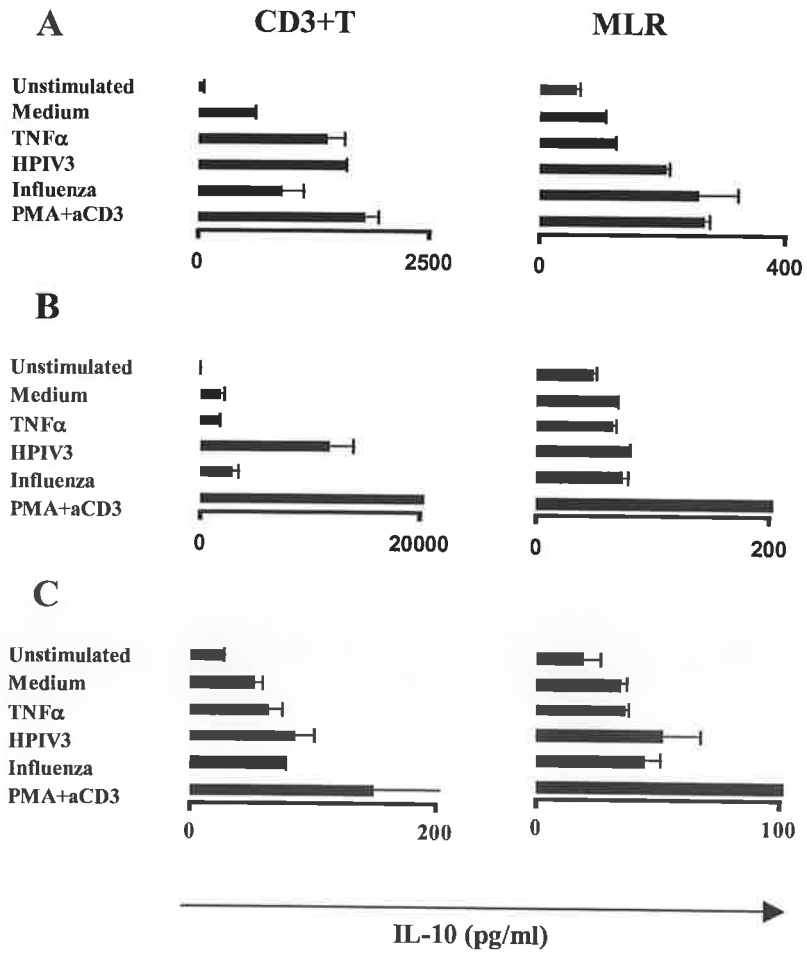

Figure 2.3.8 IL-10 secretion from the cocultures. Cells were cultured with purified CD3+ T cells and MLR, as described above (figure 2.3.6). After 3 days, supernatants were harvested from the

cocultures and tested for IL-10 secretion by ELISA. Data reflects the mean ± SD for A) IL-4 DC, B) IFN-DC and C) monocyte cocultures and are representative of two to four independent experiments (for raw data from repeat experiment refer to appendix 8, table 8.F).

2.4 DISCUSSION

Our results highlight the importance of DC generation pathways in initiating the appropriate immune response to viral infections. It has been well established that the microenvironment surrounding a viral infection is a critical factor in influencing the cells circulating in that area (Sato and Iwasaki 2004, Qu *et al* 2003). This was the reason why investigators started exploring alternative DC generation pathways to IL-4 generated DCs, leading to the creation of the IFN-DCs, which were generated from type I IFNs (Parlato *et al* 2001, Mohty *et al* 2003), commonly secreted during viral infections (Diebold *et al* 2003). However, we speculated that these artificially generated or pre-primed DCs, particularly IL-4 DCs which have been used for several years to study the immune response to viral infections *in vitro* (Cella *et al* 1999, Plotnicky-Gilquin *et al* 2001) may mask or skew the genuine immune response. By scrutinizing the differences in cell surface marker expression, cytokine production, apoptosis and T cell proliferation and polarisation, between virally infected monocytes, IL-4 DCs, IFN-DCs and A549 DCs, we hoped to elucidate which DC would be the most likely to occur during a viral infection *in vivo* and by doing so, determine which DC should be used in *ex vivo* assays when studying viral immune responses.

In order to carry out a comprehensive, comparative, phenotypic analysis of the virally infected cells, we firstly examined the cell populations in terms of cell size and granularity. As one would expect, the pre-primed DCs were much larger in size and granularity compared to the monocytes. Then we investigated the expression of an array of different surface markers on the cell subsets. We demonstrated that direct viral infection of monocytes and A549 DCs generated from monocytes cultured with supernatants from infected epithelial cells, induced distinct DC subsets from the IL-4 DCs and IFN-DCs. These pre-primed DC subsets showed strong upregulation of costimulatory markers and MHC Class II expression following maturation after TNFα treatment, while TNFα induced little or no effect on the surface marker expression of the monocytes. Interestingly, virally infected IL-4 DCs and IFN-DCs, also induced distinct DC subsets from each other, emphasising the critical nature of different DC generation pathways in shaping or directing the overall immune response.

The virally infected cell subsets also induced their own distinct cytokine secretion profile. Although, significantly high levels of IFNα were produced from all the HPIV3 infected cells, directing Th1 bias, differences were observed between the various subsets; HPIV3 infected IL-4 DCs secreted large amounts of TNFα compared to the other subsets and higher levels of IL-10 were secreted from the HPIV3 infected IL-4 DCs and monocytes compared to the HPIV3 infected IFN-DCs and A549 DCs. As IL-10 is a potent immunoregulatory cytokine (O'Garra *et al* 2004), it can have important implications on polarising T cells, such as shifting the T helper bias towards a regulatory T cell, such as Tr1, as demonstrated by McGuirk et al. (McGuirk *et al* 2002). Little or no cytokines were secreted from the influenza infected cells, which we hypothesise, is a result of its NS1 protein, which is known to suppress cytokine production from cells (Fernandez-Sesma *et al* 2006). Thus, the different cytokines secreted from the infected cell subsets, can greatly influence the polarising capacity of T cells.

Again, we observed very different levels of apoptosis induced from the virally infected cell populations. Surprisingly, the IL-4 DCs showed the greatest sensitivity to viral induced apoptosis compared to the infected IFN-DCs and monocytes. As IL-4 DCs are the most commonly used DC in *in vitro* assays (Senechal *et al* 2004, Plotnicky-Gilquin *et al* 2001, Cella *et al* 1999) the fact that these DCs appear to be hypersensitive to viral induced apoptosis, could have vast implications on viral studies, resulting in inaccurate or misleading conclusions from results. IFN-DCs appeared to be the most resistant to viral induced apoptosis, although similar levels of apoptosis were observed from the influenza infected monocytes and IFN-DCs. From this data, one can speculate, that certain DC generation pathways appear to be more prone to viral induced apoptosis.

Subsequently, we investigated the immunostimulatory capacity of these virally infected cells, to examine their functional relevance *in vitro*. Similar T cell proliferation profiles were observed from both the virally infected IL-4 DC and IFN-DC cocultures, with the purified T cells and the MLR, exhibiting strong proliferation from the influenza infected cocultures and limited proliferation from the HPIV3

infected cocultures, which corroborates previous reports (Fonteneau *et al* 2003, Plotnicky-Gilquin *et al* 2001). Virally infected monocytes and A549 DC MLR cocultures, also displayed a similar proliferation pattern to the virally infected IL-4 DC and IFN-DC cocultures, however, the inhibition of T cell proliferation observed from all HPIV3 infected cocultures in the MLR, appeared to be restored with the purified T cells from the HPIV3 infected monocyte and A549 DC cocultures. Thus, again we see differences in the T cell proliferative capacity of the virally infected cell subsets.

Lastly, we determined the T cell polarising capacity of these virally infected cells. We observed a similar pattern of IFNγ secretion from each of the virally infected cell subsets, cultured with the purified T cells, which also exhibited high levels of IFNγ production. Influenza is a strong inducer of IFNγ, so these results are consistent with the literature (Brown *et al* 2004). This IFNγ pattern was retained with the virally infected cell MLR cocultures, however, lower levels of IFNγ, in general, were evident from the IFN-DC MLR coculture, while elevated levels were secreted from the virus infected monocyte MLR cocultures. Therefore, overall the virus infected cell subsets are inducing Th1 cell development, but the varying quantities of IFNγ produced from the infected cell cocultures, could have dramatic implications on the overall immune response. We also examined T cell secretion of IL-10, as we speculated that this immunoregulatory cytokine may be involved in T cell suppression, which was observed in some of the HPIV3 infected cell cocultures. High levels of IL-10 were secreted from the HPIV3 infected IFN-DCs, cultured with the purified T cells, while little differences in the levels of IL-10 were observed from the various MLR treated cocultures. There was little variation in IL-10 production from the virus infected monocyte and IL-4 DC cocultures, however, slightly elevated levels of IL-10 were secreted from the HPIV3 infected monocyte cocultures and from the purified T cell cocultures of the HPIV3 infected and TNFα treated IL-4 DCs. From these results, it is clear that the virally infected cell cocultures stimulate different IL-10 secretion profiles and that this IL-10 pattern does not mimic the pattern observed from the reduced T cell proliferation, associated with some of the HPIV3 infected cell cocultures. Hence, in this case, IL-10 does not appear to be linked to T cell suppression.

From this data, we feel that pre-primed DCs may not be the most appropriate cell to use in *in vitro* assays when studying viral infections, as they appear to skew immune responses. Direct viral infection of monocytes and A549 DCs generated from monocytes cultured with supernatants from infected epithelial cells, appears to be the most natural pathway of DC generation. Also, blood DCs, closely resemble monocytes (O'Doherty *et al* 1994), in terms of size and morphology, so one questions the relevance of these pre-primed, more mature DCs in models of *in vivo* immune responses. We propose that this DC generation pathway could aid therapeutic advances in viral studies by representing a more accurate human *ex vivo* model for viral *in vitro* studies. However, perhaps pre-primed DCs may still be used when studying poorly immunostimulatory viruses, but in our case HPIV3 is a potent inducer of DC generation, therefore this human *ex vivo* model represents a more accurate method for us, when studying immune responses to HPIV3 infection.

INNATE AND T CELL RESPONSES TO HPIV3 INFECTIONS

3.1 INTRODUCTION

Infectious challenges to the body are met by a wealth of humoral and cellular responses, which are effective at eliminating the pathogen but may result in adverse consequences for the host, resulting in collateral tissue damage or immunopathology (Artavanis-Tsakonas *et al* 2003). This damage to the host might be more intense were it not for the many regulatory mechanisms that control the zeal of both innate and adaptive responses (Mills 2004, Jiang and Chess 2004). This was clearly demonstrated by Suvas *et al*, when they depleted regulatory T cells from mice and then infected them with herpes simplex virus (HSV). These mice exhibited increased Th1 responses and developed more severe T cell mediated lesions in the cornea, from this lack of regulatory T cells (Suvas *et al* 2004). It is now well established that these T regulatory cells play a crucial role in suppressing responses to self and preventing autoimmunity (Sakaguchi 2005), in addition to their control of immune responses to infectious disease (McGirk *et al* 2002, Kinter *et al* 2004). Most recent reports further suggest that these responses, while beneficial to the host, may offer yet another means by which infectious organisms subvert protective immune responses (Marshall *et al* 2003, Accapazzato *et al* 2004). By suppressing T cell activity, such as virus specific CTL responses, this would reduce viral clearance, enabling the virus to persist and induce chronic infection in the host (Accapazzato *et al* 2004). Thus, regulation of immune responses to viruses by host cells is imperative to the overall control of infections.

Human Parainfluenza virus type 3 (HPIV3) is a major respiratory pathogen responsible for bronchiolitis, pneumonia and croup. Initial infection occurs during infancy and early childhood but reinfection is a common event and may occur several times even in adolescents and adults (Henrickson 2003, Chanock *et al* 2001). This repeated occurrence of HPIV3 infection cannot be explained by antigenic change as the virus is relatively stable (Chanock *et al* 2001). Furthermore persistence of HPIV3

infection has been described in several cases (Goswami *et al* 1984). The ability to reinfect within a short time and to induce persistent infection suggests that HPIV3 fails to induce a state of lasting immunity. This feature of the virus has led to successive failures in the design of a protective vaccine against this major pathogen. Earlier studies have suggested that this failure to induce memory T cell responses may be due to limited T cell proliferation following infection with HPIV3 (Seig *et al* 1994). A further report from this group, demonstrated that infection of peripheral blood mononuclear cells with HPIV3, stimulated IL-10 production, which could be a contributing factor in this limited T cell proliferation (Sieg *et al* 1996). Also, HPIV3 infection can contribute to viral persistence through selective downregulation of granzyme B mRNA, resulting in cytotoxic dysfuncion of killer cells and virus survival (Sieg *et al* 1995). More recently, Plotnicky-Gilquin *et al*, demonstrated that IL-4 and GM-CSF generated DCs were sensitive to HPIV3 induced apoptosis. However, the virus did induce DC maturation but again was unable to stimulate T cell proliferation. It was suggested that DC modulation by HPIV3 might affect T cell responses, thus preventing the development of efficient and long-lasting immune responses (Plotnicky- Gilquin *et al* 2001). Also, HPIV3 can block interferon signalling (Young *et al* 2000), which is important for antiviral immunity, enabling the virus to survive and persist in host cells. Therefore, viral persistence and recurrent viral infections may stem from both virus modulation of immune responses and host regulatory responses to virus infections.

However allowing for the prevalence of apoptosis during several diverse viral infections and in the light of the era of immune regulation we proposed to revisit the investigation into the immune mechanisms at play during infection with HPIV3. In chapter two we described the development of a human *ex vivo* immune model, which could generate DCs that would most likely resemble naturally occurring DCs generated *in vivo* during a virus infection. For the present study, this human *ex vivo* model was used to investigate the phenotypic profile, cytokine production and T cell proliferation and polarisation capacity of HPIV3 infected cells, focusing mainly on the T cell proliferation of allogeneic purified CD3+ T cells compared to mixed leukocyte reactions (MLR) (Noone *et al*, accepted for publication). To generate a more comprehensive study of this virus, we compared the immune responses of

HPIV3, to those generated from influenza A virus infection. Influenza is a well documented respiratory virus that can stimulate strong immune and memory responses to the same virus strain (Doherty *et al* 2006) and therefore serves as a useful comparison to HPIV3 immune responses. It was anticipated that this comparative study would provide us with a better understanding of the mechanisms involved in HPIV3 subversion of immune responses.

3.2 MATERIALS AND METHODS

Table 3.2.1 Additional reagents to table 2.2.1 (chapter 2) used in this study.

Product	Catalog #	Company
Human IL-2 Duoset ELISA kit	DY202	R&D Systems Europe Ltd., Oxon, UK
TRI REAGENT™	T9424	Sigma-Aldrich, Dublin 24, Ireland
Chloroform ($CHCl_3$)	277106P	BDH, Poole, England
2-propanol ($CH_3CH(OH)CH_3$)	1.09634.2511	Merck, Darmstadt, Germany
Ethanol absolute	H314	Romil Ltd., Cambridge, UK
Nuclease-free water	P1193	Promega, Madison, USA
PCR nucleotide mix	C1145	Promega, Madison, USA
Oligo$(dT)_{12-18}$ primer	18418-012	Invitrogen, Carlsbad, USA
SUPERSCRIPT™ II RNaseH⁻Reverse Transcriptase	18064-014	Invitrogen, Carlsbad, USA
Ribonuclease Inhibitor	15518-012	Invitrogen, Carlsbad, USA
Taq DNA polymerase in storage buffer A	M1861	Promega, Madison, USA
1kb DNA ladder	G5711	Promega, Madison, USA
Deoxynucleotide triphosphates (dNTPs)	U1240	Promega, Madison, USA
Blue/orange 6X loading dye	G190A	Promega, Madison, USA
Agarose	A0576	Sigma-Aldrich, Dublin 24, Ireland
Boric acid (H_3BO_3)	1.00165.1000	Merck, Darmstadt, Germany
Recombinant human IL-2	11340025	Immunotools, Friesoythe, Germany
0.2μm tissue culture inserts (transwells)	136730	Nunc, Roskilde, Denmark

Table 3.2.2 Additional equipment to table 2.2.2 (chapter 2) used in this study.

Equipment	Model	Company
Biophotometer		Eppendorf, Hamburg, Germany
Mastercycler gradient	5331	Eppendorf, Hamburg, Germany
Wide mini sub-cell GT electrophoresis system	1704468	Biorad, Hercules, USA
Syngene Gene Genius Bioimaging system	3088S	American Instrument Exchange, Inc., USA

3.2.1 Cell isolation and purification

Human PBMCs were obtained from buffy coats of healthy donors, as described in section 2.2.1. CD14+ monocytes and CD3+ T cells were purified from PBMCs by positive selection on a MACS column with anti-CD14 and anti-CD3 microbeads (refer to section 2.2.6), respectively. Rountinely purity was >90% for CD14+ monocytes and >95% for CD3+ T cells as assessed by flow cytometry. The CD14-CD3- population was obtained by depleting the CD14- fraction of CD3+ T cells.

Contaminating CD14+ monocytes and CD3+ T cells was <2% of the CD14-CD3- population after purification (see appendix 1C).

3.2.2 Virus stocks and infections

CD14+ monocytes were cultured in complete RPMI on a 24 well plate and were subsequently infected with HPIV3 at a $TCID_{50}$/ml of 6 or influenza virus at a $TCID_{50}$/ml of 7 for 2h at 37°C, as previously described in section 2.2.7.1. Cells were washed following incubation to remove excess virus and cultured for a further 24h or 48h.

3.2.3 Flow cytometry

Staining of cells for flow cytometry was performed in accordance to the protocol in section 2.2.5. Abs used in this study for flow cytometric staining are summarised in table 2.2.1, of the previous chapter. Apoptosis of lymphocytes was determined using the Annexin V-FITC Apoptosis Detection Kit I (BD Pharmingen, section 2.2.8).

3.2.4 ELISA

Human IL-10, IFNγ (table 2.2.5) and IL-2 (table 3.2.1) Duoset ELISA developmental kits and human IFNα ELISA kit (table 2.2.5) were used to quantify the cytokines secreted into cell supernatants. ELISA kits were used in accordance with the manufacturers instructions (R&D) and sample concentration was determined from the standard curve for each cytokine (section 2.2.9).

3.2.5 RNA isolation

RNA from samples was isolated using TRI REAGENT™, which is a reagent that is comprised of a mixture of guanidine thiocyanate and phenol in a mono-phase solution. This reagent is very effective at inhibiting RNase activity, which is highly beneficial, considering RNA is generally unstable and can degrade readily. TRI REAGENT™ can also be used to isolate DNA and protein. After cells have been lysed with TRI REAGENT™, chloroform is added to the sample and then centrifuged. The resulting mixture separates into three phases: 1) an upper aqueous phase containing RNA, 2) an interphase containing DNA and 3) an organic phase containing proteins. RNA can then be precipitated from the aqueous phase by addition of isopropanol, followed by washing with ethanol, before it can be solubilised (www.sigma-aldrich.com).

RNA was isolated from cells according to the manufacturers guidelines (Sigma). Briefly, $1X10^6$ cells were lysed with 500µl of TRI REAGENT™ by repeated pipeting. 100µl of chloroform (0.2ml of chlorform/ml of TRI REAGENT™) was added to samples, shaken vigorously for 15 seconds and allowed to stand for 15mins at RT. Samples were then centrifuged at 13000rpm for 15mins at 4°C. Centrifugation separated the samples into three phases or layers, where the upper aqueous layer (RNA) was then removed. 250µl of isopropanol was added to samples, inverted twice and left to stand for 10mins at RT, followed again by centrifugation at 13000rpm for 10mins at 4°C. The supernatant from the samples was decanted and the RNA pellets were washed with 1ml of 75% ethanol, vortexed and centrifuged at 9000rpm for 5mins at 4°C. Sample supernatants were decanted and the RNA pellets were left to air-dry for 10-14min. Lastly, RNA pellets were resuspended in 50µl of nuclease free water (pre-heated to 55°C) and stored at –80°C.

3.2.6 Quantification of RNA

Nucleic acids can absorb UV light at 260nm. Therefore the concentration of RNA in a sample can be determined by UV spectrophotometry. An absorbance reading of 1 unit

at 260nm is equal to a concentration of 40µg/ml RNA. In contrast to nucleic acids, proteins have an absorption maximum of 280nm. This reading indicates the extent of protein contamination in a given sample. Thus, non-contaminated RNA should have an Abs (absorbance) 260/280 ratio of ≥1.7. To quantify RNA, 10µl of sample was mixed with 490µl of nuclease free water in a quartz cuvette and the absorbance reading at 260nm and the ratio of Abs260/280 was recorded from the spectrophotometer. The concentration of total RNA was calculated as follows:

RNA concentration (µg/ml) = Abs260 X dilution factor (50) X conversion factor (40)

3.2.7 Reverse transcription of RNA

Reverse transcription is a process in which single stranded RNA is converted or reverse transcribed into complementary DNA (cDNA), using a reverse transcriptase (RT) enzyme. This cDNA product is fairly stable and can be used as a template in the polymerase chain reaction (PCR). Messenger RNA from samples was reverse transcribed using the following protocol:

1) 2µg of RNA was added per 20µl reaction volume.
2) The sample (approximately 10µl) was added to a mastermix or reaction solution and the mastermix was made according to table 3.2.3

Table 3.2.3 Summarises the reagents used to make the mastermix for cDNA synthesis

Reagent	Single reaction (µl)
10X buffer	2
5mM Mg^{2+} buffer	4
0.8mM dNTPs (deoxynucleotide triphosphates)	1.6
0.5µg oligo $(dT)_{12-18}$ primer	2
25 Units RNase inhibitor	0.5
62.5 Units reverse transcriptase (superscript)	0.125

3) The following temperatures were set in the thermocycler for cDNA synthesis:
   - 25°C for 10mins (primer annealing)
   - 42°C for 60mins (cDNA synthesis)
   - 95°C for 5mins (stops reaction)
   - 4°C for 10mins

4) The resulting cDNA was used as a template for amplification in the PCR.

3.2.8 Polymerase chain reaction (PCR)

PCR is a method for synthesising and amplifying specific DNA sequences. Firstly, the DNA is denatured by heating at 95°C, which unfolds or separates the double-stranded molecule into single strands of DNA. A limited stretch of nucleotides on each side of the target gene is used to design complementary single-stranded oligonucleotides (~20bp), which serve as primers (forward and reverse) for the PCR reaction. These specific primers hybridise or anneal (temperature is specific to each primer pair) to opposite strands of DNA and flank the target DNA sequence to be amplified. Elongation of primers is catalysed by a DNA polymerase enzyme, such as Taq polymerase (72°C). This enzyme is a thermostable polymerase and so is able to withstand the high temperatures needed in PCR. These three different steps involving denaturation, primer annealing and elongation are referred to as a cycle and numerous cycles (~30-40) are needed to detect the PCR product.

The primers used in this study to identify particular genes were designed from the complete coding sequence for each gene, found on the entrez nucleotides database (http://www.ncbi.nlm.nih.gov/entrez/query.fcgi?db=Nucleotide), with the aid of the primer design software from cybergene (http://www.cybergene.se/primertools/index.html) and were ordered from MWG-Biotech AG (Germany). Primer pairs were as follows:

Human IFNβ:

Annealing temp. = 55°C
Product size = 526bp

5′-TGCTCTCCTGTTGTGCTTCT-3′ (forward)

5′-GGTAACCTGTAAGTCTGTT-3′ (reverse)

HPIV3 NP:

Annealing temp. = 54°C
Product size = 548bp

5′-TTGGAAGTGACCTGGATTAT-3′ (forward)

5′-GGATACAGATAAAAGGAGC-3′ (reverse)

Influenza A virus NP: (H3N2)

Annealing temp. = 59°C
Product size = 619bp

5′-CTTACGAACAGATGGAGACT-3′ (forward)

5′-TGTTTTCCGCCCATTCTCAC-3′ (reverse)

Human β-actin:

Annealing temp. = 55°C
Product size = 619bp

5′-TACAATGAGCTGCGTGTG-3′ (forward)

5′-TGTTGGCGTACAGGTCTT-3′ (reverse)

A 25µl reaction was performed for each sample using 1µl of cDNA as a template. As a control, PCR was performed on all samples using primers specific for the housekeeping gene β-actin. Also to check for genomic contamination, PCR amplification was performed on 100ng/ml of RNA from each sample using β-actin primers. The mastermix or reaction solution for PCR was made according to table 3.2.4.

Table 3.2.4 Summarises the reagents and quantities used in the mastermix for PCR

Reagent	Single reaction (µl)
10X buffer	2.5
2.5mM Mg^{2+} buffer	2.5
2mM dNTPs	2
Forward primer (stock=400pmol/µl)	1
Reverse primer (stock=400pmol/µl)	1
1.25 Units Taq DNA polymerase	0.2
Nuclease free water	14.8

The following temperatures were set in the thermocycler for PCR, with changes only made to the annealing temperatures:

- 95°C for 5mins
- 95°C for 45seconds

- X °C for 45seconds
- 72°C for 1min
- Go to step 2, repeat X 35
- 72°C for 10mins
- 4°C hold

DNA electrophoresis was performed on all samples using a 1% agarose gel (made in 1 X Tris-borate EDTA (TBE)) (10X TBE = 108g of 890mM tris base, 55g of 890mM boric acid, 40ml of 0.5M EDTA, make up to 1l with dH_20 and autoclave) containing 2µl (~0.3µg/ml) ethidium bromide (stock concentration = 10mg/ml). In all cases 8µl of sample product was added to 4µl of 6X blue/orange loading dye on the gel, which was run for approximately 45mins at 100V and 350mA in 1 X TBE running buffer. The 1kb molecular weight marker (Promega) was run simultaneously on each gel to act as a reference for the size of the visualised bands. Products were visualised under ultraviolet light (UV) on the gel containing ethidium bromide, which can bind to DNA and fluoresce under UV light. The syngene gene genius bioimaging system was used to analyse the data.

3.2.9 ^{3}H-Thymidine proliferation/Coculture assays

Control and infected CD14+ monocytes were gamma irradiated and were seeded at $2x10^4$ into 96-well flat-bottomed plates. Cocultures of CD14+ monocytes and allogeneic CD3+ T cells or mixed leukocyte reactions (MLR: CD14- population) were performed at 1:10 ratios for all experiments (refer to section 2.2.9). In some cases, recombinant human IL-2 (stock concentration = 100µg/ml) was added to certain wells of HPIV3 infected cocultures (1ng/ml), to evaluate T cell proliferation. In later experiments $2x10^4$ CD14-CD3- cells were added to the cocultures above in keeping with the same ratio. After 5 days incubation, proliferation was evaluated by adding 2.5µCi/well ^{3}H-thymidine to the cocultures for the last 5h of incubation. Cells were then harvested onto filter mats and analysed on a scintillation counter, as previously described (see section 2.2.11).

3.2.10 Transwell cultures

Irradiated CD14+ monocytes were cultured with CD14-CD3- cells in the upper chamber of an 8 well strip insert with 0.2-μm pores on a 96-well flat-bottomed plate. Beneath the insert in the lower chamber, $1x10^5$ CD3+ T cells were cultured with irradiated CD14+ monocytes. As in the cocultures above, a 1:10 ratio of APC:T cell was enforced to ensure comparable results. Cultures were incubated for 5 days and then analysed for proliferative responses as described above.

3.2.11 Statistical analysis

Statistical significance between samples was determined as described in section 2.2.12.

3.3 RESULTS

3.3.1 HPIV3 infection induces differentiation of human CD14+ monocytes into highly activated dendritic cells

To assess the type of antigen presenting cells induced by HPIV3 infection we isolated and infected fresh CD14+ monocytes from human blood donation and compared the results to influenza infection, a well known respiratory virus related to HPIV3 but more commonly associated with acute rather than persistent infection. Cells were also examined following TNFα treatment or medium alone. Surface marker expression demonstrated strongly activated and mature DCs following HPIV infection with an up regulation of surface markers CD83, CD40, CD80, CD86, and MHC Class II and down regulation of CD11c and CD14 (figure 3.3.1) consistent with the generation of IFNα primed DCs (Mohty *et al* 2003). Interestingly, there was a strong upregulation of CD123 (IL-3Rα) on HPIV3 infected cells, which is found on hematopoietic cells and high levels of CD123 have also been associated with IFNα primed DCs (Parlato *et al* 2001) and plasmacytoid DCs (Lui 2005). Treatment with TNFα induced little or no effect in surface marker expression compared to unstimulated controls (figure 3.3.1). However, influenza infected monocytes generated a distinct DC from HPIV3 infected monocytes. Although infection with influenza generated similar but less intense phenotypic profiles to HPIV3 infected cells, in terms of upregulation of costimulatory markers and MHC Class II; myeloid markers, CD11c and CD14, remained relatively high on influenza infected cells (figure 3.3.1). Thus, HPIV3 infection generated a highly potent, distinct DC population compared to the influenza generated DCs.

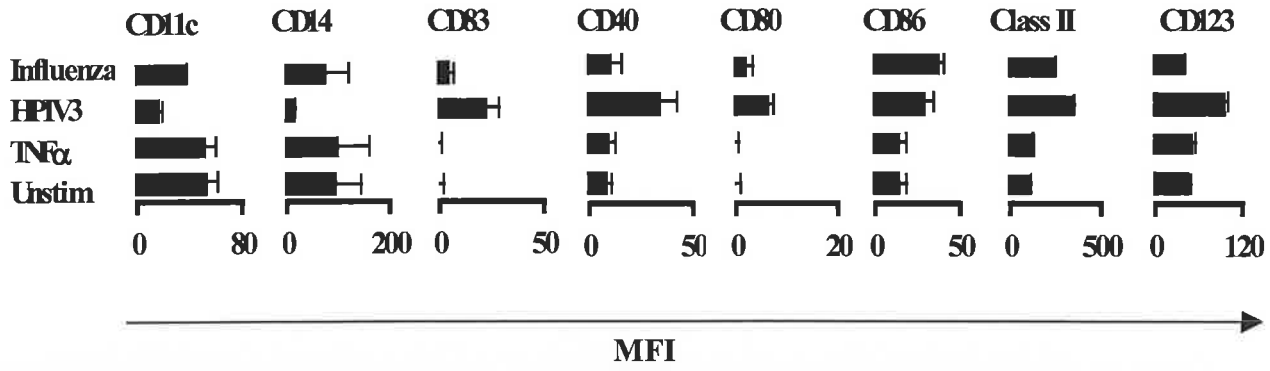

Figure 3.3.1 CD14+ responses to infection or TNF treatment. Freshly isolated CD14+ cells were infected with influenza ($TCID_{50}$=7), HPIV ($TCID_{50}$=6) or treated with TNFα (25ng/ml) or left unstimulated (medium) (section 2.2.7) for 48h. After incubation, cells were harvested and surface markers (CD11c, CD14, CD83,CD40,CD83,CD86, Class 11, CD123) were assessed by flow cytometery as mean fluorescence intensity (MFI). Results are a culmination of at least three separate experiments.

3.3.2 High levels of IFNα and IL-10 are produced from HPIV3 infected monocytes

Cytokine secretion from the virally infected cells was examined. Interestingly, significant levels of the regulatory cytokine, IL-10 were secreted from HPIV3 infected monocytes at 48h, compared to the influenza infected, TNFα treated or unstimulated cells (figure 3.3.2A). However, copious amounts of IFNα were also produced from the HPIV3 infected cells compared to the other treatments (figure 3.3.2B), reinforcing the strong influence of HPIV3 on innate cell activation. Also, upregulated levels of IFNβ mRNA were observed from HPIV3 infected cells after 24h (figure3.3.2C), emphasising the strength of this virus in stimulating type I IFN production from these cells. In contrast to HPIV3 infection, influenza infected monocytes secreted little or no cytokines (figure 3.3.2A-C). Therefore, we checked for viral replication in these cells, to assess if this lack of cytokine production could be due to inefficient viral replication and subsequent loss of stimulation in these cells. However, similar levels of the viral nucleocapsid protein (NP) mRNA was evident

from both HPIV3 infected and influenza infected cells (figure 3.3.2C). Thus, this lack of IFNα detected with influenza virus is perhaps linked to the inhibition of the type I IFN pathway by the non-structural protein (NS1) of the virus (Wang *et al* 2000). Hence, this data suggests that HPIV3 generated DCs are potent antigen presenting cells, capable of secreting large amounts of cytokines.

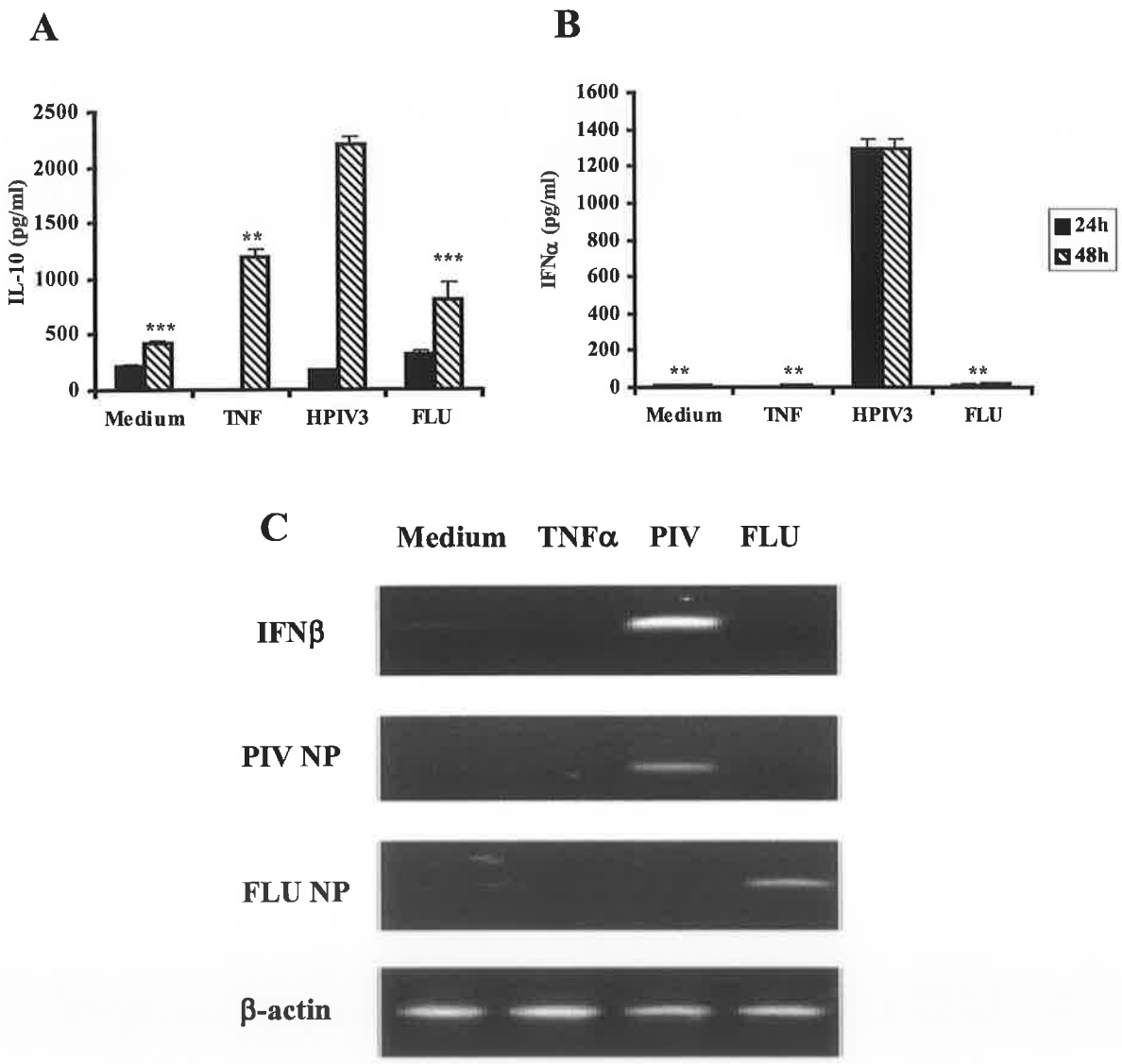

Figure 3.3.2 Cytokine expression and secretion from virally infected monocytes. Monocytes were infected with HPIV3 or influenza and cultured for indicated time points (section 2.2.7). Supernatants were then harvested at 24h and 48h and IL-10 (A) and IFNα (B) secretion from cells was determined by ELISA, where the data reflects the mean concentration ± SD for each sample. Results are representative of two to three independent experiments (for statistics from repeat experiments refer to appendix 7, table 7.B and C). $^{**}P \leq 0.01$, $^{***}P \leq 0.001$. (C) After 24h incubation, mRNA expression of

IFNβ, PIV NP, FLU NP and β-actin from infected cells was determined by RT-PCR as described in sections 3.2.5-3.2.8. Results are representative of two separate experiments.

3.3.3 HPIV3 generated DCs failed to induce proliferation of allogeneic mixed leukocytes but not allogeneic purified CD3+ T cells

We next evaluated the capacity of these infected or treated DCs to stimulate T cell proliferation and polarisation. HPIV3 generated DCs consistently failed to induce allogeneic mixed leukocyte cell proliferation compared with influenza infected, TNFα treated or unstimulated cells (5 donors: figure 3.3.3A). Despite this lack of proliferation, lymphocytes were polarised with high levels of IFNγ produced (figure 3.3.3B). Several recent studies have suggested that lymphoid derived APCs, so called plasmacytoid DCs, may be potent activators of T cell responses and that these cells are critical to the immune responses generated from viral infection (Cella *et al* 2000, Schlecht *et al* 2004). In order to investigate if plasmacytoid DCs may compensate for reduced proliferation associated with HPIV3 infected myeloid (CD14+) derived DCs, we investigated allogeneic T cell responses from directly infected CD14 CD3 depleted populations. Interestingly, HPIV3 infected "lymphoid" derived DCs also failed to induce significant allogeneic T cell proliferation (refer to appendix 3). We found identical T cell proliferation profiles compared with the CD14+ cells suggesting that HPIV3 infection of both myeloid and lymphoid innate immune cells fails to induce T cell proliferation compared with influenza virus, treatment with TNFα or unstimulated cells (figure 3.3.3A and appendix 3). Most interestingly however, over several donors, proliferation of CD3+ purified T cells cultured with HPIV3 infected cells were not significantly lower than those observed with influenza infected or TNFα treated samples (figure 3.3.3A). Thus, culturing HPIV3 infected cells with purified CD3+ T cells appeared to restore this inhibition of T cell proliferation observed from HPIV3 infected MLR cocultures. Surprisingly, IL-10 was not significantly induced in T cells stimulated by HPIV3 infected monocytes compared to influenza infection or TNFα treatment (figure 3.3.3C), which was in contrast to earlier observations from direct infection of monocytes with HPIV3 (figure

3.3.2A). We also looked for secretion of the suppressive cytokine TGFβ from infected cocultures, but only low levels of TGFβ were produced from all treatments (appendix 4). Thus, these results suggest that the failure of the mixed leukocytes to proliferate to HPIV3 infected cells is not due to IL-10, but rather points towards the presence of a regulatory group of cells in the mixed leukocyte population.

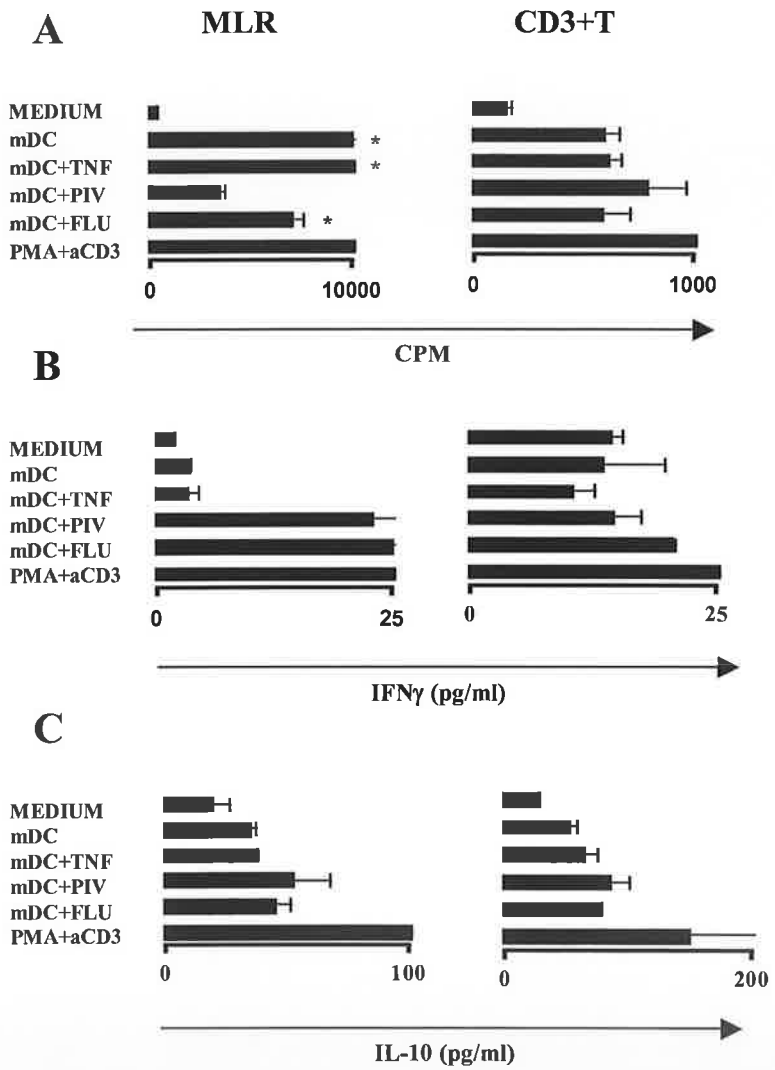

Figure 3.3.3 Mixed leukocyte and purified CD3+ T cell proliferation and cytokine profiles. CD14+ cells were left untreated (mDC) or treated with TNFα (mDC+TNF) or infected with influenza (mDC+FLU) or HPIV3 (mDC+PIV) and co cultured in allogeneic mixed leukocyte reactions (MLR) or with allogeneic purified CD3+ T cells (section 2.2.10). Proliferation was measured by ^{3}H incorporation after 5 days in culture (section 3.2.9) . Cytokines were measured by ELISA after 3 days in culture. (A) Represents the proliferation profiles from the monocyte cocultures. Data reflects the mean cpm ± SE for each sample and are representative of five independent experiments (for statistics from repeat experiments refer to appendix 7, table 7.D and for raw data see appendix 8, table 8.D).*$P \leq 0.05$. (B)

Represents IFNγ secretion and (C) represents IL-10 secretion from the monocyte cocultures. Results reflect the mean concentration ± SD for the various samples and are representative of four separate experiments (for raw data from repeat experiments refer to appendix 8, table 8.E and.F).

3.3.4 Inhibition of T cell proliferation from HPIV3 infected MLR cocultures is IL-2 dependent

As IL-2 is considered a crucial growth factor for T cells (Gaffen and Liu 2004), we examined the levels of this cytokine produced by HPIV3 infected cells cocultured with mixed leukocytes. We found a significant reduction in IL-2 secretion from the HPIV3 infected cells cocultured with the mixed leukocytes compared to the influenza infected or TNFα treated cocultures (figure 3.3.4A). However, addition of IL-2 at the start of the five day culture, completely abrogated this inhibitory effect, observed from the HPIV3 infected MLR coculture (figure 3.3.4B). As a control, IL-2 was also added to HPIV3 infected monocytes that were cocultured with purified CD3+ T cells, to ensure that the quantity of IL-2 added to the cocultures, did not induce significant T cell proliferation. This result was confirmed, when data demonstrated no significant increase in T cell proliferation between the untreated and IL-2 treated HPIV3 infected cocultures (figure 3.3.4C). Hence, this inhibition of T cell proliferation observed from HPIV3 infected MLR cocultures, was due to a lack of IL-2.

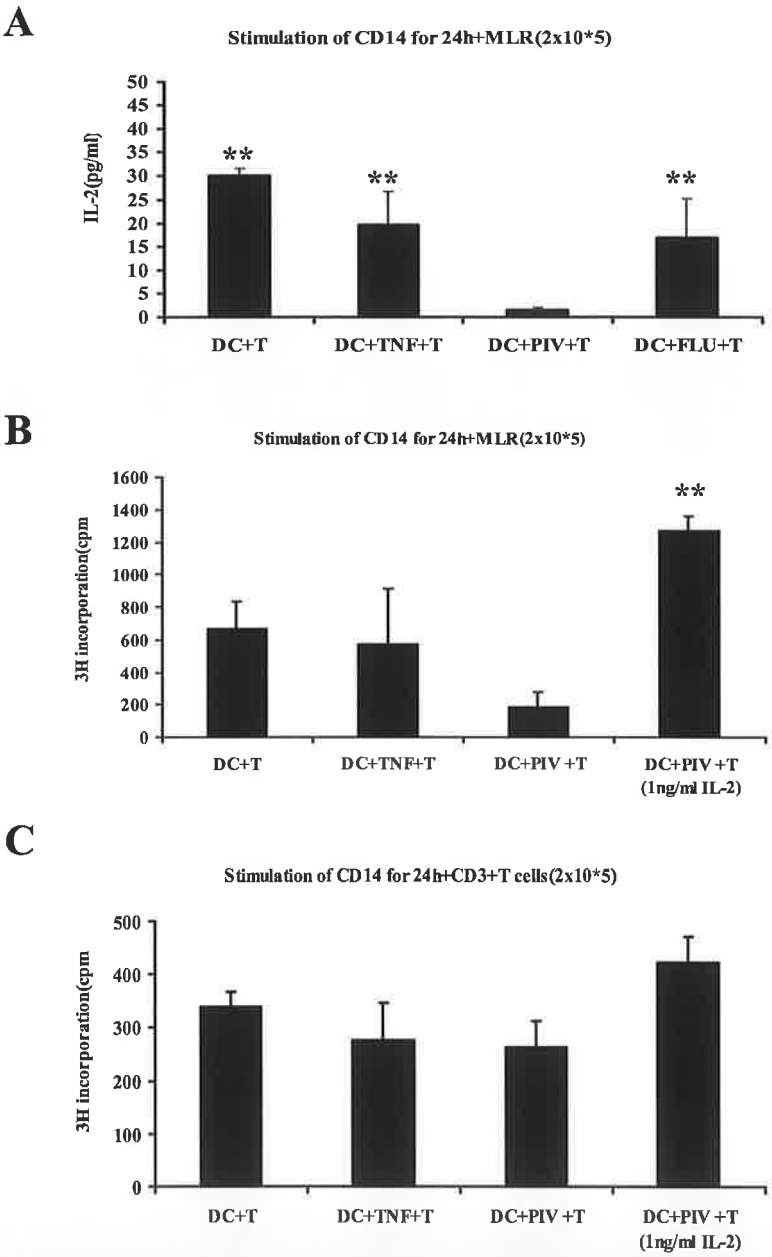

Figure 3.3.4 IL-2 secretion from allogeneic mixed leukocytes and the effect of IL-2 on T cell proliferation. CD14+ cells were cultured with purified CD3+ T cells and in a MLR, as described above (figure 3.3.3). After 3 days, supernatants were harvested and tested for IL-2 secretion by ELISA (A). Data reflects the mean concentration $\pm$ SD for each sample. Results are representative of three independent experiments. $^{**}P \leq 0.01$. IL-2 (1ng/ml) was added to MLR cocultures (B) and purified CD3+ T cell cocultures (C) at the start of the five day incubation period and T cell proliferation was assessed by ^{3}H incorporation (section 3.2.9). Results reflect the mean cpm $\pm$ SE for each sample and are representative of two separate experiments (for statistics from repeat experiments refer to appendix 7, table 7.E). $^{**}P \leq 0.01$.

3.3.5 Inhibition of T cell proliferation is not due to apoptosis of lymphocytes in HPIV3 infected MLR cocultures

Earlier studies have suggested that HPIV3 induced apoptosis of APCs may have a role in the inadequate priming of viral specific memory responses (Plotnicky-Gilquin *et al* 2001). We have already shown in previous experiments (figure 2.3.5) that HPIV3 does induce moderate levels of apoptosis of monocytes, however these cells are capable of inducing similar levels of T cell proliferation from the purified CD3+T cell cocultures compared the other treatments (figure 3.3.3A), so we believe that in this case apoptosis of APCs is not responsible for the limited T cell proliferation observed from HPIV3 infected MLR cocultures. Therefore, we investigated apoptosis of lymphocytes from HPIV3 infected cocultures. Interestingly, there was only a 1% difference in the percentage of apoptotic lymphocytes from HPIV3 and influenza infected MLR cocultures (figure 3.3.5A). Even the HPIV3 infected cells cocultured with purified CD3+ T cells displayed only minor variations in the levels of early apoptotic cells (34%) compared to cells from influenza infected, TNFα treated and untreated cocultures (figure 3.3.5B). Thus, it is apparent from these results that this inhibition of T cell proliferation from HPIV3 infected MLR cocultures is not linked to virus induced apoptosis of lymphocytes.

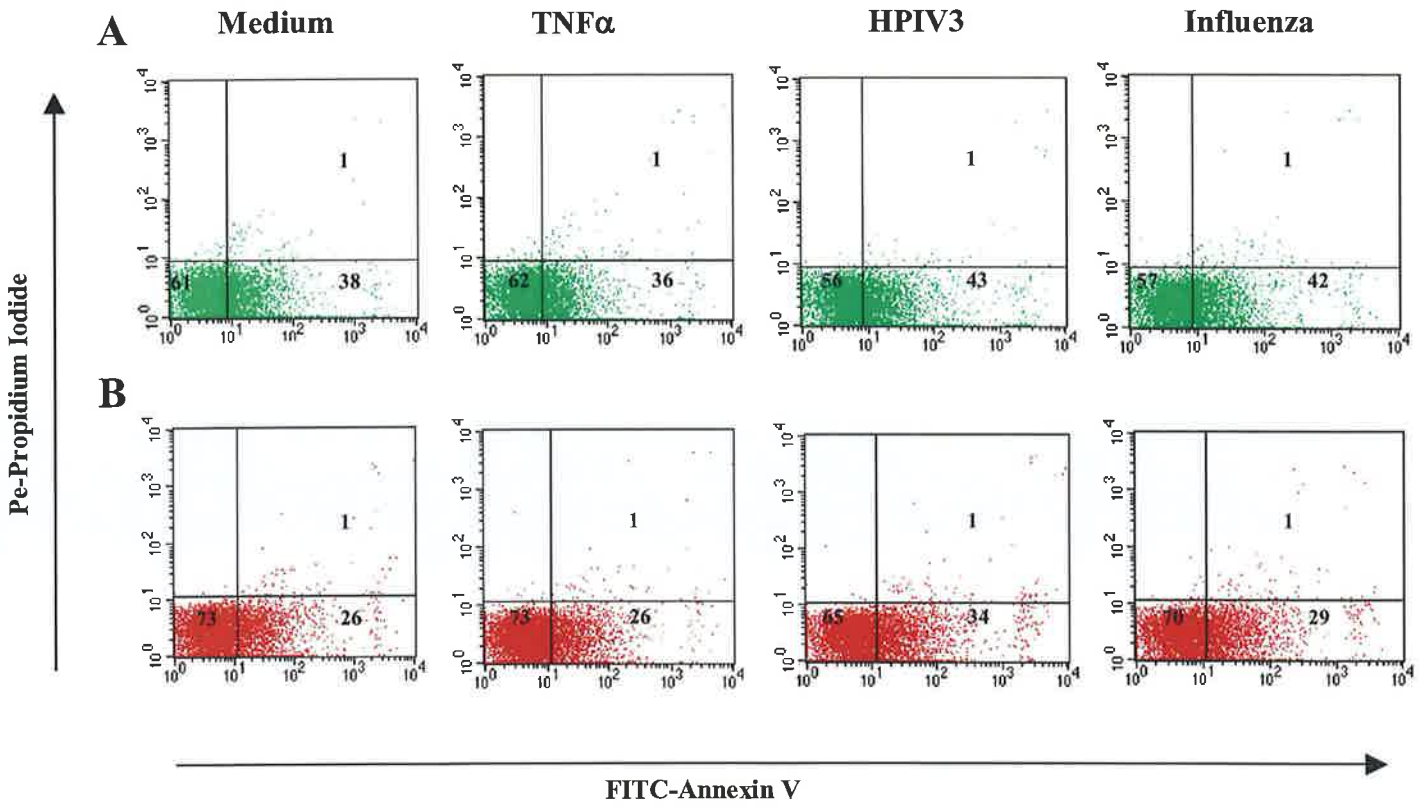

Figure 3.3.5 Apoptosis of lymphocytes from mixed leukocyte and purified CD3+ T cell cocultures. CD14+ cells were left untreated or treated with TNFα or infected with influenza or HPIV3 and co cultured in allogeneic MLRs or with allogeneic purified CD3+ T cells for 5 days (section 2.2.10). Lymphocyte populations were gated and apoptosis of lymphocytes from (A) MLR cocultures and (B) purified CD3+ T cells was determined by flow cytometry using the FITC-labelled annexin V detection kit I (section 2.2.8). Quadrants markers were set based on isotype controls and values reflect the percentage of cells in each quadrant; where the lower left quadrant represents living cell, the lower right quadrant represents early apoptotic cells and the upper right quadrant represents late apoptotic cells. Data are representative of three separate experiments (for raw data from repeat experiments refer to appendix 8, table 8.G).

3.3.6 A third population of cells that are autologous with the CD3+ T cell populations are responsible for this T cell inhibition from HPIV3 infected MLR cocultures

Studies with the purified CD3 populations (figure 3.3.3A) suggested that the failure of the mixed leukocyte cells to adequately proliferate to HPIV3 generated DCs was due to a third CD3- CD14- population of cells. In order to investigate this we isolated CD3- CD14- cell populations by cell depletion and restored them to the CD3+ T cell cocultures. As a control, we also cultured these CD3- CD14- populations with mixed leukocyte cocultures. Interestingly, addition of these cells to HPIV3 infected cocultures significantly reduced CD3+ T cell proliferation, only if the CD3- CD14- populations were autologous with the T cell population (figure 3.3.6A). This was evident from the high levels of CD3+ T cell proliferation observed from HPIV3 infected cocultures containing allogeneic CD3- CD14- cells which were comparable to the levels observed from the various other samples (figure 3.3.6A). In contrast, T cell inhibition was consistently observed from all HPIV3 infected MLR cocultures containing either allogeneic or autologous CD3- CD14-cell populations. Hence, these results suggest that this third population of cells may be responsible for this limited T cell proliferation observed in HPIV3 infected MLR cocultures and that this regulation appears to involve highly specific interactions between the T cells and the third cell population.

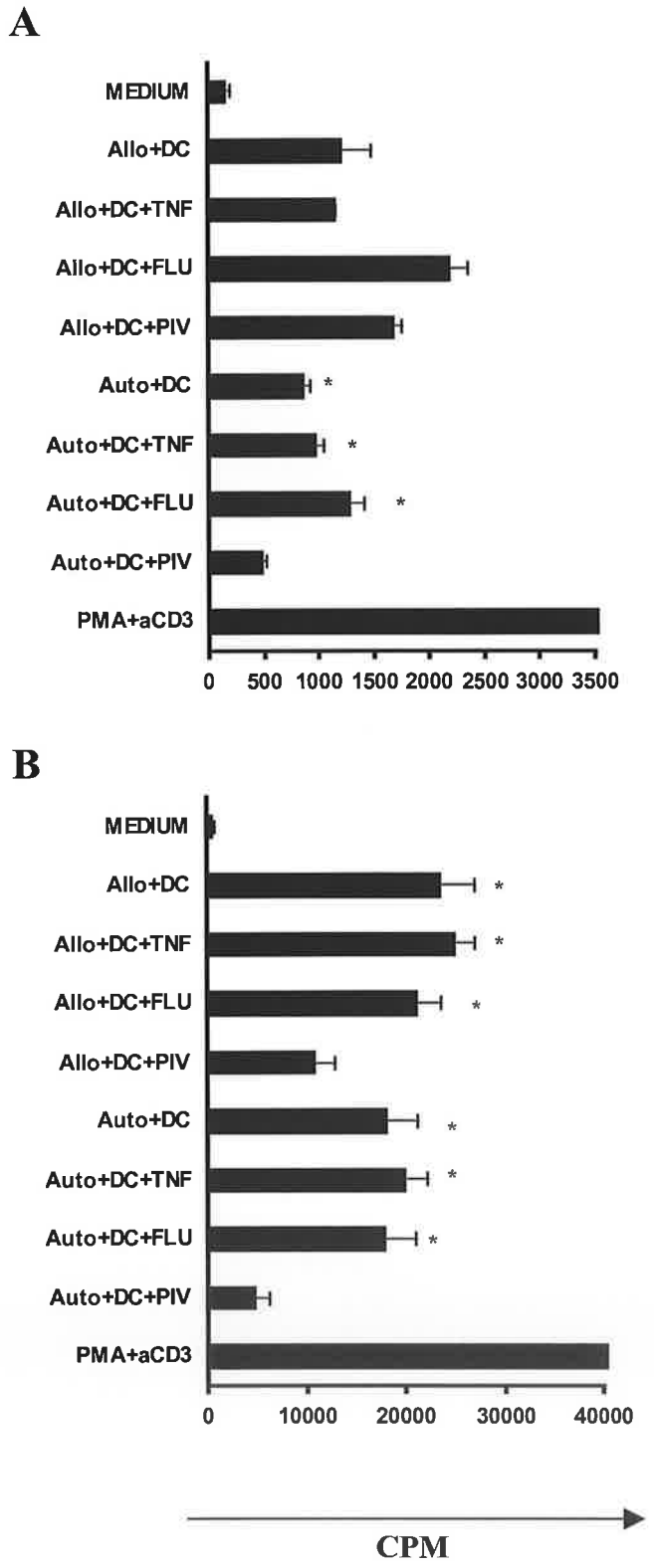

Figure 3.3.6. T cell proliferation profiles from purified CD3+ T cell cocultures and MLR cocultures reconstituted with autologous and allogeneic CD3- CD14- cell populations. (A) Purified CD3+ T cells and (B) mixed leukocytes were cocultured alone (MEDIUM), with CD14+ cells (DCs) and allogeneic or autologous CD14- CD3- cells (allo/auto+DC), with TNFα treated cells and

allogeneic or autologous CD14- CD3- cells (allo/auto+DC+TNF), with HPIV3 infected monocytes and allogeneic or autologous CD14- CD3- cells (allo/auto+DC+PIV) and with influenza infected monocytes and allogeneic or autologous CD14- CD3- cells (allo/auto+DC+FLU)(section 3.2.9). Proliferation profiles were measured by ^{3}H incorporation after 5 days. Results reflect the mean cpm $\pm$ SE for each sample and are representative of three independent experiments (for statistics from repeat experiments refer to appendix 7, table 7.F and G). *$P \leq 0.05$.

3.3.7 Differential cytokine secretion from purified CD3+ T cells stimulated with HPIV3 infected APCs and autologous CD3- CD14- populations does not appear to be responsible for T cell inhibition

Next we investigated T cell polarisation of the purified CD3+ T cells cocultured with HPIV3 generated DCs and autologous CD3- CD14- cell populations, to see if differential cytokine production by T cells, induced by this third cell population, may mediate this inhibition in T cell proliferation. Surprisingly, there was only slightly elevated levels of IL-10 produced from HPIV3 infected cocultures compared to the influenza infected and untreated cocultures, while similar levels of IFNγ were secreted from each of the different cocultures containing autologous CD3- CD14- cells (figure 3.3.7A and B). Also, this cytokine secretion profile is comparable to that observed from the purified CD3+ T cell cocultures in figure 3.3.3B and C, which suggests that differential expression of IL-10 and IFNγ do not appear to be linked to this reduction in CD3+ T cell proliferation observed from HPIV3 infected cocultures containing autologous CD3- CD14- cells.

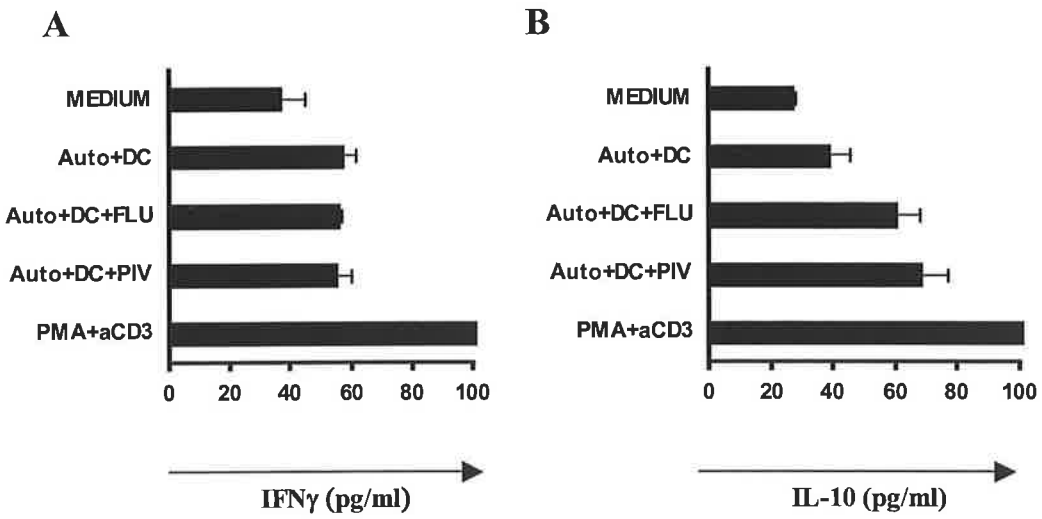

Figure 3.3.7 Cytokine secretion from purified CD3+ T cell cocultures reconstituted with autologous CD3- CD14- cell populations. Purified CD3+ T cells were cultured alone (MEDIUM), with CD14+ cells (DCs) and autologous CD14- CD3- cells (auto+DC), with HPIV3 infected monocytes and autologous CD14- CD3- cells (auto+DC+PIV) and with influenza infected monocytes and autologous CD14- CD3- cells (auto+DC+FLU)(section 3.2.9). After 3 days, supernatants were harvested from cells and (A) IFNγ and (B) IL-10 secretion was determined by ELISA. Data reflects the mean concentration ± SD for each sample. Results are representative of two to three individual experiments (for raw data from repeat experiments refer to appendix 8, table 8.H).

3.3.8 Autologous CD3- CD14- cells mediate CD3+ T cell inhibition of HPIV3 infected cocultures through contact dependent mechanisms

From our results we have demonstrated that specific interactions between T cells and the third cell population are required for this limited CD3+ T cell proliferation observed from HPIV3 infected cocultures containing CD3- CD14- cells. This inhibition is not related to increased IL-10 or TGFβ secretion, so we speculated that inhibition might be mediated through contact dependent mechanisms. To investigate this hypothesis, we repeated the experiments with autologous CD3- CD14- populations in transwells inserted above the CD3+ T cell cocultures. Consistently separation of the cells resulted in restored proliferative capacity of the CD3+ T cell

population, from the HPIV3 cocultured cells (figure 3.3.8). Thus, overall these results suggest that T cell inhibition is not due to soluble mediators but to a contact dependent inhibition of T cell proliferation by an autologous CD3- CD14- cell population(s) in the allogeneic mixed leukocyte culture of HPIV3 infected cells.

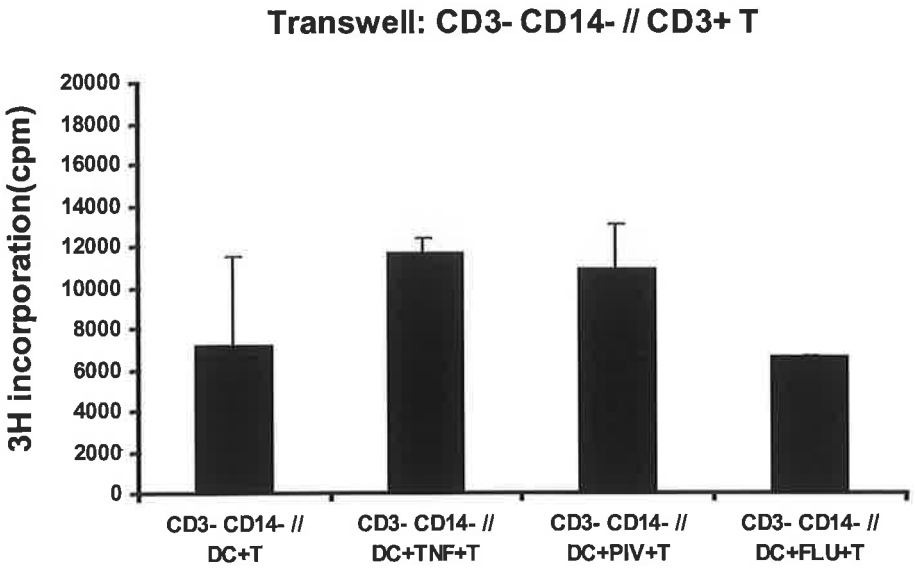

Figure 3.3.8 Transwell proliferation studies on purified CD3+ T cell cocultures. Purified CD3+ T cells were cocultured with allogeneic DCs and autologous CD14- CD3- cells, with TNFα treated allogeneic DCs and autologous CD14- CD3- cells, with HPIV3 generated DCs and autologous CD14- CD3- cells and with influenza generated DCs and autologous CD14- CD3- cells in transwells (section 3.2.10). Proliferation was measured by ^{3}H incorporation after 5 days (section 3.2.9). Results reflect the mean cpm $\pm$ SE for each sample and are representative of three separate experiments (for raw data from repeat experiments refer to appendix 8, table 8.I).

3.4 DISCUSSION

Current thinking on immune regulation has suggested that, in addition to the control of responses to self, regulatory mechanisms are at play which limit collateral damage during infection (O'Garra *et al* 2004) and that this response, while manageable often comes with the forfeit of appropriate immune activation resulting in chronic or persistent infections (Accapazzato *et al* 2004). This new vantage point of immune regulation has already provided insights to the mechanisms that define persistence and chronicity associated with hepatitis C virus (HCV) and HIV (Boettler *et al* 2005, Weiss *et al* 2004). While immune regulation is likely to influence the outcome of all infections we felt that it may be key to the host's inability to mount responses against certain pathogens that persist within the host. One such an offending organism is HPIV3. We began this investigation with a comprehensive look at the innate immune responses to HPIV3 taking into account the known features that flag the influence of immune regulation. By using a human *ex vivo* model to generate DCs, we compared the responses of HPIV3 infection to stimulation with a proinflammatory cytokine TNFα and the well-characterised influenza virus that, under normal immune conditions, is associated with acute rather than persistent infections (Cox and Subbarao 1999). Then we scrutinised the functional capacity of these APCs, in terms of T cell proliferation and polarisation. From our results we identified that the failure to induce T cell proliferation by HPIV3 infected APC populations could be restored by purification of the CD3+ T cell population from allogeneic mixed leukocytes. We also demonstrated that this inability to respond to the virally infected DC was due to the presence of a third population of cells, which were CD3- CD14-, from the mixed leukocyte reaction and that this influence was exerted in a contact dependent manner.

Initially, we discovered that HPIV3 induces the generation of a distinct DC from direct infection of monocytes. These DCs acquired a highly activated phenotype, displaying upregulation of costimulatory markers, MHC Class II and the DC maturation marker, CD83; which would indicate that it had all the attributes of a professional APC. This contradicts a previous report by Plotnicky-Gilquin *et al.* which suggested no upregulation of costimulatory markers and MHC Class II from HPIV3 infected monocytes (Plotnicky-Gilquin *et al* 2001). However, these findings

were not accompanied by data (ie: data not shown) making it difficult to comment on the discrepancy found between the present study and those reported by Plotnicky-Gilquin *et al.* Furthermore, HPIV3 generated DCs exhibited phenotypic similarities to other APCs, such as the IFNα generated DCs and plasmacytoid DCs (Mohty *et al* 2003, Lui 2005), confirming their position within the DC family. Significant levels of IL-10 and IFNα were also secreted from these highly potent DCs compared to the influenza infected, TNFα treated or untreated cells. This is in agreement with previous studies, which demonstrated potent IL-10 secretion from HPIV3 infected peripheral blood mononuclear cells (Sieg *et al* 1996). Also, it has been well documented that paramyxoviruses can downregulate the IFN response, as a means of evading immune abolition (Hengel *et al* 2005, Gotoh *et al* 2002), therefore we were surprised by the extremely high levels of type I IFN produced from HPIV3 infected cells. However in the study by Young *et al*, they demonstrated an inhibition in IFN signalling from a HPIV3 infected fibroblast cell line (Young *et al* 2000), but did not investigate if this inhibition affected antiviral protein production in these cells. Also, fibroblasts are not considered immune cells, so perhaps the virus induces diverse stimulatory affects on different cell types.

From these innate observations, including the strong activating nature of HPIV3 and its propensity to induce elevated levels of IL-10, we speculated that the solution to the riddle of persistence and the failure to induce memory may be due to immune regulation or control of over zealous activation. In order to prove this we investigated allogeneic mixed leukocyte responses and purified CD3+ T cell responses to each of the matured DCs and TNFα treated and untreated cells. We observed significant reduction in T cell proliferation from HPIV3 infected MLR cocultures compared to influenza infected, TNFα treated and untreated MLR cocultures. Inhibition of T cell proliferation from HPIV3 infection has been documented in several reports (Sieg *et al* 1994, Plotnicky-Gilquin *et al* 2001), so these results are in accordance with previous findings. However, when purified CD3+ T cells were stimulated with HPIV3 generated DCs, proliferation was restored in the coculture, which induced comparable levels of proliferation to those observed from the other CD3+ T cell cocultures. This result was baffling but we speculated that it might be due to differences in T cell polarisation. Sieg *et al.* reported that increased IL-10 production from HPIV3 infected

PBMCs was responsible for T cell inhibition and viral persistence (Sieg *et al* 1996), so perhaps elevated levels of IL-10 were responsible for this inhibition in T cell proliferation from HPIV3 infected MLR cocultures. However similar levels of IL-10 and IFNγ were secreted from both the purified CD3+ T cells and mixed leukocyte populations that had been cultured with HPIV3 infected monocytes. Thus, this inhibition does not appear to be related to increased IL-10 secretion.

As IL-2 is imperative for T cell growth and proliferation (Gaffen and Liu 2004) and a lack of IL-2 has been associated with T cell suppression in some virus infections (Andrews *et al* 2001, Flamand *et al* 1995), we investigated IL-2 secretion from HPIV3 infected MLR cocultures. A significant reduction in IL-2 production was noticeable from HPIV3 infected MLR cocultures compared to the other stimulated cocultures. However T cell proliferation was restored when exogenous IL-2 was added at the start of the culture period. Paiardini *et al.* demonstrated a similar effect on lymphocytes from HIV infected individuals, where addition of IL-2 corrected abnormalities in the cell cycle of HIV infected lymphocytes (Paiardini *et al* 2001). Thus, we concluded that this inhibition was IL-2 dependent. Next we investigated if this T cell inhibition from HPIV3 generated DCs cocultured with mixed leukocytes could be due to virus induced apoptosis of lymphocytes. Virus induced apoptosis of lymphocytes has been linked to several viruses, such as HIV (Gougeon *et al* 1996), however similar numbers of apoptotic lymphocytes were observed from both HPIV3 infected and influenza infected MLR cocultures, ruling out the involvement of apoptosis in this T cell inhibition.

Thus, from these results it was hypothesised that T cell inhibition from HPIV3 infected MLR cocultures may be due to a regulatory, third population of cells that are CD3- CD14-, from the mixed leukocytes. Coculture studies revealed that reconstitution of the autologous but not allogeneic CD3- CD14- cells resulted in inhibition of the CD3+ T cell population from HPIV3 infected cocultures. These results emphasise the fact that specific interactions must exist between this regulatory population and its cognate T cell in order to exert this suppression. Again, we noticed no increase in the level of IL-10 secretion from the purified CD3+ T cells that had been cultured with HPIV3 generated DCs and autologous CD3- CD14- cells

compared to the other samples, ruling out its involvement in suppression. However, other mechanisms involving cell-cell contact that are independent of regulatory cytokines have been implicated in studies involving T cell suppression (Kinter *et al* 2004, Boettler *et al* 2005). To explore this possibility in our study, transwells were used to separate the cell populations. A striking restoration in the proliferative capacity of the purified CD3+ T cells from the HPIV3 infected coculture was observed, demonstrating that autologous CD3- CD14- cells from the mixed leukocyte population appear to mediate this inhibition of T cell proliferation evident from HPIV3 infected MLR cocultures, through contact dependent mechanisms. Interestingly, another related virus RSV, also mediated inhibition of T cell proliferation through a direct cell contact mechanism involving cells expressing RSV F protein to mitogen activated PBMCs (Schlender *et al* 2002). Thus perhaps this contact mediated suppression is a common feature employed by viruses from the *Paramyxoviridae* family to enable viral persistence.

In summation, from this data we have identified an autologous, regulatory CD3-CD14- cell population from mixed leukocyte cells that appears to be responsible for the T cell inhibition observed from HPIV3 generated DCs that were cultured with mixed leukocytes. This inhibition is mediated through contact dependent mechanisms but suppression can be reversed by addition of exogenous IL-2. Thus, one can speculate that these regulatory cells that seem to suppress T cell proliferation to HPIV3 generated DCs, may in fact be limiting collateral damage to a highly activated DC population that may induce unrestrained, robust T cell responses *in vivo*.

NK CELL REGULATION OF T CELL RESPONSES DURING HPIV3 INFECTIONS

4.1 INTRODUCTION

It is now abundantly clear that there are multiple pathways to control over zealous immune responses. The cells implicated in regulating these immune responses or pathways, have been regulatory T cells (Mills 2004), overlooking the possibility that other immune cells may be involved. NK cells are important effectors in innate immunity (Hamerman *et al* 2005) and the critical role that these cells play in antiviral and anti-tumour immunity has been well documented (Arnon *et al* 2004, Wallace and Smyth 2005). However, in the grander scheme of regulation, these cells have been largely ignored.

This is puzzling, considering many studies of autoimmune diseases have revealed a regulatory role of NK cells in controlling disease progression (Pazmany 2005). Observations of decreased NK cell activity or cytotoxicity has been associated with several autoimmune diseases, such as multiple sclerosis (MS) (Kastrukoff *et al* 2003) and rheumatoid arthritis (RA) (Combe *et al* 1984), implicating an essential role for these cells in disease abolition. The most convincing data, linking a regulatory role to NK cells in autoimmunity, came from a study investigating experimental autoimmune encephalomyelitis (EAE), which demonstrated that NK cells derived from the bone marrow of rats could inhibit syngenic T cell proliferation in response to the self-antigen, myelin basic protein, as well as to concanavalin A (potent mitogen) stimulated T cells (Smeltz *et al* 1999). *In vivo* depletion studies have also revealed that NK cells can negatively regulate T cell responses during virus infections (Su *et al* 2001). This report demonstrated an increase in CD4 and CD8 T cell proliferation and IFNγ expression, during murine cytomegalovirus (MCMV) infection, when NK cells had been depleted (Su *et al* 2001). Moreover, activated NK cells have been shown to express costimulatory markers and upregulate MHC class II molecules that can regulate T cell activation and function (Zingoni *et al* 2005, Hanna *et al* 2004). One such marker is the OX40 ligand, which has been shown to be expressed on activated

NK cells and can bind to OX40 on T cells, thereby enhancing T cell proliferation and cytokine production of autologous CD4+ T cells in a cell contact dependent manner (Zingoni *et al* 2004). The role of NK cells in downregulating T cell responses has also been observed. Trivedi *et al* found that NK cells could inhibit proliferation of polyclonally activated syngenic T cells, through upregulation of the cell cycle inhibitor, p21, resulting in a G0/G1 cell cycle arrest. This inhibition was contact dependent, reversible and non-antigen specific (Trivedi *et al* 2005). Thus, this preconceived idea that NK cell regulation only involves cytotoxic measures is now being replaced, as new mechanisms are emerging for NK regulation.

Increasing evidence is also emerging that NK cells are also directly involved in DC maturation and regulation (Degli-Esposti and Smyth 2005, Zhang *et al* 2006). This activation appears to be reciprocal, involving both cell-cell contact dependent mechanisms and cytokine secretion (Hamerman *et al* 2005, Walzer *et al* 2005). Piccioli *et al* showed that activated NK cells cultured with autologous immature monocyte derived DCs, at low NK:DC ratios, induced DC maturation, which was mediated by soluble factors such as TNFα and IFNγ, in addition to cell-cell contact. However, at high NK:DC ratios, NK mediated cytotoxicity of immature DCs ensued (Piccioli *et al* 2002). Furthermore, another report found that a small NK cell subset in lymph nodes, expressing CD94/NKG2A receptors, but not killer Ig-like receptors (KIRs) was capable of killing not only immature DCs but mature DCs, to prevent overactivation of DCs (Della Chiesa *et al* 2003). Other studies have demonstrated the ability of mature DCs, stimulated by viruses and microbial compounds, to activate NK cells and their cytotoxic and effector functions (Gerosa *et al* 2005, Romagnani *et al* 2005, Andoniou *et a*l 2005). Again, this activation was observed through secretion of cytokines, such as IL-12 and type I IFNs and also cell-cell contact (Gerosa *et al* 2005). These interactions between NK cells and DCs can greatly influence adaptive immunity, thereby shaping the overall immune response.

Previous studies undertaken demonstrated that in spite of strong innate immune activation, human mixed leukocytes failed to proliferate to HPIV3 infected DCs. However, purified human CD3+ T cells were capable of expanding to these antigen presenting cells. Further investigation revealed that the presence of autologus but not

allogeneic human CD14-CD3- cell population in the MLR was responsible for this control of T cell proliferation. From these results, it was concluded that regulatory T cells did not appear to be involved in this T cell inhibition, as this population expresses the surface marker, CD3. As NK cells display many regulatory roles in adaptive immunity and immune responses to virus infections (Su *et al* 2001, Trivedi *et al* 2005), they appeared to be a strong candidate, which may contribute to this T cell suppression. Therefore, the aim of this study was to investigate if NK cells played a role in the T cell inhibition observed from HPIV3 infected MLR cocultures and to identify and possibly eliminate other populations that may be involved. Hence, firstly the expression of different cell surface markers from the CD3- CD14- population was scrutinised, to identify the most abundant cell types present in this population. Using this information, we then reconstituted select cell populations, identified from the CD3- CD14- cells, to HPIV3 infected DC/CD3+ T cell cultures, in order to see if they restored this inhibitory effect on T cell expansion. Lastly, the molecular mechanisms that may be responsible for inducing T cell suppression were investigated, to generate a thorough picture. It was hoped that this study could provide us with a better understanding of the immune responses to HPIV3 and by focusing on the crucial importance of immunoregulatory cells in directing overall immune responses to virus infections, some light may be shed on the lack of memory T cell responses associated with HPIV3 infections.

4.2 MATERIALS AND METHODS

Table 4.2.1 Lists additional reagents to tables 2.2.1/3.2.1 used in this study.

Product	Catalog #	Company
Human NK cell isolation kit II	130-091-152	Miltenyi Biotec, Gladbach, Germany
Human CD19 microbeads	130-050-301	Miltenyi Biotec, Gladbach, Germany
Human CD56 microbeads	130-050-401	Miltenyi Biotec, Gladbach, Germany
sterile 6-well plate (flat bottom)	140675	Nunc, Roskilde, Denmark
Propidium iodide solution	P4864-10ml	Sigma-Aldrich, Dublin 24, Ireland
RNase A	R4642	Sigma-Aldrich, Dublin 24, Ireland
Glycine (H_2NCH_2COOH)	5.00190.1000	Merck, Darmstadt, Germany
Hydrochloric acid (HCl) 32%	O7115	Sigma-Aldrich, Dublin 24, Ireland
Sodium dodecyl sulphate (SDS)	442442F	BDH, Poole, England
Methanol	RSA007	Reagecon, Shannon, Ireland
Glycerol	G5516	Sigma-Aldrich, Dublin 24, Ireland
Bromophenol blue	B0126	Sigma-Aldrich, Dublin 24, Ireland
β-mercaptoethanol	M3148	Sigma-Aldrich, Dublin 24, Ireland
Cell extraction buffer	FNN0011	Biosource International, California, USA
Protease inhibitor cocktail	P2714	Sigma-Aldrich, Dublin 24, Ireland
Phenylmethylsulfonyl fluoride (PMSF)	P7626	Sigma-Aldrich, Dublin 24, Ireland
Temed	T9281	Sigma-Aldrich, Dublin 24, Ireland
Ammonium persulfate	A9164	Sigma-Aldrich, Dublin 24, Ireland
Acrylamide/Bis-acrylamide, 29:1 ration	A2792	Sigma-Aldrich, Dublin 24, Ireland
Ponceau S solution	P7170	Sigma-Aldrich, Dublin 24, Ireland
Bicinchoninic acid (BCA) reagent A	23228	MSC Ltd., Dublin 15, Ireland
Bicinchoninic acid (BCA) reagent B	23224	MSC Ltd., Dublin 15, Ireland
Mini trans filter paper	4962422	Biorad, Hercules, USA
Nitrocellulose membrane	66485	Pall Life Sciences, MI, USA
Full range Rainbow molecular weight marker	RPN800V	GE Healthcare UK Ltd., Buckinghamshire, UK
Immobilon™ chemiluminescent HRP substrate	WBKLS0050	Millipore, MA, USA
Hyperfilm ECL	RPN1674K	GE Healthcare UK Ltd., Buckinghamshire, UK
Kodak GBX developer	P7042	Sigma-Aldrich, Dublin 24, Ireland
Kodak GBX fixer	P7167	Sigma-Aldrich, Dublin 24, Ireland
Monoclonal anti-human $p21^{cip1}$ Ab	MAB1047	R&D Systems Europe Ltd., Oxon, UK
Monoclonal anti-human $p27^{kip1}$ Ab	MAB2256	R&D Systems Europe Ltd., Oxon, UK
Anti-mouse IgG-HRP Ab	HAF007	R&D Systems Europe Ltd., Oxon, UK
Phospho-Retinoblastoma ($pSer^{249}$/$pThr^{252}$) ELISA	CS0060	Sigma-Aldrich, Dublin 24, Ireland

Table 4.2.2 Lists additional equipment to tables 2.2.2/3.2.2 used in this study.

Equipment	Model	Company
Gel box (electrophoresis)	AE6450	MSC Ltd., Dublin 15, Ireland
Semi-dry transer cassette	AE6675L	MSC Ltd., Dublin 15, Ireland
Mini orbital shaker	SSM1	MSC Ltd., Dublin 15, Ireland
Platform rocker	STR6	MSC Ltd., Dublin 15, Ireland

4.2.1 Cell isolation and purification

Human PBMCs were obtained from buffy coats of healthy donors, as described in section 2.2.1. CD14+ monocytes and CD3+ T cells were purified from PBMCs by positive selection on a MACS column with anti-CD14 and anti-CD3 microbeads (refer to section 2.2.6), respectively and purity was >90% for CD14+ monocytes and >95% for CD3+ T cells as assessed by flow cytometry. The CD14-CD3- population was obtained by depleting the CD14- fraction of CD3+ T cells. Contaminating CD14+ monocytes and CD3+ T cells was <2% of the CD14-CD3- population after purification (see appendix 1C). CD19+ B cells were purified from PBMCs by positive selection on a MACS column with anti-CD19 microbeads (>90% purity). CD56+ CD3- CD14- NK cells were obtained from the CD3- CD14- population by positive selection with anti-CD56 microbeads. Routinely, purity was >90% for CD56+ NK cells. NK cell depletion was carried out on the CD14- cell fraction (MLR) using the NK Cell Isolation Kit II (Miltenyi Biotec). Following positive selection of the non-NK cell population, contaminating NK cells were ≤ 2% on this NK cell depleted fraction (appendix 1D).

4.2.2 Virus stocks and infections

CD14+ monocytes were cultured in complete RPMI on a 24 well plate and were subsequently infected with HPIV3 at a $TCID_{50}$/ml of 6 or influenza virus at a $TCID_{50}$/ml of 7 for 2h at 37°C, as previously described in section 2.2.6.1. In later experiments, CD3- CD14- cells were also infected with HPIV3 at a $TCID_{50}$/ml of 6 for 2h at 37°C. Cells were washed following incubation to remove excess virus and cultured for a further 24h or 48h.

4.2.3 Flow cytometry

4.2.3.1 Cell surface staining

Staining of cells for flow cytometry was performed in accordance to the protocol in section 2.2.5. Additional Abs used in this study, along with Abs from table 2.2.1 (chapter 2) for flow cytometric staining are summarised below in table 4.2.3.

Table 4.2.3 Lists additional human cells surface mAbs used in this study.

Antibody	Fluorochrome	Catalog #	Company
CD40	FITC	11-0409	eBioscience
CD4	FITC	11-0049	eBioscience
CD11b	Pe	12-0113	eBioscience
CD1a	FITC	11-0019	eBioscience
CD56	APC	555518	BD-Pharmingen
CD19	APC	17-0199	eBioscience
DC-SIGN	APC	17-2099	eBioscience
CD56	FITC	11-0569	eBioscience
HLA-A, B, C	FITC	11-9983	eBioscience
rat IgG2a	APC	17-4321	eBioscience
IgG2a	FITC	11-4729	eBioscience

4.2.3.2 Determination of cell cycle progression

Background

The cell cycle can be divided into four phases in proliferating cells. The G1 (gap 1) phase is where the cells are growing and proliferating. Then they enter the S (synthesis) phase, where DNA replication occurs, which is followed by a second G2 phase during which growth and preparation for cell division or mitosis occurs. Lastly, mitosis and the production of two daughter cells occur in the M (mitosis) phase. Also, there is another phase that some cells may enter if the appropriate signals are not present, known as the G0 phase, which is a quiescent, nonproliferative stage (http://users.rcn.com/jkimball.ma.ultranet/BiologyPages/C/CellCycle.html).

Propidium iodide (PI) is the most commonly used dye for cell cycle analysis. It binds to dsDNA by intercalating between the bases and can be excited at 488nm by the

argon laser of the flow cytometer. As PI can also bind to dsRNA, it is essential to treat cells with RNase for optimal DNA resolution. PI fluorescence is usually detected by the FL2 channel of the flow cytometer (http://www.cbm.uam.es/confocal/Manuales/Ioduro%20propidio.pdf). The different phases of the cell cycle can be observed from PI staining as shown in figure 4.2.1.

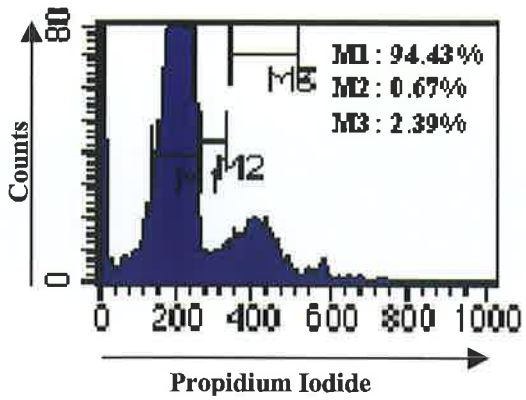

Figure 4.2.1 Illustrates the different phases of the cell cycle. The percentage of cells in each phase: M1=G1 phase, M2=S/M phase and M3=G2 phase, is represented in the histogram.

Method

Cells (>1X10^6 cells) were harvested following three day incubations and washed with ice-cold PBS. They were centrifuged at 800g for 5mins and resuspended in 1ml PBS containing 0.1%BSA. Cells were fixed with 3ml of ice-cold absolute ethanol, vortexed and either incubated for 1h at 4°C or stored at –20°C for several weeks prior to staining. Then, cells were washed with ~3ml ice-cold PBS and centrifuged again at 800g for 5mins and resuspended in 1ml of propidium iodide staining solution (staining solution = PI (40μg/ml) + RNase A (100μg/ml) in PBS). Cells were incubated at 37°C (water bath) in the dark for 30mins and then analysed by flow cytometry (http://www.molbio.princeton.edu/facility/flowcyt/Cycle1.html).

4.2.4 Coculture assays

Cocultures of unstimulated CD14+ monocytes, TNFα treated or virus infected monocytes and allogeneic CD3+ T cells or mixed leukocyte reactions (MLR: CD14- population) were performed at 1:10 ratios for all experiments (refer to section 2.2.10).

In some experiments, CD19+ B cells or CD56+ NK cells were added to the cocultures above in keeping with the same ratio. Later experiments involving NK depleted mixed leukocytes were also performed at the ratio above. Cells were either cultured on 96 well, 24 well or 6 well plates for indicated time points.

4.2.5 Western blot analysis

Table 4.2.3 Lists the buffers used in western blotting.

Tris-Glycine 1L 10X Stock(pH 8.2)
- 30.27g Trizma base
- 144g Glycine
Reservoir Buffer
- 50ml 10X Tris-glycine
- 5ml 10% SDS (10g SDS in 100mld.H_2O)
- 445ml upd.H_2O
Semi-Dry Transfer Buffer
- 50ml 10X Tris-glycine(pH 8.4) } Make up to 500ml dH_20
- 100ml Methanol
- 2.5ml 10% SDS
Washing Buffer 2L
- 200ml 10X PBS
- 1ml Tween 20
- 1800ml dH_20
Upper Tris(4X)
- 0.5M - 60.55g Trizma base
- Made up to 1L
- Ph to 6.8 with HCl
Lower Tris(4X)
- 1.5M – 181.65g Trizma base
- Made up to 1L
- Ph to 8.8 with HCl
4X Sample Solubilisation Buffer (pH6.8)50ml
- 4g SDS, 0.04g Bromophenol blue
- 20ml Glycerol, 24ml 0.25M Tris-HCl
- 2ml β-mercaptoethanol

Background

Western blotting or immunoblotting is a method used to detect specific proteins in a cell lysate. Firstly, cell lysates were prepared from the cells using a cell extraction buffer and protein concentration is quantified. Samples are boiled in a sample buffer solution, containing dye, a sulfurous compound - typically beta-mercaptoethanol, a detergent known as sodium dodecyl sulfate or SDS and glycerol. This boiling denatures the proteins completely. The protein sample is then run on a polyacrylamide gel by electrophoresis (SDS-PAGE [polyacrylamide gel electrophoresis]) and the proteins are separated according to their molecular weight. The proteins are transferred to a stable support such as a nitrocellulose membrane and specific proteins are detected by primary antibodies (mAbs) that bind to their corresponding protein on the membrane. To detect the primary antibody, a secondary antibody directed at the species specific portion of the primary antibody is incubated with the protein membrane.This antibody is commonly, a horsradish peroxidase-linked secondary Ab, which is used in conjunction with a chemiluminescent agent, which react together forming a product that produces luminescence in proportion to the amount of protein. A sensitive sheet of photographic film is placed against the membrane, and exposure to the light from the reaction creates an image of the antibodies bound to the blot (Janeway *et al* 2005).

4.2.5.1 Preparation of cell lysates

Cells (~5.5X10^6 cells) were harvested from 6 well plates following two day cultures. Cells were washed with ice-cold PBS, centrifuged at 800g for 5mins and then lysed in 100µl of cell extraction buffer (Biosource), supplemented with phenylmethylsulfonyl fluoride (PMSF) and protease cocktail inhibitor. Cells were incubated on ice for 30mins in the cell extraction buffer, with vortexing at 10min intervals and then centrifuged at 13000rpm for 10mins at 4°C. The clear lysates were transferred to fresh tubes and aliquoted and stored at –80°C (www.biosource.com).

4.2.5.2 Protein quantification

The protein concentration of samples was measured using the bicinchoninic acid protein (BCA) assay according to the manufacturer's instructions (Pierce). Briefly, BSA standards were prepared by diluting samples 1:2 in dH_2O:

0.0mg/ml

0.125mg/ml

0.25mg/ml

0.5mg/ml

1.0mg/ml

2.0mg/ml

A 96 well plate was loaded as follows:

- 10ul of each protein lysate sample
- 10ul of each BSA standard
- 10ul of lysis buffer (cell extraction)

All of the samples were added to separate wells in triplicate and 200ul BCA reagent (50:1 dilution of BCA reagents A: B) was added to each well. The 96 well plate was incubated at 37°C for 30mins and the absorbance was read at a wavelength of 560nm. The protein concentration of unknown samples was determined from the standard curve generated, much in the same way as that of a sandwich ELISA (2.2.9.2).

4.2.5.3 SDS-PAGE

80µg of protein (cell lysate) was added to sample solubilisation buffer (SSB) and boiled at 95°C for 7mins (total volume = 20-25µl). A 10% resolving gel was prepared as follows:

- 2.9ml lower tris buffer
- 3.5ml acyl (polyacrylamide) stock
- 6.6ml dH_2O
- 116.5µl 10% SDS (made in dH_2O)
- 58.4µl ammonium persulfate (AP) (made in dH_2O)
- 17.5µl temed

(enough for two gels)

A 5% stacking gel was prepared as follows:

- 2ml upper tris buffer
- 1ml acyl stock
- 5ml dH_2O
- 80µl 10% SDS (made in dH_2O)
- 40µl ammonium persulfate
- 12µl temed

Samples were loaded onto wells in the stacking gel and the gel was run at 150V, 90mA and 150W for approximately 2h. A molecular weight marker was also run alongside the samples on the gel to determine protein sizes.

4.2.5.4 Western blot analysis

Following SDS-PAGE the gel was placed on top of two filters, with a nitocellulose membrane (7 X 9cm) on top of the gel, followed by another two filters on top of the membrane, in a semi-dry electroblotting cassette. The filters and membrane were presoaked in semi-dry transfer buffer prior to use. Bubbles were expelled from the gel by gentle rolling over the filter mats with a pipette. The cassette was run at 80V, 400mA and 150W for 45mins. The membrane was then removed from the gel and filter mats and placed in ~10ml Ponceau S staining solution to verify the efficiency and consistency of protein loading and transfer. Figure 4.2.2 illustrates the typical Ponceau staining observed from our cells.

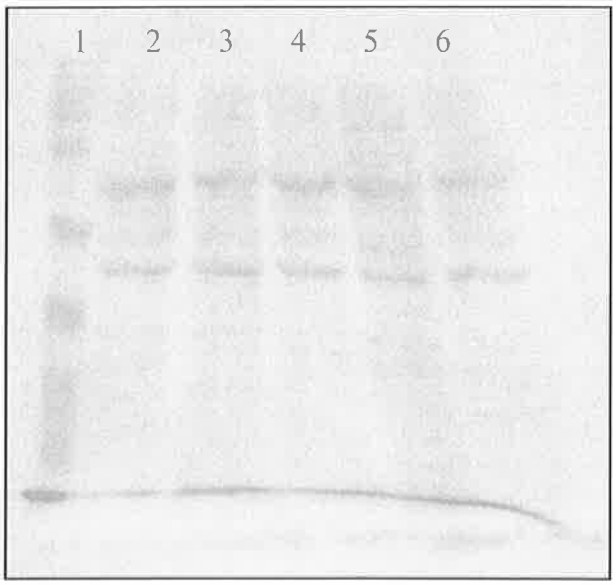

Figure 4.2.2 Illustrates a typical Ponceau S stain. Ponceau stains all proteins on the membrane (from gel). Lane 1 shows the molecular weight marker, while the other five lanes (2-6) contain protein samples. Higher molecular weight proteins reside as thicker bands at the top of the membrane, while smaller molecular weight proteins are visible as thinner bands near the end of the membrane.

The membrane was then blocked for 1h at room temperature (on rocker at 0.2rpm) using 5% marvel (made in washing buffer). The membrane was washed twice at 15min intervals in washing buffer (shaker at 0.1rpm). Primary antibody (diluted in 5% marvel) was incubated overnight with the membrane at 4°C (rocker at 0.2rpm). The following day, the membrane was left at RT for 30mins, before repeating the wash step above. The secondary antibody (diluted in 5% marvel) was then added to the membrane and incubated for a further 2h at RT (rocker at 0.2rpm). The membrane was washed again and incubated with a high sensitivity chemiluminescent HRP substrate (Immobilon™ Western) for 5mins, then placed in a cassette with fresh film covering the blot for 15mins and developed manually. Blot densitometry was analysed using Kodak 1D image analysis software. Antibodies used for Western blotting in this study are summarised in table 4.2.1.

4.2.6 Phospho-Retinoblastoma ($pSer^{249}/pThr^{252}$) ELISA

Background

Phospho-Retinoblastoma (Rb) ($pSer^{249}/pThr^{252}$) ELISA is a phosphorylation site specific assay, that quantifies the amount of Rb protein phosphorylated at both serine 249 and threonine 252 sites. Rb is a tumour suppressor gene, whose product (110kDa protein) plays an important role in regulating cell growth. Mutations in the Rb gene can lead to various forms of cancer. It functions as a negative regulator of cell cycle by binding to transcription factors such as E2F-1, PU.1, ATF-2, UBF, Elf-1 and c-abl. The ability of the Rb protein to bind to these transcription factors is controlled by its phosphorylation state; for example, hypophosphorylated Rb can bind strongly to these transcription factors, while hyperphosphorylated Rb loses this binding affinity. Most notably, hypophosphorylated Rb binds to members of the E2F/DP transcription factor family, preventing the transcription of genes required to pass through the G1 to S phase boundary of the cell cycle. The inhibitory effect of Rb is abrogated when Rb undergoes phosphorylation, catalysed by the cyclin-dependent protein kinases (cdks), which releases the transcription factors enabling them to progress through the cell cycle. Rb contains at least 16 consensus serine/ threonine sequences for cdk phosphorylation. Once dephosphorylated, Rb can then return to its active state of suppression (Giacinti and Giordano 2006).

Method

Phospho-Retinoblastoma (Rb) ($pSer^{249}/pThr^{252}$) ELISA was performed according to the manufacturers instructions (Sigma). Cell lysates were prepared as described above (section 4.2.5.1) and standards and samples were plated in duplicate wells on the pre-coated plate provided. The OD values were then read at 450nm and used to calculate the concentration of phosphorylated Rb in the unknown samples.

4.2.7 ^{3}H-Thymidine Proliferation

After 5 days incubation, proliferation was evaluated by adding 2.5μCi/well ^{3}H-thymidine to the cocultures for the last 5h of incubation. Cells from the 96 well plate were then harvested onto filter mats and analysed on a scintillation counter, as previously described (see section 2.2.11).

4.2.8 Statistical analysis

Statistical significance between samples was determined as described in section 2.2.12.

4.3 RESULTS

4.3.1 CD19+ B cells and CD56+ NK cells are the most abundant cell types found in the CD3- CD14- population

To assess the different cell subsets found in the heterogenous CD3- CD14- population, phenotypic analysis of this cell population was carried out, by looking at an array of surface markers. As expected, ≤ 2% of these cells expressed lineage markers CD14 and CD3, following purification (figure 4.3.1). A high percentage of cells (~15%) expressed the myeloid marker, CD11c, however the B cell marker, CD19 appeared to be the most common cell subset found in this CD3- CD14- population (10%). The next most abundant cell type evident from this population, was NK cells, with 8% of cells expressing the NK cell marker, CD56, closely followed by the myeloid marker CD11b (7%), frequently used to identify macrophage (figure 4.3.1). A smaller population of cells (~5-7%) expressed CD4 and CD123, which are markers generally associated with plasmacytoid DCs. The DC maturation marker, CD83 was found on approximately 6% of cells, while DC-SIGN, a C-type lectin expressed by many DC subsets (ie: myeloid DCs, IL-4 DCs) was undetectable on these cells. This CD3- CD14- population also expressed similar levels of the costimulatory molecules, CD80 and CD86 (~ 4-5%), while a large portion of cells (43%) expressed CD40, a costimulatory molecule commonly found on antigen presenting cells (figure 4.3.1). So, these results identify B cells and NK cells as the most numerous cell subsets found in the CD3- CD14- population.

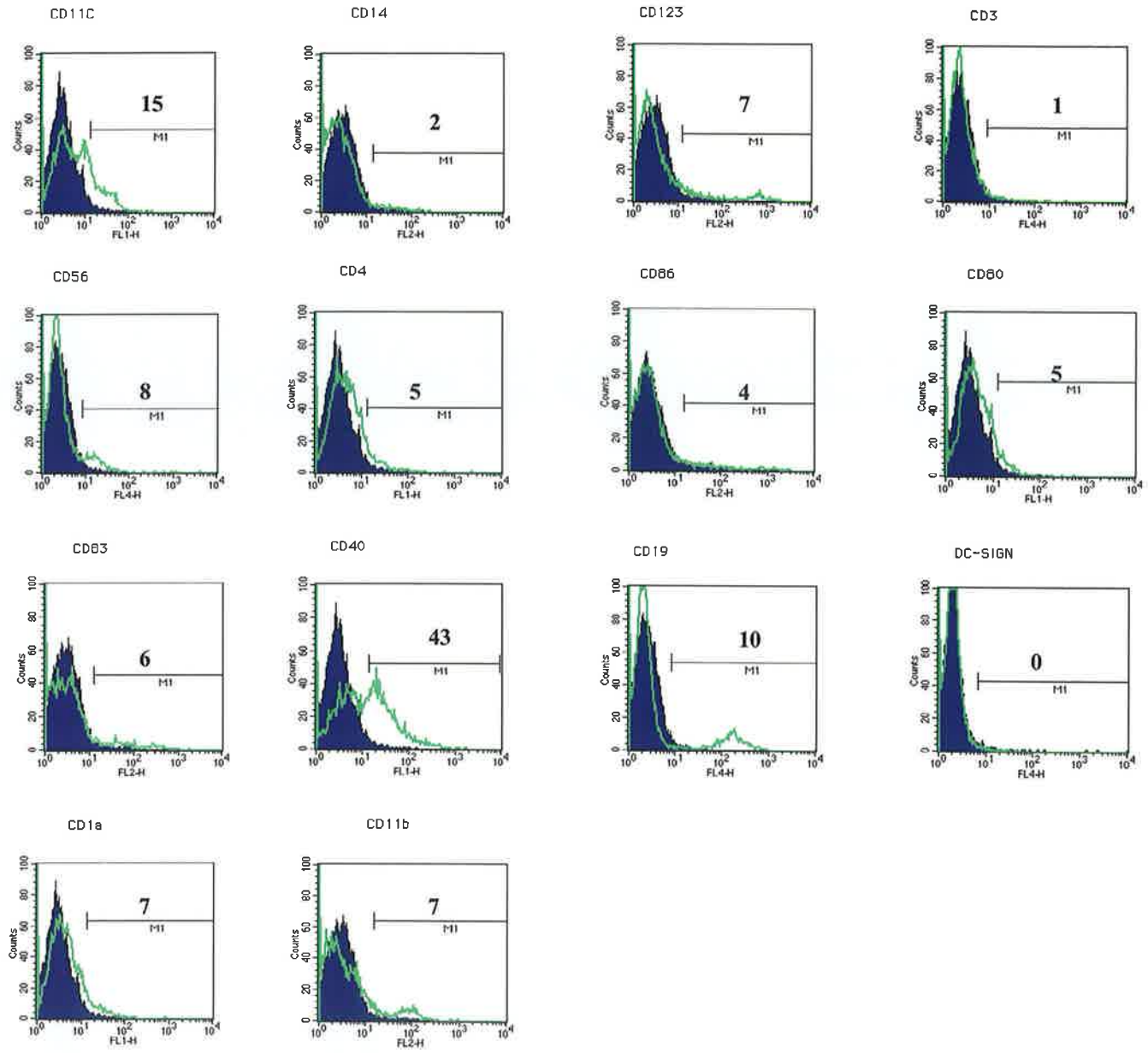

Figure 4.3.1 Phenotypic profile of CD3- CD14- cells. CD3- CD14- cells were purified from human PBMCs as described in section 3.2.1 and surface marker expression of CD11c, CD14, CD40,CD83,CD80, CD86, CD123,CD4, CD56, CD19, DC-SIGN, CD11b, CD1a and CD3 were assessed by flow cytometery. The purple histogram represents the isotype contol for each marker and the green line shows the number and intensity of cells that express that particular marker. The M1 region shows the percentage of positive cells for specific markers. Results are respresentative of two separate experiments (for raw data from repeat experiment refer to appendix 8, table 8.J).

4.3.2 Autologous CD19+ B cells from the CD3- CD14- population are not responsible for T cell inhibition in HPIV3 infected MLR cocultures

Previous studies have already identified that an autologous CD3- CD14- cell population appeared to be responsible for the limited T cell proliferation observed from HPIV3 infected MLR cocultures. Therefore, the next objective was to identify the particular cell subset(s) involved. The most prominent cell type found in the CD3- CD14- population was B cells (figure 4.3.1), hence we investigated if this CD19+ B cell population played a role in regulating T cells from the mixed leukocytes that had been cultured with HPIV3 generated DCs. In order to investigate this, we isolated autologous CD19+ B cells by cell enrichment and restored them to the CD3+ T cell cocultures. These autologous CD19+ B cells were also cultured with mixed leukocyte cocultures, as a control. Previous studies have already revealed that autologous CD3- CD14- cells could reduce CD3+ T cell proliferation when cultured in HPIV3 infected cocultures (3.3.6A-chapter 3). However, clearly, addition of these CD19+ B cells resulted in no decrease in CD3+ T cell proliferation from HPIV3 infected cocultures (figure 4.3.2A). Proliferation was even slightly elevated in these HPIV3 infected cocultures compared to influenza infected, TNFα treated and untreated cocultures (figure 4.3.2A). Furthermore, T cell proliferation was still suppressed in HPIV3 infected MLR cocultures containing autologous CD19+ B cells compared to the other treatments (figure 4.3.2B). This result excludes B cells as a possible cell subset from the CD3- CD14- population that could be involved in T cell inhibition from HPIV3 infected MLR cocultures.

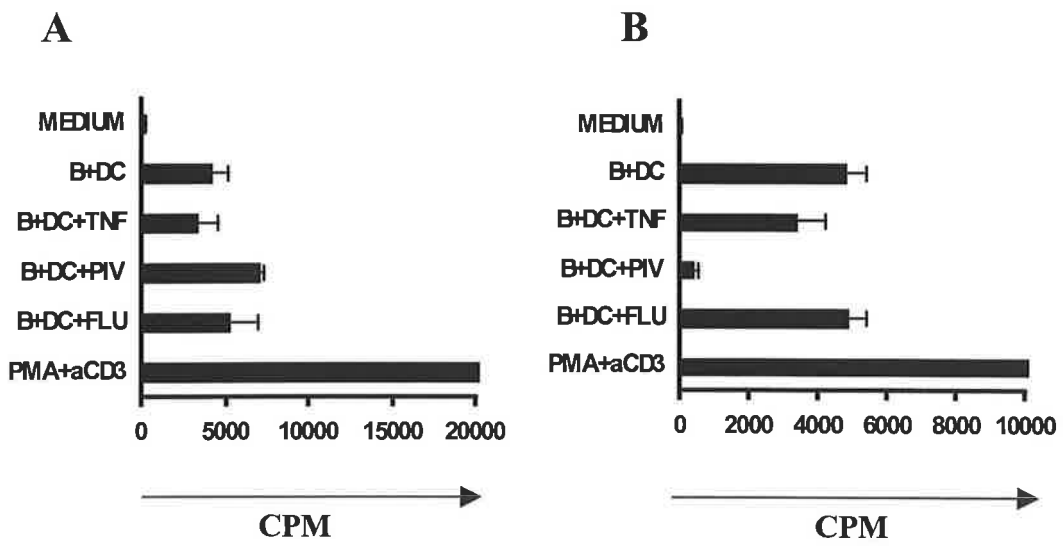

Figure 4.3.2 T cell proliferation profiles from purified CD3+ T cell cocultures and MLR cocultures reconstituted with autologous B cells. (A) Purified CD3+ T cells and (B) mixed leukocytes were co cultured alone (MEDIUM), with CD14+ cells (DCs) and autologous B cells (B+DC), with TNFα treated DC and autologous B cells (B+DC+TNF), with HPIV infected DCs and autologous B cells (B+DC+PIV) and with influenza infected DCs and autologous B cells (B+DC+FLU) (section 4.2.4). Proliferation profiles were measured by ^{3}H incorporation after 5 days (section 4.2.7). Results reflect the mean cpm $\pm$ SE for each sample and are representative of two to three independent experiments (for raw data from repeat experiments refer to appendix 8, table 8.K).

4.3.3 Direct infection of CD3- CD14- cells with HPIV3 upregulates the NK cell marker CD56

B cells were the most common cell subset found in the CD3- CD14- population but did not appear to be involved in T cell inhibition. Repeating these experiments with diverse cell subsets isolated from the CD3- CD14- population, could be a lengthy and laborious task. Therefore, we decided to directly infect the CD3- CD14- cells with HPIV3, to see if any differences were observed in the various surface markers between unstimulated and infected cells, which could aid in the identification of a particular cell type. An extensive array of surface markers was examined but the only notable difference observed between unstimulated and HPIV3 infected CD3- CD14- cells, was an upregulation of the NK cell marker, CD56, on HPIV3 infected cells (figure 4.3.3A and B); however, this result was not reproducible over repeat experiments. There was no increase in the B cell marker, CD19, costimulatory

marker, CD80 or MHC Class I and II, between unstimulated and HPIV3 infected cells (figure 4.3.3A and B). Thus, NK cells may play a role in the observed immune responses associated with HPIV3 infections.

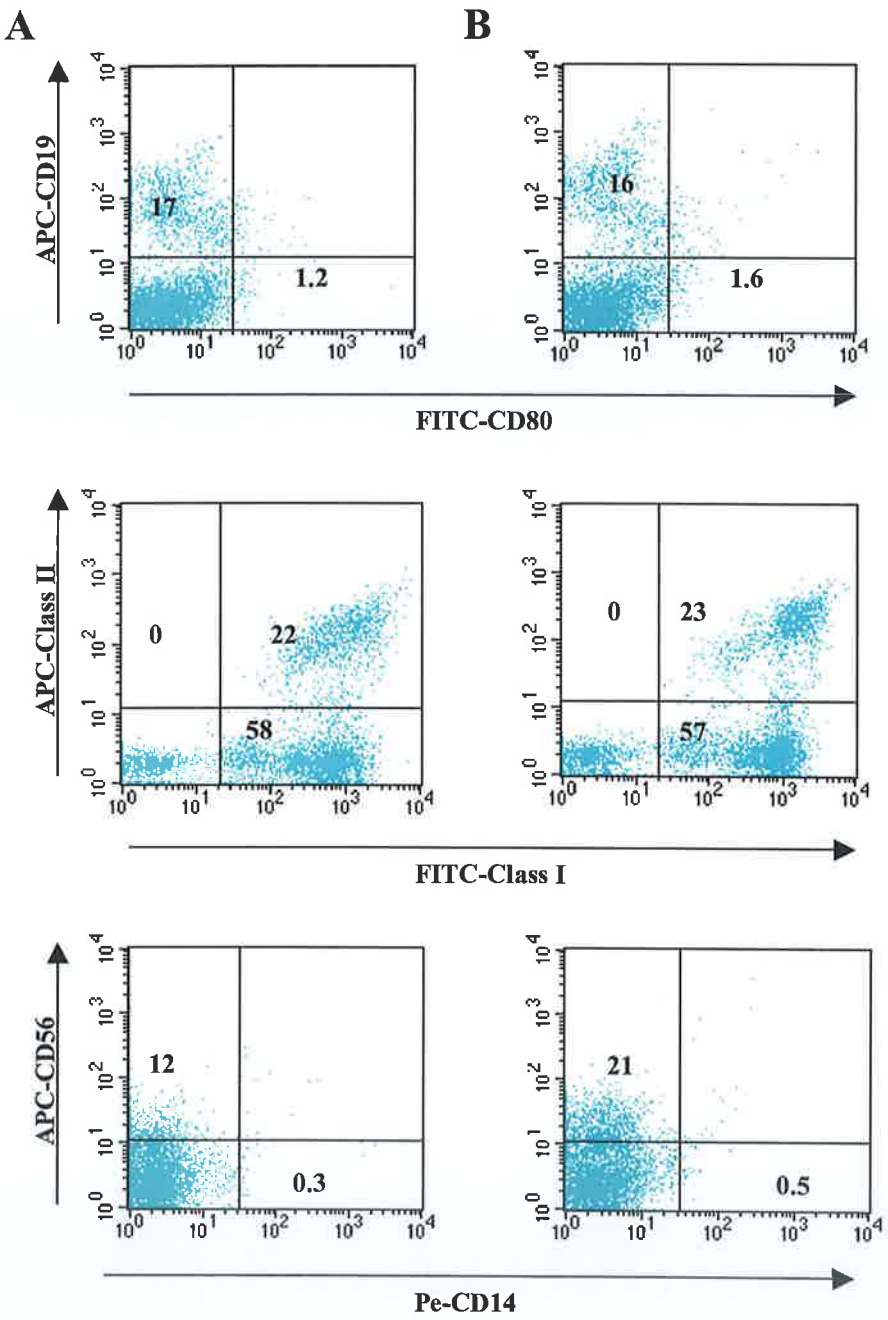

Figure 4.3.3 Expression of surface markers on unstimulated and HPIV3 infected CD3- CD14- cells. (A) Unstimulated CD3- CD14- cells and (B) HPIV3 infected CD3- CD14- cells were harvested after 24h and the cell surface markers CD19, CD80, MHC Class II, MHC Class I, CD14 and CD56, expressed on these cells were assessed by flow cytometry. Quadrant markers were set based on isotype controls and values reflect the percentage of cells in each quadrant. Results are representative of three independent experiments for all surface markers examined, except for CD56 (for raw data from repeat experiments refer to appendix 8, table 8.L).

4.3.4 Autologous CD56+ NK cells can inhibit proliferation of purified CD3+ T cells from HPIV3 infected cocultures

From the results to date, one could speculate that NK cells may be involved in this inhibition, therefore the potential of autologous NK cells to inhibit purified CD3+ T cell proliferation from HPIV3 infected cocultures was investigated. Again, for control purposes, the effect of NK cells on HPIV3 infected MLR cocultures, was also examined. Consistently, addition of these autologous NK cells to purified CD3+T cell cocultures, significantly reduced T cell proliferation from HPIV3 infected cocultures compared to influenza infected, TNFα treated or untreated cocultures (figure 4.3.4A). Moreover, inhibition was still observed in the control experiment from HPIV3 infected MLR cocultures containing autologous NK cells compared to the other cocultures (figure 4.3.4B). This result suggests that autologous NK cells from this CD3- CD14- population may be the regulatory population responsible for the T cell inhibition observed from HPIV3 infected MLR cocultures.

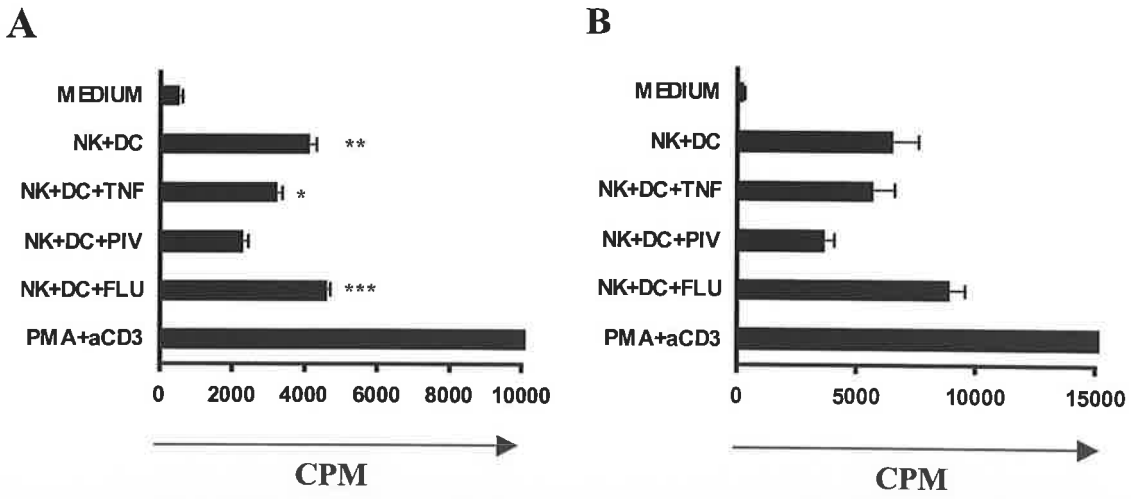

Figure 4.3.4 Proliferation profiles from purified CD3+ T cell cocultures and MLR cocultures reconstituted with autologous NK cells. (A) Purified CD3+ T cells and (B) mixed leukocytes were co cultured alone (MEDIUM), with CD14+ cells (DCs) and autologous NK cells (NK+DC), with TNFα treated DC and autologous NK cells (NK+DC+TNF), with HPIV infected DCs and autologous NK cells (NK+DC+PIV) and with influenza infected DCs and autologous NK cells (NK+DC+FLU) (section 4.2.4). Proliferation profiles were measured by ^{3}H incorporation after 5 days (section 4.2.7). Data reflects the mean cpm $\pm$ SE for each sample. Results are representative of three separate experiments (for statistics from repeat experiments refer to appendix 7, table 7.H and for raw data see appendix 8, table 8.M). *$P \leq 0.05$, **$P \leq 0.01$, ***$P \leq 0.001$.

4.3.5 Lymphocytes from HPIV3 infected MLR cocultures are arrested in the G0/G1 phase of the cell cycle while progression is restored by depletion of CD56+ NK population

Results have demonstrated that NK cells can inhibit T cell proliferation from HPIV3 infected cocultures and previous work has shown that this inhibition does not appear to result in cell death but another arrest mechanism that is overridden by the addition of IL-2. In the light of these observations and earlier reports suggesting a regulatory role of NK cells in T cell cycle progression (Trivedi *et al* 2005), it was investigated if NK cells may be interfering specifically with the cell cycle progression of T cells. Hence, the cell cycle status of the mixed leukocyte populations cocultured with allogeneic CD14+ monocytes infected with HPIV3 or influenza, or treated with TNFα, were examined using PI staining. Consistent with ^{3}H incorporation studies, fewer lymphocytes progressed to the S phase, where DNA synthesis was occurring, when cocultures were infected with HPIV3 (0.19%) compared to influenza infected (1.04%), TNFα treated (0.25%) or medium alone (0.27%)(figure 4.3.5A). Subsequently, only a minor fraction of cells from the HPIV3 infected coculture entered the G2 phase of the cell cycle, compared to the other cocultures (figure 4.3.5A). However, when CD56+ NK cells were depleted from the mixed leukocyte cocultures, a striking increase in the percentage of cells entering the S (1.26%) and G2 (2.52%) phase of the cell cycle was evident from the HPIV3 infected cocultures (figure 4.3.5B). This increase in cell number was comparable to that of influenza infected cocultures and was higher than that of the TNFα treated and untreated cocultures (figure 4.3.5B). Also, lymphocytes were functionally capable of extensively progressing through the different stages of the cell cycle, as evident from the positive control (PMA+aCD3), which contained a high percentage of cells in the S and G2 phases (figure 4.3.5Aand B). Thus, lymphocytes from HPIV3 infected MLR cocultures appear to be arrested in the G0/G1 phase of the cell cycle but progression can be restored by depletion of NK cells from these cocultures. These results strongly suggest a role for NK cells in regulating T cell responses during infection with HPIV3.

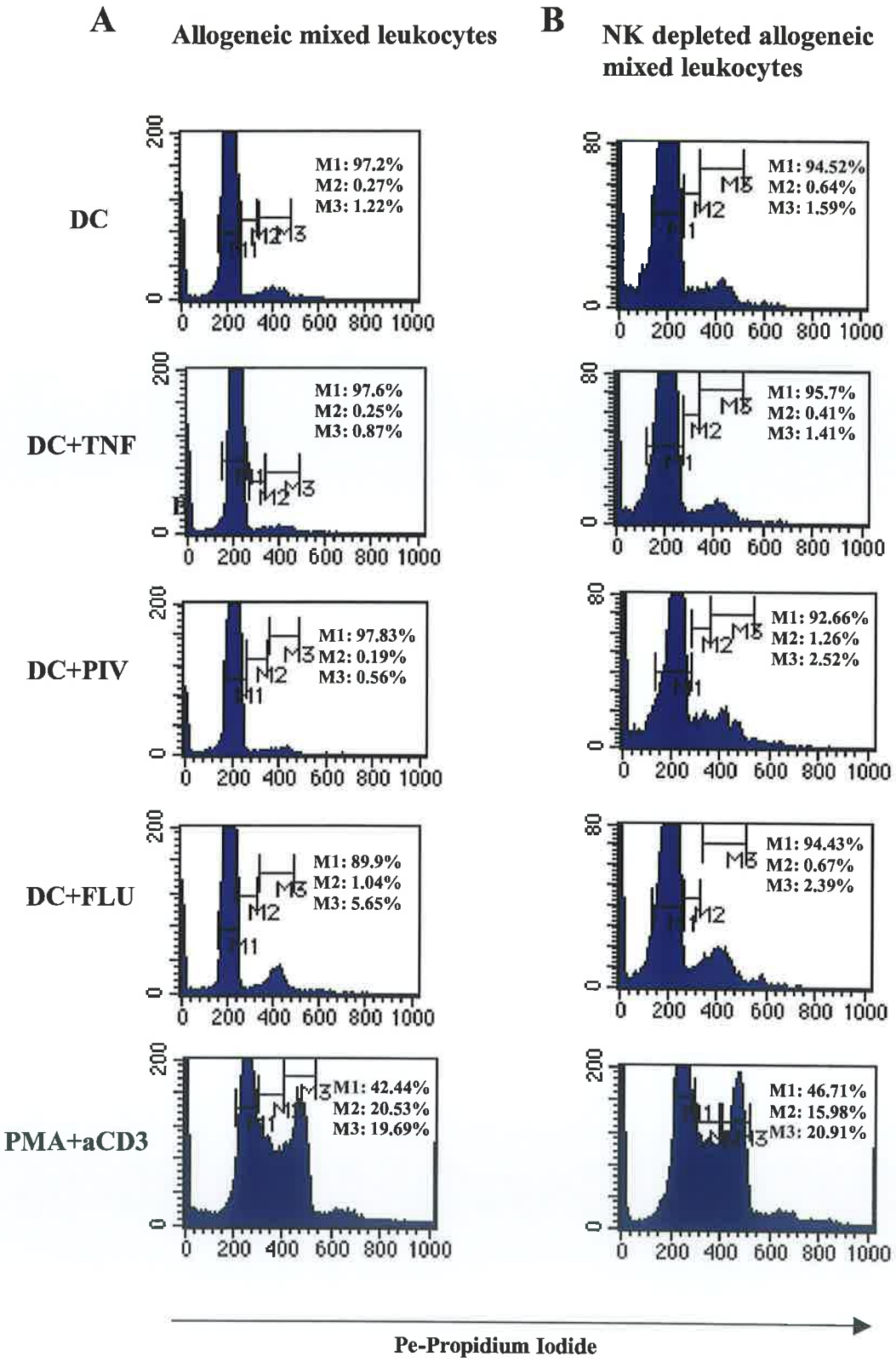

Figure 4.3.5 Cell cycle analysis from mixed leukocyte cocultures and NK depleted mixed leukocyte cocultures. CD14+ cells (DCs) were left untreated or treated with TNFα (DC+TNF) or infected with HPIV3 (DC+PIV) or influenza (DC+FLU) and cocultured with mixed leukocytes or CD56+ NK depleted mixed leukocytes. Cells were harvested from the cocultures at 72h and stained

with propidium iodide and the DNA content from gated lymphocytes was analysed by flow cytometry (section 4.2.3.2). M1 represents the percentage of cells in the G0/G1 phase, M2 represents S phase and M3 represents G2 phase. (A) Cell cycle progression of lymphocytes from allogeneic mixed leukocyte cocultures. (B) Cell cycle progression of lymphocytes from CD56+ NK depleted allogeneic mixed leukocyte cocultures. Results are representative of three independent experiments (for raw data from repeat experiments refer to appendix 8, table 8.N).

4.3.6 NK cells partially prevent p27 degradation in HPIV3 infected MLR cocultures

T cell progression from the G0/G1 phase to S phase of the cell cycle is controlled by the activity of cyclins and cyclin-dependent kinases (cdks). G1 phase progression firstly requires the activity of cyclin D-cdk4/6 complexes and then cyclin E-cdk2 activity is necessary for the G1-S transition. These cyclin-cdk complexes regulate the cell cycle through phosphorylation of the retinoblastoma protein (pRb). Rb hyperphosphorylation results in the release of the transcription factor E2F, which can then activate genes necessary for the S phase of the cell cycle. However, the activities of these cyclin-cdk complexes are tightly regulated by cdk inhibitors, such as p27 and p21 proteins, which are members of the Cip/Kip family of cdk inhibitors (Sherr and Roberts 1999). Therefore, to determine the molecular basis of the HPIV3 infected monocyte induced T cell cycle arrest in the G0/G1 phase, we investigated the status of these cell cycle inhibitors by western blot analysis. Interestingly, high levels of p27 were observed from the HPIV3 generated DCs that were cultured with the mixed leukocytes, which were similar to the levels observed from unstimulated lymphocytes (figure 4.3.6A). However, increased degradation of p27 was evident from the untreated monocyte and influenza infected MLR cocultures compared to the HPIV3 infected MLR coculture (figure 4.3.6A). In contrast, there was a higher level of p27 degradation found in the NK depleted mixed leukocytes cocultured with HPIV3 generated DCs compared to the levels found in unstimulated lymphocytes and even those observed from influenza infected cocultures (figure 4.3.6B). As expected, reduced levels of p27 were evident from the polyclonally activated samples (figure 4.3.6A and B). Conversely, the presence of p21 was only observed in unstimulated lymphocytes from MLR cocultures and faint bands were detected from all samples in

NK depleted MLR cocultures (appendix 5), however, this result was irreproducible. Thus, NK cells appear to partially prevent the degradation of p27 from HPIV3 infected MLR cocultures, resulting in increased levels of p27, which may induce T cell cycle arrest in the G0/G1 phase.

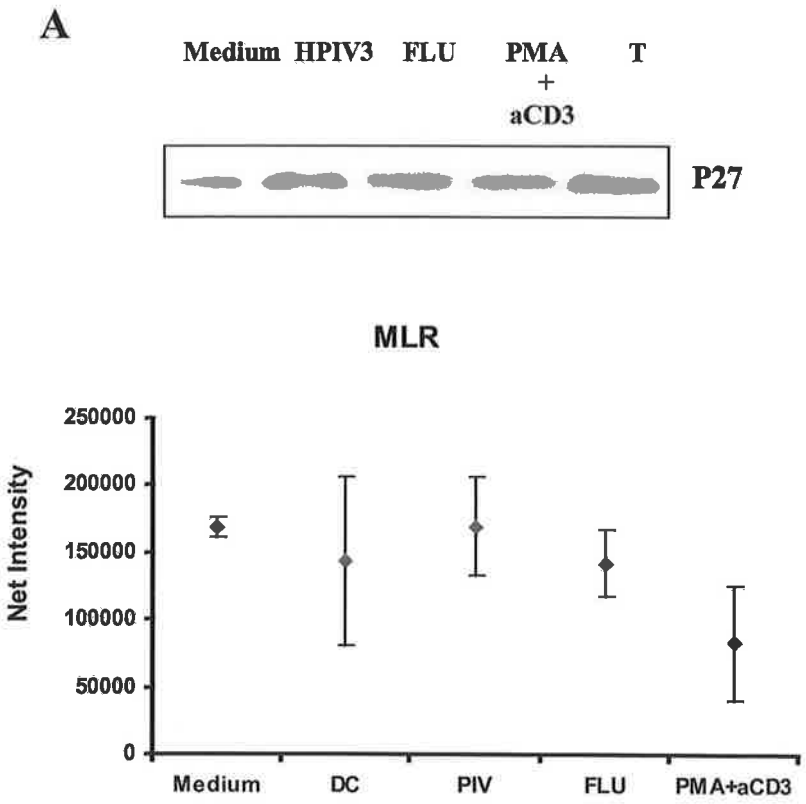

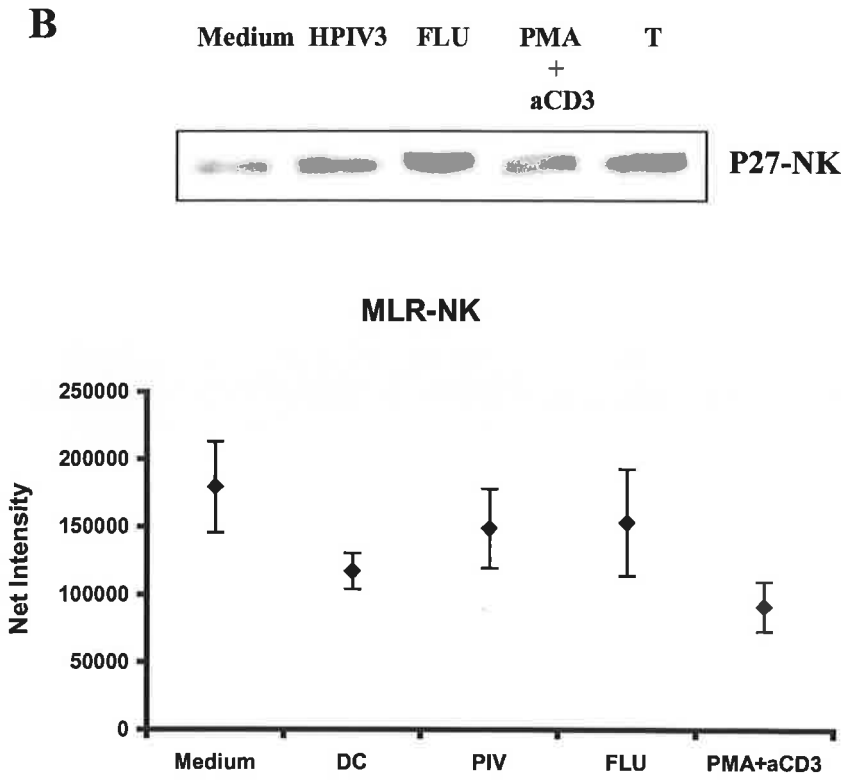

Figure 4.3.6 Western blot analysis of the cell cycle inhibitor p27. Cells were cocultured as described above (figure 4.3.5) and cell lysates were prepared from 48h cultures and analysed for p27 by Western blot (section 4.2.5). Blots and densitometry graphs (net intensity-culmination of two experiments) for p27 are shown for (A) mixed leukocyte cocultures and (B) NK depleted mixed leukocyte cocultures. Blots are representative of two independent experiments.

4.3.7 NK cells exhibit an overall anti proliferative effect on T cells from mixed leukocyte cocultures

Lastly, we investigated if retinoblastoma phosphorylation was impaired, due to the higher levels of p27 observed in HPIV3 infected MLR cocultures. We examined phosphorylation of Rb in both mixed leukocyte cocultures and NK depleted mixed leukocyte cocultures. Interestingly, only small levels of phosphorylated Rb were detected from all MLR cocultures, showing little or no difference between each sample (figure 4.3.7). However, significant levels of phosphorylated Rb were

produced from untreated monocytes, HPIV3 generated DCs and influenza generated DCs that were cultured with NK depleted mixed leukocytes compared to their corresponding non depleted mixed leukocyte cultures (figure 4.3.7). This result suggests that NK cells can exert an overall suppressive effect on Rb phosphorylation or G1-S phase transition. Also, the higher level of p27 observed from HPIV3 infected MLR cocultures does not appear to affect Rb phosphorylation.

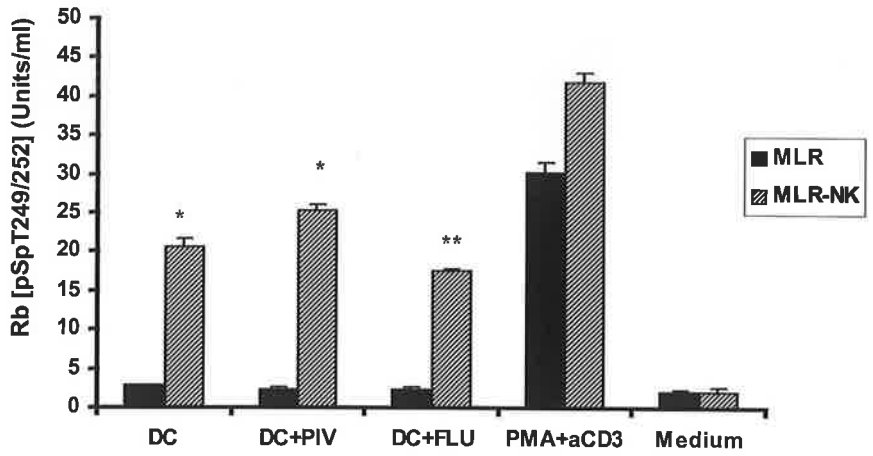

Figure 4.3.7 Rb phosphorylation from mixed leukocyte cocultures and NK depleted mixed leukocyte cocultures. Cells were cocultured as described above (figure 4.3.5) and cell lysates were prepared from 48h cultures. The phosphorylation site specific ($pSer^{249}/pThr^{252}$) ELISA was used to measure the amount of phosphorylated Rb protein (section 4.2.6). Data reflects the mean concentration $\pm$ SD for each sample. Results are representative of two separate experiments (for statistics from repeat experiments refer to appendix 7, table 7.I). $*P \leq 0.05$, $**P \leq 0.01$.

4.4 DISCUSSION

Immune regulation is key to the control of autoimmunity and excessive immune responses to foreign pathogens. This self-protective feature of the host is controlled by a complex regulatory system, consisting of immune cells such as regulatory T cells. These regulatory T cells have played centre stage for many years, as the most pivotal cell type in controlling immune responses (Jiang and Chess 2004). However, recently other immune cells are emerging as critical effectors in regulation (Zhang *et al* 2006). One such cell is the NK cell. NK cells are not only involved in mediating target cell killing of cells but can also regulate innate and adaptive immune responses (Walzer *et al* 2005). They have been shown to be essential regulators in controlling autoimmune diseases (Smeltz *et al* 1999, Kastrukoff *et al* 2003). Also, the role of NK cells in regulating T cell responses to virus infections has been reported (Su *et al* 2001). Thus, our aim was to investigate the regulatory mechanisms at play during HPIV3 infections, paying particular attention to NK cells as possible contenders in this regulatory process. The lack of memory T cell responses associated with HPIV3 infections has been thought to result from T cell suppression (Sieg *et al* 1994, Plotnicky-Gilquin *et al* 2001). Our previous study has already implicated a role for an autologous CD3- CD14- population in suppressing T cell responses during HPIV3 infection. This finding prompted the investigation into the nature of the reduced T cell proliferation exerted by this virus and the exact cell type involved. Therefore, to begin this investigation, the different cell subsets found in this heterogenous CD3- CD14- population were firstly scrutinised. Results demonstrated that the inhibition of T cell proliferation observed from HPIV3 infected MLR cocultures was due to the CD56+ NK cell component of the MLR. Of interest however, the regulation was not exerted by normal NK cytotoxicity but by arrest/delay of cell cycle progression in the G0/G1 transition via degradation of p27 cdk inhibitor.

Through extensive examination of various surface markers, we identified that CD19+ B cells were the most abundant cell type found in the CD3- CD14- population. B cells have been shown to regulate DC function *in vivo* affecting T cell responses (Moulin *et al* 2000), therefore we investigated if these cells played a regulatory role in our system. Autologous B cells did not reduce CD3+ T cell proliferation from HPIV3

infected cocultures compared to influenza infected, TNFα treated and untreated cocultures, eliminating them as the possible cell subset responsible for T cell inhibition. The next most numerous cell type found in the CD3- CD14- population was CD56+ NK cells and interestingly, direct infection of CD3- CD14- cells with HPIV3, upregulated CD56. This clue and several recent reports demonstrating both positive and negative NK cell regulation of T cell proliferation (Zingoni *et al* 2004, Trivedi *et al* 2005) led to the speculation that this group of cells may be involved in the failure of T cells to proliferate to HPIV3 infection. This hypothesis was confirmed by the significant reduction in proliferation of the purified CD3+ T cells upon addition of purified autologous CD56+ NK cells to the HPIV3 generated DC and T cell cocultures.

In the light of these findings we sought to dissect the mechanism exerted by these autologous NK cells to regulate T cell proliferation. NK cells have been shown to inhibit T cell proliferation of polyclonally activated T cells by arresting them in the G0/G1 phase of the cell cycle (Trivedi *et al* 2005). Also, a recent report demonstrated that an increased binding of human NK cells to autologous T cells occurs during mitosis, which was not accompanied by traditional NK killing type responses (Nolte-'t Hoen *et al* 2006). From these studies, it could be speculated that one mode in which NK cells may exert regulatory functions over T cells, is by controlling cell cycle progression. Therefore, the cell cycle progression of lymphocytes from HPIV3 infected mixed leukocyte cocultures and NK depleted mixed leukocytes cocultured with HPIV3 generated DCs was analysed. Lymphocytes from HPIV3 infected MLR cocultures appeared to be arresting in the G0/G1 phase of the cell cycle, with only a small percentage of cells progressing through the S and G2 phases compared to other stimulations. However, interestingly, in the absence of the CD56+ NK populations from HPIV3 infected MLR cocultures, cell cycle progression was restored to levels comparable with influenza infected cocultures.

Inhibition of T cell proliferation by cell cycle arrest has been documented in several studies, involving immunosuppressive viruses, such as HCV or SIV (Yao *et al* 2003, Ndolo *et al* 2002) and respiratory viruses, such as RSV (Schlender *et al* 2002), which is closely related to HPIV3. HCV core protein was shown to prevent degradation of

the cell cycle inhibitor p27 in mitogen activated T cells, inducing cell cycle arrest in the G0/G1 phase (Yao *et al* 2003), while the SIV Nef protein suppressed CD4+ T cell proliferation by preventing the progression of cells into the S phase of the cell cycle, through reduced degradation of the cdk inhibitors p21 and p27 and downregulation of cyclins (Ndolo *et al* 2002). Also, Trivedi *et al* demonstrated that the cell cycle arrest observed in activated T cells that was induced by NK cells was due to increased expression of p21 (Trivedi *et al* 2005). Another report also suggested that the cell cycle inhibitor p27 regulates T cell progression in an IL-2 dependent and independent manner (Appleman *et al* 2000). Therefore, these studies led to the investigation of whether the T cell cycle arrest (G0/G1 phase) observed in lymphocytes from HPIV3 infected MLR cocultures, was due to the expression of the cdk inhibitors, p21 and p27. The levels of p27 and p21 protein degradation from HPIV3 infected monocytes cocultured with mixed leukocytes or with NK depleted mixed leukocytes were analysed. Interestingly, NK cells appeared to partially prevent degradation of p27 but not p21 from HPIV3 infected MLR cocultures. Similar levels of p27 were observed from both the HPIV3 infected MLR coculture and unstimulated lymphocytes, while increased p27 degradation was evident from the HPIV3 generated DCs that had been cocultured with NK depleted mixed leukocytes compared to the unstimulated lymphocytes. Also, p21 and p27 induced G0/G1 arrest can be associated with low phosphorylation of the retinoblastoma (Rb) protein, which has been demonstrated in several studies (Chen *et al* 2004, Yao *et al* 2003). Hence, we investigated the phosphorylation of Rb from our infected cocultures. The high level of p27 observed from HPIV3 infected MLR cocultures did not appear to effect Rb phosphorylation. However, as phosphorylated Rb levels were so low in this assay, we cannot categorically prove this statement. Interestingly, significant Rb phosphorylation was observed from all the NK depleted mixed leukocyte cocultures compared to their corresponding non- depleted mixed leukocyte cocultures. Thus, our results implicate that NK cells may exert a more general, anti-proliferative role in controlling immune responses.

In conclusion, we have identified that autologous NK cells from HPIV3 infected MLR cocultures appear to be responsible for the T cell inhibition observed from these infected cocultures. NK cell regulation of T cell proliferation did not involve cytotoxic measures but was mediated through direct cell contact dependent

mechanisms, which ultimately resulted in T cell cycle arrest in the G0/G1 phase, via an IL-2 dependent mechanism involving the cell cycle inhibitor p27. Thus, the role of NK cells in HPIV3 infections could be to limit immunopathology induced by over zealous immune responses, but this response may inadvertently lead to HPIV3 persistence and reduce the memory T cell repertoire, by limiting T cell proliferation.

IMMUNE RESPONSES TO A NOVEL REPLICATION DEFICIENT HPIV3 VACCINE

5.1 INTRODUCTION

Human Parainfluenza virus type 3 (HPIV3) is a major cause of respiratory illness in both adults and children (Chanock *et al* 2001, Marx *et al* 1999). Despite years of research, a licensed vaccine for HPIV3 is still unavailable. The lack of durable immunity, and recurrent infections associated with HPIV3 and the dearth of understanding, regarding its complexity in terms of host/virus relationship, are obstacles to effective immunisation. This has led to successive failures in HPIV3 vaccine development. Initially, inactivated vaccines were developed, such as the formalin-killed whole HPIV1, 2 and 3 trivalent vaccine (Henrickson 2003, Fulginiti *et al* 1969). Although children immunised with this vaccine, developed antibodies to all serotypes, the levels produced were lower than that of the natural infection, thus failing to protect children against these viral strains (Fulginiti *et al* 1969). More recently, two live attenuated HPIV3 vaccines appear more promising (Durbin and Karron 2003). HPIV3cp45 vaccine is an attenuated HPIV3 vaccine produced by 45 passages of the virus in primary monkey kidney cells at low temperatures (Belshe and Hissom 1982). This vaccine was shown be to immunogenic and safe in seronegative children (Belsche *et al* 2004). The antigenically related attenuated bovine PIV3 vaccine has also been shown to be protective, safe and immunogenic in infants (Karron *et al* 1995). However, both vaccine candidates were found to be overattenuated in adults and seropositive children (Clements *et al* 1991, Karron *et al* 1995a, Karron *et al* 1995). Also, due to further advances in genetic engineering, recombinant DNA technology has enabled the development of chimeric or hybrid vaccines such as the attenuated bovine-human PIV3 virus developed by Haller *et al* (Haller *et al* 2000). This vaccine consists of a temperature sensitive recombinant bovine PIV3 backbone, containing the HN and F genes of HPIV3 and was shown to be safe and protect against challenge with wild type HPIV3 in hamsters (Haller *et al* 2000). Thus, these technological advances in vaccine design should facilitate the development of improved HPIV3 vaccines.

On this project, collaborators (Wolfgang Neubert, Max-Planck-Institute of Biochemisty, Munich, Germany and Grazia Cusi, Department of Molecular Biology, Siena, Italy) have developed, a novel sendai virus (SeV) replication deficient vaccine, expressing RSV F and HPIV3 F and HN genes. SeV is the murine form of HPIV1 and is considered to be non-pathogenic in humans (Bitzer *et al* 2003). This replication deficient SeV vector, has a truncated P gene, which is needed for virus replication, enabling the vaccine to be replication deficient and so providing essential safety features to the vaccine's design. Then inserted into its genome are chimeric HPIV3 F and HN genes and a mutated RSV F gene, which are major glycoproteins of these viruses and are important viral epitopes associated with inducing protective immunity (Chanock *et al* 2001). In this study, the chief objective was to compare immune responses to this novel SeV replication deficient vaccine in both the human *ex vivo* model and a murine *in vivo* model. Although HPIV3 does not replicate efficiently in mice, this model provides a good readout for immunological responses *in vivo*. Our focus was mainly on the HPIV3 component of the vaccine and its immune responses *in vivo*, in terms of antibody production and T cell responses. Trial vaccine contructs were firstly analysed for their immunogenicity *in vivo*, to enable background information to be gathered for efficient vaccine design. Virosomes, which are empty viruses that contain only envelop proteins were considered as possible vectors for delivering the vaccine, as they can provide essential adjuvant properties, required for poorly immunostimulatory vaccines. Thus, T cell proliferation to different virosomes was also assessed from the human *ex vivo* model. Previous studies using the human *ex vivo* model, have demonstrated that HPIV3 can inhibit T cell proliferation from mixed leukocyte cocultures. Therefore, by thoroughly investigating immune responses to the vaccine *in vivo* and in the developed human *ex vivo* model, it was hoped that this would demonstrate if the vaccine could possibly circumvent the T cell suppressive immune responses associated with HPIV3 infections.

5.2 MATERIALS AND METHODS

Table 5.2.1 Additional reagents to table 2.2.1 (chapter 2) used in this study.

Product	Catalog #	Company
purified anti mouse CD3	553057	BD pharmingen, Oxford, England
HRP-rat anti mouse IgG	40990572	Zymed laboratories Inc.,San Francisco, USA
Mouse IFNg duoset ELISA kit	DY485	R&D Systems Europe Ltd., Oxon, UK
Mouse IL-5 duoset ELISA kit	DY405	R&D Systems Europe Ltd., Oxon, UK
Bicarbonate buffer capsules	C3041	Sigma-Aldrich, Dublin 24, Ireland
70μm cell strainer	352350	BD Biosciences Europe, Belgium
Vetalar V (ketamine)	23111	Bioresource Unit, TCD
Chanazine (2%)/xylazine (2%)	L18376/B	Bioresource Unit, TCD

5.2.1 *In vivo* animal studies

Six-week old female Balb/c mice were purchased from Harlan UK Limited and were housed in pathogen-free conditions. All immunisations were subsequently carried out two weeks post delivery. Each mouse (~ 20g) received 200μl anaesthetics, which were administered intraperitoneally, prior to immunisation. Anaesthetics were prepared as follows: 0.5ml ketamine + 0.25ml xylazine + 4.25ml diluent (0.9% sterile sodium chloride in distilled water). In all experiments either intranasal (i.n) or intraperitoneal (i.p) immunisations were performed and animals were reboosted two weeks prior to sacrafice, on day 35.

5.2.1.1 Immunisations

***5.2.1.1.1 Experiment 1:* *In vivo* immune responses to SeV wild type and SeV expressing chimeric HPIV3 F and HN genes**

Mice were infected with either sendai virus (SeV) wild type (wt) or with SeV expressing chimeric HPIV3 proteins F and HN (produced by our collaborators Wolfgang Neubert, Max-Planck-Institute of Biochemisty, Munich, Germany and Grazia Cusi, Department of Molecular Biology, Siena, Italy). Chimera 1 (ch) = HN (composed of HPIV3 ectodomain and SeV transmembrane and cytoplasmic domains)

and chimera 3 = F (composed of HPIV3 ectodomain and SeV transmembrane and cytoplasmic domains).

SeV genome structure: 3'- ld- | N | P | M | F | HN | L | -tr-5'

SeV expressing chimeric HPIV3 F and HN:

3'- ld - | N | P | M | F^{ch} | HN^{ch} | L | -tr-5'

Method

SeV wt (stock= $727X10^6$ pfu/ml) and SeV (ch1+ch3) (stock= $150X10^6$ pfu/ml) were diluted to $1X10^7$ pfu/ml and $1X10^5$ pfu/ml in diluent (0.1% sterile BSA in PBS). For i.n immunisations, units were given 30µl of virus per nose and for i.p mmunisations, units were injected with 150µl of virus. Eight groups altogether were immunised with four units per group (table 5.2.2)

Table 5.2.2 Summarises the experimental design used for experiment 1.

Group	Concentration (pfu/ml)	Intranasal Immunisation (30µl)	Intraperitoneal Immunisation (150µl)
1) Control (diluent ie. PBS)	–	Yes	–
2) SeV wt	$1X10^7$	Yes	–
3) SeV wt	$1X10^5$	Yes	–
4) SeV (ch1+ch3)	$1X10^7$	Yes	–
5) SeV (ch1+ch3)	$1X10^5$	Yes	–
6) Control	–	–	Yes
7) SeV wt	$1X10^7$	–	Yes
8) SeV (ch1+ch3)	$1X10^7$	–	Yes

Day 35, mice were sacrificed and spleens and serum samples were taken. Spleens and were isolated into complete RPMI and mashed through 70μm filters. Filters were washed with ~3ml cRPMI and samples were centrifuged at 1200rpm for 7mins. Supernatants were decanted and pellets were resuspended in 2ml cRPMI. Cells were counted (1:50 dilution) using EB/AO staining (section 2.2.2) and plated in triplicate wells at $2X10^6$cells/ml on 96 well plates. After a three day incubation, supernatants were harvested from cells and stored at –20°C.

Blood was collected in microtubes and left to stand at room temperature for 1h, followed by incubation at 4°C for 1h. Samples were centrifuged at 13000rpm for 5mins and the clear upper layer or serum (IgG) was removed and stored at –80°C.

T cell responses were investigated by restimulating cells from spleens with particular antigens. UV inactivated (20mins) SeV wt at a concentration of $1X10^6$ pfu/ml and $1X10^4$ pfu/ml and BPL (β-propiolactone) inactivated HPIV3 (stock=9mg/ml) at a concentration of 10, 5 and 1μg/ml were used as antigens. PMA (concentration of 25ng/ml) and anti-mouse CD3 mAb (concentration of 1μg/ml) were diluted in cRPMI and used as a positive control in these experiments.

5.2.1.1.2 Experiment 2: ***In vivo*** **immune responses to wild type SeV and a replication deficient SeV vector (SeVV)**

Mice were immunised with either SeV wt or replication deficient SeV vector (SeVV) produced by Wolfgang Neubert and Sascha Bossow, Max-Planck-Institute of Biochemisty, Munich. This replication deficient SeVV expressed a truncated P gene (Δ2-77). The truncated P gene inhibits virus replication, as functional P, along with L and N, are required for virus replication. For amplification purposes, this SeVV also expressed a mutated F gene, which enabled the virus to infect many different cell types, as usually infection is restricted to epithelial cells of the respiratory tract, which contain tryptase clara (trypsin-like protease), required to activate F. Therefore, this mutated F gene has purposely been designed to overcome cell tropism, permitting F activation by an ubiquitously expressed protease, furin, instead.

SeVV genome structure: 3'- ld-

N	$P_{\Delta 2\text{-}77}$	M	Fmut	HN	L

-tr-5'

Method

SeV wt and the replication deficient SeVV (stock= $26X10^6$ ciu [cell infectious units]/ml) were diluted to $1X10^7$ and $1X10^5$ pfu or ciu/ml in diluent. All units were immunised intranasally and each group contained four units (table 5.2.3).

Table 5.2.2 Summarises the experimental design used for experiment 2.

Group	Concentration	Intranasal Immunisation (30µl)
1) Control (PBS)	–	Yes
2) SeV wt	$1X10^7$ pfu/ml	Yes
3) SeV wt	$1X10^5$ pfu/ml	Yes
4) Replication deficient SeVV	$1X10^7$ ciu/ml	Yes
5) Replication deficient SeVV	$1X10^5$ ciu/ml	Yes

Day 35, units were sacrificed and spleens and serum were isolated and treated as described above. UV inactivated SeV wt at a concentration of $1X10^6$ pfu/ml and $1X10^4$ pfu/ml was used to restimulate T cells from spleens and lymph nodes and PMA and aCD3 (concentrations as for experiment 1) were used as positive controls.

***5.2.1.1.3 Experiment 3*: *In vivo* immune responses to the replication competent final vaccine**

Mice were intranasally immunised with the replication competent final vaccine (SePIV47E) produced by Wolfgang Neubert and Sascha Bossow, Max-Planck-Institute of Biochemisty, Munich. SePIV47E contained both chimera 1 and 3 and the mutated F gene from RSV lacking the transmembrane and cytoplasmic domains which was inserted behind the P gene.

SePIV47E genome structure:

3'- ld - | N | P [RSV $_{Fmut}$] | M | F^{ch} | HN^{ch} | L | -tr-5'

Method

SePIV47E (stock= $3.6X10^9$ ciu/ml) was diluted to $1X10^7$ and $1X10^5$ ciu/unit in diluent and administered intranasally. Each group contained five units (table 5.2.4).

Table 5.2.2 Summarises the experimental design used for experiment 3.

Group	Concentration (ciu/unit)	Intranasal Immunisation (30µl)
1) Control (diluent ie. PBS)	–	Yes
2) SePIV47E	$1X10^7$	Yes
3) SePIV47E	$1X10^5$	Yes

Day 35, units were sacrificed and spleens and serum were isolated and treated as described above. UV inactivated SeV wt at a concentration of $1X10^6$ pfu/ml and $1X10^4$ pfu/ml and BPL inactivated HPIV3 at a concentration of 10, 5 and 1µg/ml were used as antigens to restimulate T cells from spleens and lymph nodes and PMA and aCD3 (concentrations as for experiment 1) were used as positive control antigens.

5.2.1.1.4 Experiment 4: ***In vivo*** **immune responses to the replication deficient final vaccine**

Mice were immunised with the replication deficient final vaccine (SePIV56) produced by Wolfgang Neubert and Sascha Bossow, Max-Planck-Institute of Biochemisty, Munich. SePIV56 contained both chimera 1 and 3 and the mutated F gene from RSV which was inserted behind a truncated P gene (Δ2-77). The truncated P gene inhibits virus replication.

SePIV56 genome structure:

3'- ld -

N	$P_{\Delta 2\text{-}77}$ [RSV_{Fmut}]	M	F^{ch}	HN^{ch}	L

-tr-5'

Method

Due to limited stocks, SePIV56 (stock= $4.36X10^6$ciu/ml) at a concentration of $1.3X10^5$ and $1.3X10^4$ ciu/unit was prepared and administered intranasally. Each group contained five units (table 5.2.5).

Table 5.2.2 Summarises the experimental design used for experiment 4.

Group	Concentration (ciu/unit)	Intranasal Immunisation (30µl)
1) Control (diluent ie. PBS)	_	Yes
2) SePIV56	$1.3X10^5$	Yes
3) SePIV56	$1.3X10^4$	Yes

Day 35, units were sacrificed and spleens and serum were isolated and treated as described above. BPL inactivated HPIV3 at a concentration of 10, 5 and 1µg/ml was used to restimulate T cells from spleens and lymph nodes and PMA and aCD3 (concentrations as for experiment 1) were used as positive controls.

5.2.2 Antibody ELISA

Background

An indirect ELISA can be used to quantify the amount of antibody produced in a sample. Indirect ELISAs are similar to sandwich ELISAs (section 2.2.9) but instead of coating the 96 well plate with a mAb, the plate is coated with a particular antigen, known to induce the antibody to be detected (figure 5.2.1). The antibody sample is then added to the wells on the plate, where it binds to its particular antigen. For

detection, an enzyme-linked antibody (such as a HRP-conjugated Ab) specific for the antibody of interest is added to the plate, followed by a substrate (such as TMB). The enzyme catalyses the conversion of the substrate into a coloured product, which is directly proportional to the amount of antibody present.

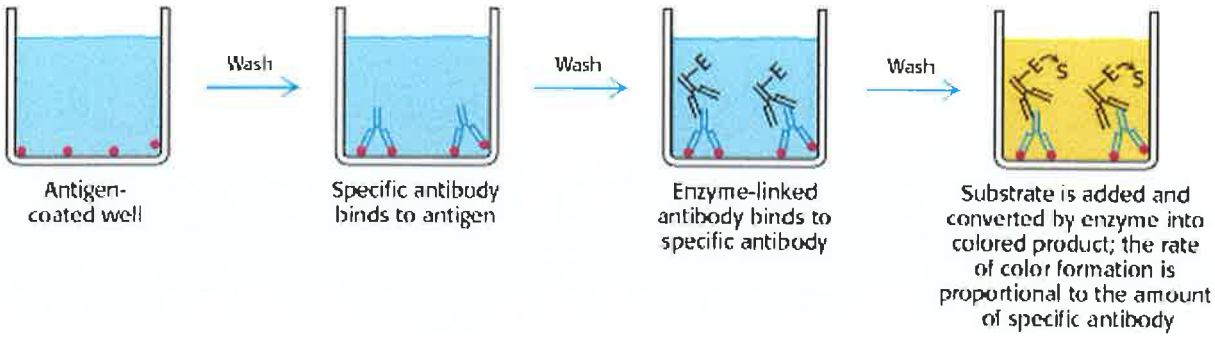

Figure 5.2.1 Illustrates the principles of an indirect ELISA.
(Taken from: http://www.ncbi.nlm.nih.gov/books/bv.fcgi?rid=stryer.figgrp.515)

5.2.2.1 IgG ELISA

96 well plates were coated with antigen (inactivated virus) dissolved in bicarbonate buffer at a concentration of 1µg/ml (100µl/well) and incubated overnight at 4°C. The following day, plates were washed three times in 1X PBS, containing 0.05% TWEEN and were blocked with 1% BSA in bicarbonate buffer (200µl/well) for 2h at room temperature. Plates were washed again and samples (serum or lung) were plated at 1/50 dilutions (50µl bicarbonate buffer was firstly added to each well of the 96 well plate. Samples were diluted 1/25 with bicarbonate buffer [i.e. 8µl sample + 192µl bicarbonate buffer] and 50µl of diluted samples were added to triplicate wells at the top of the plate containing 50µl bicarbonate buffer). Samples were mixed and diluted 1/2 (doubling dilutions) down the 96 well plate and left to incubate overnight at 4°C. The plates were washed again and IgG (serum) antibodies were detected as follows:

IgG: HRP-rat anti-mouse IgG Ab was diluted 1/500 in bicarbonate buffer (100µl/well) and incubated at room temperature for 2h. Plates were washed again and antibody was detected using TMB (100µl/well). The reaction was stopped by adding sulphuric acid to the plate and samples were read at 450nm in the plate reader.

5.2.2.2 Calculating results

The optical density (OD) mean and standard deviation X 2 (2SD) of the control samples (usually PBS) are used to determine the standard line. On a graph, the OD values were plotted (y axis) against $\log_{10}$ of the reciprocal end point titre (x axis) ($\log_{10}$ of the reciprocal end point e.g. 1/400 is $\log_{10}$ 400) and the standard line was drawn on the graph. The values for OD vs $\log_{10}$ reciprocal end point for each of the test samples were plotted and the line of best fit through these points was drawn until it transected the standard or control sample line. At this point a perpendicular line was drawn down to read the end point titre ($\log_{10}$ reciprocal) off the x axis for each sample.

5.2.3 ELISA

Murine IFNγ and IL-5 Duoset ELISA (table 5.2.1) developmental kits (sandwich ELISA) were used to quantify cytokines secreted into cell supernatants. ELISA kits were used in accordance to the manufacturers instructions (R&D) and sample concentration was determined from the standard curve for each cytokine (section 2.2.9).

5.2.4 Human *ex vivo* infections

Human CD14+ monocytes ($1x10^6$ cells/ml) were cultured in complete RPMI on a 24 well plate and were subsequently infected with UV inactivated SePIV56, live SePIV56 at $1x10^6$ ciu/ml, HPIV3 ($TCID_{50}$ 10^6/ml) or influenza virus ($TCID_{50}$ 10^7/ml). CD14+ monocytes were also infected with immunopotentiating reconstituted virosomes (IRV), which are empty viruses that contain only envelope proteins. IRIV (influenza virosome: stock= 150μg/ml), IRPV (HPIV3 virosome: stock= 10μg/ml) and IRSV (SeV virosome: stock= 80μg/ml) were produced by Marius Loetscher, Berna Biotech AG, Switzerland and were used at a concentration of 5μg/ml to infect monocytes. Cells were cultured for 2h at 37°C as previously described in section 2.2.7

(chapter 2). Following incubation cells were washed to remove excess virus and cultured for a further 24h.

5.2.5 Human coculture assays

Cocultures of unstimulated CD14+ monocytes ($2X10^4$ cells/ml) and virus infected monocytes and allogeneic purified CD3+ T cells or mixed leukocyte reactions (MLR: CD14- population) were performed at 1:10 ratios ($2X10^5$ cells/ml) for all experiments (refer to section 2.2.10) on 96 well plates.

5.2.6 ^{3}H-Thymidine Proliferation

After 5 days, proliferation was evaluated by adding 2.5μCi/well ^{3}H-thymidine to the cocultures for the last 5h of incubation. Cells from the 96 well plate were then harvested onto filter mats and analysed on a scintillation counter, as previously described (see section 2.2.11).

5.3 RESULTS

5.3.1 *In vivo* immune responses to SeV wild type and SeV expressing chimeric HPIV3 F and HN genes

Preliminary experiments involved examining immune responses to different vaccine components or constructs. Firstly, it was necessary to investigate if there was cross reactivity between SeV and HPIV3 antigens. Balb/c mice received either i.n or i.p immunisations with SeV wt and SeV expressing chimeric HPIV3 F and HN genes. As expected, high levels of anti-SeV serum IgG were produced *in vivo* in response to i.n infections at the higher dose of SeV (10^7) compared to the lower dose (10^5), while moderate levels of IgG were only detected in serum from the chimeric SeV at the higher dose (10^7) of infection, when UV inactivated whole SeV antigen was used for detection (figure 5.3.1A). However, when BPL inactivated whole HPIV3 antigen was used to detect anti-HPIV3 serum specific IgG, elevated levels of IgG were produced in serum samples from the chimeric SeV at both concentrations compared to moderate to low titres detected in serum from the SeV wt samples (figure 5.3.1B). Similar results were obtained from the serological studies performed on serum samples from i.p immunisations (figure 5.3.1C and D). Thus, SeV and chimeric SeV induce potent antibody responses in mice. Also, modest levels of cross reactivity were observed between SeV and HPIV3 antigens, indicating that whole HPIV3 can be used to detect serum specific HPIV3 IgG induced by F and HN antigens, without major cross reactivity with the SeV backbone.

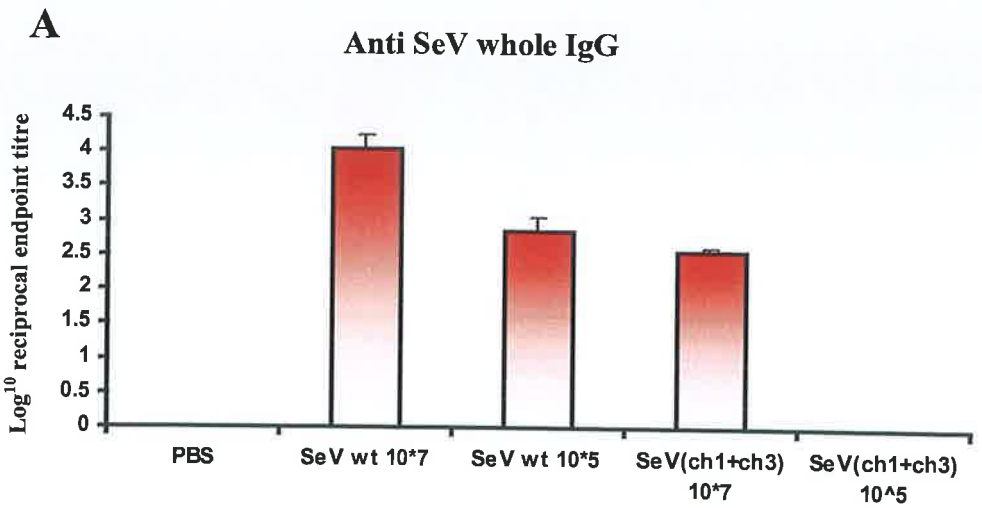

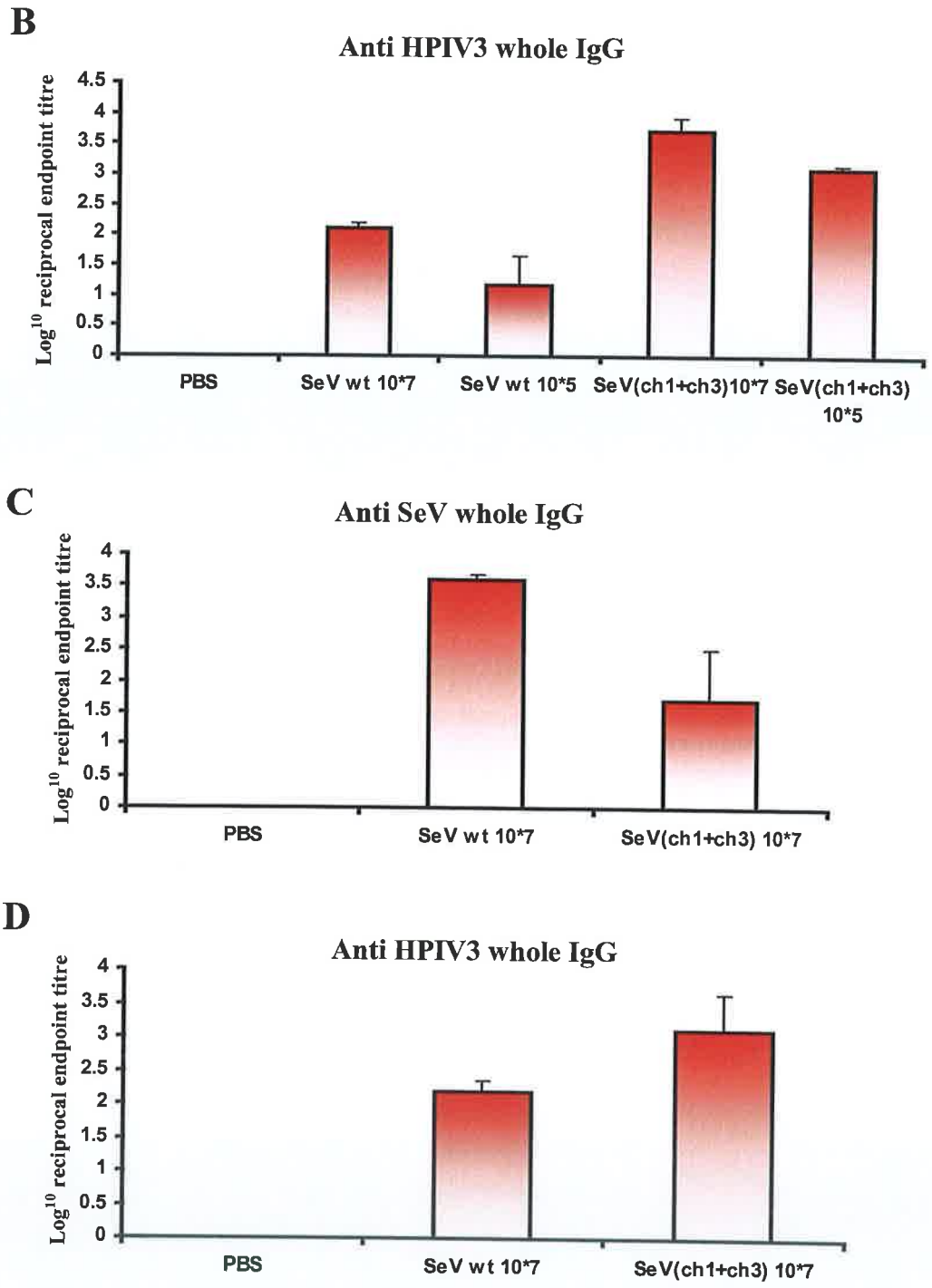

Figure 5.2.1 Serological responses against SeV wt and SeV expressing chimeric HPIV3 F (ch3) and HN (ch1) genes. Balb/c mice were intranasally (A and B) and intraperitoneally (C and D) immunised with SeV and SeV(ch1+ch3) as described in section 5.2.1 (experiment 1) and sacrificed on day 35. Serum samples were prepared (section 5.2.1.2) and UV inactivated SeV (A and C) and BPL inactivated HPIV3 (B and D) antigens at 1μg/ml were used to detect whole IgG by indirect ELISA

(section 5.2.2). Results reflect the mean $\log_{10}$ of the reciprocal end point titre $\pm$ SE for each group immunised.

T cell responses from mice immunised intranasally and intraperitoneally with SeV wt and chimeric SeV were also investigated. High levels of IFNγ were secreted from mice receiving SeV 10^7 when splenocytes were restimulated with SeV antigen at both concentrations, while reduced but moderate levels of IFNγ were produced from animals immunised with chimeric SeV 10^7 (figure 5.3.2A and B). In contrast, increased IFNγ production was detected at the higher concentration of HPIV3 antigen used to restimulate cells from chimeric SeV 10^7 immunised mice compared to mice receiving wild type SeV 10^7 (figure 5.3.2A and B). Elevated levels of IFNγ were also produced by both SeV 10^5 and chimeric SeV 10^5 immunised animal, when the higher concentration of SeV antigen was used to restimulate cells (figure 5.3.2C and D). However, IFNγ production was noticeably increased in supernatants from splenocytes isolated from mice immunised with chimeric SeV 10^5 compared to wild type SeV 10^5, when splenocytes were restimulated with either concentration of HPIV3 antigens (figure 5.3.2C and D). Also, little or no IFNγ was detected in the control group except from the polyclonally activated or positive control sample (figure 5.3.2E). Again, similar results were observed from T cells following i.p immunisations, exhibiting high IFNγ secretion from supernatants of chimeric SeV 10^7 compared to wild type SeV 10^7, when cells were restimulated with HPIV3 antigens (figure 5.3.3A-C). In addition to IFNγ secretion from cells, IL-5 production was also investigated. However, IL-5 was not detected in any of the immunised or control groups (appendix 6A and B). Thus, SeV wild type and chimeric SeV induce polarised Th1 responses in mice and whole HPIV3 antigens only induce strong IFNγ production from chimeric SeV immunised mice, exhibiting little cross reactivity with the SeV backbone.

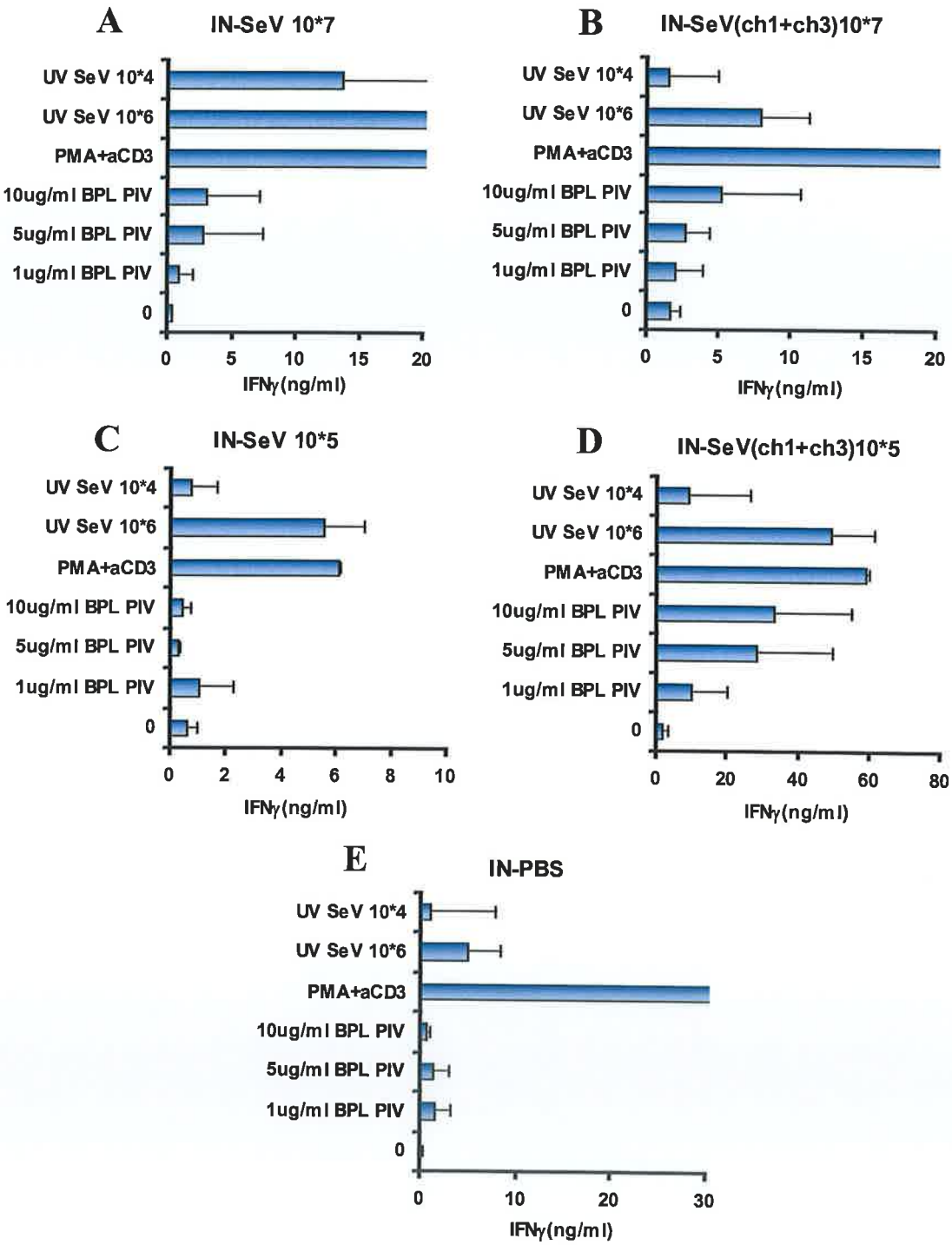

Figure 5.2.2 T cell responses following intransal infection with SeV and SeV expressing chimeric HPIV3 F (ch3) and HN (ch1) genes. Mice were immunised intransally with SeV and SeV(ch1+ch3) as described in section 5.2.1 (experiment 1) and sacrificed on day 35. Spleen cells were restimulated with UV inactivated SeV, BPL inactivated HPIV3 and PMA+aCD3 (section 5.2.1). After 3 days,

supernatants were harvested from (A) SeV 10^7, (B) SeV(ch1+ch3) 10^7, (C)) SeV 10^5, (D) SeV(ch1+ch3) 10^5 and (E) PBS (control) cultures and tested for IFNγ secretion by ELISA (section 5.2.3). Data reflects the mean concentration ± SD for each sample per group.

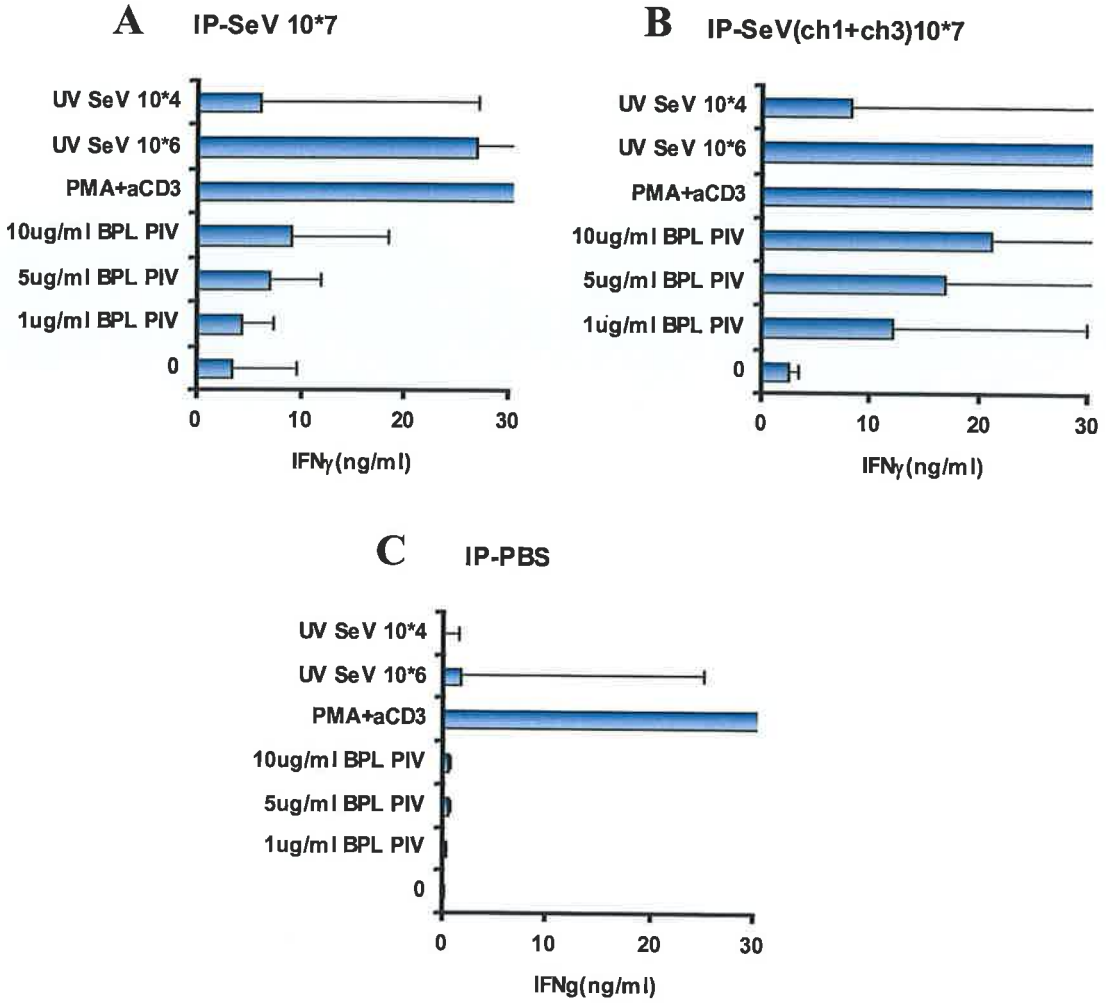

Figure 5.2.3 T cell responses following intraperitoneal infection with SeV and SeV expressing chimeric HPIV3 F (ch3) and HN (ch1) genes. Mice were immunised with SeV and SeV(ch1+ch3) as described in section 5.2.1 (experiment 1) and sacrificed on day 35. Spleen cells were restimulated with UV inactivated SeV, BPL inactivated HPIV3 and PMA+aCD3 (section 5.2.1). After 3 days, supernatants were harvested from (A) SeV 10^7, (B) SeV(ch1+ch3) 10^7 and (C) PBS (control) cultures and tested for IFNγ secretion by ELISA (section 5.2.3). Data reflects the mean concentration ± SD for each sample per group.

5.3.2 *In vivo* immune responses to wild type SeV and a replication deficient SeV vector (SeVV)

Next we investigated immune responses to a replication deficient SeVV, which had been made replication incompetent by truncating the P gene and compared these responses to wild type SeV. Therefore, mice were immunised intranasally with SeV wt and with the replication deficient SeVV and UV inactivated SeV was used to detect serum IgG produced. Notably, high levels of anti SeV serum IgG were produced from mice infected with the replication deficient SeVV at the higher dose (10^7), which was comparable to the levels produced by wild type SeV 10^5 (figure 5.3.4). In contrast, no serum IgG was detected when the lower dose (10^5) of the replication deficient SeVV was used to immunise mice. Therefore, the replication deficient SeVV induces robust IgG production in mice, only when high concentrations of the vector are used for infections.

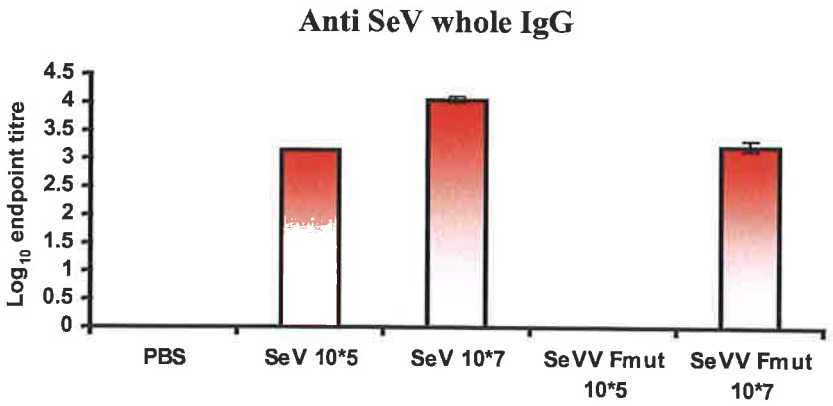

Figure 5.3.4 Serological responses against a replication deficient SeVV (Fmut) and wild type SeV. Mice were immunised intranasally with a replication deficient SeVV (Fmut) and SeVwt as described in section 5.2.1 (experiment 2) and sacrificed on day 35. Serum samples were prepared (section 5.2.1.2) and UV inactivated SeV antigen at 1μg/ml were used to detect whole IgG by indirect ELISA (section 5.2.2). Results reflect the mean $\log_{10}$ of the reciprocal end point titre ± SE for each group immunised.

From our T cell studies of mice intranasally immunised with the replication deficient SeVV or with SeV wt, only modest amounts of IFNγ were produced at both 10^7 and 10^5 from the replication deficient SeVV compared to wild type SeV 10^5 (figure 5.3.5). Also, IL-5 was not produced from cultures containing either immunised or control

cells (appendix 6C). So, the replication deficient SeVV can induce only modest IFNγ secretion from T cells, but still generates a Th1 bias similar to wild type SeV.

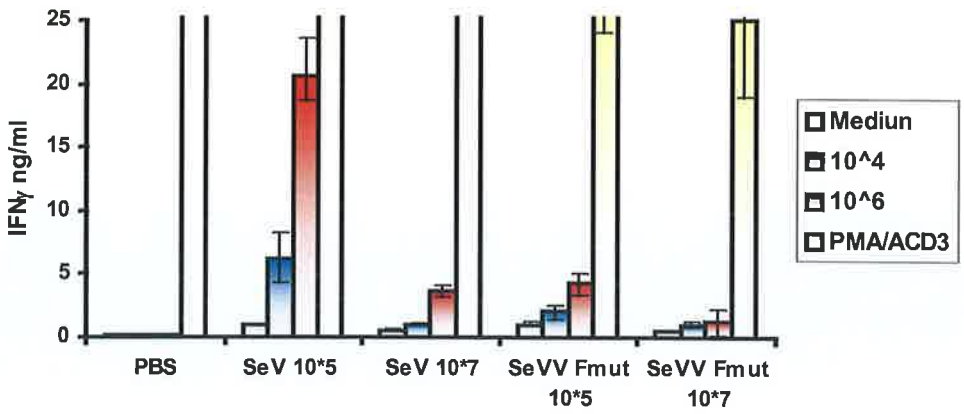

Figure 5.3.5 T cell responses following intranasal infection with a replication deficient SeVV (Fmut) and SeV wt. Mice were immunised with a replication deficient SeVV (Fmut) and SeVwt as described in section 5.2.1 (experiment 2) and sacrificed on day 35. Spleen cells were restimulated with UV inactivated SeV and PMA+aCD3 (section 5.2.1) and cultured for 3 days. Following incubation, supernatants were harvested from PBS (control), SeV 10^5, SeV10^7, SeVV Fmut 10^5 and SeVV Fmut 10^7 cultures and tested for IFNγ secretion by ELISA (section 5.2.3). Data reflects the mean concentration ± SD for each sample per group.

5.3.3 *In vivo* immune responses to the replication competent final vaccine

Subsequently, immune responses to the replication competent final vaccine construct SePIV47E, which expresses a mutated RSV F gene and the chimeric HPIV3 F and HN genes were examined. Mice were intranasally immunised with two different doses of SePIV47E and again antibody and T cell responses to this vaccine contruct were investigated. Replication competent SePIV47E induced high levels of anti HPIV3 specific serum IgG production *in vivo* when mice were infected with the higher dose (10^7) of the vaccine compared to the lower dose (10^5) (figure 5.3.6). Therefore, the replication competent SePIV47E vaccine can induce robust anti HPIV3 IgG at high infectious doses.

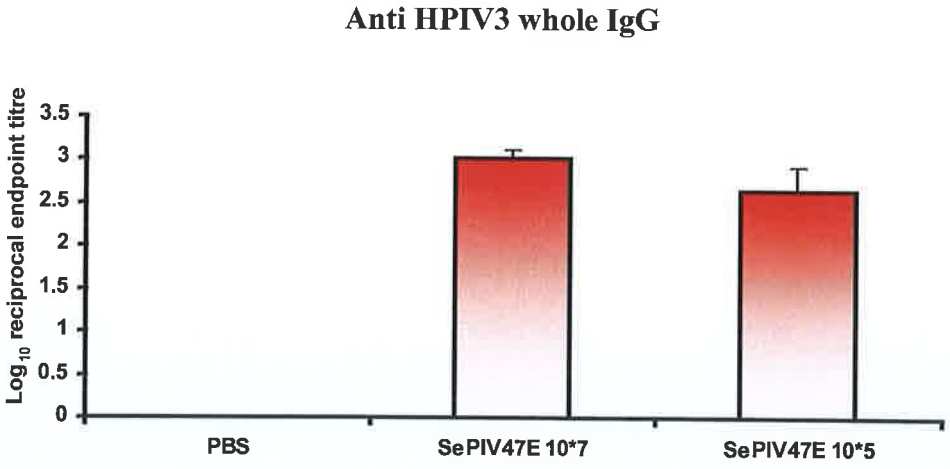

Figure 5.3.6 Serological responses against the replication competent final vaccine. Mice were immunised intranasally with the replication competent SePIV47E vaccine as described in section 5.2.1 (experiment 3) and sacrificed on day 35. Serum samples were prepared (section 5.2.1.2) and BPL inactivated HPIV3antigen at 1μg/ml were used to detect whole IgG by indirect ELISA (section 5.2.2). Results reflect the mean $\log_{10}$ of the reciprocal end point titre ± SE for each group immunised.

Splenocytes from mice that were infected at both doses of the replication competent SePIV47E vaccine and were restimulated with BPL inactivated HPIV3, secreted large amounts of IFNγ in response to the higher antigen concentrations used (figure 5.3.7A and B). Modest levels of IFNγ were produced from SePIV47E immunised mice when cells were restimulated with UV inactivated SeV 10^6, as the vaccine backbone is SeV, so minor responses to SeV are inevitable (figure 5.3.7A and B). Furthermore, little or no IFNγ was detected from the control group restimulations, demonstrating a lack of immune response to the mock infections (figure 5.3.7C). In line with previous experiments, IL-5 levels were also tested from control and immunised cultures, to examine Th2 cytokine production. However, no IL-5 was detected in supernatants from any group (appendix 6D). Thus, the replication competent SePIV47E vaccine induces strong polarised Th1 responses in mice at both doses investigated.

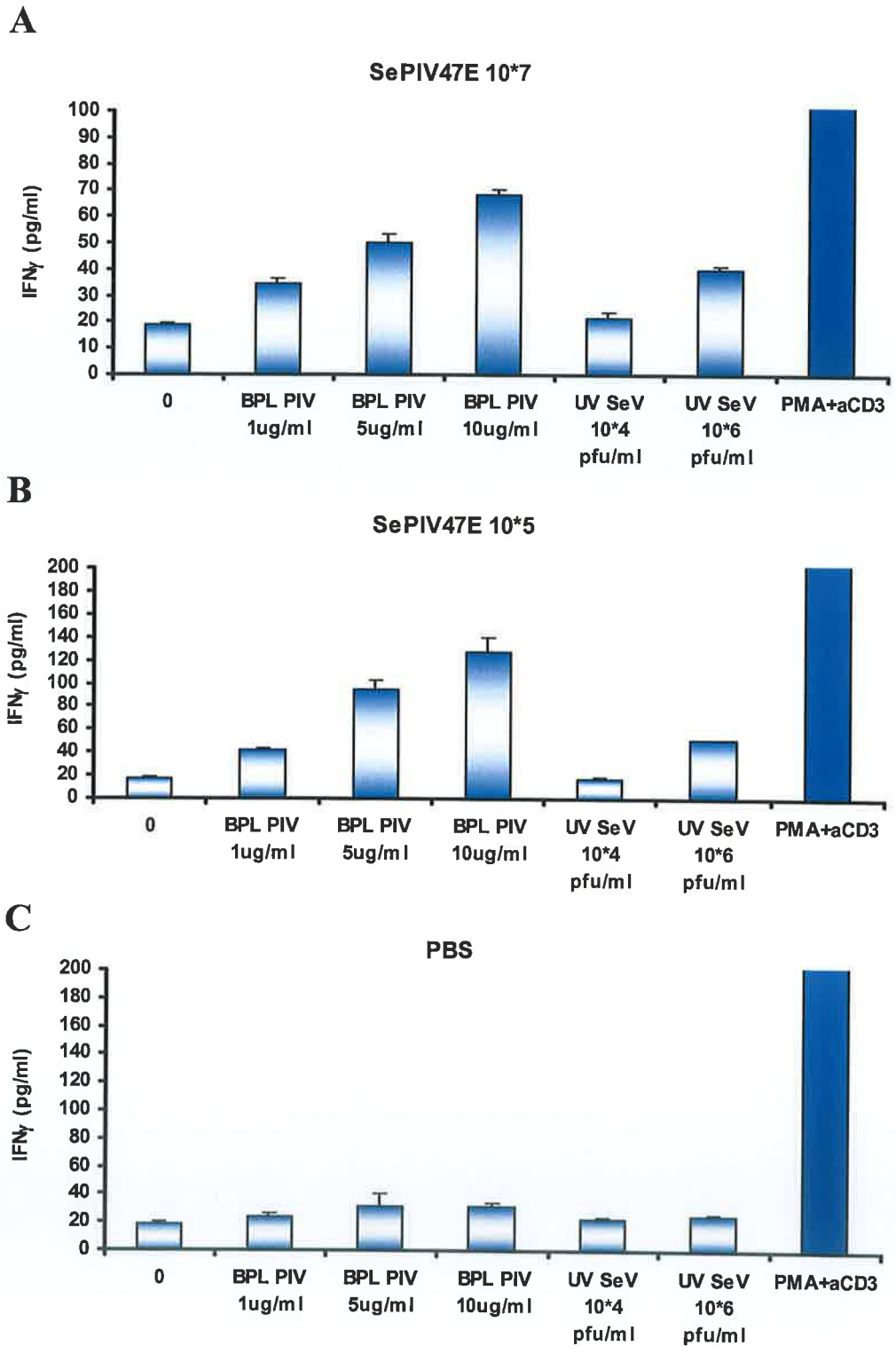

Figure 5.2.7 T cell responses following intransal immunisation with the replication competent final vaccine. Mice were immunised with the replication competent SePIV47E vaccine as described in section 5.2.1 (experiment 3) and sacrificed on day 35. Spleen cells were restimulated with UV inactivated SeV, BPL inactivated HPIV3 and PMA+aCD3 (section 5.2.1). After 3 days, supernatants

were harvested from (A) SePIV47E 10^7, (B) SePIV47E 10^5 and (C) PBS (control) cultures and tested for IFNγ secretion by ELISA (section 5.2.3). Data reflects the mean concentration ± SD for each sample per group.

5.3.4 *In vivo* immune responses to the replication deficient final vaccine

Lastly, we investigated immune responses *in vivo* to the replication deficient final vaccine SePIV56, which expresses a mutated RSV F gene and the chimeric HPIV3 F and HN genes, but has been made replication incompetent by truncating the P gene. Mice were intranasally immunised with the SePIV56 at $1.3X10^5$ and $1.3X10^4$. Due to limited vaccine stocks $1.3X10^5$ was the highest dose that could be used for infection. However, noticeably high levels of anti HPIV3 specific serum IgG was produced *in vivo* in response to mice immunised at the higher dose of vaccine (10^5) (figure 5.3.8). Only low levels of IgG were detected from SePIV56 infected mice at 10^4. Thus, elevated levels of anti HPIV3 serum IgG are induced by high concentrations of SePIV56 from immunised mice.

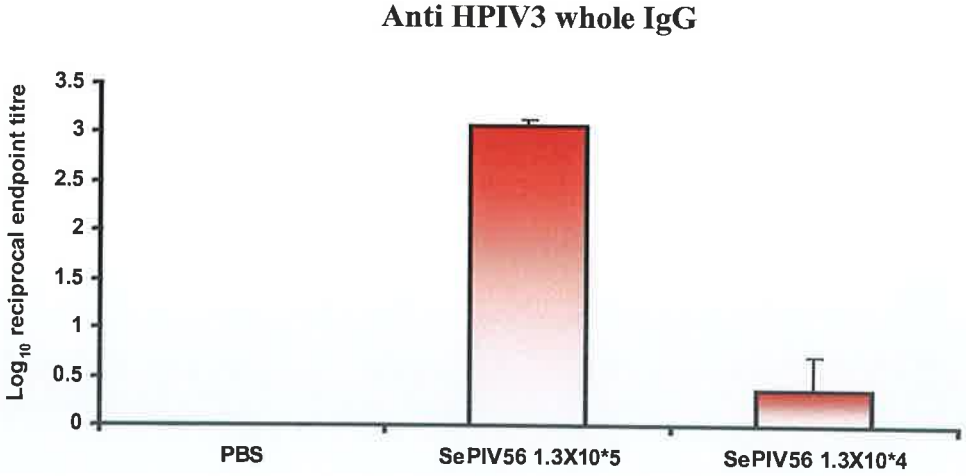

Figure 5.3.8 Serological responses against the replication deficient final vaccine. Mice were immunised intranasally with the replication deficient SePIV56 vaccine as described in section 5.2.1 (experiment 4) and sacrificed on day 35. Serum samples were prepared (section 5.2.1.2) and BPL inactivated HPIV3antigen at 1μg/ml were used to detect whole IgG by indirect ELISA (section 5.2.2). Results reflect the mean $\log_{10}$ of the reciprocal end point titre ± SE for each group immunised.

T cell responses from the replication deficient SePIV56 1.3X10^5 infected mice demonstrated high levels of HPIV3 specific IFNγ production, when spleen cells were restimulated with the highest concentration of BPL inactivated HPIV3 (figure 5.3.9A). In contrast, little IFNγ was secreted from cultures containing cells from either SePIV56 1.3X10^4 or PBS (control) immunised mice (figure 5.3.9B and C). Also, IL-5 was not produced from any of the immunised group cultures (appendix 6E). Hence, the replication deficient final vaccine induces strong polarised Th1 responses *in vivo* at the higher dose of SePIV56 but not at the lower dose.

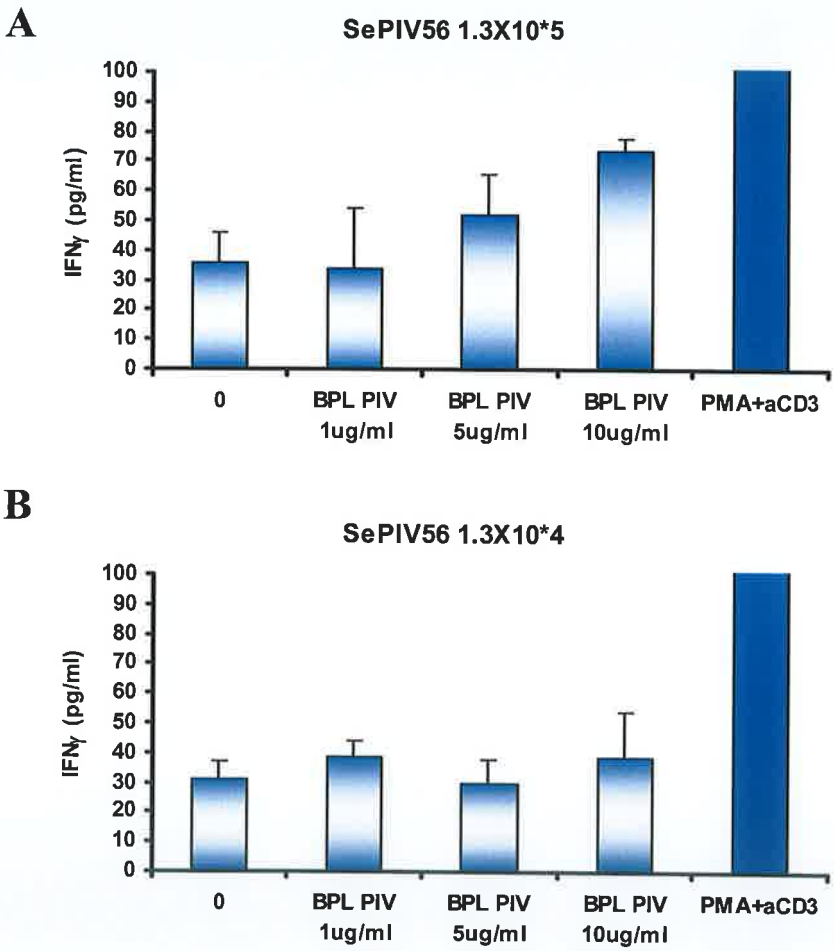

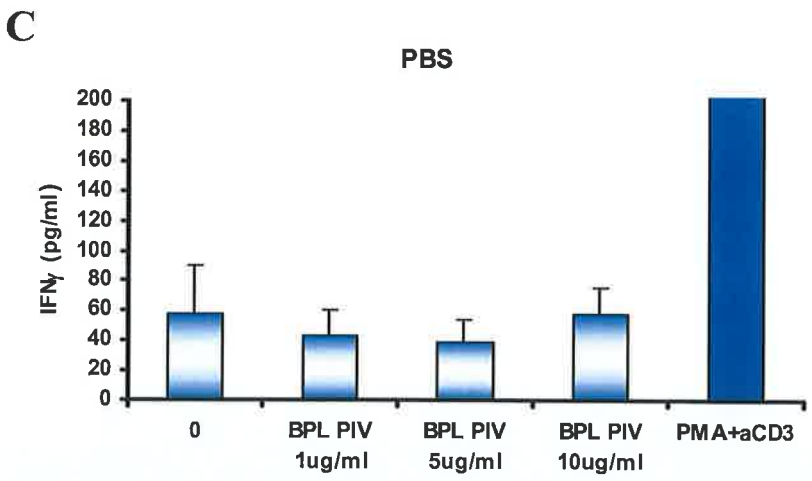

Figure 5.2.9 T cell responses following intransal immunisation with the replication deficient final vaccine. Mice were immunised with the replication deficient SePIV56 vaccine as described in section 5.2.1 (experiment 4) and sacrificed on day 35. Spleen cells were restimulated with BPL inactivated HPIV3 and PMA+aCD3 (section 5.2.1). After 3 days, supernatants were harvested from (A) SePIV56 $1.3X10^5$, (B) SePIV56 $1.3X10^4$ and (C) PBS (control) cultures and tested for IFNγ secretion by ELISA (section 5.2.3). Data reflects the mean concentration $\pm$ SD for each sample per group.

5.3.5 Adaptive immune responses induced by virosome infected human *ex vivo* monocytes

In parallel with the *in vivo* studies, human T cell responses to virus constructs were also investigated. Firstly, T cell responses to the envelope components of HPIV3 were examined, in order to assess if HPIV3 glycoproteins had a suppressive effect on T cell proliferation. Monocytes were infected with SeV (IRSV), HPIV3 (IRPV) and influenza virus (IRIV) virosomes, which are empty virus shells comprised of envelope proteins, but contain no genetic material. Interestingly, T cell proliferation was suppressed from the mixed leukocytes that were cocultured with IRPV infected monocytes compared to IRIV and IRSV infected cocultures, which induced moderate levels and high levels of T cell proliferation, respectively (figure 5.3.10B). However, this inhibition in T cell proliferation was restored when IRPV infected monocytes were cocultured with purified CD3+ T cells, as proliferation was comparable to that observed from the other virosome infected cocultures (figure 5.3.10A). These results, along with our human studies of T cell proliferation (chapter 2) strongly implicate

HPIV3 glycoproteins F and HN as major contributors to T cell suppression, which is associated with HPIV3 infections. Results also suggest that SeV envelope proteins are capable of inducing strong T cell proliferation, possibly eliminating the necessity for the vaccine to be encapsidated in a virosome.

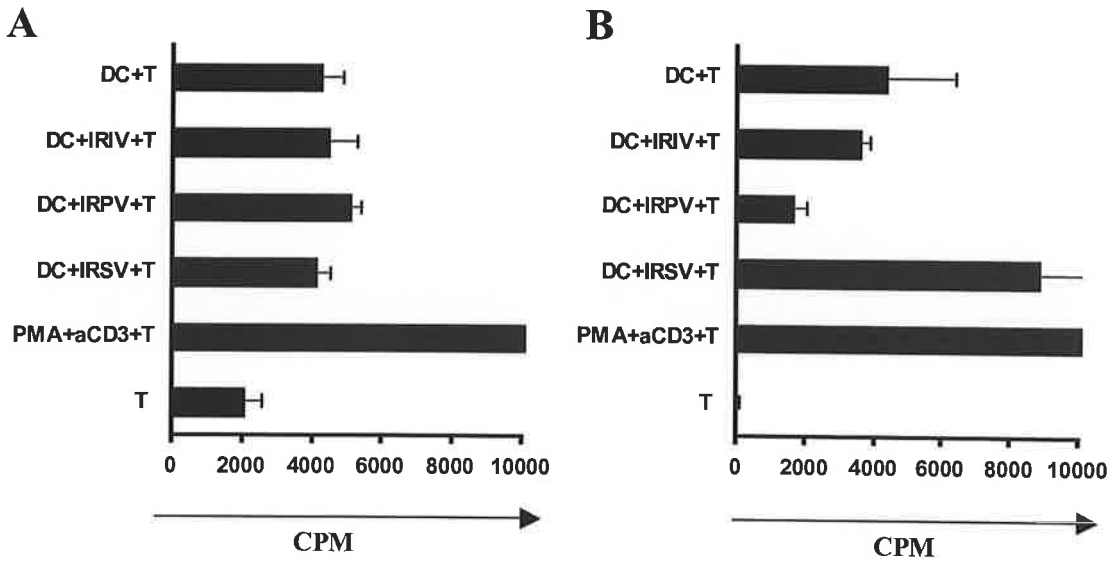

Figure 5.3.10 T cell proliferation profiles from purified CD3+ T cell cocultures and MLR cocultures reconstituted with allogeneic virosome infected monocytes. (A) Purified CD3+ T cells and (B) mixed leukocytes were cocultured alone (T), with CD14+ cells (DCs), with IRIV infected monocytes (DC+IRIV), with IRPV infected monocytes (DC+IRPV) and with IRSV infected monocytes (DC+IRSV) (section 5.2.4/5). Proliferation profiles were measured by ^{3}H incorporation after 5 days (section 5.2.6). Results reflect the mean cpm $\pm$ SE for each sample and are representative of two independent experiments (for raw data from repeat experiment refer to appendix 8, table 8.O).

5.3.6 T cell proliferation induced by human *ex vivo* monocytes infected with the replication deficient vaccine

Lastly, we examined T cell proliferation in response to the replication deficient SePIV56 vaccine infected monocytes to investigate if this novel vaccine could induce T cell proliferation. Therefore monocytes were infected with both UV inactivated SePIV56 and live SePIV56 and T cell responses induced by the vaccine were compared with those induced by HPIV3 infected monocytes. Similar CD3+ T cell proliferation profiles were observed from all the infected cocultures (figure 5.3.11A). However, although T cell proliferation was limited in the HPIV3 infected MLR

coculture and it was also decreased in the UV inactivated SePIV56 infected MLR coculture, a modest increase in T cell proliferation was evident from the SePIV56 infected MLR coculture which was comparable to the levels observed from the influenza infected coculture (figure 5.3.11B). Thus, this novel vaccine appears to bypass the inhibitory T cell effects inflicted by HPIV3 infection, by inducing enhanced T cell proliferation compared to HPIV3 infected cells.

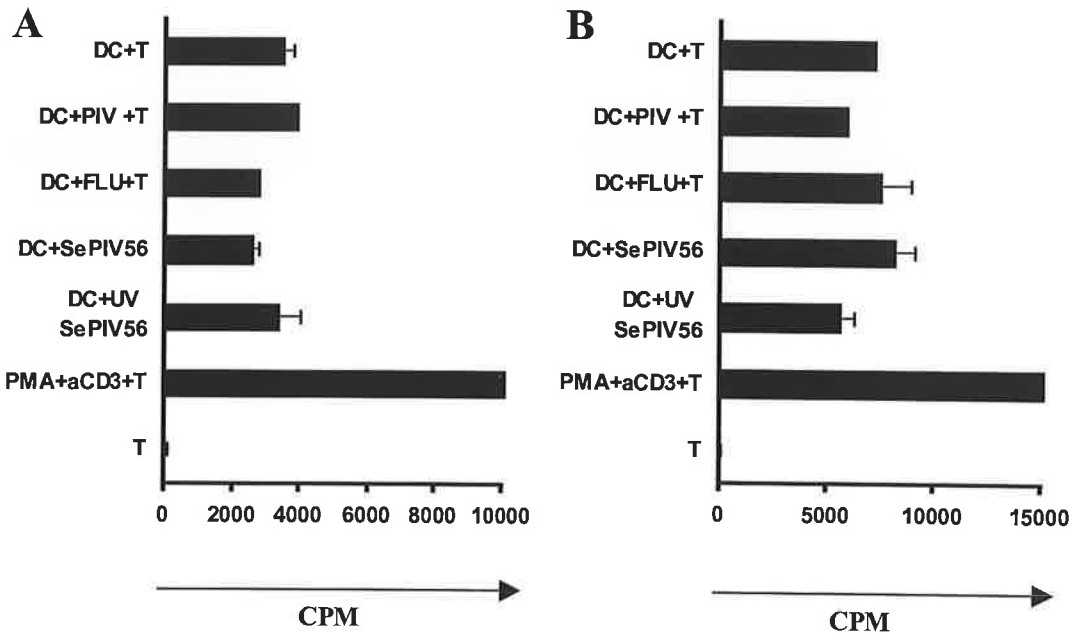

Figure 5.3.11 T cell proliferation profiles from purified CD3+ T cell cocultures and MLR cocultures reconstituted with vaccine infected monocytes. (A) Purified CD3+ T cells and (B) mixed leukocytes were cocultured alone (T), with CD14+ cells (DCs), with HPIV3 infected monocytes (DC+PIV), with influenza infected monocytes (DC+FLU), with SePIV56 infected monocytes (DC+SePIV56) and with UV inactivated SePIV56 infected monocytes (DC+UV SePIV56) (section 5.2.4/5). Proliferation profiles were measured by ^{3}H incorporation after 5 days (section 5.2.6). Results reflect the mean cpm $\pm$ SE for each sample and are representative of three separate experiments (for raw data from repeat experiments refer to appendix 8, table 8.P).

5.4 DISCUSSION

In a world where one is constantly under threat of new and re-emerging diseases, vaccines are key to our survival and protection against infectious pathogens. By preventing or modifying the severity of illness in an individual they can reduce the transmission of pathogens to other susceptible beings. However, virus interactions with the immune system are highly complex, hindering successful vaccine developments. One such virus, with no licensed vaccine as yet, is HPIV3. A high frequency of reinfection is one of the main problems associated with HPIV3 infections (Hall 2001). Several reports have suggested that this lack of lifelong immunity may be due to T cell suppression during HPIV3 infections (Plotnicky-Gilquin *et al* 2001, Sieg *et al* 1994) and as robust T cell proliferation is essential for the development of longlived memory T cells (Esser *et al* 2003), this is a plausible theory. Thus, an effective HPIV3 vaccine would need to be able to overcome the suppressive effects associated with HPIV3 infections. Therefore the aim of these studies was to test the immunogenicity of a novel replication deficient sendai virus (SeV) vaccine expressing RSV F and HPIV3 F and HN antigens (designed and produced by our project collaborators) in an animal *in vivo* model and human *ex vivo* model, focusing on the HPIV3 components of the vaccine. Preliminary experiments were performed *in vivo* on various virus constructs that would eventually lead to the development of the final vaccine product. *In vivo* murine serological and T cell responses to these constructs and the final replication deficient vaccine were assessed and compared to T cell responses generated from infection of the human *ex vivo* model with the final vaccine. Results demonstrated that the replication deficient SeV vaccine was capable of inducing robust anti HPIV3 serum IgG production and strong polarised Th1 responses *in vivo*. These elevated T cell responses were also consistently observed from infection of the human *ex vivo* model with the replication deficient SeV vaccine, where the vaccine demonstrated promising potential to bypass HPIV3 suppressive responses, by inducing elevated levels of T cell proliferation.

Initially, *in vivo* immune responses to SeV expressing chimeric HPIV3 F and HN genes were investigated. These glycoproteins are the main antigens known to stimulate antiviral immunity against HPIV3 infections (Chanock *et al* 2001), so it was

imperative that antibody and T cell responses to these glycoproteins could be detected. SeV expressing chimeric HPIV3 F and HN genes appeared to induce robust anti HPIV3 serum IgG production and polarised Th1 responses *in vivo* when compared to wild type SeV. Also, minimal crossreactivity was observed between SeV and HPIV3 antigens, enabling whole inactivated HPIV3 to be used as a readout for HPIV3 specific responses. Other vaccine vectors, such as the chimeric bovine/human PIV3 vaccine where the F and HN genes of bovine PIV3 are replaced with those from HPIV3, displayed similarly high HPIV3 specific antibody responses to these glycoproteins in hamsters (Haller *et al* 2000).

One of the most critical requirements in vaccine development is vaccine safety *in vivo*. A previous study showed that SeV replicated nearly as efficiently as HPIV1 in chimpanzees and African green monkeys (Skiadopoulos *et al* 2002). This raises doubts as to whether SeV would be sufficiently attenuated in humans in an unmodified form. Therefore it is essential that live HPIV3 vaccines are attenuated or engineered to be replication deficient *in vivo*, to limit the chance of infection in the host but without compromising immunogenicity. So we examined immune responses to a replication deficient SeVV (Fmut) *in vivo*. High levels of anti SeV serum IgG were produced *in vivo* in response to the higher dose of SeVV used in immunisations. However, only modest amounts of IFNγ were secreted from T cells, possibly due to the lack of viral replication. Nonetheless, T cells were still directed towards a Th1 bias, mimicking their wild type counterpart SeV, demonstrating that a replication deficient SeVV could induce sufficient immune responses while protecting the host from the threat of infection.

Then the immunostimulatory ability of the replication competent final vaccine was determined, which expressed a mutated RSV F gene and chimeric HPIV3 F and HN genes. This replication competent vaccine induced potent anti HPIV3 serum IgG at high infectious doses and exhibited strong polarised Th1 responses *in vivo*, evident from the high levels of IFNγ produced. These results were promising but to ensure complete safety *in vivo*, this vaccine was engineered to be replication deficient by truncating the P gene, which is an essential component for virus replication (Bitzer *et al* 2003). Subsequently, immune responses to this replication deficient final vaccine

construct were assessed *in vivo*. Interestingly, the replication deficient final vaccine induced robust anti HPIV3 specific serum IgG at $1.3X10^5$ciu/unit, which was the lower dose used throughout these experiments. Also a strong polarised Th1 response was evident from mice immunised at the higher concentration ($1.3X10^5$) of the vaccine. Thus, even though this vaccine was replication deficient, it was still capable of inducing potent immune responses to HPIV3 *in vivo*. Similar promising results were obtained from a replication defective chimeric alphavirus replicon expressing the HN glycoprotein of HPIV3. This vaccine showed strong PIV3 specific IgG responses following *in vivo* immunisations and protected hamsters against challenge with mucosal PIV3 (Greer *et al* 2006).

Many studies have implicated viral glycoproteins as mediators of T cell suppression, including RSV (Dubois *et a*l 2001, Schlender *et al* 2001). The F (fusion) protein from this related virus was shown to suppress T cell proliferation of mitogen activated lymphocyes (Schlender *et al* 2001). Therefore we sought to investigate T cell responses to HPIV3 glycoproteins, by infecting human monocytes with HPIV3 (IRPV), SeV (IRSV) and influenza virus (IRIV) virosomes and coculturing them with T cells. Interestingly, HPIV3 virosomes appeared to mimic live HPIV3 infections, exhibiting suppressive effects on T cells from mixed leukocyte cultures while inducing no inhibitory effects on proliferating purified CD3+ T cells. Also, as the vaccine backbone is SeV, it was encouraging to see such high levels of T cell proliferation induced by the SeV virosome, which influenced the collaborators decision, not to encapsidate the final vaccine in a virosome. Thus, from these results one could speculate that these glycoproteins play a major role in suppressing T cell responses in HPIV3 infections. However, in order to observe if this replication deficient vaccine was immunogenic in humans, T cell responses to human *ex vivo* monocytes infected with the vaccine were also investigated. Interestingly, this replication deficient vaccine appeared to overcome the suppressive effects imposed by HPIV3, restoring normal levels of T cell proliferation to mixed leukocyte cultures. Hence, this data corroborates results from the *in vivo* studies. In both models this novel vaccine is capable of inducing strong immune responses against HPIV3 and may represent a promising vaccine in future years against HPIV3 infections. Also, this human *ex vivo* model could potentially be used to validate immune responses to vaccines in animal models, in order to develop more competent vaccines.

6.1 FINAL DISCUSSION

The immune system has evolved to protect the host against foreign pathogens and autoimmune disease, through a complex network involving both effector and regulatory mechanisms. This maintenance or preservation of 'self', is pivotal to the hosts survival, enabling the host to control excessive immune responses induced by foreign pathogens, thus limiting immunopathology to self tissue (O'Garra *et al* 2004). Such control can be implemented by regulatory T cells, which have been shown to suppress T cell induced proinflammatory responses to both infectious pathogens and self-antigens (Suvas *et al* 2004, Masteller *et al* 2005). However, dampening down effector responses can inadvertently lead to persistent or chronic infections, induced by opportunistic pathogens (Weiss *et al* 2004, Boettler *et al* 2005). One such pathogen that may subvert immune responses and has been associated with persistent infections is HPIV3 (Goswami *et al* 1984). HPIV3 is a major respiratory pathogen responsible for both upper and lower respiratory tract infections of adults, neonates and infants (Marx *et al* 1999, Henrickson 2003, Chanock *et al* 2001). Recurrent infections are a hallmark of this virus (Henrickson 2003), suggesting that HPIV3 fails to induce a state of lifelong immunity. Hence, the aim of this study was to investigate immune responses to HPIV3, focusing mainly on the cellular aspects of immunity, which are responsible for generating memory T cells. Our findings demonstrated that HPIV3 was a strong inducer of innate immune activation, generating a highly potent DC, attributed with elevated costimulatory and polarising capabilities. However, most interestingly, this HPIV3 generated DC was unable to stimulate T cell proliferation from mixed leukocyte cocultures. Moreover, this phenomena was abolished when HPIV3 generated DCs were cocultured with purified CD3+ T cells, which exhibited similar levels of T cell proliferation comparable to influenza (a closely related human virus) infected, TNFα treated or untreated cocultures. Further studies revealed that an autologous CD3- CD14- population was responsible for this T cell inhibition observed from HPIV3 infected MLR cocultures. This effect was not due to apoptosis, required cellular contact and was dependent on IL-2. Follow on studies identified autologous CD56+ NK cells as the cell population from the MLR responsible for this T cell inhibition observed from HPIV3 infected MLR cocultures. NK cells exerted this regulatory effect on T cells by inducing their cell cycle arrest in the G0/G1 phase,

via inhibition of p27 degradation. Lastly, it was demonstrated that a novel replication deficient HPIV3 vaccine induced robust humoral and cell-mediated responses *in vivo* in a murine model and strong proliferative responses in the human *ex vivo* model.

Initially, current methods of DC generation and viral immune responses induced by various DC subsets were investigated (summarised in chapter 2), to evaluate the most appropriate or accurate model of DC generation, which should be used when studying HPIV3 infections. Current procedures used to generate DCs involve culturing monocytes with cytokines, such as GM-CSF and IL-4 or IFNα, which generates IL-4 DCs and IFN-DCs, respectively (Cella *et al* 1999, Mohty *et al* 2003). Through extensive examination of the differences observed in cell surface marker expression, cytokine production, apoptosis and T cell proliferation and polarisation, between virally infected monocytes, IL-4 DCs, IFN-DCs and A549 DCs (generated from culturing virally infected A549 supernatants with monocytes), we demonstrated that both influenza and HPIV3 induced a distinctive type of DC from each of the DC subsets analysed. Virus generated A549 DCs appeared to mimic direct viral infection of monocytes, in terms of their phenotype and functionality, while virally infected pre-primed DCs were not only phenotypically and functionally distinct from each other, they were also distinct from the A549 DCs and virus infected monocytes. From these conflicting results, it was thought that pre-treated or pre-primed DCs may mask genuine immune responses to viruses, as they were artificially generated through culture with cytokines, which may not be present, at least at physiological concentrations, during *in vivo* viral infections (Sato and Iwasaki 2004). Interestingly, IL-4 DCs were found to be extremely sensitive to virus induced apoptosis. As these DCs represent the most widely used cell type in viral *in vitro* assays (Cella *et al* 1999, Senechal *et al* 2004, Plotnicky-Gilquin *et al* 2001), this highlights the inaccuracies that could be obtained from viral studies using IL-4 DCs. Hence, the most natural pathway of DC generation appeared to be the virally infected monocytes and A549 DCs generated from monocytes cultured with supernatants from infected epithelial cells, as no artificial treatment of these monocytes was employed during DC generation. As monocytes are precursor cells, known to be capable of differentiating into DCs *in vivo* (Randolph *et al* 1999), it is not surprising that they appeared to produce the most naturally occurring DCs. Thus, these results emphasise the

importance of accounting for the microenvironment when designing *in vitro* studies around infectious organisms. This is further highlighted by experiments involving stromal and endothelial cells, which demonstrated that these cells were capable of directing DC development in response to infectious pathogens (Svensson *et al* 2004, Qu *et al* 2003). So, future studies assessing viral immune responses *in vitro* should employ other methods for DC generation, such as the human *ex vivo* model described, to help produce more accurate and realistic results, rather than using conventional approaches to DC development, which may inappropriately skew immune responses. In our case, this human *ex vivo* model represented the most natural way of developing virus induced DCs that could mimic *in vivo* virus generated DCs and was therefore used in subsequent studies evaluating immune responses to HPIV3 infections.

Next, the pathogenesis of HPIV3 and the mechanisms at play during HPIV3 infections were investigated (summarised in chapter 3 and 4). Infection of the human *ex vivo* model with HPIV3 generated a highly activated DC, capable of secreting large amounts of IL-10 and type I IFNs. However, HPIV3 generated DCs inhibited allogeneic T cell proliferation in a mixed leukocyte reaction in contrast to influenza infection, treatment with TNFα or untreated cells. Surprisingly, we found that proliferation of the purified CD3+ T cell populations from these donors was not inhibited by HPIV3 generated DCs. Due to the high levels of the immunoregulatory cytokine IL-10 (O'Garra *et al* 2004) secreted from HPIV3 infected monocytes during the innate immune response and evidence suggesting that HPIV3 may suppress T cell proliferation through production of elevated levels of IL-10 (Sieg *et al* 1996), we examined IL-10 secretion from HPIV3 infected MLR cocultures. Interestingly, HPIV3 infection induced a polarised Th1 response from both mixed leukocyte and purified CD3+ T cell cocultures, which produced similar levels of IFNγ and IL-10. Furthermore, HPIV3 infected MLR cocultures secreted comparable levels of these cytokines to influenza infected MLR cocultures, excluding an involvement of IL-10 in T cell suppression. Also, as IL-2 is considered a crucial growth factor for T cells (Gaffen and Lui 2004), the levels of IL-2 produced from HPIV3 infected MLR cocultures were examined. IL-2 secretion from leukocytes was significantly impaired in HPIV3 infected cocultures compared to the other cocultures. However, addition of

IL-2 to these cultures restored the proliferating capacity of these cells, demonstrating that T cell inhibition induced by HPIV3 is a transient, IL-2 dependent process. Moreover, as viral induced apoptosis of lymphocytes has been linked to immune suppression (Gougeon *et al* 1996), this possibility was investigated in this study. However, there was no increase in lymphocyte apoptosis from HPIV3 infected cocultures compared to influenza infected cocultures, confirming that virus induced apoptosis was not responsible for T cell inhibition.

These studies suggested that a regulatory population of cells, which were CD3- CD14- within the allogeneic MLR was responsible for T cell inhibition observed from HPIV3 infection. Regulatory cells play a major role in controlling not only immune responses to self but also to infectious pathogens (Mills 2004, Jiang and Chess 2004). However, these responses while protecting the integrity of the host through reduced immunopathology (O'Garra *et al* 2004) can result in inadequate immune responses against infectious organisms, hindering pathogen eradication and often resulting in pathogen persistence (Accapazzato *et al* 2004). This study demonstrated that addition of autologous but not allogeneic CD3- CD14- cells to the purified CD3+ T cell coculture containing HPIV3 generated DCs, restored this inhibition of T cell proliferation in a contact dependent manner, reliant on IL-2 production. Clearly a novel mechanism of regulation involving CD3- CD14- cells was afoot. These findings prompted us to investigate the nature of the reduced T cell proliferation and the exact cell type involved. The CD14- CD3- populations consist of a heterogenous group of cells with CD19+ (B cells) and CD56+ (NKs) cells predominating. Recently a study showed that NK cells may regulate the expansion of polyclonally activated T cells by cell cycle arrest (Trivedi *et al* 2005) while another report demonstrated an increase in the binding of NK cells to autologous T cells during mitosis, which did not induce T cell cytotoxicity (Nolte-'t Hoen *et al* 2006). Also, we observed an expansion of CD56 (NK cell marker) positive cells in HPIV3 infected CD3- CD14- cells during preliminary investigations. NK cells need to be activated before they can exert effector function and as direct infection of monocytes with HPIV3 induces significant IFNα production, which is known to activate and enhance NK responses (Wallace and Smyth 2005, Degli-Esposti and Smyth 2005), it is plausible that this cytokine could play a role in inducing NK cell activation in the HPIV3 infected MLR

cocultures. Therefore it was speculated that this group of cells might be involved in the failure of T cells to proliferate to HPIV3 infection. This hypothesis was confirmed by the significant reduction in proliferation of the purified CD3+ T cells upon addition of autologous NK cells to the HPIV3 infected coculture. This effect was not observed following the addition of purified autologous CD19+ cells to HPIV3 infected cocultures.

Interestingly, although NK cells inhibited T cell proliferation, they did not induce T cell death. Previous studies investigating NK cell regulation (Trivedi *et al* 2005), in combination with our own observations, such as the lack of significant apoptosis and the reversible nature of the reduced proliferation, led us to speculate that NK cells may target components of the cell cycle pathway. In our study, NK cells appeared to arrest T cell cycle progression in the G0/G1 phase by partially preventing degradation of the cell cycle inhibitor protein, p27. Other viruses, such as HCV and SIV have been shown to use similar methods to suppress T cell proliferation, through reduced degradation of cyclin dependent kinase inhibitors p21 and p27, resulting in T cell cycle arrest (Yao *et al* 2003, Ndolo *et al* 2002). The fact that only partial prevention of p27 degradation was observed, is in keeping with the low levels of cells that are affected in the cell cycle studies and is consistent with the clinical outcome of this infection whereby different individuals will mount different proliferative responses. The use of NK depletion studies from donors as opposed to artificial NK:T cell ratio experiments reflects more accurately this variation within the human population. This control of T cell proliferation by reversible cell cycle arrest rather than cell cytotoxicity would represent a cleaver departure for NKs where T cell death might be too costly for the host. Also, HPIV3 infection has been shown to contribute to viral persistence through downregulation of granzyme B mRNA, which results in cytotoxic dysfunction of killer cells (Sieg *et al* 1995). This virus survival strategy would obviously affect NK cell cytotoxic responses, forcing NK cells to evolve other mechanisms to control or regulate immune responses. In addition, control of proliferation of these cells does not seem to affect appropriate T cell polarisation to Th1 cells. Thus cell arrest rather than cell death permits at least some defence against the invading organism. From these results and other reports (Nolte-'t Hoen *et al* 2006) we hypothesise that NK cells engage in surveillance of T cell activation and regulate proliferation of overactive T cells that may be induced during HPIV3

infections. This prevents bystander immune activation and limits immune damage, the ultimate price being viral persistence and poor memory T cell responses. Future studies should focus on components of the signalling pathway of IL-2, as T cell inhibition induced from HPIV3 infection is IL-2 dependent and IL-2 is essential for T cell proliferation (Gaffen and Liu 2004), which is ultimately responsible for the generation of memory T cells (Esser *et al* 2003).

Of wider interest, in studies looking at the overall cell cycle status of these cells we observed that all NK depleted cocultures had significantly enhanced phosphorylation of retinoblastoma, a key event that drives cell cycle progression (Sherr and Roberts 1999). These results strongly suggest that NK cells regulate all lymphocyte proliferation. NK cell regulation has largely been overshadowed by regulatory T cells (Zhang *et al* 2006). Regulatory T cells play a pivotal role in suppressing responses to self (Sakaguchi 2005), thus preventing autoimmunity, in addition to infectious pathogens (McGuirk *et al* 2002, Kinter *et al* 2004). However, several studies investigating autoimmune diseases have suggested a regulatory role for NK cells in controlling disease progression (Smeltz *et al* 1999, Pazmany 2005, Zhang *et al* 2006). NK cells have also been shown to control T cell responses during viral infections (Su *et al* 2001, Zhang *et al* 2006). One study showed that depletion of NK cells *in vivo* during murine cytomegalovirus (MCMV) infection actually enhanced the number of IFNγ specific T cells (Su *et al* 2001). Interestingly, the NK cell natural cytotoxic receptor NKp46 has been shown to bind to HA on influenza virus and HN on SeV, activating NK cells to lyse the virus infected cells (Mandelboim *et al* 2001). SeV (murine form of HPIV1) is related to HPIV3 (Chanock *et al* 2001) so one could speculate that NKp46 may also recognise HN from HPIV3. However, cellular cytotoxicity is not detected during HPIV3 infections, so perhaps NK receptors have a more flexible role than previously thought. Thus, NK regulation is a critical feature in shaping the immune responses to viruses and autoimmune diseases. Overall, our results have demonstrated a novel mechanism of immune regulation by NK cells and not only shed new light on the complex and multi faceted human response to danger but reveal a new cell cycle control mechanism, demonstrated from the retinoblastoma experiments, that may provide important clues to the development of cancer.

Lastly, immune responses to a novel replication deficient SeV vaccine (expressing RSV F and HPIV3 F and HN antigens) against HPIV3 were evaluated, by comparing immune responses generated against the vaccine in a murine *in vivo* model, to those produced from our human *ex vivo* model (summarised in chapter 5). In parallel, we also investigated human T cell responses to the envelope glycoproteins of HPIV3, influenza and SeV, through the use of virosomes, to assess if HPIV3 viral glycoproteins F and HN contributed to immune suppression. Other viruses, including RSV, which is closely related to HPIV3, have been shown to mediate T cell suppression through direct cell contact with viral envelope glycoproteins (Schlender *et al* 2001, Dubois *et a*l 2001). Therefore, it was appealing to speculate that a similar mechanism was occurring in our system. A similar pattern of T cell proliferation was observed from the HPIV3 virosome infected cocultures to live HPIV3 infected cocultures, which demonstrated reduced T cell proliferation from MLR cocultures but induced no inhibitory effects on proliferating purified CD3+ T cells. Thus, these results suggest that the major envelope proteins of HPIV3 appear to play a role in this T cell suppression associated with HPIV3 infections. In addition, SeV virosome infected cocultures stimulated high levels of T cell proliferation, which was an encouraging result, considering the vaccine is designed on a SeV backbone. Hence, the strong T cell proliferative response induced by SeV could potentially override the suppressive effects induced by HPIV3.

Our studies investigating immune responses to a novel replication deficient vaccine, revealed that this novel vaccine was capable of inducing robust anti HPIV3 specific serum IgG and polarised Th1 responses in mice *in vivo*. Similar encouraging immune responses were observed from infection of the human *ex vivo* model with the vaccine. Interestingly, the vaccine appeared to bypass the suppressive effects exerted by HPIV3, restoring normal levels of T cell proliferation to mixed leukocyte cultures. Thus, this novel replication deficient vaccine may be capable of overriding the suppressive effects imposed by HPIV3 enabling T cells to proliferate normally and generate an extensive repertoire of memory T cells, representing a promising vaccine against HPIV3 in the future. At present there is no licensed vaccine for HPIV3, although, two live attenuated HPIV3 vaccines have reached phase II in clinical trials (Belshe *et al* 2004, Greenberg *et al* 2005). So future prospects of acquiring a licensed HPIV3 vaccine are optimistic and through advancements, not only in genetic

engineering but also in research, this will enable more competent vaccines to be developed. Also, as animal models are widely used to evaluate immune responses to novel vaccines, the developed human *ex vivo* model could potentially be used to corroborate findings *in vivo*, providing additional information and a human perspective on developing vaccines.

APPENDICES

Appendix 1: Analysis of cell purity by flow cytometry

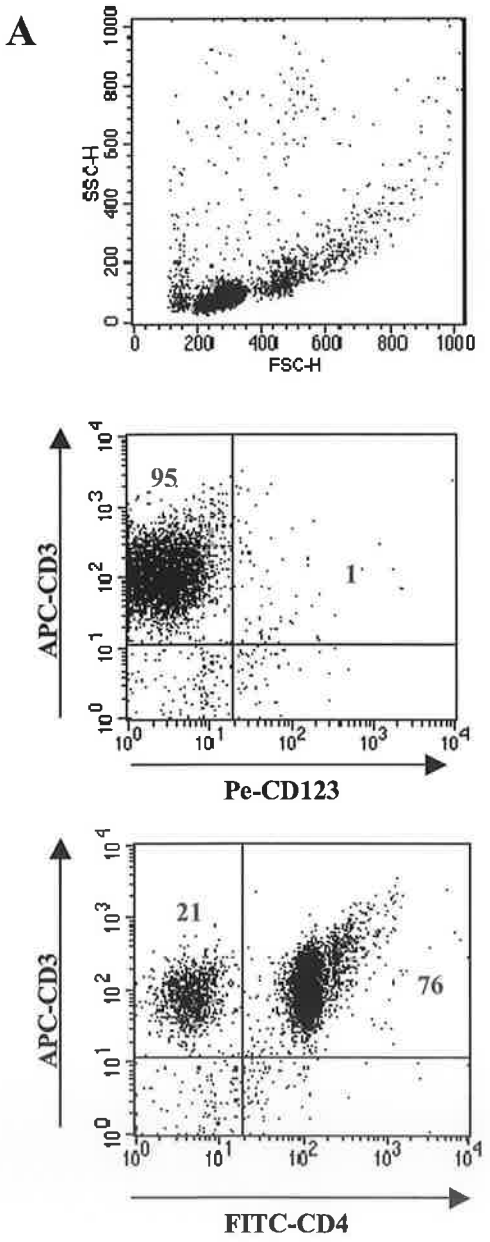

Purity of CD3+ T cells isolated from human PBMCs. Cells were positively selected and stained with anti-human FITC-CD4, APC-CD3 and Pe-CD123 and purity was assessed by flow cytometry. Quadrants markers were set based on isotype controls and values reflect the percentage of cells in each quadrant, which exhibit positive or negative staining for a particular marker. The CD3 enriched population had a purity > 95%.

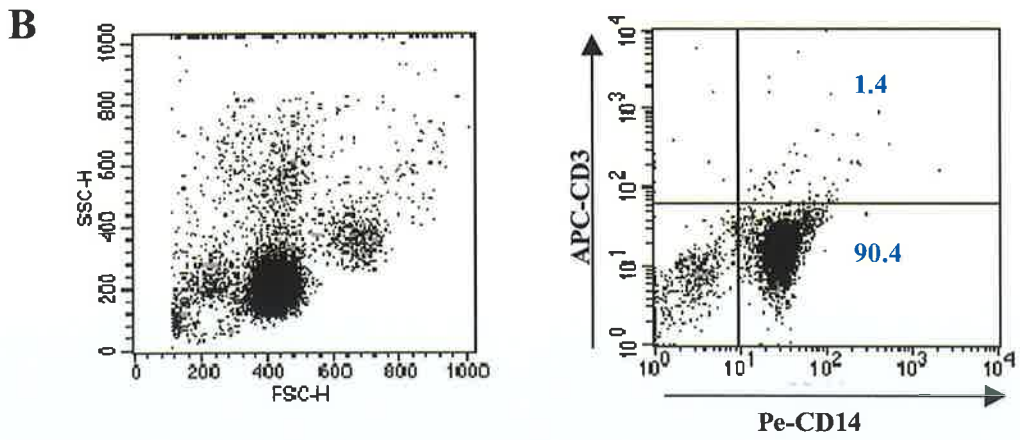

Purity of CD14+ monocytes isolated from human PBMCs. Cells were positively selected and stained with anti-human APC-CD3 and Pe-CD14 and purity was assessed by flow cytometry. Quadrant markers were set based on isotype controls and values reflect the percentage of cells in each quadrant, which exhibit positive or negative staining for a particular marker. The CD14 enriched population had a purity > 90% with < 2% contaminating CD3+ T cells.

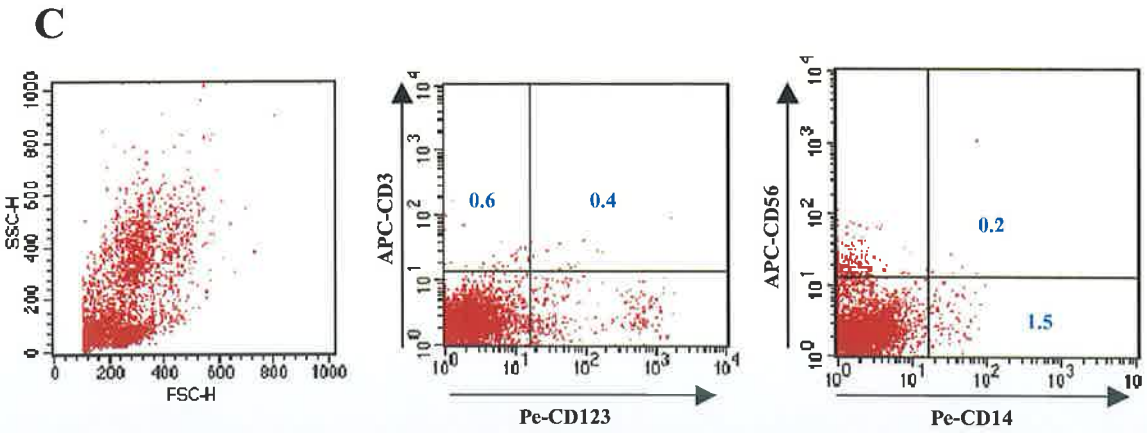

Purity of CD3- CD14- cells isolated from mixed leukocytes (CD14- fraction). The CD14- cell fraction was collected and depleted of CD3+ cells, using anti-CD3 microbeads. Cells were stained with anti-human APC-CD3, Pe-CD123, APC-CD56 and Pe-CD14 and purity was assessed by flow cytometry. Quadrants markers were set based on isotype controls and values reflect the percentage of cells in each quadrant, which exhibit positive or negative staining for a particular marker. Contaminating CD14+ monocytes and CD3+ T cells were found to be <2% of the CD14-CD3- population after purification.

D

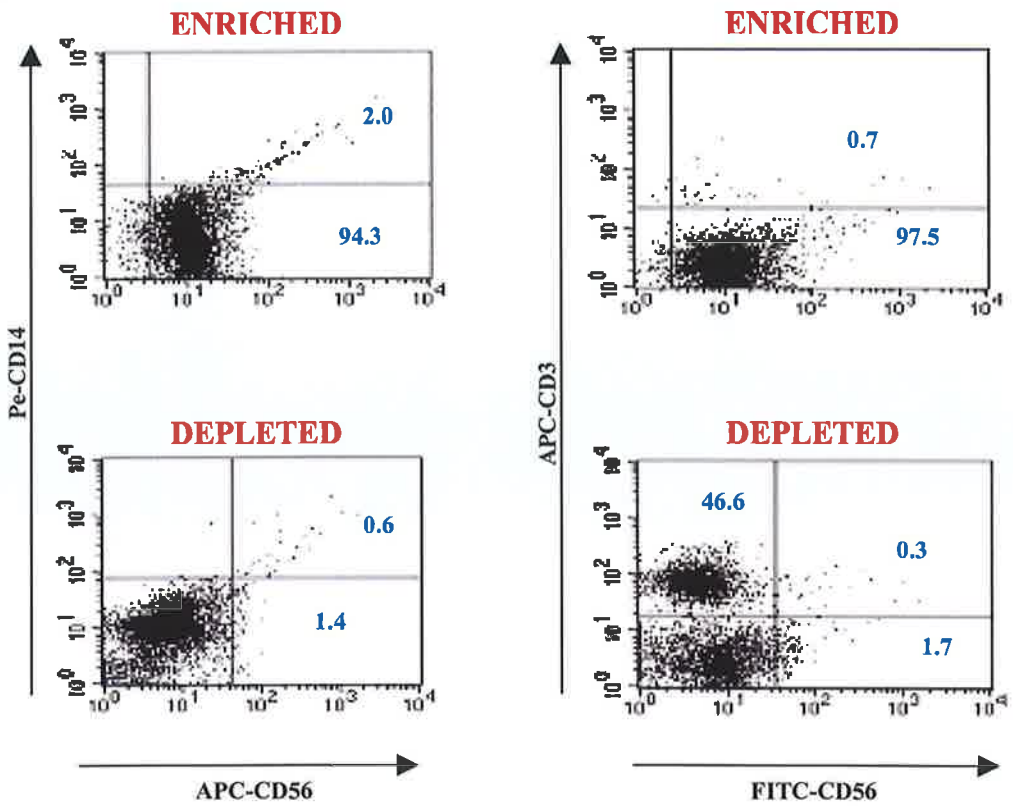

Purity of CD56+ NK cells isolated from human PBMCs. Cells were positively selected using the NK Cell Isolation Kit II and stained with anti-human APC-CD3, Pe-CD14 and FITC/APC-CD56 and purity was assessed by flow cytometry. Quadrant markers were set based on isotype controls and values reflect the percentage of cells in each quadrant, which exhibit positive or negative staining for a particular marker. The NK enriched population had a purity > 90% with < 2% contaminating CD3+ and CD14+ cells, while the depleted fraction contained < 2% CD56+ cells.

Appendix 2: T cell secretion from A549 DC/MLR cocultures

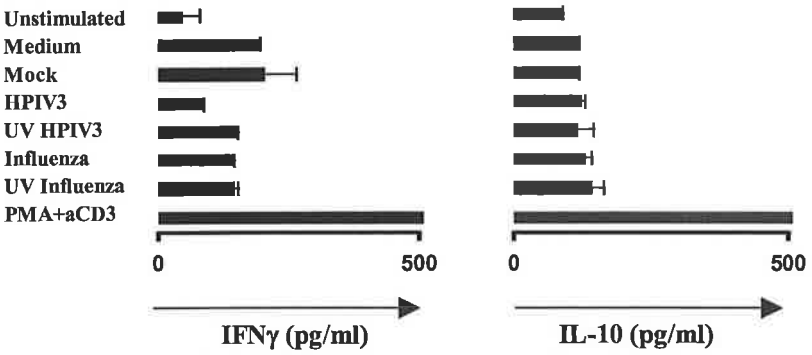

T cell secretion from mixed leukocytes cocultured with A549 DCs. Cells were infected with HPIV3 or influenza virus and were cultured for 24h (section 2.2.7). Cocultures of A549 DCs with allogeneic mixed leukocytes (MLR: CD14 depleted fraction) were set up at a 1:10 ratio and incubated for 3 days (section 2.2.10). Supernatants were harvested from the cocultures and tested for IFNγ and IL-10 secretion by ELISA. Data reflects the mean concentration ± SD for A549 DC/MLR cocultures.

Appendix 3: T cell proliferation from HPIV3 infected CD3- CD14- cells

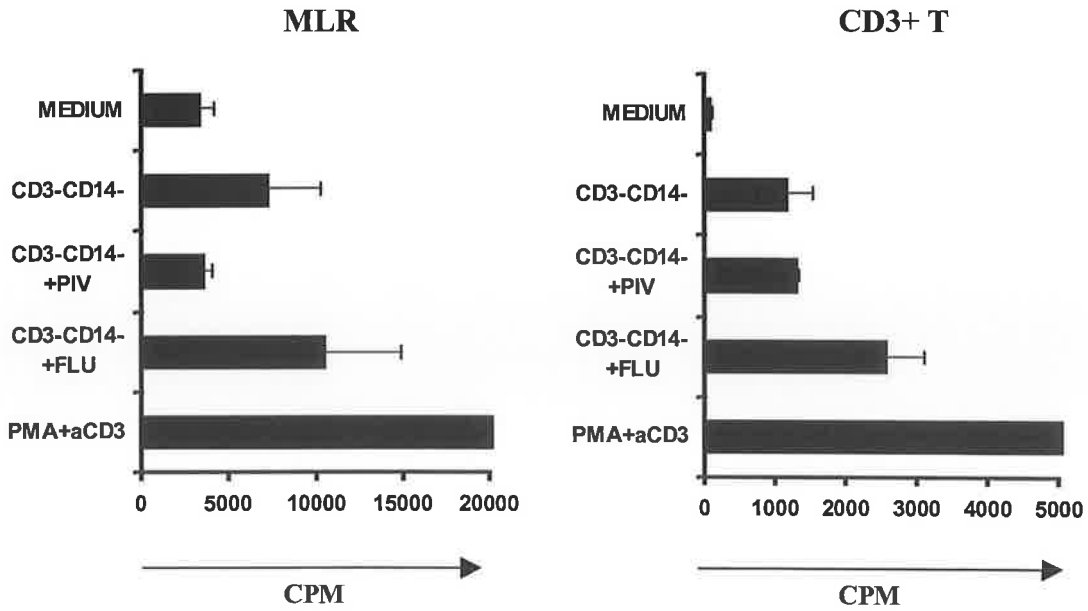

Mixed leukocyte and purified CD3+ T cell proliferation. CD3- CD14- cells were left untreated (CD3- CD14-) or infected with influenza (CD3-CD14-+FLU) or HPIV3 (CD3-CD14-+PIV) and co cultured in allogeneic mixed leukocyte reactions (MLR) or with allogeneic purified CD3+ T cells

(section 2.2.10). Proliferation was measured by ^{3}H incorporation after 5 days in culture (section 3.2.9). Data reflects the mean cpm $\pm$ SE for each sample.

Appendix 4: TGFβ secretion from HPIV3 infected cocultures

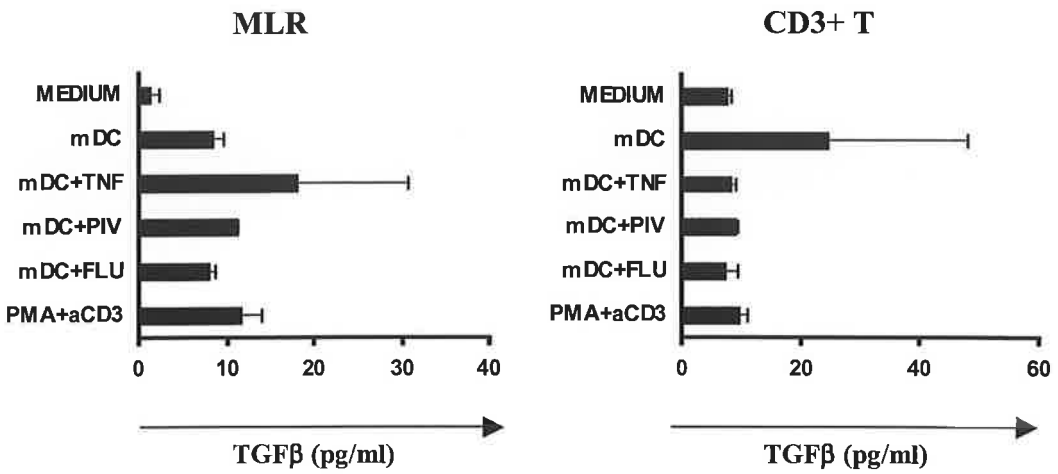

TGFβ secretion from mixed leukocyte and purified CD3+ T cell cocultures. CD14+ cells were left untreated (mDC) or treated with TNFα (mDC+TNF) or infected with influenza (mDC+FLU) or HPIV3 (mDC+PIV) and cocultured in allogeneic mixed leukocyte reactions (MLR) or with allogeneic purified CD3+ T cells (section 2.2.10). TGFβ was measured by ELISA (Duoset kit, R&D) after 3 days in culture. Results reflect the mean concentration $\pm$ SD for each sample from the various cocultures.

Appendix 5: Expression of p21 from mixed leukocyte and NK depleted mixed leukocyte cocultures

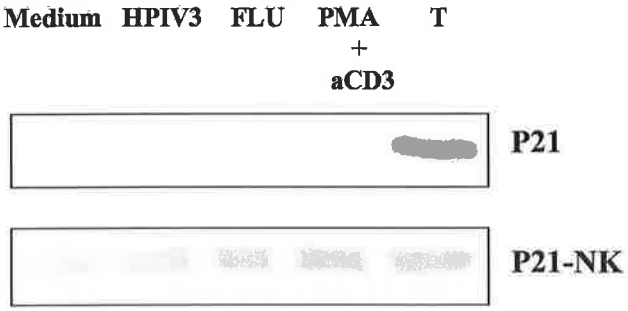

Western blot analysis of the cell cycle inhibitor p21. CD14+ cells were left untreated or infected with HPIV3 or influenza and cocultured with mixed leukocytes or CD56+ NK depleted mixed leukocytes. Cell lysates were prepared from 48h cultures and analysed for p21 by western blot (section 4.2.5). Blots depict p21expression from mixed leukocyte cocultures (p21) and NK depleted mixed leukocyte cocultures (p21-NK).

Appendix 6: IL-5 secretion from antigen restimulated splenocytes of immunised mice

A

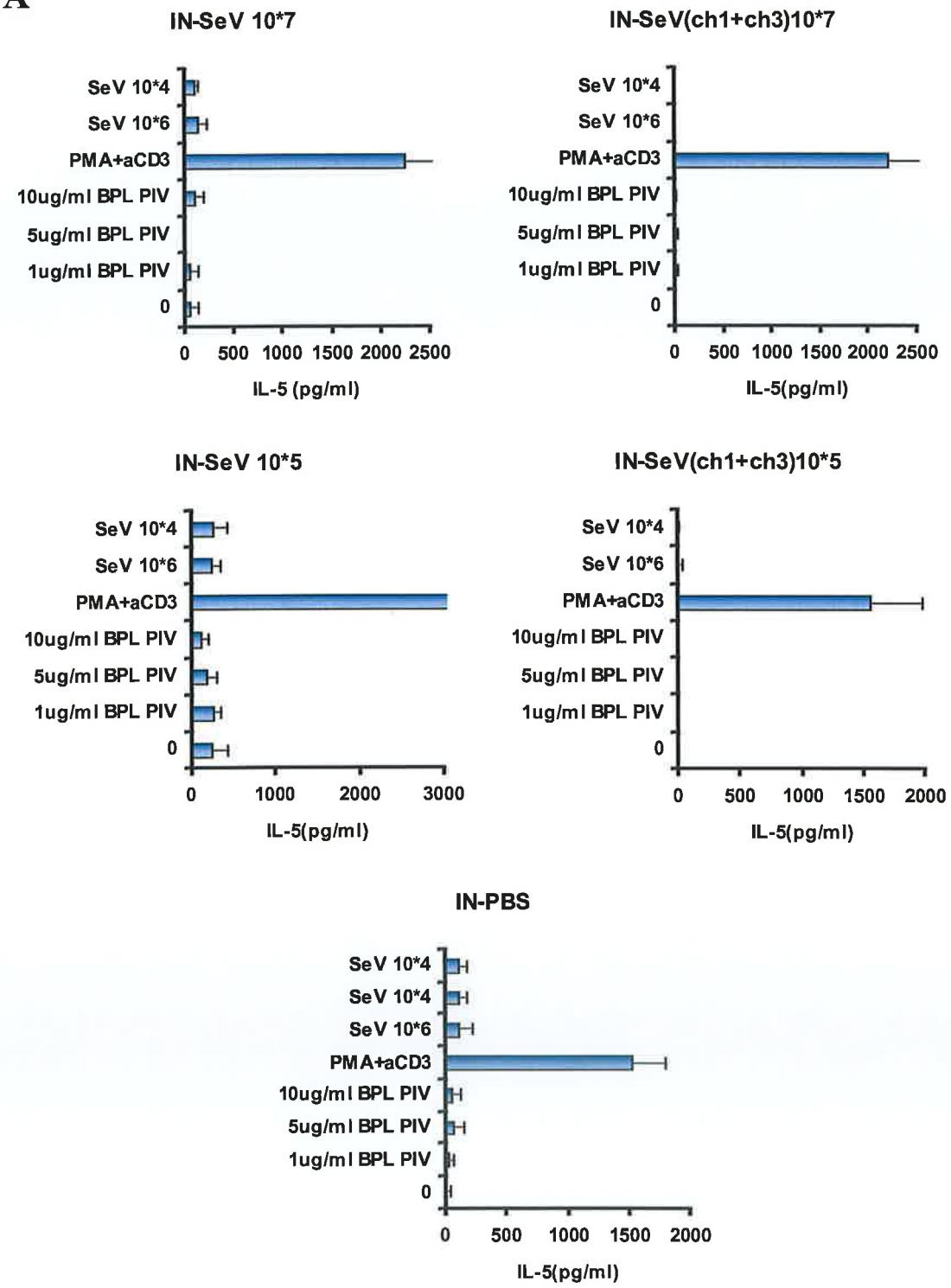

T cell responses following intransal infection with SeV and SeV expressing chimeric HPIV3 F (ch3) and HN (ch1) genes. Mice were immunised intransally with SeV and SeV(ch1+ch3) as described in section 5.2.1 (experiment 1) and sacrificed on day 35. Spleen cells were restimulated with UV inactivated SeV, BPL inactivated HPIV3 and PMA+aCD3 (section 5.2.1). After 3 days, supernatants were harvested from SeV 10^7, SeV(ch1+ch3) 10^7, SeV 10^5SeV(ch1+ch3) 10^5 and PBS (control) cultures and tested for IL-5 secretion by ELISA (section 5.2.3). Data reflects the mean concentration $\pm$ SD for each sample per group.

B

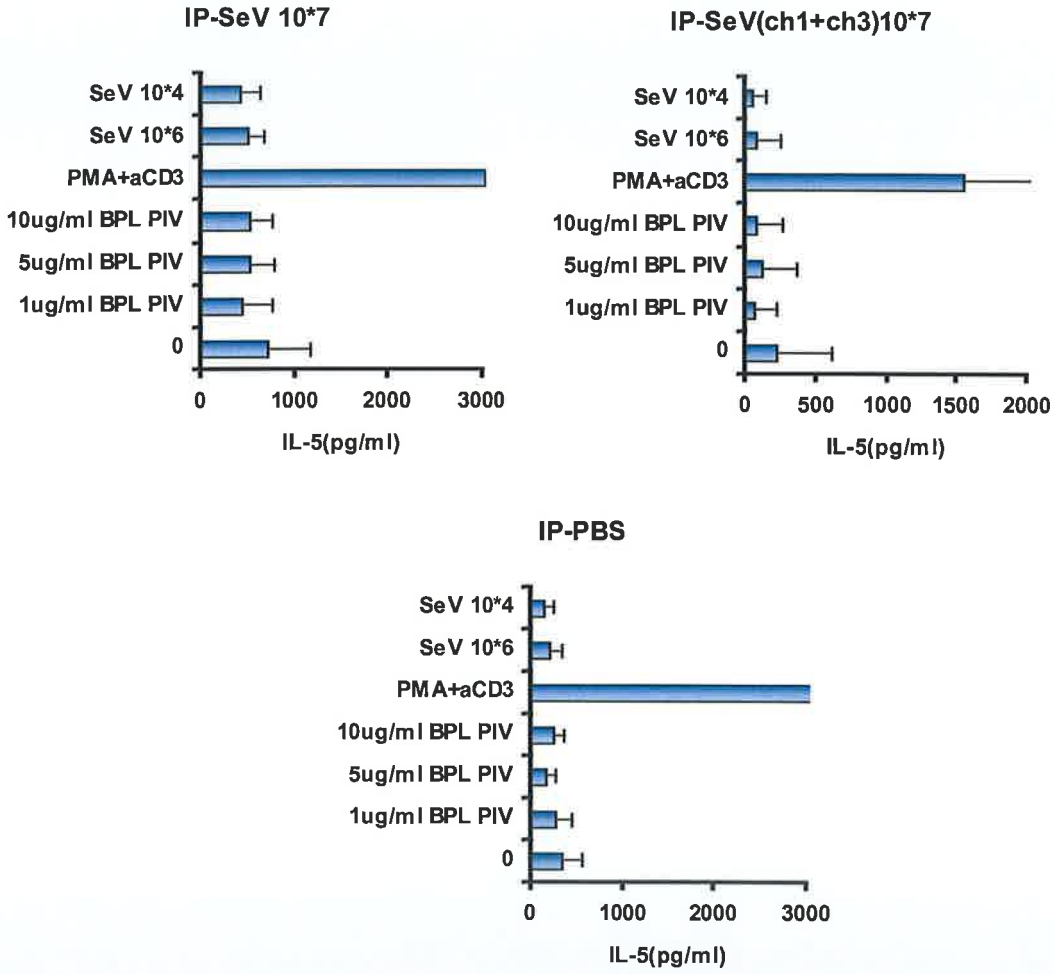

T cell responses following intraperitoneal infection with SeV and SeV expressing chimeric HPIV3 F (ch3) and HN (ch1) genes. Mice were immunised with SeV and SeV(ch1+ch3) as described in section 5.2.1 (experiment 1) and sacrificed on day 35. Spleen cells were restimulated with UV inactivated SeV, BPL inactivated HPIV3 and PMA+aCD3 (section 5.2.1). After 3 days, supernatants were harvested from SeV 10^7, SeV(ch1+ch3) 10^7 and PBS (control) cultures and tested for IL-5 secretion by ELISA (section 5.2.3). Data reflects the mean concentration $\pm$ SD for each sample per group.

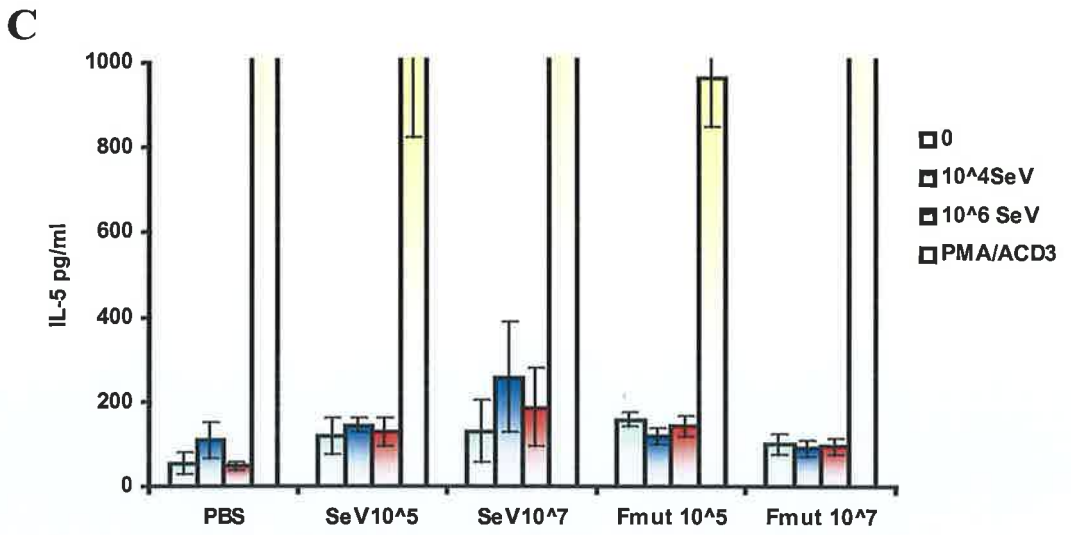

T cell responses following intranasal infection with a replication deficient SeVV (Fmut) and SeV wt. Mice were immunised with a replication deficient SeVV (Fmut) and SeVwt as described in section 5.2.1 (experiment 2) and sacrificed on day 35. Spleen cells were restimulated with UV inactivated SeV and PMA+aCD3 (section 5.2.1) and cultured for 3 days. Following incubation, supernatants were harvested from PBS (control), SeV 10^5, SeV10^7, SeVV Fmut 10^5 and SeVV Fmut 10^7 cultures and tested for IL-5 secretion by ELISA (section 5.2.3). Data reflects the mean concentration $\pm$ SD for each sample per group.

D

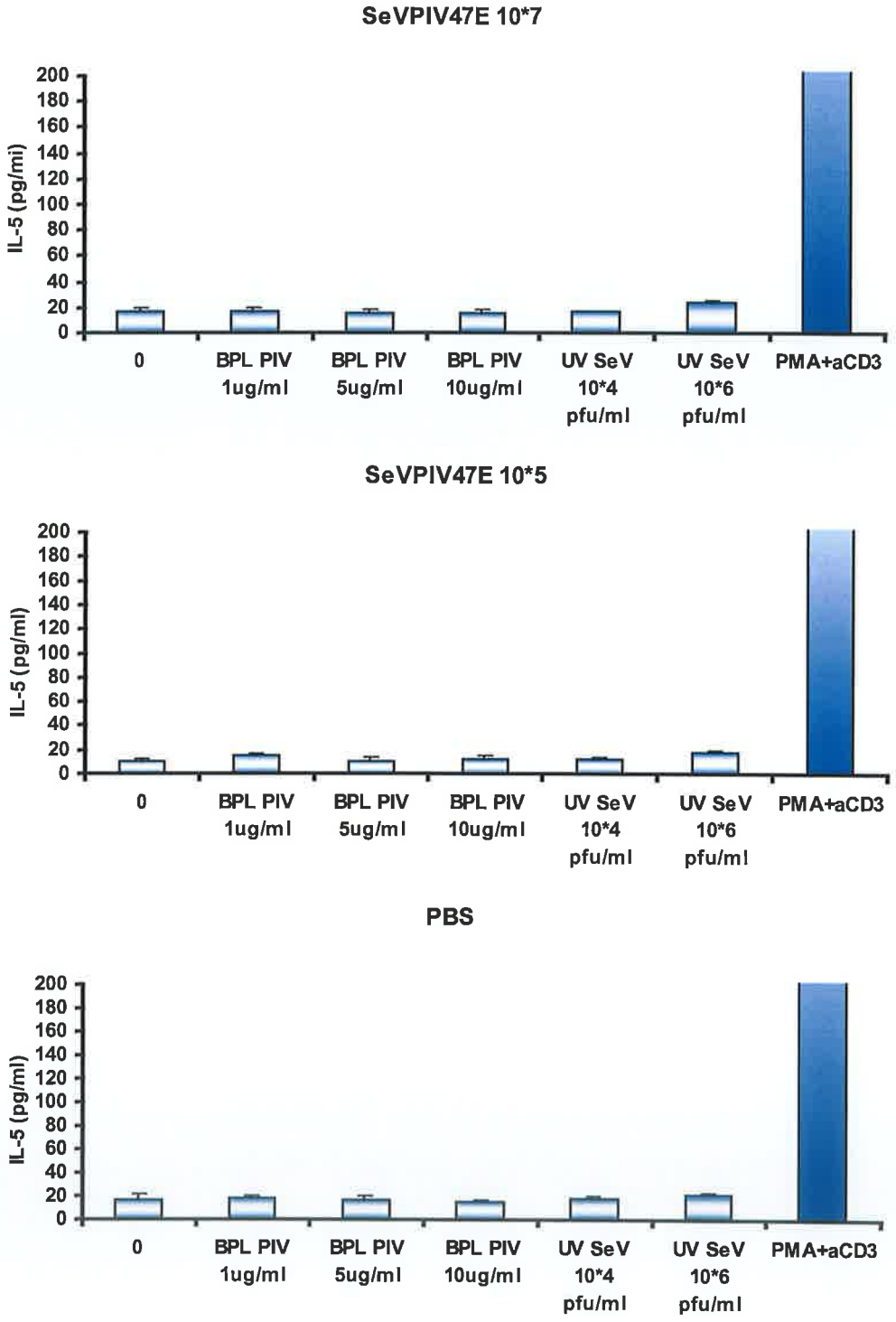

T cell responses following intransal immunisation with the replication competent final vaccine. Mice were immunised with the replication competent SePIV47E vaccine as described in section 5.2.1 (experiment 3) and sacrificed on day 35. Spleen cells were restimulated with UV inactivated SeV, BPL inactivated HPIV3 and PMA+aCD3 (section 5.2.1). After 3 days, supernatants were harvested from SePIV47E 10^7, SePIV47E 10^5 and PBS (control) cultures and tested for IL-5 secretion by ELISA (section 5.2.3). Data reflects the mean concentration $\pm$ SD for each sample per group.

E

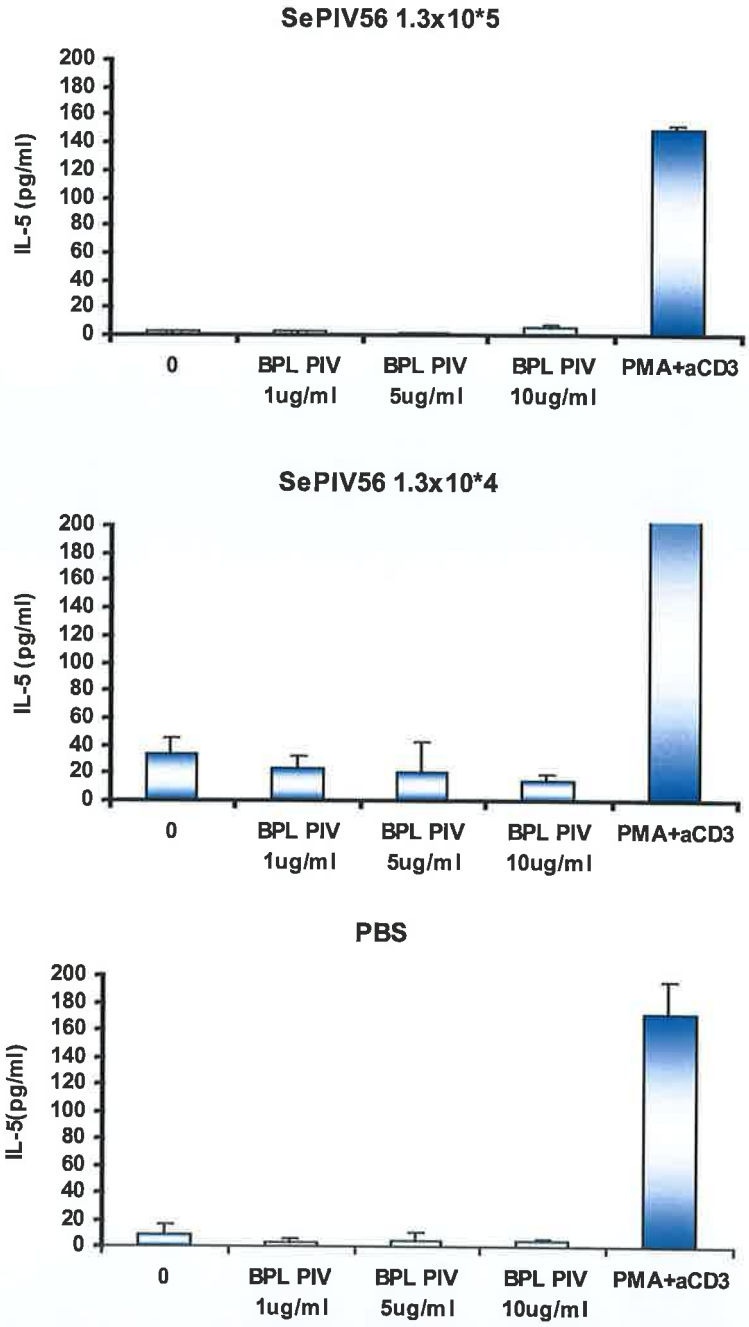

T cell responses following intransal immunisation with the replication deficient final vaccine. Mice were immunised with the replication deficient SePIV56 vaccine as described in section 5.2.1 (experiment 4) and sacrificed on day 35. Spleen cells were restimulated with BPL inactivated HPIV3 and PMA+aCD3 (section 5.2.1). After 3 days, supernatants were harvested from SePIV56 $1.3X10^5$, SePIV56 $1.3X10^4$ and PBS (control) cultures and tested for IL-5 secretion by ELISA (section 5.2.3). Data reflects the mean concentration $\pm$ SD for each sample per group.

Appendix 7: Additional statistics

Table 7.A Displays the statistical differences (P values) between HPIV3 samples and other treatments for IFNα production.

	MED-V-PIV	MOCK-V-PIV	TNFα-V-PIV	FLU-V-PIV	UV FLU-V-PIV
IL-4DC (28-10-04)	P=0.012	*	P=0.005	P=0.036	*
IFN-DC (26-4-06)	P=0.041	*	P=0.033	P=0.033	*
A549 DC (19-7-04)	P=0.013	P=0.013	*	P=0.013	P=0.013
A549 DC (UV:19-7-04)	P=0.02	P=0.021	*	P=0.021	P=0.02
CD14+ (6-9-04)A	P=0.007	*	P=0.006	P=0.009	*
CD14+ (6-9-04)B	P=0.045	*	P=0.045	P=0.05	*

Table 7.B Shows the statistical differences (P values) between HPIV3 samples and other treatments for IFNα production from CD14+ monocytes.

IFNα	MED-V-PIV	TNFα-V-PIV	FLU-V-PIV
CD14+ 24h (6-9-04)B	P=0.02	P=0.02	P=0.02
CD14+ 48h (6-9-04)B	P=0.045	P=0.045	P=0.05
CD14+ 24h(19-7-04)	P=0.017	P=0.017	P=0.018
CD14+ 48h(19-7-04)	P=0.019	P=0.019	P=0.019

Table 7.C Shows the statistical difference (P values) between HPIV3 samples and other treatments for IL-10 production from CD14+ monocytes.

IL-10	MED-V-PIV	TNFα-V-PIV	FLU-V-PIV
CD14+ 48h (20-7-04)B	P=0.003	P=0.008	P=0.007

Table 7.D Shows the statistical differences (P values) between HPIV3 infected MLR cocultures and the other MLR cocultures for T cell proliferation (cpm).

MLR	DC-V-DC+PIV	DC+TNFα–V-DC+PIV	DC+FLU-V-DC+PIV
DONOR 2 (1-9-04)	P=0.006	P=0.012	P=0.046
DONOR 3 (13-7-05)	P=0.05	NS*	P=0.005
DONOR 4 (26-7-05)	P=0.005	P=0.006	P=0.003
DONOR 5 (12-10-05)	P=0.05	P=0.014	P=0.047

*NS (not significant)

Table 7.E Shows the statistical difference (P values) between non-treated and IL-2 treated HPIV3 infected MLR cocultures for T cell proliferation (cpm).

MLR	DC+PIV-V-DC+PIV(1ng/ml)
DONOR 2 (6-12-05)	P=0.017

Table 7.F Shows the statistical differences (P values) between HPIV3 infected CD3+ T cell cocultures (containing autologous CD3- CD14- cells) and the other CD3+ T cell cocultures (containing autologous CD3- CD14- cells) for T cell proliferation (cpm).

CD3+T	DONOR 2 (03/08/2005)	DONOR 3 (29/06/2005)
AUTO+DC	P=0.036	P=0.05
AUTO+TNF	P=0.05	P=0.05
AUTO+FLU	P=0.05	P=0.006

Table 7.G Shows the statistical differences (P values) between HPIV3 infected MLR cocultures (containing autologous or allogeneic CD3- CD14- cells) and the other MLR cocultures (containing autologous or allogeneic CD3- CD14- cells) for T cell proliferation (cpm).

MLR	DONOR 2 (03/08/2005)	DONOR 3 (07/07/2005)
AUTO+DC	P=0.046	P=0.046
AUTO+TNF	P=0.05	P=0.035
AUTO+FLU	NS*	P=0.043
ALLO+DC	P=0.05	P=0.000
ALLO+TNF	P=0.015	P=0.024
ALLO+FLU	P=0.043	P=0.028

*NS (not significant)

Table 7.H Shows the statistical differences (P values) between HPIV3 infected CD3+ T cell cocultures (containing autologous NK cells) and the other CD3+ T cell cocultures (containing autologous NK cells) for T cell proliferation (cpm).

CD3+T	NK+DC-V-NK+DC+PIV	NK+DC+TNF-V-NK+DC+PIV	NK+DC+FLU-V-NK+DC+PIV
DONOR 2 (26-4-06)	P=0.001	P=0.047	P=0.045
DONOR 3 (6-12-05)	P=0.047	NS*	p=0.05

*NS (not significant)

Table 7.I Shows the statistical difference (P values) between samples for Rb phosphorylation from mixed leukocyte cocultures and NK depleted mixed leukocyte cocultures.

DONOR 2	MLR-V-MLR-NK
DC	P=0.013
DC+PIV	P=0.007
DC+FLU	P=0.05

Appendix 8: Raw data from repeat experiments

Table 8.A Purity of CD14+ monocytes (% of cells staining positive for CD11c and CD14) isolated from human PBMCs.

	Unseparated	CD14 depleted	CD14 enriched
CD11c-V-CD14 (% positive cells)-14/10/03	16.8	2.1	90.2
CD11c-V-CD14 (% positive cells)-4/3/04	22.3	1.8	91

Table 8.B Cytokine (IL-10, IL-12p40 and TNFα) secretion profile (mean concentration pg/ml) of virally infected IL-4 DCs, IFN-DCs, monocytes and A549 DCs.

			MEAN (pg/ml)				
IL-10	MED	MOCK	TNFα	HPIV3	UV HPIV3	FLU	UV FLU
IL-4DC (22-6-06)	95.03	*	126.02	138.84	*	93.56	*
IFN-DC (26-4-06)	64	*	45.71	42.48	*	42.48	*
A549 DC (20-7-04)	540.38	876.43	*	969.17	1679.86	874.3	891.62
CD14+ (20-7-04)B	540.38	*	949.18	1679.85	*	876.43	*
IL-12p40	MED	MOCK	TNFα	HPIV3	UV HPIV3	FLU	UV FLU
IL-4DC (28-10-04)	7057.04	*	17319.87	1490.78	*	281.1	*
IFN-DC (26-4-06)	37.87	*	64.79	34.23	*	21.89	*
A549 DC (20-7-04)	9.96	31.8	*	22.35	39.1	16.57	12.4
CD14+ (7-9-04)B	40.15	*	24.61	34.69	*	13.63	*
CD14+ (7-9-04)A	27.47	*	39.62	39.62	*	14.53	*
CD14+ (7-9-04)B	40.15	*	24.61	34.69	*	13.63	*
CD14+ (7-9-04)A	27.47	*	39.62	39.62	*	14.53	*
TNFα	MED	MOCK	TNFα	HPIV3	UV HPIV3	FLU	UV FLU
IL-4DC (28-10-04)	244.21	*	8305.78	1126.32	*	156.49	*
IFN-DC (26-4-06)	113.61	*	8636.45	226.85	*	18.88	*
A549 DC (20-7-04)	22.31	26.5	*	142.3	121.36	56.2	10.1
CD14+ (7-9-04)B	8.47	*	5277.76	1254.09	*	89.98	*

Table 8.C Virus induced apoptosis of IL-4 DCs, IFN-DCs and monocytes.

		% OF APOPTOTIC CELLS		
IL-4DC (22/06/2006)	MED	TNFα	HPIV3	FLU
LL	30	76	29	51
LR	42	17	53	33
UR	26	6	17	13
IFN-DC (20/06/2006)	MED	TNFα	HPIV3	FLU
LL	72	79	66	70
LR	16	11	26	20
UR	12	9	5	9
UR	12	9	5	9
CD14+ (15/07/2005)	MED	TNFα	HPIV3	FLU
LL	68	67	51	64
LR	18	18	30	22
UR	11	14	16	13

The lower left (LL) quadrant represents living cells, the lower right (LR) quadrant represents early apoptotic cells and the upper right (UR) quadrant represents late apoptotic cells.

Table 8.D T cell proliferation profiles (mean cpm) from purified CD3+ T cell and MLR cocultures reconstituted with virally infected IL-4 DCs, IFN-DCs, monocytes and A549 DCs.

				Mean ^{3}H-thymidine incorporation (cpm)					
CD3+T	T	MED	MOCK	TNFα	HPIV3	UV HPIV3	FLU	UV FLU	PMA+aCD3
IL-4DC (25/10/04)B	218	36454	*	39885	6614.67	*	33343.3	*	45630
IL-4DC (30/1/06)	127	31271	*	42015	24405	*	31818	*	44563
IFN-DC (30/4/06)	109	13582	*	9069	3983	*	8937	*	11370
A549 DC (2/5/06)B	63	2158	1522	*	1149	1241	1506	2044	38614
CD14+ (26/10/04)	93	563.67	*	426	422	*	540	*	5650
CD14+ (11/5/05)	161	294.33	*	259.33	238.33	*	198.67	*	50323
CD14+ (21/6/05)	268	1022	*	1619	1968	*	2316	*	37481
CD14+ (3/8/05)	771	4706	*	5484	4482	*	5109	*	28964.67

				Mean ^{3}H-thymidine incorporation (cpm)					
MLR	T	MED	MOCK	TNFα	HPIV3	UV HPIV3	FLU	UV FLU	PMA+aCD3
IL-4DC (25/10/04)B	4157	79520.7	*	87958	59549	*	71481	*	89563.2
IL-4DC (30/1/06)	166	12031.3	*	36969	8903.33	*	17290.7	*	42955
IFN-DC (30/4/06)	313	13710	*	13534	6889	*	7300	*	45183
A549 DC (2/5/06)B)	178	3433	3347	*	2305	2025	2676	2904	41929
CD14+ (13/7/05)	36	5686	*	1174	146	*	3394	*	41090
CD14+ (26/7/05)	600	15538	*	16172	4688	*	15149	*	50163
CD14+ (12/10/05)	110	2841.5	*	2677	642.5	*	6080	*	35179
CD14+ (1/9/04)	72	10143	*	8025	912	*	6737	*	80136

Table 8.E IFNγ (mean concentration pg/ml) secretion from purified CD3+ T cell and MLR cocultures reconstituted with virally infected IL-4 DCs, IFN-DCs and monocytes.

			MEAN (pg/ml)			
CD3+T-IFNγ	T	MED	TNFα	HPIV3	FLU	PMA+aCD3
IL-4DC (2-11-04)D.2	14.45	357.49	892.89	1774.06	1401.43	1950
IFN-DC (23-11-04)D.2	17.03	4108.22	3182.59	3986.71	3885.58	3713.34
CD14+ (5/4/05)	8.37	17.18	18.94	17.59	21.84	2847.45
CD14+ (25/5/05)	16.2	45.2	49.01	38.73	54.69	2140.6
CD14+ (26/4/05)C	11.2	20.88	18.51	40.97	20.1	2007.75

			MEAN (pg/ml)			
MLR-IFNγ	T	MED	TNFα	HPIV3	FLU	PMA+aCD3
IL-4DC (2-11-04)D.2	401.25	2254.02	2377.88	2293.8	2328.76	2597.15
IFN-DC (23-11-04)D.2	25.1	1798.17	2494.06	2829.42	3615.27	3588.83
CD14+ (5/4/05)	4.52	14.86	11.67	25.53	22.42	2637.96
CD14+ (25/5/05)	3.2	13.78	12.06	14.66	15.16	1769
CD14+ (26/4/05)C	3.58	10.2	10.52	16.84	15.41	1715.58

Table 8.F IL-10 (mean concentration pg/ml) secretion from purified CD3+ T cell and MLR cocultures reconstituted with virally infected IL-4 DCs, IFN-DCs and monocytes.

			MEAN (pg/ml)			
CD3+T-IL-10	T	MED	TNFα	HPIV3	FLU	PMA+aCD3
IL-4DC (2-11-04)D.2	71.44	321.3	463.53	1398.99	720.51	2560
IFN-DC (23-11-04)D.2	57.3	3598.7	2081.17	13735	5703.43	43845.91
CD14+ (5/4/05)	40.5	79.83	101.01	148.88	151.04	5077.7
CD14+ (11/5/05)	24.76	75.52	67.37	130.67	135.08	8267.36
CD14+ (26/4/05)C	4.76	139.49	113.7	288.84	118.41	7964.14

			MEAN (pg/ml)			
MLR-IL-10	T	MED	TNFα	HPIV3	FLU	PMA+aCD3
IL-4DC (2-11-04)D.2	58.09	111.6	161.58	261.35	277.59	264.6
IFN-DC (23-11-04)D.2	37.37	68.57	68.7	107.61	101.13	9280.86
CD14+ (5/4/05)	10.5	18.74	29.97	36.89	67.81	4059.95
CD14+ (11/5/05)	8.9	14.26	24.82	65.23	75.36	3977.06
CD14+ (26/4/05)C	14.95	35.09	37.88	125.03	89.19	2475.31

Table 8.G Apoptosis of lymphocytes from mixed leukocytes and purified CD3+ T cells cocultured with virally infected monocytes.

MLR		% OF APOPTOTIC CELLS		
06/12/2005	MED	TNFα	HPIV3	FLU
LL	68	64	63	58
LR	28	31	31	36
UR	4	5	5	6
19/04/2005	MED	TNFα	HPIV3	FLU
LL	59	57	52	54
LR	37	38	39	41
UR	4	5	8	4

CD3+T		% OF APOPTOTIC CELLS		
06/12/2005	MED	TNFα	HPIV3	FLU
LL	82	70	69	61
LR	17	29	30	38
UR	1	1	1	1
19/04/2005	MED	TNFα	HPIV3	FLU
LL	71	71	64	70
LR	23	23	28	25
UR	3	4	7	5

The lower left (LL) quadrant represents living cells, the lower right (LR) quadrant represents early apoptotic cells and the upper right (UR) quadrant represents late apoptotic cells.

Table 8.H Cytokine (IFNγ and IL-10) secretion (mean concentration pg/ml) from purified CD3+ T cell cocultures reconstituted with autologous CD3- CD14- cell populations.

			MEAN (pg/ml)		
CD3+T-IFNγ	T	Auto+DC	Auto+DC+FLU	Auto+DC+HPIV3	PMA+aCD3
22/07/2005	68.08	118.31	127.85	126.5	2356

			MEAN (pg/ml)		
CD3+T-IL-10	T	Auto+DC	Auto+DC+FLU	Auto+DC+HPIV3	PMA+aCD3
11/10/2005	92.47	115.22	137.6	129.96	2221.59
22/07/2005	87.92	140.36	136.77	149.44	2634.62

Table 8.I Transwell proliferation (mean cpm) studies on purified CD3+ T cells cultured with allogeneic DCs (unstimulated, TNFα treated or virus infected) and autologous CD14- CD3- cells.

TRANSWELLS		Mean ^{3}H-thymidine incorporation (cpm)		
CD3+T	Auto // DC+T	Auto // DC+TNF+T	Auto // DC+PIV+T	Auto // DC+FLU+T
07/07/2005	741	331	392	296
7/6/06 D.2	559	2393.5	2611	1110.5

Table 8.J Phenotypic profile of CD3- CD14- cells (M1 region shows the % of positive cells for specific markers)..

CD3- CD14- Cells	% OF POSITIVE CELLS IN M1
CD11c	16
CD14	1
CD123	5
CD3	1
CD56	11
CD4	6
CD86	4
CD80	5
CD83	5
CD40	37
CD19	15
DC-SIGN	0
CD1a	8
CD11b	6

Table 8.K T cell proliferation profiles (mean cpm) from purified CD3+ T cell and MLR cocultures (containing infected allogeneic monocytes) reconstituted with autologous B cells.

			Mean ^{3}H-thymidine incorporation (cpm)			
CD3+T	T	B+DC	B+DC+TNF	B+DC+PIV	B+DC+FLU	PMA+aCD3
26/07/2005	167	1052	730	889	2633	39572
13/07/2005	85	2691	1944	1789	1895	40054.33

			Mean ^{3}H-thymidine incorporation (cpm)			
MLR	T	B+DC	B+DC+TNF	B+DC+PIV	B+DC+FLU	PMA+aCD3
26/07/2005	600	24455	21447.67	12057	19954	50163

Table 8.L Expression of surface markers on unstimulated and HPIV3 infected CD3- CD14- cells.

% positive cells (10/11/05)	Unstimulated	HPIV3
CD19+/CD80+	1.0	1.0
CD19+/CD80-	15.1	15.3
CD19-/CD80+	1.7	1.8
Class II+/Class I+	17.2	17.9
Class II+/Class I-	0.0	0.0
Class II-/Class I+	52.3	52.6
CD56+/CD14+	0.0	0.0
CD56+/CD14-	8.5	8.7
CD56-/CD14+	1.1	1.4

% positive cells (2/12/05)	Unstimulated	HPIV3
CD19+/CD80+	0.0	0.0
CD19+/CD80-	19.2	18.9
CD19-/CD80+	1.1	1.3
Class II+/Class I+	20.1	22.6
Class II+/Class I-	0.0	0.0
Class II-/Class I+	54.5	54.8
CD56+/CD14+	0.0	0.0
CD56+/CD14-	11.5	11.8
CD56-/CD14+	0.1	0.2

Table 8.M T cell proliferation profiles (mean cpm) from MLR cocultures (containing infected allogeneic monocytes) reconstituted with autologous NK cells.

			Mean ^{3}H-thymidine incorporation (cpm)			
MLR	T	NK+DC	NK+DC+TNF	NK+DC+PIV	NK+DC+FLU	PMA+aCD3
03/08/2005	104	3807	3970	1011	2962	31729
09/11/2005	65	256	459	148	450	32844

Table 8.N Cell cycle analysis from mixed leukocyte and NK depleted mixed leukocyte cocultures reconstituted with allogeneic DCs (unstimulated, TNFα treated or virus infected).

		% OF CELLS	
MLR	M1	M2	M3
DC (19/12/05)	99.24	0.12	0.27
DC+TNF	99.04	0.13	0.47
DC+PIV	99.41	0.11	0.11
DC+FLU	98.81	0.18	0.59
PMA+aCD3	53.79	18.18	14.74
DC (31/5/06)D.2	96.57	0.17	0.61
DC+TNF	96.33	0.15	0.66
DC+PIV	96.37	0.13	0.41
DC+FLU	96.24	0.18	0.46
PMA+aCD3	46.71	15.98	20.91
		% OF CELLS	

NK depleted MLR	M1	M2	M3
DC (23/5/06)	95.51	0.30	0.64
DC+TNF	96.82	0.59	0.60
DC+PIV	95.13	0.31	0.64
DC+FLU	96.63	0.39	1.02
PMA+aCD3	34.46	11.09	11.39
DC (31/5/06)D.2	93.71	0.58	1.06
DC+TNF	93.41	0.66	1.09
DC+PIV	96.32	0.43	1.09
DC+FLU	96.69	0.41	0.93
PMA+aCD3	47.23	16.82	20.95

M1 represents the percentage of cells in the G0/G1 phase, M2 represents S phase and M3 represents G2 phase.

Table 8.O T cell proliferation profiles (mean cpm) from purified CD3+ T cell cocultures and MLR cocultures reconstituted with allogeneic virosome infected monocytes.

			Mean ^{3}H-thymidine incorporation (cpm)			
CD3+T	T	DC+T	DC+IRIV+T	DC+IRPV+T	DC+IRSV+T	PMA+aCD3
13/04/2005	124	1336	1210	1649	1377	41097
MLR	T	DC+T	DC+IRIV+T	DC+IRPV+T	DC+IRSV+T	PMA+aCD3
13/04/2005	147	6697	4697	3686	8106	33833

IRIV (influenza virosome), IRPV (parainfluenza virosome) and IRSV (sendai virosome)

Table 8.P T cell proliferation profiles (mean cpm) from purified CD3+ T cell cocultures and MLR cocultures reconstituted with vaccine (SePIV56) infected monocytes.

				Mean ^{3}H-thymidine incorporation (cpm)			
CD3+T	T	DC+T	DC+PIV+T	DC+FLU+T	DC+SePIV56	DC+UV SePIV56	PMA+aCD3
7/6/06 D.1	125	5069	4120	2609	5787	3510	44526
25/07/2006	170	2568	5403	7616	2803	2733	18092

				Mean ^{3}H-thymidine incorporation (cpm)			
MLR	T	DC+T	DC+PIV+T	DC+FLU+T	DC+SePIV56	DC+UV SePIV56	PMA+aCD3
7/6/06 D.1	54	1597	1451	1539	1702	1503	33406
25/07/2006	153	562	537	2290	512	508	15376

BIBLIOGRAPHY

Abbas, A.K.A.H.L.a.J.S.P. (1997) *Cellular And Molecular Immunology*. W. B. Saunders Company, Philadelphia, US.

Abed, Y., Boivin, G. (2006) Treatment of respiratory virus infections. *Antiviral Res* **14**, 14.

Accapezzato, D., Francavilla, V., Paroli, M., Casciaro, M., Chircu, L.V., Cividini, A., Abrignani, S., Mondelli, M.U., Barnaba, V. (2004) Hepatic expansion of a virus-specific regulatory CD8(+) T cell population in chronic hepatitis C virus infection. *J Clin Invest.* **113**, 963-72.

Akira, S., Takeda, K., Kaisho, T. (2001) Toll-like receptors: critical proteins linking innate and acquired immunity. *Nat Immunol.* **2**, 675-80.

Akira, S., Takeda, K. (2004) Toll-like receptor signalling. *Nat Rev Immunol.* **4**, 499-511.

Andoniou, C.E., van Dommelen, S.L., Voigt, V., Andrews, D.M., Brizard, G., Asselin-Paturel, C., Delale, T., Stacey, K.J., Trinchieri, G., Degli-Esposti, M.A. (2005) Interaction between conventional dendritic cells and natural killer cells is integral to the activation of effective antiviral immunity. *Nat Immunol.* **6**, 1011-9. Epub 2005 Sep 4.

Andrejeva, J., Childs, K.S., Young, D.F., Carlos, T.S., Stock, N., Goodbourn, S., Randall, R.E. (2004) The V proteins of paramyxoviruses bind the IFN-inducible RNA helicase, mda-5, and inhibit its activation of the IFN-beta promoter. *Proc Natl Acad Sci U S A.* **101**, 17264-9. Epub 2004 Nov 24.

Andrews, D.M., Andoniou, C.E., Granucci, F., Ricciardi-Castagnoli, P., Degli-Esposti, M.A. (2001) Infection of dendritic cells by murine cytomegalovirus induces functional paralysis. *Nat Immunol* **2**, 1077-84.

Appleman, L.J., Berezovskaya, A., Grass, I., Boussiotis, V.A. (2000) CD28 costimulation mediates T cell expansion via IL-2-independent and IL-2-dependent regulation of cell cycle progression. *J Immunol.* **164**, 144-51.

Appleman, L.J., Boussiotis, V.A. (2003) T cell anergy and costimulation. *Immunol Rev.* **192**, 161-80.

Armstrong, G.L., Conn, L.A., Pinner, R.W. (1999) Trends in infectious disease mortality in the United States during the 20th century. *Jama.* **281**, 61-6.

Arnon, T.I., Achdout, H., Lieberman, N., Gazit, R., Gonen-Gross, T., Katz, G., Bar-Ilan, A., Bloushtain, N., Lev, M., Joseph, A., Kedar, E., Porgador, A., Mandelboim, O. (2004) The mechanisms controlling the recognition of tumor- and virus-infected cells by NKp46. *Blood* **103**, 664-72. Epub 2003 Sep 22.

Artavanis-Tsakonas, K., Tongren, J.E., Riley, E.M. (2003) The war between the malaria parasite and the immune system: immunity, immunoregulation and immunopathology. *Clin Exp Immunol.* **133**, 145-52.

Arvin, A.M., Greenberg, H.B. (2006) New viral vaccines. *Virology.* **344**, 240-9.

Ashkar, A.A., Bauer, S., Mitchell, W.J., Vieira, J., Rosenthal, K.L. (2003) Local delivery of CpG oligodeoxynucleotides induces rapid changes in the genital mucosa and inhibits replication, but not entry, of herpes simplex virus type 2. *J Virol.* **77**, 8948-56.

Banchereau, J., Steinman, R.M. (1998) Dendritic cells and the control of immunity. *Nature.* **392**, 245-52.

Banchereau, J., Briere, F., Caux, C., Davoust, J., Lebecque, S., Liu, Y.J., Pulendran, B., Palucka, K. (2000) Immunobiology of dendritic cells. *Annu Rev Immunol.* **18**, 767-811.

Barchet, W., Cella, M., Colonna, M. (2005) Plasmacytoid dendritic cells--virus experts of innate immunity. *Semin Immunol* **17**, 253-61.

Belshe, R.B., Hissom, F.K. (1982) Cold adaptation of parainfluenza virus type 3: induction of three phenotypic markers. *J Med Virol.* **10**, 235-42.

Bergmann, M., Garcia-Sastre, A., Carnero, E., Pehamberger, H., Wolff, K., Palese, P., Muster, T. (2000) Influenza virus NS1 protein counteracts PKR-mediated inhibition of replication. *J Virol* **74**, 6203-6.

Bitzer, M., Armeanu, S., Lauer, U.M., Neubert, W.J. (2003) Sendai virus vectors as an emerging negative-strand RNA viral vector system. *J Gene Med.* **5**, 543-53.

Blom, B., Ho, S., Antonenko, S., Liu, Y.J. (2000) Generation of interferon alpha-producing predendritic cell (Pre-DC)2 from human CD34(+) hematopoietic stem cells. *J Exp Med.* **192**, 1785-96.

Boettler, T., Spangenberg, H.C., Neumann-Haefelin, C., Panther, E., Urbani, S., Ferrari, C., Blum, H.E., von Weizsacker, F., Thimme, R. (2005) T cells with a CD4+CD25+ regulatory phenotype suppress in vitro proliferation of virus-specific CD8+ T cells during chronic hepatitis C virus infection. *J Virol.* **79**, 7860-7.

Brombacher, F., Kastelein, R.A., Alber, G. (2003) Novel IL-12 family members shed light on the orchestration of Th1 responses. *Trends Immunol.* **24**, 207-12.

Brown, D.M., Roman, E., Swain, S.L. (2004) CD4 T cell responses to influenza infection. *Semin Immunol.* **16**, 171-7.

Brown, D.M., Dilzer, A.M., Meents, D.L., Swain, S.L. (2006) CD4 T cell-mediated protection from lethal influenza: perforin and antibody-mediated mechanisms give a one-two punch. *J Immunol.* **177**, 2888-98.

Carbonneil, C., Saidi, H., Donkova-Petrini, V., Weiss, L. (2004) Dendritic cells generated in the presence of interferon-alpha stimulate allogeneic CD4+ T-cell proliferation: modulation by autocrine IL-10, enhanced T-cell apoptosis and T regulatory type 1 cells. *Int Immunol.* **16**, 1037-52. Epub 2004 Jun 7.

Cella, M., Salio, M., Sakakibara, Y., Langen, H., Julkunen, I., Lanzavecchia, A. (1999) Maturation, activation, and protection of dendritic cells induced by double-stranded RNA. *J Exp Med* **189**, 821-9.

Cella, M., Facchetti, F., Lanzavecchia, A., Colonna, M. (2000) Plasmacytoid dendritic cells activated by influenza virus and CD40L drive a potent TH1 polarization. *Nat Immunol* **1**, 305-10.

Chan, C.W., Crafton, E., Fan, H.N., Flook, J., Yoshimura, K., Skarica, M., Brockstedt, D., Dubensky, T.W., Stins, M.F., Lanier, L.L., Pardoll, D.M., Housseau, F. (2006) Interferon-producing killer dendritic cells provide a link between innate and adaptive immunity. *Nat Med.* **12**, 207-13. Epub 2006 Jan 29.

Chanock, R.M.B.R.M.a.P.L.C. (2001) Parainfluenza Viruses. In *Field Virology*, Volume 4th edition (D. M. a. P. M. H. Knipe, ed) Lippincott Williams and Wilkins, Philadelphia, US 1341-1379.

Chen, C.J., Sugiyama, K., Kubo, H., Huang, C., Makino, S. (2004) Murine coronavirus nonstructural protein p28 arrests cell cycle in G0/G1 phase. *J Virol.* **78**, 10410-9.

Clements, M.L., Belshe, R.B., King, J., Newman, F., Westblom, T.U., Tierney, E.L., London, W.T., Murphy, B.R. (1991) Evaluation of bovine, cold-adapted human, and wild-type human parainfluenza type 3 viruses in adult volunteers and in chimpanzees. *J Clin Microbiol.* **29**, 1175-82.

Coelho, A.L., Hogaboam, C.M., Kunkel, S.L. (2005) Chemokines provide the sustained inflammatory bridge between innate and acquired immunity. *Cytokine Growth Factor Rev* **16**, 553-60. Epub 2005 Jun 20.

Collier, L.a.J.O. (2006) *Human Virology*. Oxford University Press Inc, New York, US.

Colonna, M., Trinchieri, G., Liu, Y.J. (2004) Plasmacytoid dendritic cells in immunity. *Nat Immunol* **5**, 1219-26.

Combe, B., Pope, R., Darnell, B., Talal, N. (1984) Modulation of natural killer cell activity in the rheumatoid joint and peripheral blood. *Scand J Immunol.* **20**, 551-8.

Cox, N.J., Subbarao, K. (1999) Influenza. *Lancet.* **354**, 1277-82.

Crowe, J.E., Jr., Williams, J.V. (2003) Immunology of viral respiratory tract infection in infancy. *Paediatr Respir Rev.* **4**, 112-9.

de Jong, E.C., Vieira, P.L., Kalinski, P., Schuitemaker, J.H., Tanaka, Y., Wierenga, E.A., Yazdanbakhsh, M., Kapsenberg, M.L. (2002) Microbial compounds selectively induce Th1 cell-promoting or Th2 cell-promoting dendritic cells in vitro with diverse th cell-polarizing signals. *J Immunol.* **168**, 1704-9.

Degli-Esposti, M.A., Smyth, M.J. (2005) Close encounters of different kinds: Dendritic cells and NK cells take centre stage. *Nat Rev Immunol* **5**, 112-124.

Della Chiesa, M., Vitale, M., Carlomagno, S., Ferlazzo, G., Moretta, L., Moretta, A. (2003) The natural killer cell-mediated killing of autologous dendritic cells is confined to a cell subset expressing CD94/NKG2A, but lacking inhibitory killer Ig-like receptors. *Eur J Immunol.* **33**, 1657-66.

Denny, F.W., Clyde, W.A., Jr. (1986) Acute lower respiratory tract infections in nonhospitalized children. *J Pediatr.* **108**, 635-46.

Diebold, S.S., Montoya, M., Unger, H., Alexopoulou, L., Roy, P., Haswell, L.E., Al-Shamkhani, A., Flavell, R., Borrow, P., Reis e Sousa, C. (2003) Viral infection switches non-plasmacytoid dendritic cells into high interferon producers. *Nature* **424**, 324-8.

Diebold, S.S., Kaisho, T., Hemmi, H., Akira, S., Reis e Sousa, C. (2004) Innate antiviral responses by means of TLR7-mediated recognition of single-stranded RNA. *Science* **303**, 1529-31. Epub 2004 Feb 19.

Doherty, P.C., Turner, S.J., Webby, R.G., Thomas, P.G. (2006) Influenza and the challenge for immunology. *Nat Immunol.* **7**, 449-55.

Dong, C. (2006) Diversification of T-helper-cell lineages: finding the family root of IL-17-producing cells. *Nat Rev Immunol.* **6**, 329-34.

Dubois, B., Lamy, P.J., Chemin, K., Lachaux, A., Kaiserlian, D. (2001) Measles virus exploits dendritic cells to suppress CD4+ T-cell proliferation via expression of surface viral glycoproteins independently of T-cell trans-infection. *Cell Immunol.* **214**, 173-83.

Durbin, A.P., Karron, R.A. (2003) Progress in the development of respiratory syncytial virus and parainfluenza virus vaccines. *Clin Infect Dis.* **37**, 1668-77. Epub 2003 Nov 20.

Esser, M.T., Marchese, R.D., Kierstead, L.S., Tussey, L.G., Wang, F., Chirmule, N., Washabaugh, M.W. (2003) Memory T cells and vaccines. *Vaccine.* **21**, 419-30.

Fauci, A.S. (2006) Emerging and re-emerging infectious diseases: influenza as a prototype of the host-pathogen balancing act. *Cell.* **124**, 665-70.

Fernandez-Sesma, A., Marukian, S., Ebersole, B.J., Kaminski, D., Park, M.S., Yuen, T., Sealfon, S.C., Garcia-Sastre, A., Moran, T.M. (2006) Influenza Virus Evades Innate and Adaptive Immunity via the NS1 Protein. *J Virol.* **80**, 6295-304.

Flamand, L., Gosselin, J., Stefanescu, I., Ablashi, D., Menezes, J. (1995) Immunosuppressive effect of human herpesvirus 6 on T-cell functions: suppression of interleukin-2 synthesis and cell proliferation. *Blood.* **85**, 1263-71.

Fonteneau, J.F., Gilliet, M., Larsson, M., Dasilva, I., Munz, C., Liu, Y.J., Bhardwaj, N. (2003) Activation of influenza virus-specific CD4+ and CD8+ T cells: a new role for plasmacytoid dendritic cells in adaptive immunity. *Blood* **101**, 3520-6. Epub 2003 Jan 2.

Forster, R., Schubel, A., Breitfeld, D., Kremmer, E., Renner-Muller, I., Wolf, E., Lipp, M. (1999) CCR7 coordinates the primary immune response by establishing functional microenvironments in secondary lymphoid organs. *Cell.* **99**, 23-33.

Fulginiti, V.A., Eller, J.J., Sieber, O.F., Joyner, J.W., Minamitani, M., Meiklejohn, G. (1969) Respiratory virus immunization. I. A field trial of two inactivated respiratory virus vaccines; an aqueous trivalent parainfluenza virus vaccine and an alum-precipitated respiratory syncytial virus vaccine. *Am J Epidemiol.* **89**, 435-48.

Gaffen, S.L., Liu, K.D. (2004) Overview of interleukin-2 function, production and clinical applications. *Cytokine* **28**, 109-23.

Garcia-Sastre, A. (2002) Mechanisms of inhibition of the host interferon alpha/beta-mediated antiviral responses by viruses. *Microbes Infect.* **4**, 647-55.

Garcia-Sastre, A., Biron, C.A. (2006) Type 1 interferons and the virus-host relationship: a lesson in detente. *Science.* **312**, 879-82.

Gerosa, F., Gobbi, A., Zorzi, P., Burg, S., Briere, F., Carra, G., Trinchieri, G. (2005) The reciprocal interaction of NK cells with plasmacytoid or myeloid dendritic cells profoundly affects innate resistance functions. *J Immunol* **174**, 727-34.

Giacinti, C., Giordano, A. (2006) RB and cell cycle progression. *Oncogene.* **25**, 5220-7.

Gilliet, M., Boonstra, A., Paturel, C., Antonenko, S., Xu, X.L., Trinchieri, G., O'Garra, A., Liu, Y.J. (2002) The development of murine plasmacytoid dendritic cell precursors is differentially regulated by FLT3-ligand and granulocyte/macrophage colony-stimulating factor. *J Exp Med.* **195**, 953-8.

Gordon, S., Taylor, P.R. (2005) Monocyte and macrophage heterogeneity. *Nat Rev Immunol* **5**, 953-64.

Goswami, K.K., Cameron, K.R., Russell, W.C., Lange, L.S., Mitchell, D.N. (1984) Evidence for the persistence of paramyxoviruses in human bone marrows. *J Gen Virol.* **65**, 1881-8.

Gotoh, B., Komatsu, T., Takeuchi, K., Yokoo, J. (2002) Paramyxovirus strategies for evading the interferon response. *Rev Med Virol.* **12**, 337-57.

Gougeon, M.L., Lecoeur, H., Dulioust, A., Enouf, M.G., Crouvoiser, M., Goujard, C., Debord, T., Montagnier, L. (1996) Programmed cell death in peripheral lymphocytes from HIV-infected persons: increased susceptibility to apoptosis of CD4 and CD8 T cells correlates with lymphocyte activation and with disease progression. *J Immunol.* **156**, 3509-20.

Greenberg, D.P., Walker, R.E., Lee, M.S., Reisinger, K.S., Ward, J.I., Yogev, R., Blatter, M.M., Yeh, S.H., Karron, R.A., Sangli, C., Eubank, L., Coelingh, K.L., Cordova, J.M., August, M.J., Mehta, H.B., Chen, W., Mendelman, P.M. (2005) A bovine parainfluenza virus type 3 vaccine is safe and immunogenic in early infancy. *J Infect Dis.* **191**, 1116-22. Epub 2005 Feb 22.

Greer, C.E., Zhou, F., Legg, H.S., Tang, Z., Perri, S., Sloan, B.A., Megede, J.Z., Uematsu, Y., Vajdy, M., Polo, J.M. (2006) A chimeric alphavirus RNA replicon gene-based vaccine for human parainfluenza virus type 3 induces protective immunity against intranasal virus challenge. *Vaccine* **7**, 7.

Grouard, G., Rissoan, M.C., Filgueira, L., Durand, I., Banchereau, J., Liu, Y.J. (1997) The enigmatic plasmacytoid T cells develop into dendritic cells with interleukin (IL)-3 and CD40-ligand. *J Exp Med.* **185**, 1101-11.

Guidotti, L.G., Chisari, F.V. (2000) Cytokine-mediated control of viral infections. *Virology.* **273**, 221-7.

Hall, C.B. (2001) Respiratory syncytial virus and parainfluenza virus. *N Engl J Med.* **344**, 1917-28.

Haller, A.A., Miller, T., Mitiku, M., Coelingh, K. (2000) Expression of the surface glycoproteins of human parainfluenza virus type 3 by bovine parainfluenza virus type 3, a novel attenuated virus vaccine vector. *J Virol.* **74**, 11626-35.

Hamerman, J.A., Ogasawara, K., Lanier, L.L. (2005) NK cells in innate immunity. *Curr Opin Immunol* **17**, 29-35.

Hanna, J., Gonen-Gross, T., Fitchett, J., Rowe, T., Daniels, M., Arnon, T.I., Gazit, R., Joseph, A., Schjetne, K.W., Steinle, A., Porgador, A., Mevorach, D., Goldman-Wohl, D., Yagel, S., LaBarre, M.J., Buckner, J.H., Mandelboim, O. (2004) Novel APC-like properties of human NK cells directly regulate T cell activation. *J Clin Invest* **114**, 1612-23.

Harandi, A.M., Svennerholm, B., Holmgren, J., Eriksson, K. (2001) Differential roles of B cells and IFN-gamma-secreting CD4(+) T cells in innate and adaptive immune control of genital herpes simplex virus type 2 infection in mice. *J Gen Virol.* **82**, 845-53.

Harper, D.R. (1998) *Molecular Virology.* BIOS Scientific Publishers Ltd, Oxford, UK.

Heil, F., Hemmi, H., Hochrein, H., Ampenberger, F., Kirschning, C., Akira, S., Lipford, G., Wagner, H., Bauer, S. (2004) Species-specific recognition of single-stranded RNA via toll-like receptor 7 and 8. *Science.* **303**, 1526-9. Epub 2004 Feb 19.
Henderson, F.W. (1981) Anti-viral cytotoxic lymphocyte response in hamsters with parainfluenza virus type 3 infection. *Adv Exp Med Biol.* **134**, 215-9.

Hengel, H., Koszinowski, U.H., Conzelmann, K.K. (2005) Viruses know it all: new insights into IFN networks. *Trends Immunol.* **26**, 396-401.
Henrickson, K.J. (2003) Parainfluenza viruses. *Clin Microbiol Rev.* **16**, 242-64.

Hilleman, M.R. (2002) Realities and enigmas of human viral influenza: pathogenesis, epidemiology and control. *Vaccine.* **20**, 3068-87.

Hou, S., Doherty, P.C., Zijlstra, M., Jaenisch, R., Katz, J.M. (1992) Delayed clearance of Sendai virus in mice lacking class I MHC-restricted CD8+ T cells. *J Immunol.* **149**, 1319-25.

Ito, T., Liu, Y.J., Kadowaki, N. (2005) Functional diversity and plasticity of human dendritic cell subsets. *Int J Hematol* **81**, 188-96.

Iwasaki, A., Medzhitov, R. (2004) Toll-like receptor control of the adaptive immune responses. *Nat Immunol.* **5**, 987-95.

Janeway, C.A.J.p.T., M. Walport and M. J. Shomchik (2001) *Immunobiology: the immune system in health and disease.*, Churchill Livingstone, New York.

Janeway, C.A., Jr., Medzhitov, R. (2002) Innate immune recognition. *Annu Rev Immunol.* **20**, 197-216. Epub 2001 Oct 4.

Janeway, C.A.J.p.T., M. Walport and M. J. Shomchik (2005) *Immunobiology: the immune system in health and disease.*, Churchill Livingstone, New York.

Jiang, H., Chess, L. (2004) An integrated view of suppressor T cell subsets in immunoregulation. *J Clin Invest* **114**, 1198-208.

Jinushi, M., Takehara, T., Tatsumi, T., Kanto, T., Groh, V., Spies, T., Suzuki, T., Miyagi, T., Hayashi, N. (2003) Autocrine/paracrine IL-15 that is required for type I IFN-mediated dendritic cell expression of MHC class I-related chain A and B is impaired in hepatitis C virus infection. *J Immunol.* **171**, 5423-9.

Julkunen, I., Hovi, T., Seppala, I., Makela, O. (1985) Immunoglobulin G subclass antibody responses in influenza A and parainfluenza type 1 virus infections. *Clin Exp Immunol.* **60**, 130-8.

Kadowaki, N., Ho, S., Antonenko, S., Malefyt, R.W., Kastelein, R.A., Bazan, F., Liu, Y.J. (2001) Subsets of human dendritic cell precursors express different toll-like receptors and respond to different microbial antigens. *J Exp Med.* **194**, 863-9.

Kagnoff, M.F., Eckmann, L. (1997) Epithelial cells as sensors for microbial infection. *J Clin Invest.* **100**, 6-10.

Karron, R.A., Wright, P.F., Hall, S.L., Makhene, M., Thompson, J., Burns, B.A., Tollefson, S., Steinhoff, M.C., Wilson, M.H., Harris, D.O., et al. (1995) A live attenuated bovine parainfluenza virus type 3 vaccine is safe, infectious, immunogenic, and phenotypically stable in infants and children. *J Infect Dis.* **171**, 1107-14.

Karron, R.A., Wright, P.F., Newman, F.K., Makhene, M., Thompson, J., Samorodin, R., Wilson, M.H., Anderson, E.L., Clements, M.L., Murphy, B.R., et al. (1995a) A live human parainfluenza type 3 virus vaccine is attenuated and immunogenic in healthy infants and children. *J Infect Dis.* **172**, 1445-50.

Kastrukoff, L.F., Lau, A., Wee, R., Zecchini, D., White, R., Paty, D.W. (2003) Clinical relapses of multiple sclerosis are associated with 'novel' valleys in natural killer cell functional activity. *J Neuroimmunol.* **145**, 103-14.

Kawai, T., Akira, S. (2006) Innate immune recognition of viral infection. *Nat Immunol.* **7**, 131-7.

Kinter, A.L., Hennessey, M., Bell, A., Kern, S., Lin, Y., Daucher, M., Planta, M., McGlaughlin, M., Jackson, R., Ziegler, S.F., Fauci, A.S. (2004) CD25(+)CD4(+) regulatory T cells from the peripheral blood of asymptomatic HIV-infected individuals regulate CD4(+) and CD8(+) HIV-specific T cell immune responses in vitro and are associated with favorable clinical markers of disease status. *J Exp Med* **200**, 331-43. Epub 2004 Jul 26.

Krug, A., Veeraswamy, R., Pekosz, A., Kanagawa, O., Unanue, E.R., Colonna, M., Cella, M. (2003) Interferon-producing cells fail to induce proliferation of naive T cells but can promote expansion and T helper 1 differentiation of antigen-experienced unpolarized T cells. *J Exp Med.* **197**, 899-906. Epub 2003 Mar 31.

Lamb, R.A.a.R.M.K. (2001) Orthomyxoviridae: The Viruses and Their Replication. In *Field Virology*, Volume 4th edition (D. M. a. P. M. H. Knipe, ed) Lippincott Williams and Wilkins, Philadelphia, US 1487-1531.

Le Bon, A., Etchart, N., Rossmann, C., Ashton, M., Hou, S., Gewert, D., Borrow, P., Tough, D.F. (2003) Cross-priming of CD8+ T cells stimulated by virus-induced type I interferon. *Nat Immunol.* **4**, 1009-15. Epub 2003 Sep 21.

Liu, Y.J. (2005) IPC: professional type 1 interferon-producing cells and plasmacytoid dendritic cell precursors. *Annu Rev Immunol* **23**, 275-306.

Lutz, M.B., Schuler, G. (2002) Immature, semi-mature and fully mature dendritic cells: which signals induce tolerance or immunity? *Trends Immunol* **23**, 445-9.

Mandelboim, O., Lieberman, N., Lev, M., Paul, L., Arnon, T.I., Bushkin, Y., Davis, D.M., Strominger, J.L., Yewdell, J.W., Porgador, A. (2001) Recognition of haemagglutinins on virus-infected cells by NKp46 activates lysis by human NK cells. *Nature.* **409**, 1055-60.

Mangan, P.R., Harrington, L.E., O'Quinn, D.B., Helms, W.S., Bullard, D.C., Elson, C.O., Hatton, R.D., Wahl, S.M., Schoeb, T.R., Weaver, C.T. (2006) Transforming growth factor-beta induces development of the T(H)17 lineage. *Nature.* **441**, 231-4. Epub 2006 Apr 30.

Marshall, N.A., Vickers, M.A., Barker, R.N. (2003) Regulatory T cells secreting IL-10 dominate the immune response to EBV latent membrane protein 1. *J Immunol.* **170**, 6183-9.

Marx, A., Gary, H.E., Jr., Marston, B.J., Erdman, D.D., Breiman, R.F., Torok, T.J., Plouffe, J.F., File, T.M., Jr., Anderson, L.J. (1999) Parainfluenza virus infection among adults hospitalized for lower respiratory tract infection. *Clin Infect Dis.* **29**, 134-40.

Masteller, E.L., Warner, M.R., Tang, Q., Tarbell, K.V., McDevitt, H., Bluestone, J.A. (2005) Expansion of functional endogenous antigen-specific CD4+CD25+ regulatory T cells from nonobese diabetic mice. *J Immunol.* **175**, 3053-9.

Matzinger, P. (1994) Tolerance, danger, and the extended family. *Annu Rev Immunol.* **12**, 991-1045.

104. Mayer, G. (2003) Virus-host interactions. MBIM (Microbiology and Immunology on-line).

McGuirk, P., McCann, C., Mills, K.H. (2002) Pathogen-specific T regulatory 1 cells induced in the respiratory tract by a bacterial molecule that stimulates interleukin 10 production by dendritic cells: a novel strategy for evasion of protective T helper type 1 responses by Bordetella pertussis. *J Exp Med.* **195**, 221-31.

McHeyzer-Williams, M.G. (2003) B cells as effectors. *Curr Opin Immunol.* **15**, 354-61.

McKenna, K., Beignon, A.S., Bhardwaj, N. (2005) Plasmacytoid dendritic cells: linking innate and adaptive immunity. *J Virol* **79**, 17-27.

Miller, J.S. (2001) The biology of natural killer cells in cancer, infection, and pregnancy. *Exp Hematol.* **29**, 1157-68.

Mills, K.H. (2004) Regulatory T cells: friend or foe in immunity to infection? *Nat Rev Immunol* **4**, 841-55.

Mohty, M., Vialle-Castellano, A., Nunes, J.A., Isnardon, D., Olive, D., Gaugler, B. (2003) IFN-alpha skews monocyte differentiation into Toll-like receptor 7-expressing dendritic cells with potent functional activities. *J Immunol.* **171**, 3385-93.

Morelli, A.E., Zahorchak, A.F., Larregina, A.T., Colvin, B.L., Logar, A.J., Takayama, T., Falo, L.D., Thomson, A.W. (2001) Cytokine production by mouse myeloid dendritic cells in relation to differentiation and terminal maturation induced by lipopolysaccharide or CD40 ligation. *Blood.* **98**, 1512-23.

Moscona, A. (2005) Entry of parainfluenza virus into cells as a target for interrupting childhood respiratory disease. *J Clin Invest* **115**, 1688-98.

Moulin, V., Andris, F., Thielemans, K., Maliszewski, C., Urbain, J., Moser, M. (2000) B lymphocytes regulate dendritic cell (DC) function in vivo: increased interleukin 12 production by DCs from B cell-deficient mice results in T helper cell type 1 deviation. *J Exp Med* **192**, 475-82.

Moutaftsi, M., Mehl, A.M., Borysiewicz, L.K., Tabi, Z. (2002) Human cytomegalovirus inhibits maturation and impairs function of monocyte-derived dendritic cells. *Blood.* **99**, 2913-21.

Munz, C., Steinman, R.M., Fujii, S. (2005) Dendritic cell maturation by innate lymphocytes: coordinated stimulation of innate and adaptive immunity. *J Exp Med* **202**, 203-7.

Ndolo, T., Dhillon, N.K., Nguyen, H., Guadalupe, M., Mudryj, M., Dandekar, S. (2002) Simian immunodeficiency virus Nef protein delays the progression of CD4+ T cells through G1/S phase of the cell cycle. *J Virol.* **76**, 3587-95.

Neirynck, S., Deroo, T., Saelens, X., Vanlandschoot, P., Jou, W.M., Fiers, W. (1999) A universal influenza A vaccine based on the extracellular domain of the M2 protein. *Nat Med.* **5**, 1157-63.

Ngo, V.N., Tang, H.L., Cyster, J.G. (1998) Epstein-Barr virus-induced molecule 1 ligand chemokine is expressed by dendritic cells in lymphoid tissues and strongly attracts naive T cells and activated B cells. *J Exp Med.* **188**, 181-91.

Nolte-'t Hoen, E., Almeida, C., Cohen, N., Nedvetzki, S., Yarwood, H., Davis, D. (2006) Increased surveillance of cells in mitosis by human NK cells suggests a novel strategy for limiting tumor growth and viral replication. *Blood* **7**, 7.

O'Doherty, U., Peng, M., Gezelter, S., Swiggard, W.J., Betjes, M., Bhardwaj, N., Steinman, R.M. (1994) Human blood contains two subsets of dendritic cells, one immunologically mature and the other immature. *Immunology.* **82**, 487-93.

O'Garra, A. (1998) Cytokines induce the development of functionally heterogeneous T helper cell subsets. *Immunity.* **8**, 275-83.

O'Garra, A., Vieira, P.L., Vieira, P., Goldfeld, A.E. (2004) IL-10-producing and naturally occurring CD4+ Tregs: limiting collateral damage. *J Clin Invest.* **114**, 1372-8.

O'Neill, L.A. (2004) TLRs: Professor Mechnikov, sit on your hat. *Trends Immunol.* **25**, 687-93.

Paiardini, M., Galati, D., Cervasi, B., Cannavo, G., Galluzzi, L., Montroni, M., Guetard, D., Magnani, M., Piedimonte, G., Silvestri, G. (2001) Exogenous interleukin-2 administration corrects the cell cycle perturbation of lymphocytes from human immunodeficiency virus-infected individuals. *J Virol.* **75**, 10843-55.

Palese, P. (2006) Making better influenza virus vaccines? *Emerg Infect Dis.* **12**, 61-5.

Parham, P. (2005) Putting a face to MHC restriction. *J Immunol.* **174**, 3-5.

Parlato, S., Santini, S.M., Lapenta, C., Di Pucchio, T., Logozzi, M., Spada, M., Giammarioli, A.M., Malorni, W., Fais, S., Belardelli, F. (2001) Expression of CCR-7, MIP-3beta, and Th-1 chemokines in type I IFN-induced monocyte-derived dendritic cells: importance for the rapid acquisition of potent migratory and functional activities. *Blood.* **98**, 3022-9.

Pazmany, L. (2005) Do NK cells regulate human autoimmunity? *Cytokine.* **32**, 76-80. Epub 2005 Oct 5.

Piccioli, D., Sbrana, S., Melandri, E., Valiante, N.M. (2002) Contact-dependent stimulation and inhibition of dendritic cells by natural killer cells. *J Exp Med.* **195**, 335-41.

Platanias, L.C. (2005) Mechanisms of type-I- and type-II-interferon-mediated signalling. *Nat Rev Immunol* **5**, 375-86.

Plotnicky-Gilquin, H., Cyblat, D., Aubry, J.P., Delneste, Y., Blaecke, A., Bonnefoy, J.Y., Corvaia, N., Jeannin, P. (2001) Differential effects of parainfluenza virus type 3 on human monocytes and dendritic cells. *Virology* **285**, 82-90.

Qu, C., Moran, T.M., Randolph, G.J. (2003) Autocrine type I IFN and contact with endothelium promote the presentation of influenza A virus by monocyte-derived APC. *J Immunol* **170**, 1010-8.

Randolph, G.J., Inaba, K., Robbiani, D.F., Steinman, R.M., Muller, W.A. (1999) Differentiation of phagocytic monocytes into lymph node dendritic cells in vivo. *Immunity.* **11**, 753-61.

Raulet, D.H., Vance, R.E. (2006) Self-tolerance of natural killer cells. *Nat Rev Immunol.* **6**, 520-31.

Reis e Sousa, C. (2004a) Toll-like receptors and dendritic cells: for whom the bug tolls. *Semin Immunol.* **16**, 27-34.

Reis e Sousa, C. (2004) Activation of dendritic cells: translating innate into adaptive immunity. *Curr Opin Immunol.* **16**, 21-5.

Romagnani, C., Della Chiesa, M., Kohler, S., Moewes, B., Radbruch, A., Moretta, L., Moretta, A., Thiel, A. (2005) Activation of human NK cells by plasmacytoid dendritic cells and its modulation by CD4(+) T helper cells and CD4(+) CD25(hi) T regulatory cells. *Eur J Immunol* **5**, 5.

Russell, J.H., Ley, T.J. (2002) Lymphocyte-mediated cytotoxicity. *Annu Rev Immunol.* **20**, 323-70. Epub 2001 Oct 4.

Sakaguchi, S. (2005) Naturally arising Foxp3-expressing CD25+CD4+ regulatory T cells in immunological tolerance to self and non-self. *Nat Immunol.* **6**, 345-52.

Sallusto, F., Lanzavecchia, A. (1994) Efficient presentation of soluble antigen by cultured human dendritic cells is maintained by granulocyte/macrophage colony-stimulating factor plus interleukin 4 and downregulated by tumor necrosis factor alpha. *J Exp Med.* **179**, 1109-18.

Santini, S.M., Di Pucchio, T., Lapenta, C., Parlato, S., Logozzi, M., Belardelli, F. (2003) A new type I IFN-mediated pathway for the rapid differentiation of monocytes into highly active dendritic cells. *Stem Cells.* **21**, 357-62.

Sato, A., Iwasaki, A. (2004) Induction of antiviral immunity requires Toll-like receptor signaling in both stromal and dendritic cell compartments. *Proc Natl Acad Sci U S A.* **101**, 16274-9. Epub 2004 Nov 8.

Schlecht, G., Garcia, S., Escriou, N., Freitas, A.A., Leclerc, C., Dadaglio, G. (2004) Murine plasmacytoid dendritic cells induce effector/memory CD8+ T-cell responses in vivo after viral stimulation. *Blood.* **104**, 1808-15. Epub 2004 May 27.

Schlender, J., Walliser, G., Fricke, J., Conzelmann, K.K. (2002) Respiratory syncytial virus fusion protein mediates inhibition of mitogen-induced T-cell proliferation by contact. *J Virol.* **76**, 1163-70.

Schwartz, R.H. (2005) Natural regulatory T cells and self-tolerance. *Nat Immunol.* **6**, 327-30.

Senechal, B., Boruchov, A.M., Reagan, J.L., Hart, D.N., Young, J.W. (2004) Infection of mature monocyte-derived dendritic cells with human cytomegalovirus inhibits stimulation of T-cell proliferation via the release of soluble CD83. *Blood.* **103**, 4207-15. Epub 2004 Feb 12.

Sherr, C.J., Roberts, J.M. (1999) CDK inhibitors: positive and negative regulators of G1-phase progression. *Genes Dev.* **13**, 1501-12.

Shortman, K., Liu, Y.J. (2002) Mouse and human dendritic cell subtypes. *Nat Rev Immunol* **2**, 151-61.

Sieg, S., Muro-Cacho, C., Robertson, S., Huang, Y., Kaplan, D. (1994) Infection and immunoregulation of T lymphocytes by parainfluenza virus type 3. *Proc Natl Acad Sci U S A* **91**, 6293-7.

Sieg, S., Xia, L., Huang, Y., Kaplan, D. (1995) Specific inhibition of granzyme B by parainfluenza virus type 3. *J Virol* **69**, 3538-41.

Sieg, S., King, C., Huang, Y., Kaplan, D. (1996) The role of interleukin-10 in the inhibition of T-cell proliferation and apoptosis mediated by parainfluenza virus type 3. *J Virol.* **70**, 4845-8.

Skiadopoulos, M.H., Surman, S.R., Riggs, J.M., Elkins, W.R., St Claire, M., Nishio, M., Garcin, D., Kolakofsky, D., Collins, P.L., Murphy, B.R. (2002) Sendai virus, a murine parainfluenza virus type 1, replicates to a level similar to human PIV1 in the upper and lower respiratory tract of African green monkeys and chimpanzees. *Virology.* **297**, 153-60.

Smeltz, R.B., Wolf, N.A., Swanborg, R.H. (1999) Inhibition of autoimmune T cell responses in the DA rat by bone marrow-derived NK cells in vitro: implications for autoimmunity. *J Immunol.* **163**, 1390-7.

Smyth, M.J., Takeda, K., Hayakawa, Y., Peschon, J.J., van den Brink, M.R., Yagita, H. (2003) Nature's TRAIL--on a path to cancer immunotherapy. *Immunity.* **18**, 1-6.

Su, H.C., Nguyen, K.B., Salazar-Mather, T.P., Ruzek, M.C., Dalod, M.Y., Biron, C.A. (2001) NK cell functions restrain T cell responses during viral infections. *Eur J Immunol* **31**, 3048-55.

Suvas, S., Azkur, A.K., Kim, B.S., Kumaraguru, U., Rouse, B.T. (2004) CD4+CD25+ regulatory T cells control the severity of viral immunoinflammatory lesions. *J Immunol.* **172**, 4123-32.

Svensson, M., Maroof, A., Ato, M., Kaye, P.M. (2004) Stromal cells direct local differentiation of regulatory dendritic cells. *Immunity* **21**, 805-16.

Tato, C.M., O'Shea J, J. (2006) Immunology: What does it mean to be just 17? *Nature.* **441**, 166-8.

Theofilopoulos, A.N., Baccala, R., Beutler, B., Kono, D.H. (2005) Type I interferons (alpha/beta) in immunity and autoimmunity. *Annu Rev Immunol.* **23**, 307-36.

Tosi, M.F. (2005) Innate immune responses to infection. *J Allergy Clin Immunol.* **116**, 241-9; quiz 250.

Trapani, J.A., Smyth, M.J. (2002) Functional significance of the perforin/granzyme cell death pathway. *Nat Rev Immunol.* **2**, 735-47.

Traver, D., Akashi, K., Manz, M., Merad, M., Miyamoto, T., Engleman, E.G., Weissman, I.L. (2000) Development of CD8alpha-positive dendritic cells from a common myeloid progenitor. *Science.* **290**, 2152-4.

Trivedi, P.P., Roberts, P.C., Wolf, N.A., Swanborg, R.H. (2005) NK cells inhibit T cell proliferation via p21-mediated cell cycle arrest. *J Immunol* **174**, 4590-7.

Twigg, H.L., 3rd (2005) Humoral immune defense (antibodies): recent advances. *Proc Am Thorac Soc.* **2**, 417-21.

van Kooyk, Y., Geijtenbeek, T.B. (2003) DC-SIGN: escape mechanism for pathogens. *Nat Rev Immunol.* **3**, 697-709.

van Rijt, L.S., van Kessel, C.H., Boogaard, I., Lambrecht, B.N. (2005) Respiratory viral infections and asthma pathogenesis: a critical role for dendritic cells? *J Clin Virol.* **34**, 161-9. Epub 2005 Aug 26.

Vidalain, P.O., Azocar, O., Lamouille, B., Astier, A., Rabourdin-Combe, C., Servet-Delprat, C. (2000) Measles virus induces functional TRAIL production by human dendritic cells. *J Virol* **74**, 556-9.

Wallace, M.E., Smyth, M.J. (2005) The role of natural killer cells in tumor control--effectors and regulators of adaptive immunity. *Springer Semin Immunopathol.* **27**, 49-64. Epub 2005 Feb 24.

Walzer, T., Dalod, M., Robbins, S.H., Zitvogel, L., Vivier, E. (2005) Natural-killer cells and dendritic cells: "l'union fait la force". *Blood* **106**, 2252-8. Epub 2005 Jun 2.
Wang, X., Li, M., Zheng, H., Muster, T., Palese, P., Beg, A.A., Garcia-Sastre, A. (2000) Influenza A virus NS1 protein prevents activation of NF-kappaB and induction of alpha/beta interferon. *J Virol.* **74**, 11566-73.

Watford, W.T., Moriguchi, M., Morinobu, A., O'Shea, J.J. (2003) The biology of IL-12: coordinating innate and adaptive immune responses. *Cytokine Growth Factor Rev.* **14**, 361-8.

Webby, R.J., Webster, R.G. (2001) Emergence of influenza A viruses. *Philos Trans R Soc Lond B Biol Sci.* **356**, 1817-28.

Weiss, L., Donkova-Petrini, V., Caccavelli, L., Balbo, M., Carbonneil, C., Levy, Y. (2004) Human immunodeficiency virus-driven expansion of CD4+CD25+ regulatory T cells, which suppress HIV-specific CD4 T-cell responses in HIV-infected patients. *Blood.* **104**, 3249-56. Epub 2004 Jul 22.

Williams, B.R. (1999) PKR; a sentinel kinase for cellular stress. *Oncogene.* **18**, 6112-20.

Woodland, D.L. (2003) Cell-mediated immunity to respiratory virus infections. *Curr Opin Immunol.* **15**, 430-5.

Wright, P.F.a.R.G.W. (2001) Orthomyxoviruses. In *Field Virology*, Volume 4th edition (D. M. a. P. M. H. Knipe, ed) Lippincott Williams and Wilkins, Philadelphia, US 1533-1579.

Yao, Z.Q., Eisen-Vandervelde, A., Ray, S., Hahn, Y.S. (2003) HCV core/gC1qR interaction arrests T cell cycle progression through stabilization of the cell cycle inhibitor p27Kip1. *Virology.* **314**, 271-82.

Young, D.F., Didcock, L., Goodbourn, S., Randall, R.E. (2000) Paramyxoviridae use distinct virus-specific mechanisms to circumvent the interferon response. *Virology.* **269**, 383-90.

Zhang, C., Zhang, J., Tian, Z.G. (2006) The Regulatory Effect of Natural Killer Cells: Do "NK-reg Cells" Exist? *Cell Mol Immunol.* **3**, 241-54.

Zingoni, A., Sornasse, T., Cocks, B.G., Tanaka, Y., Santoni, A., Lanier, L.L. (2004) Cross-talk between activated human NK cells and CD4+ T cells via OX40-OX40 ligand interactions. *J Immunol.* **173**, 3716-24.

Zingoni, A., Sornasse, T., Cocks, B.G., Tanaka, Y., Santoni, A., Lanier, L.L. (2005) NK cell regulation of T cell-mediated responses. *Mol Immunol.* **42**, 451-4.